AMILTON BARBOSA BOTELHO JUNIOR

EXTRAÇÃO DE ESCÂNDIO A PARTIR DE RESERVAS NÃO EXPLORADAS UTILIZANDO ROTA HIDROMETALÚRGICA COM FOCO NO DESENVOLVIMENTO SUSTENTÁVEL

São Paulo

2021

AMILTON BARBOSA BOTELHO JUNIOR

EXTRAÇÃO DE ESCÂNDIO A PARTIR DE RESERVAS NÃO EXPLORADAS UTILIZANDO ROTA HIDROMETALÚRGICA COM FOCO NO DESENVOLVIMENTO SUSTENTÁVEL

Tese apresentada em cumprimento parcial dos requisitos para o grau de Doutor em Ciências pela Escola Politécnica da Universidade de São Paulo.

São Paulo

2021

AMILTON BARBOSA BOTELHO JUNIOR

EXTRAÇÃO DE ESCÂNDIO A PARTIR DE RESERVAS NÃO EXPLORADAS UTILIZANDO ROTA HIDROMETALÚRGICA COM FOCO NO DESENVOLVIMENTO SUSTENTÁVEL

Tese apresentada em cumprimento parcial dos requisitos para o grau de Doutor em Ciências pela Escola Politécnica da Universidade de São Paulo.

Área de concentração: Engenharia Química

Orientador: Prof. Dr. Jorge Alberto Soares Tenório

Co-orientador: Profa. Dra. Denise Crocce Romano Espinosa

São Paulo

2021

AMILTON BARBOSA BOTELHO JUNIOR

EXTRACTION OF SCANDIUM FROM NON-EXPLORED RESOURCES USING HYDROMETALLURGICAL ROUTE WITH FOCUS ON SUSTAINABLE DEVELOPMENT

São Paulo

2021

AMILTON BARBOSA BOTELHO JUNIOR

EXTRACTION OF SCANDIUM FROM NON-EXPLORED RESOURCES USING HYDROMETALLURGICAL ROUTE WITH FOCUS ON SUSTAINABLE DEVELOPMENT

Thesis submitted in partial fulfilment of the requirements for the degree of Doctor of Philosophy (PhD) in Science in Escola Politécnica da Universidade de São Paulo.

São Paulo

2021

AMILTON BARBOSA BOTELHO JUNIOR

EXTRACTION OF SCANDIUM FROM NON-EXPLORED RESOURCES USING HYDROMETALLURGICAL ROUTE WITH FOCUS ON SUSTAINABLE DEVELOPMENT

Thesis submitted in partial fulfilment of the requirements for the degree of Doctor of Philosophy (PhD) in Science in Escola Politécnica da Universidade de São Paulo.

Area of concentration: Chemical Engineering

Supervisor: Prof. Dr. Jorge Alberto Soares Tenório

Co-supervisor: Profa. Dra. Denise Crocce Romano Espinosa

São Paulo

2021

Este exemplar foi revisado e corrigido em relação à versão original, sob responsabilidade única do autor e com a anuência de seu orientador.

São Paulo, _____ de _____ de _____

Assinatura do autor: _____

Assinatura do orientador: _____

Catalogação-na-publicação

Botelho Junior, Amilton Barbosa
Extração de escândio a partir de reservas não exploradas utilizando rota hidrometalúrgica com foco no desenvolvimento sustentável / A. B. Botelho Junior -- versão corr. -- São Paulo, 2021.
243 p.

Tese (Doutorado) - Escola Politécnica da Universidade de São Paulo. Departamento de Engenharia Química.

1.ODS 2.metais críticos 3.lama vermelha 4.resíduo de bauxita 5.resíduo de mineração I.Universidade de São Paulo. Escola Politécnica. Departamento de Engenharia Química II.t.

To my parents, Amilton and Eliana,
and to my brother, Alan.

ACKNOWLEDGEMENTS

Thanks to God;

To my parents Amilton and Eliana and to my brother Alan, for their support throughout my journey

To Patricia Tachibana Jo, who, in addition to being a girlfriend, was my friend and companion in good and bad times;

To Faculdades Oswaldo Cruz;

To FAPESP/CAPES - Foundation for Research Support of the State of São Paulo (processes number 2012/51871-9, 2018/03483-6, 2018/11417-3 and 2019/11866-5), for the scholarship provided;

I would like to express my special thanks to my supervisor, Prof. Jorge Tenório, and co-supervisor, Prof. Denise Espinosa, for their kind guidance and support throughout the PhD's program. All of their words lead me to learn a lot about how to be a professor, a researcher, a professional, and human;

To my first children in academia, Iara Anes, José Helber Vinco, Lívia Martins and Lucas Guimarães for all learning and for letting me be a part of your careers;

To my children of LAREX-Tupy project, Anastássia, David, Jenesson, Maria Eduarda, Roberta, and Vinícius, for being a part of my new journey;

To all my colleagues of LAREX, in special Jorge Coleti, Carlos Rosario, Ana Carolina, Paula Aliprandini, Franco Garjulli, Jonathan Vinhal, Isabela Falconi, Thamiris Gonçalves, Rafael Piumatti, Larissa Otaviano, Giovani Pavoski, for all the learning and support I had from you during my journey;

To The University of Queensland (School of Chemical Engineering), to the research group Hydrometallurgy, and mainly to the Prof. James Vaughan for the internship which was crucial for my personal and professional growth.

"*Avanti, Palestra! Scoppia che la vittoria è nostra*"

"Cool Head, Warm Heart."

“Cabeça Fria, Coração Quente”

Ferreira, Abel

RESUMO

Escândio é um dos elementos presentes na lista de metais terras raras, sendo o mais valioso entre eles. O elemento é amplamente utilizado em ligas leves de alumínio, aparelhos eletrônicos, lasers, iluminação e células de combustível de óxido sólido (SOFCs). Escândio e todos os elementos terras raras são considerados críticos pela União Europeia, Brasil e pelos EUA devido aos riscos de interrupção na cadeia de fornecimento, importância econômica, reservas limitadas, baixa taxa de reciclagem e praticamente insubstituível na aplicação de tecnologias verdes. Por esta razão, é essencial o estudo de rotas extrativas de escândio a partir de novas reservas para desenvolver um processo economicamente e tecnicamente viável. Assim, a demanda atual e crescente de um elemento crucial para o desenvolvimento de uma sociedade sustentável pode ser atendida. Bauxitas são consideradas a principal fonte de escândio no mundo, o qual é a matéria-prima para produção de alumina pelo processo Bayer. Após a extração da alumina, praticamente todo o escândio vai para o resíduo gerado no processo conhecido como resíduo de bauxita (ou lama vermelha). Estima-se que pelo menos 4 bilhões de toneladas do resíduo estão armazenados em barragens no mundo, contendo 30-100mg/kg de escândio, o que pode valer entre US$400 – 4,500 bilhões. O elemento representa 95% do valor econômico do resíduo. Zircônio é reportado como o segundo mais valioso. A literatura tem mostrado que fontes contento acima de 20mg/kg merecem exploração devido a viabilidade econômica. Ainda, a descoberta de novas reservas primárias é crucial para atender a demanda de escândio. Entre as técnicas de extração, a rota hidrometalúrgica atinge as maiores taxas de extração principalmente em concentrações traço. Por outro lado, há dois problemas principais: a síntese de sílica gel que reduz a extração de escândio e aumenta o consumo de ácido, e a separação de escândio dos contaminantes. Por esta razão, o objetivo desta tese foi estudar a extração de escândio de duas reservas não exploradas: resíduo de bauxita de um processo Brasileiro e do minério silicatado de uma fonte Canadense. Técnicas de lixiviação e de separação foram estudadas. A caracterização dos materiais foi realizada por difração de raios-X, fluorescência de raios-X por energia dispersiva, distribuição granulométrica, microscopia eletrônica de varredura acoplado com energia dispersiva, perda ao fogo, carbono orgânico total, e espectrometria de emissão ótica com plasma indutivamente acoplado. Experimentos de lixiviação do resíduo de bauxita foram realizados usando H_2SO_4 e H_3PO_4, onde o efeito da relação sólido-líquido, tempo, temperatura, dosagem de H_2O_2, e concentração de ácido foram avaliados. Lixiviação direta e digestão à seco/sulfatação seguido por lixiviação com água foram estudados para extração de escândio do minério a base de silicato usando H_2SO_4. O efeito da dosagem de ácido e da temperatura de calcinação também foram estudados. A técnica de extração por solventes foi estudada para separação de escândio usando Alamine 336, D2EHPA, e Cyanex 923. O efeito do pH, temperatura, concentração de extratante, mistura com TBP e relação A/O foram explorados. Resultados mostraram que a concentração de escândio e zircônio foi de 43.5mg/kg e 1329.8mg/kg, respectivamente, e 36.4% de Fe_2O_3, 23.3% de Al_2O_3 21.6% de SiO_2. As principais fases minerais foram quartzo, sodalita, gibbsita, goetita, hematita, boehmita e gibbsita. Teores de escândio e zircônio minério à base de sílica foi 191mg/kg e 8,090mg/kg, respectivamente. O material continha 36.3% de Fe_2O_3, 4.61% de Al_2O_3, e 39.4% de SiO_2. As principais fases minerais era dickite, ferrohornblende, fayalite, hedenbergite e albite. A extração de escândio resíduo de bauxita atingiu 92% usando H_2SO_4 20%, relação sólido-líquido igual a 1/10 for 8h e 90°C. Houve praticamente 0% de lixiviação de silício. O H_2O_2 teve

pouca contribuição na formação de dióxido de silício durante a lixiviação ácida do resíduo de bauxita. As taxas extração na lixiviação com H_3PO_4 foram similares à lixiviação com H_2SO_4, onde a eficiência de lixiviação de escândio, alumínio, e ferro atingiu 90%, enquanto que silício foi de 13%. A extração de metais valiosos do minério a base de silicato por lixiviação direta aumentou de 40% (25°C) para 80% (90°C). A extração de escândio por lixiviação direta e por sulfatação seguido por lixiviação com água foi de 13,5% e 5,6%, respectivamente. Todo zircônio foi separado da solução usando Alamine 336 10% em querosene, relação A/O igual a 1:1, pH 1.0 por 15min a 25°C. Não foi observado efeito sinérgico entre o extratante amina e o TBP. Cyanex 923 foi mais seletivo para escândio do que para D2EHPA, onde o fator de separação para Sc/Fe foi de 288 e 99, e Sc/Ti foi de 98 e 21.5, respectivamente. A eficiência de reextração do zircônio foi de 92% usando Na_2CO_3 para concentração acima de 0.25mol/L. A etapa de lavagem pode ser realizada por HCl 5mol/L com perda de escândio de 0.1%. Todo o escândio foi extraído da fase orgânica usando H_3PO_4 5mol/L. A extração de escândio e zircônio (como coproduto) atingiu 92% e 25%, respectivamente. De acordo com o fluxograma proposto, seria possível obter 4kg de escândio e 31.9kg de zircônio a partir de 100 toneladas de resíduo de bauxita. O processo poderia gerar cerca de US$ 46.626 de óxido de escândio ou US$ 1.940.980.00 de fluoreto de escândio. O processo desenvolvido e a presente tese estão estritamente ligados aos objetivos para o desenvolvimento sustentável número 7 (7.2, 7a), 8 (8.2, 8.4), 9 (9.2, 9.4, 9.5, 9b), e 12 (12.2, 12.4, 12.5, 12.6, 12a).

Palavras-chave: ODS; metais críticos, lama vermelha; resíduo de bauxita; resíduo de mineração.

ABSTRACT

Scandium is one of the elements presented in the list of rare earths metals, being the most valuable among them. It´s widely used in lightweight aluminum alloys, electronic devices, lasers, lighting, and solid oxide fuel cells (SOFCs). Scandium and all rare earth elements are considered critical by the European Union, Brazil, and the USA due to the risk of supply chain interruption, economic importance, limited resources, low recycling rate, and practically irreplaceable in green technologies application. For this reason, it is essential the study of extractive route of scandium from new resources to design an economic and technological feasible process. Therefore, the current and growing demand of an element crucial to the development of sustainable society will be met. Bauxites are considered the main source of scandium in the world, which are the raw material for alumina production by the Bayer Process. After alumina extraction, almost all scandium went through the residue generated called bauxite residue (or red mud). It's estimated up to 4 billion tons of the residue are stored in dams worldwide containing 30-100mg/kg of scandium, which may value between US$400 – 4,500billion. The rare earth element would represent 95% of the economic value of the residue. Zirconium is reported as the second most valuable. The literature has shown that sources containing more than 20mg/kg deserve exploration due to their economic feasibility. Moreover, the discovery of new primary reserves is crucial for its supply. Among the extraction techniques, hydrometallurgy achieves the highest scandium obtaining rates mainly in trace concentration. On the other hand, there are two main problems: the synthesis of silica gel which reduces scandium extraction and increases the acid consumption, and the separation of scandium from the contaminants. For this reason, the goal of the thesis was the study of scandium extraction from two sources unexplored: bauxite residue from a Brazilian process and silicate-based ore from a Canadian source. The leaching process and separation by solvent extraction were studied. The materials' characterization was carried out by X-ray diffraction, energy-dispersive X-ray fluorescence, particle size distribution, scanning electron microscopy coupled with energy-dispersive, loss of ignition, total organic carbon, and inductively coupled plasma atomic emission spectrometry. Leaching experiments of bauxite residue were carried out with H_2SO_4 and H_3PO_4, where the effect of solid-liquid ratio, time, temperature, H_2O_2 dosage, and acid concentration were evaluated. Direct leaching and dry digestion/sulfation followed by water leaching were studied for scandium extraction from silicate-based ore using H_2SO_4. The effect of acid dosage and the roasting temperature was also evaluated. Solvent extraction technique was studied for scandium separation using Alamine 336, D2EHPA, and Cyanex 923. The effect of pH, temperature, extractant concentration, TBP mixture, and A/O ratio were explored. Results show that scandium and zirconium content in bauxite residue was 43.5mg/kg and 1329.8mg/kg, respectively, and 36.4% of Fe_2O_3, 23.3% of Al_2O_3 21.6% of SiO_2. The main mineral phases of the residue were quartz, sodalite, gibbsite, goethite, hematite, boehmite, and gypsum. Scandium and zirconium content in the silicate-based ore was 191mg/kg and 8,090mg/kg, respectively. The material had 36.3% of Fe_2O_3, 4.61% of Al_2O_3, and 39.4% of SiO_2. The main mineral phases of the silicate-based ore were dickite, ferrohornblende, fayalite, hedenbergite, and albite. The extraction of scandium from bauxite residue achieved 92% using H_2SO_4 20%, solid-liquid ratio equals 1/10 for 8h at 90°C. Almost 0% of silicon was leached. The H_2O_2 little contributed to silicon oxide formation during the acid leaching of bauxite residue. The extraction rates in H_3PO_4 leaching were similar to H_2SO_4 leaching, where the efficiency for scandium, aluminum, and iron achieved up to 90%, while silicon was

13%. The extraction of the valuable elements from the silicate-based ore by direct leaching increased from 40% (25°C) to 80% (90°C). The extraction of scandium from direct leaching and sulfation followed by water leaching was 13.5% and 5.6%, respectively. All zirconium was separated from the solution using Alamine 336 10% in kerosene, A/O ratio equals 1:1, at pH 1.0 for 15min at 25°C. No synergic effect was observed between amine extractant and TBP. Cyanex 923 was more selective for scandium than D2EHPA, where the separation factor for Sc/Fe was 288 and 99, and Sc/Ti was 98 and 21.5, respectively, considering 10% of organic extractant, A/O ratio equals to 1:1 at 25°C for 15min. Stripping of zirconium achieved 92% using Na_2CO_3 for concentration above 0.25mol/L. Scrubbing of Cyanex 923 for contaminants removal may be carried out with HCl 5mol/L with losses of 0.1% of scandium. All remained scandium may be stripped using H_3PO_4 5mol/L. The extraction of scandium and zirconium (as co-product) reached 92% and 25%, respectively. According to the flowchart proposed, it would be possible to obtain 4kg of scandium and 31.9kg of zirconium from 100 tons of bauxite residue. The process would generate up to US$ 46,626 of scandium oxide or US$ 1,940,980 of scandium fluoride. The process design and this thesis are strictly connected to the sustainable development goals number 7 (7.2, 7a), 8 (8.2, 8.4), 9 (9.2, 9.4, 9.5, 9b), and 12 (12.2, 12.4, 12.5, 12.6, 12a).

Keywords: SGDs; critical metals; red mud; bauxite residue; mining waste.

LIST OF FIGURES

LIST OF TABLES

SUMÁRIO

1. INTRODUCTION

The list of rare earth elements (REE) are scandium, yttrium and the elements of lanthanide group, which are included together due to their chemical similarity [1]. The group is divided into the light rare earth elements, consisting of lanthanum to europium, and heavy rare earth elements, from gadolinium to lutetium. Yttrium exhibits similar characteristics of the heavy elements. Scandium, on the other hand, may be classified in none of them as it bears different properties [2].

Among these elements, scandium is the most valuable (Table 1). Its application are found in light-weight aluminum alloys, electronic devices, lasers, lighting [3] and as a key component of certain solid oxide fuel cells [4].

Table 1: Examples of rare earth element (oxides) price in US$/kg [3,5,6]

Compound	Price (US$/kg)
CeO_2	2
La_2O_3	2
Nd_2O_3	47
Y_2O_3	3
Pr_6O_{11}	75
Sm_2O_3	6
Gd_2O_3	24
Dy_2O_3	180
Sc_2O_3	3,800

Scandium and all REE are considered *critical* by the European Union and most countries around the world, such as the U.S.A. (U.S. Department of Energy) and Brazil [7,8]. For instance, in European Union, the light and heavy rare earth elements are considered the most critical among all materials in the list of critics. while scandium is considered more critical than cobalt, graphite and lithium (crucial for electric car batteries [9,10]), platinum group metals, indium and silicon metal (important for photovoltaic panels [11,12]), and also silver and gold [13,14].

Scandium is included, as well as magnesium, niobium, germanium and borates, in the group of *high* critical elements, while the light and heavy rare earth elements are present in the group of *very high* critical [15]. It means that these elements have a risk of interruption of supply in the short and medium-term owing to:

i) high economic importance;

ii) high control of resources by a few countries;

iii) practically irreplaceable;

iv) application in green technologies; and

iv) low recycling rate.

To the world, scandium is deemed extremely important for their development for materials and metallurgy sector, civil and military drones and 3D printers' production, and digital sector to different areas including defense and space, e-mobility and renewable energy [16]. At the same time, the element has the highest potential for transformation market growth, driving to the necessity of efforts to avoid risks on supply interruption. While the REE recycling rate is between 3% and 8%, the recycling rate for scandium is zero [17,18]. The criticality of Sc and REE's, future market potential and low recycling rates highlights the need to search for and invest in recycling technologies in addition to new sources and more efficient primary extraction and refining methods.

The main primary scandium resources are the thortveitite and lolbeckite ores ($(Sc,Y)_2Si_2O_7$), which contain up to 45% of Sc_2O_3. This scandium silicate-rich ore contains also yttrium, REEs, iron, aluminum, thorium, zirconium, and alkaline earths, which is restricted in quantity and sources. Mine processes from Madagascar and Norway produce scandium from thortveitite, and in the USA it is obtained from thortveitite tailings [19,20].

A process patented by Baptiste (1959) describes scandium extraction by fractionation sublimation in chloride medium, to obtain $ScCl_3$. The process consists of heating to 950°C the ore mixed with a carbon source. Then, dry chloride is passed

over the mixture. The sublimation temperature of scandium and yttrium chloride are 967°C and 1507°C, respectively. Silicon, titanium, aluminum, iron, and zirconium chlorides sublimation temperatures are, respectively, 57°C, 136°C, 180°C, 310°C, and 331°C. The gases go through a refractory tube where the temperature of its downstream does not fall below 400°C. According to the patent, scandium oxide can then be obtained by precipitation using ammonia into the oxide from anhydrous scandium chloride [21]. Scandium can also be obtained from thotvellite using ammonia bifluoride at 400°C in a stream of dry air [19]

Minerals with appreciable concentrations scandium are rarely found which make its extraction as primary source limited. It is estimated that only 400kg of scandium is obtained from primary sources, and the remaining 2000kg is obtained as a secondary source [20].

The main scandium resources worldwide are in Australia, Canada, China, Kazakhstan, Madagascar, Norway, the Philippines, Russia, Ukraine, and the USA while the main producers are China (66%), followed by Russia (26%) and Ukraine (7%) [17,22]. Due to Chinese control of the REE market, and the market crisis in 2011 [23–25], researchers have been looking for new sources, mainly for scandium.

In Australia, several mining companies are in various stages of development for new scandium supply. The Nyngan project in New South Wales is under development, where the reserves are estimated in 590 tonnes of scandium (155ppm of Sc) from 1.44 million tonnes of ore. It is expected to produce 39 tonnes per year of scandium oxide starting in 2020. The Syerston project, also in New South Wales, is under development, which contains 19,200 tonnes of scandium (300ppm). In Queensland, the Scandium-Cobalt-Nickel (SCONI) Project was finishing its economic feasibility study, which expects to obtain 3,000 tonnes of scandium from 12 million tonnes of mineral resource (162ppm) [22].

Associated with the availability of scandium, environmental issues related to the extraction processes has been concerning all stakeholders and put a focus on using the most sustainable techniques [26]. For example, the risks of dam accidents have been highlighted in the last years, as two of them occurred in Brazil (2015 and 2018) [27–31], and, due to the relatively low grades, a high amount of waste material

would be generated from a scandium ore if no other by-products are produced. Accordingly, the reuse of mining tailings is gaining importance.

Leading with all those aspects, the United Nations (the U.N.) released 17 Sustainable Development Goals (SDG) to be achieved by 2030 [32], focuses on objectives on three dimensions of sustainable development which are to achieve global peace, justice, and international collaboration:

1) Economic development;
2) Social inclusion;
3) Environmental sustainability

The same approach can be applied in mining and metal processing industries, considering aspects of safe work, social issues, economics and the environment [33]. Nonetheless, it is well known that extractive activities are considered non-renewable. Thus, scientific and technical developments are carried out in order to make the processing more ecofriendly with respect to environmental issues such as tailings volume and toxicity; energy use and CO_2 emissions as well as the impacts of reagents in the extractive processing stages.

Among the sources of scandium worldwide, bauxite residues (also known as red mud) are considered important due to two main reasons: first, the volume of waste material produced in the world achieved 4 billion tons in 2015, which have been considered an important source for many elements, not only scandium; second, the content of rare earth elements presented in bauxite residues are considered enough to deserve consideration for potential by-product recovery [20,34].

Moreover, among the potential resources of rare earth elements there are silicates and oxides. In the case of silicate-based ores, there is a lack in the literature due to scarcity. However, due to the growing demand for rare earth elements, these reserves have been considered even with lower rare earth elements than recognized minerals [35].

There are only a few works in the literature about direct leaching or acid baking of rare earth elements from silicate-based ores, probably because such minerals are

less common than phosphates (Monazite and Xenotime) and carbonates (Bastnasite) [35]. Moreover, there also a few works in the literature dedicated to scandium extraction from silicate ores. However, since the consumption and demand of scandium has grown over the years, it is necessary to search for new potential resources.

For this reason, it is essential the study of extractive route of scandium from different sources to supply the current and growing demand of an element crucial to the development of sustainable society.

The goal of the thesis was the study of scandium extraction from two different sources: bauxite residue, widely known as a scandium resource, and silicate-based ore, which there is a lack in the literature. The structure of the thesis is depicted in Figure 1.

This document presents five manuscripts submitted to scientific journals. The literature review has been published in the *Minerals Engineering* journal [36] and it is presented in Section 2.1. This paper aims the evaluation of scandium extraction from three different sources - primary, secondary and opportunities – focusing on clean technologies and eco-friendly processing to achieve goals 7, 8, 9, and 12 of the 17 sustainable development goals (SDGs) of the United Nations. The question “is it possible to have an ecofriendly process for scandium extraction?” - worldwide debated – was answered providing diversified opportunities for scandium extraction, demonstrating that the current development would achieve these goals.

The Results and Discussion section of the present thesis is divided into four manuscripts. The paper is presented in section 5.1 shows the results for characterization of bauxite residue used in the current thesis, as well as the studies for recovery of scandium by the leaching/ion-exchange process. The manuscript has been published in the *Mining, Metallurgy & Exploration* journal [37]. Scandium recovery using a leaching/ion exchange process may be possible with efficiency higher than 90%. The greatest challenge is the occurrence of silica gel formation during leaching.

Section 5.2 presents the results for leaching experiments of bauxite residue evaluating the synthesis of silica gel. Also, the goal of this study was obtaining a near-zero-waste process, where the final waste (leaching residue) could be used in other process. It was studied the leaching agents sulfuric acid and phosphoric acid through

the parameters time, solid-liquid ratio, temperature and acid concentration. It was explored in-depth the use of H_2O_2 to suppress the silica gel synthesis, where the effect of oxidant agent was explored. The manuscript has been published in the *Journal of Sustainable Metallurgy* [38].

The manuscript presented in Section 5.3 depicts the extraction results of scandium and rare earth elements from silicate-based ore by direct leaching and dry digestion/sulfation followed by water leaching. There are almost none studies published in the literature reporting extraction of rare earth elements from silicate ores.

The Section 5.4 shows the results of solvent extraction experiments from the bauxite residue leach solution. It is proposed the separation of scandium using Cyanex 923 and zirconium using Alamine 336. As depicted in the section 5.2, the rare earth elements represent 95% of the economic value of the solution, while zirconium represents up to 3% (the second most valuable). For this reason, it is proposed their recovery to improve the economic benefits of bauxite residue recycling. The manuscript has been published in the *Separation and Purification Technology* journal [39].

Finally, the conclusions of the manuscripts are presented in section 6 numbered. In addition to these manuscripts, it was published the following works about the topic of this thesis:

- Botelho Junior AB, Pinheiro ÉF, Espinosa DCR, Tenório JAS, Baltazar M dos PG. Adsorption of lanthanum and cerium on chelating ion exchange resins: kinetic and thermodynamic studies. Separation Science and Technology, 2021 [40];

- Botelho Junior AB, Espinosa DCR, Tenório JAS. The use of computational thermodynamic for yttrium recovery from rare earth elements-bearing residue. Journal of Rare Earths, 2021 [41].

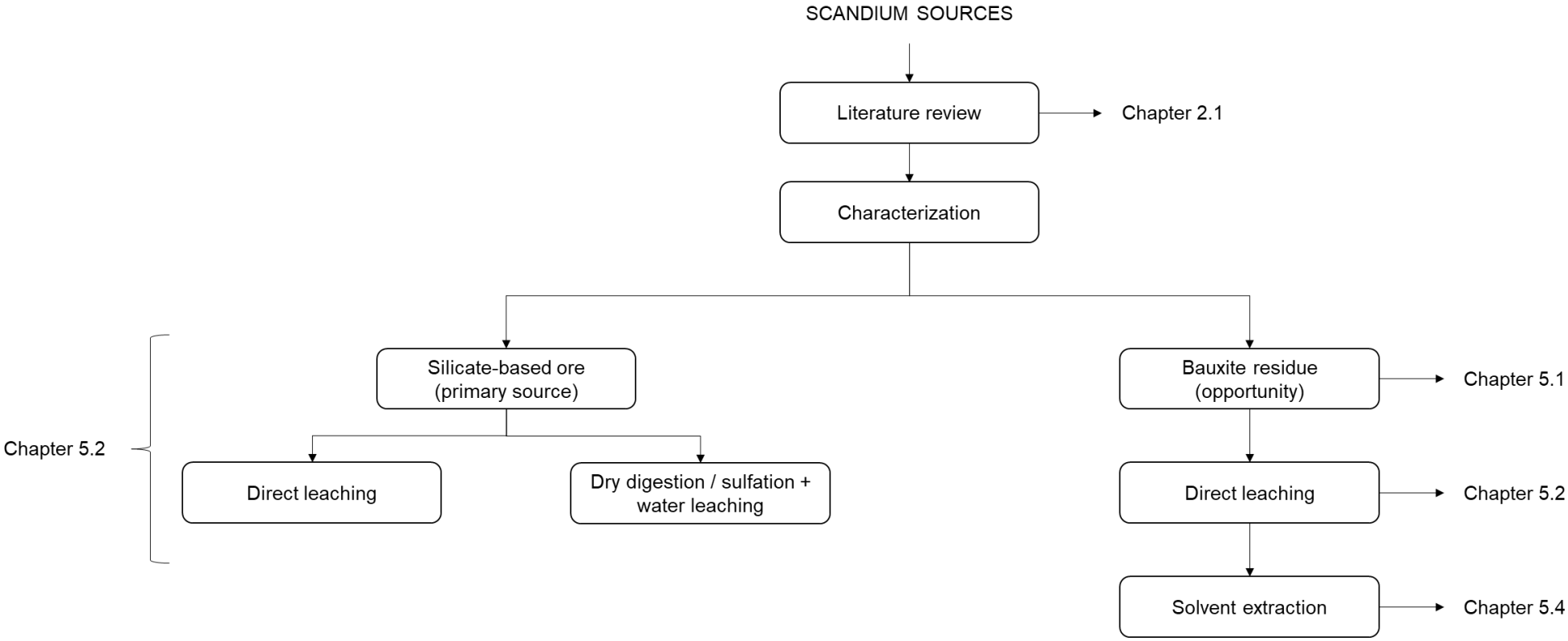

Figure 1: Structure of the thesis

1.1. SCIENTIFIC CONTRIBUTION

For this thesis, it is proposed the scandium recovery from bauxite residue. The choice of this residue for the thesis proposal is related to the 17 SDGs, mainly due to the use of an industrial waste as resource of scandium. The extraction of scandium from bauxite residue may achieves the following SDGs: 7 (*affordable and clean energy – targets 7a and 7.2*), 8 (*decent work and economic growth – targets 8.2 and 8.4*), 9 (*industry, innovation, and infrastructure – targets 9.2, 9.4, 9.5 and 9b*) and 12 (*responsible, consumption and production – targets 12.2, 12.4, 12.5, 12.6 and 12a*).

The SDG 7 in the present study is related to the increase demand for scandium in energy production (Single-crystal gadolinium– aluminum–scandium garnet (GASG) doped with nickel and chromium and production of metal halide lamps by the lighting industry, for instance [1]). The targets 9.4, 12.4 (the indicator 12.4.2), 12.5 and 12.6 are strongly related to the scandium recovery from mining waste [42]. Table 2 presents the targets related to the present thesis and their relation with scandium source studied.

The flowchart for scandium recovery from bauxite residue proposed in this thesis is presented in Figure 2. First, the bauxite residue is leached by H_2SO_4 or H_3PO_4 for scandium extraction generating a leach residue rich in SiO_2. In the present study, it was identified the possible use for the construction sector [43,44], titanium recovery [45], or production of zeolites for wastewater treatment [27,46].

For the sake of optimized leaching conditions in both H_2SO_4 and H_3PO_4 leaching was: 20% of acid concentration, solid-liquid ratio equals to 1/10, 90°C and 8h. The rare earth content varies from 2.4mg/L (scandium) to 27.6mg/L (cerium). The main elements in the solution are iron (up to 11,000mg/L) aluminum (up to 6,000mg/L) and sodium (up to 3,100mg/L). Calcium content differs according to the leaching agent, as a part of the element precipitates in the H_2SO_4 leaching as sulfate. The H_3PO_4 leached more silicon than H_2SO_4 – 454mg/L and 7.4mg/L, respectively – as well as titanium – 312mg/L and 200mg/L.

Table 2: The Sustainable Development Goals related to the scandium sources studied

SDGs	targets		bauxite residue	silicate ore
7	7.2	By 2030, increase substantially the share of renewable energy in the global energy mix 7.2.1 Renewable energy share in the total final energy consumption	X	X
	7a	By 2030, enhance international cooperation to facilitate access to clean energy research and technology, including renewable energy, energy efficiency and advanced and cleaner fossil-fuel technology, and promote investment in energy infrastructure and clean energy technology	X	X
8	8.2	Achieve higher levels of economic productivity through diversification, technological upgrading and innovation, including through a focus on high-value added and labour-intensive sectors	X	X
	8.4	Improve progressively, through 2030, global resource efficiency in consumption and production and endeavour to decouple economic growth from environmental degradation, in accordance with the 10-Year Framework of Programmes on Sustainable Consumption and Production, with developed countries taking the lead	X	
9	9.2	Promote inclusive and sustainable industrialization and, by 2030, significantly raise industry's share of employment and gross domestic product, in line with national circumstances, and double its share in least developed countries	X	
	9.4	By 2030, upgrade infrastructure and retrofit industries to make them sustainable, with increased resource-use efficiency and greater adoption of clean and environmentally sound technologies and industrial processes, with all countries taking action in accordance with their respective capabilities	X	
	9.5	Enhance scientific research, upgrade the technological capabilities of industrial sectors in all countries, in particular developing countries, including, by 2030, encouraging innovation and substantially increasing the number of research and development workers per 1 million people and public and private research and development spending	X	X
	9b	Support domestic technology development, research and innovation in developing countries, including by ensuring a conducive policy environment for, inter alia, industrial diversification and value addition to commodities	X	
12	12.2	By 2030, achieve the sustainable management and efficient use of natural resources	X	
	12.4	By 2020, achieve the environmentally sound management of chemicals and all wastes throughout their life cycle, in accordance with agreed international frameworks, and significantly reduce their release to air, water and soil in order to minimize their adverse impacts on human health and the environment	X	
	12.5	By 2030, substantially reduce waste generation through prevention, reduction, recycling and reuse	X	
	12.6	Encourage companies, especially large and transnational companies, to adopt sustainable practices and to integrate sustainability information into their reporting cycle	X	
	12a	Support developing countries to strengthen their scientific and technological capacity to move towards more sustainable patterns of consumption and production	X	

The economic analysis shows scandium as responsible for at least 95% of the solution's economic value, followed by zirconium (up to 3%) and neodymium. Comparing the costs of leaching agents, which are similar [47], the leaching with H_2SO_4 achieved the most valuable solution, which was further studied.

Separation steps are necessary for obtaining of high-pure products. It is proposed here zirconium recovery using Alamine 336 in kerosene as first step, where the best conditions were: 10% of organic extractant, A/O ratio equals to 1:1, at 25°C for 15min under stirring. All zirconium was extracted with co-extraction of aluminum and iron. Stripping using 0.25mol/L of Na_2CO_3 was enough for high-pure zirconium solution without impurities (A/O ratio equals to 1:1, at 25°C for 15min under stirring).

Results indicated Cyanex 923 as the best organic extractant for scandium separation. Scrubbing using HCl 5mol/L is required for contaminants removal from the organic phase, where the scandium losses were negligible (0.1%). Stripping step using H_3PO_4 5mol/L recovered all scandium from the organic phase.

Mass balance demonstrated that scandium extraction reached 92% of efficiency, while zirconium was 25% as co-product. Considering 100 tons of bauxite residue, an amount of 4kg of scandium and 31.9kg of zirconium may be produced. Considering the production of scandium oxide or fluoride, the process would generate up to US$ 46,626 or US$ 1,940,980, respectively.

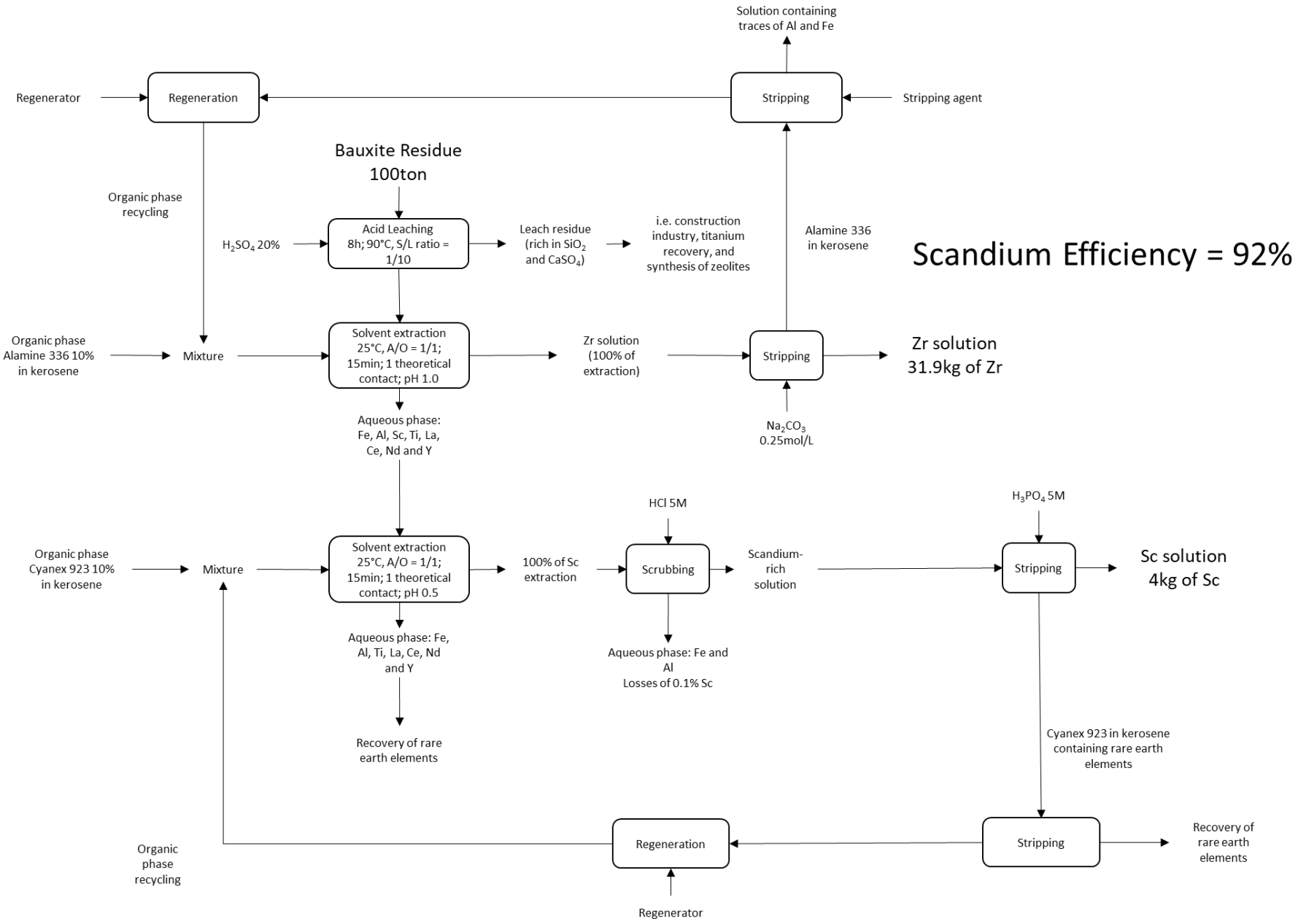

Figure 2: Flowchart proposed for scandium and zirconium recovery from bauxite residue by leaching-solvent extraction

1.2. TECHNICAL CONTRIBUTION

The extraction process of scandium from bauxite residue represents one of the most challenges owing to the synthesis of silica gel [48], which difficult the solid-liquid separation and causes losses of valuable elements, and separation step, where the Fe/Sc concentration ratio would make the process technical unfeasible [49,50].

The literature reports two main routes for scandium obtaining: pyrometallurgical and hydrometallurgy. The first focus on aluminum and iron extraction previous acid leaching for scandium extraction. Despite removal of the main contaminants would improve the separation step, the slag contains high silica content resulting in silica gel formation in the acid leaching reaction. Also, the extraction rate for scandium reaches up to 80% [51].

Sulfation followed by water leaching would represent a solution for scandium extraction avoiding silica gel synthesis and co-extraction of iron and aluminum. However, energy consumption and losses of sulfuric acid would make the process unfeasible [52].

Direct leaching of bauxite residue has represented the most advantageous technique for scandium extraction. The literature reports extraction rates up to 95% [53]. Despite the silica gel formation into the leach solution described in the literature [48,54], this thesis demonstrated that it is avoided after 8 hours of reaction. While Alkan et al. (2018) proposes the use of H_2O_2 to suppress its synthesis, the results demonstrated that it has no significant effect in the process.

Among the problematic of scandium separation from the solution, the use of Alamine 336 for zirconium removal has shown crucial for scandium recovery, since phosphinic acid extractants has selectivity for zirconium. Further, Cyanex 923 separated all scandium from the solution and scrubbing using HCl 5mol/l would be useful for contaminants removal with negligible scandium losses (0.1%). Stripping with H_3PO_4 5mol/L achieved better results than reported in the literature. For this reason, the present thesis has substantial technical benefits.

2. LITERATURE REVIEW

The literature review had carried out in three different databases: ScienceDirect, Web of Science (or Web of Knowledge), Scopus, and Taylor and Francis online. It was used the following keywords:

i. “scandium” AND “waste”;
ii. “scandium” AND “residue”;
iii. “scandium” AND "recovery”;
iv. “scandium extraction” AND “green technology”;
v. “scandium extraction” AND “clean technology”;
vi. “scandium” AND “ecofriendly”.

The aim of this work is to evaluate the possibilities of scandium recovery routes focusing on sustainable and cleaner production. Insights into the extraction processes of scandium in light of clean technologies have been lacking, such as CO_2 emission, energy consumption, sustainable management of resources, economic growth, scientific innovation, safe work, sustainable production patterns, and hazardous chemicals pollution and contamination.

It was proposed to answer the question: “*Is it possible to have an ecofriendly process for scandium extraction?*”, in order to meet the following United Nations Sustainable Development Goals (SDG): number 7 (*affordable and clean energy*), 8 (*decent work and economic growth*), 9 (*industry, innovation, and infrastructure*) and 12 (*responsible, consumption and production*). As explained by Monteiro et al. (2019), SDGs can contribute to mitigating the negative impacts of mining activities [33]. The choice of those SDGs is related to the economic and sustainable growth of industries by innovation with responsible consumption to minimize the waste generation or reuse.

The Section 2.1 presents the manuscript as published.

2.1. Recovery of scandium from various sources: a critical review of the state of the art and future prospects

A.B. BOTELHO JUNIOR[1]*; D.C.R. ESPINOSA[1]; J. VAUGHAN[2]; J.A.S. TENÓRIO[1]

[1] Department of Chemical Engineering; Polytechnic School, University of Sao Paulo, Sao Paulo – Brazil.

[2] School of Chemical Engineering; The University of Queensland, Brisbane, Queensland – Australia.

ABSTRACT

Scandium is a critical metal in increasing demand for modern technologies, such as light-weight aluminum-scandium alloys. Evaluating current and identifying new sources of the element has become a pressing need in order to provide a reliable and cost effective future supply. As current resources are limited, new sources must be explored with due consideration for the environmental aspects of the mining and processing technologies. The present review considers scandium extraction from three different sources - primary, secondary and opportunities – focusing on clean technologies and eco-friendly processing to achieve goals 7, 8, 9, and 12 of the 17 sustainable development goals of the United Nations. The main scientific databases were explored using keyword combinations. The question “is it possible to have an ecofriendly process for scandium extraction?” - worldwide debated – was answered providing diversified opportunities for scandium extraction, demonstrating that the current development would achieve these goals. Several techniques were explored and compared. As important as technical studies, economic approaches must be deeply evaluated where both acid consumption and downstream refining are equally challenging.

Keywords: Sustainable Development Goals; REEs; recycling; mining tailings; critical metals

Highlights

1. The literature review focused on SDGs number 7, 8, 9, and 12;
2. Hydrometallurgical processing is the main route for scandium recovery towards low CO_2 emission;
3. The supply of Sc and REEs in the next years will be from wastes achieving the circular economy;
4. Sc and REEs are important for technologies to produce clean energy.

2.1.1. Introduction

The rare earth elements (REEs) are considered to be scandium, yttrium and the elements of lanthanide group, which are included together due to their chemical similarity [1]. Among those, scandium is the most valuable (Table 3). Its application in modern advanced technologies are found in light-weight aluminium alloys, where scandium is used as doping agent to strengthen and lighten the alloys for the automobile and aerospace industries, electronic devices, lasers for military and medical purposes, lighting [3], as a key component of certain solid oxide fuel cells (SOFCs) improving the conductivity and lower the operation temperature, and used as a tracer in cruel oil refinery [4,55].

Scandium and all REEs are considered *critical* by the European Union and most countries around the world, such as U.S.A. (U.S. Department of Energy) and Brazil [7–9]. This means that these elements may face supply chain challenges due to several reasons: i) high economic importance; ii) localized resource in limited mining regions; iii) practically irreplaceable in green technologies application; and iv) low recycling rate. For these countries, scandium is deemed extremely important for their development. At the same time, the element has the highest potential for transformative market growth, driving to the necessity of efforts to avoid risks on supply interruption. While the REEs recycling rate is between 3% and 8%, the recycling rate for scandium is zero [17,18]. The criticality of Sc and REEs, future market potential and low recycling rates highlights the need to search for and invest in recycling technologies in addition to new sources and more efficient primary extraction and refining methods.

Table 3: Examples of rare earth element (oxides) price in US$/kg [3,5,6]

Compound	Price (US$/kg)
CeO_2	2
La_2O_3	2
Nd_2O_3	47
Y_2O_3	3
Pr_6O_{11}	75
Sm_2O_3	6
Gd_2O_3	24
Dy_2O_3	180
Sc_2O_3	3,800

The main scandium resources worldwide are in Australia, Canada, China, Kazakhstan, Madagascar, Norway, the Philippines, Russia, Ukraine, and the USA while the main producers are China (66%), followed by Russia (26%) and Ukraine (7%) [17,22]. Due to limitation of scandium sources in a few regions, and also owing to the market crisis in 2011 [23–25], researchers have been looking for new sources, mainly for scandium.

In Australia, several mining companies are in various stages of development for new scandium supply. The Nyngan project in New South Wales is under development, where the reserves are estimated in 590 tonnes of scandium (155ppm of Sc) from 1.44 million tonnes of ore. It is expected to produce 39 tonnes per year of scandium oxide starting in 2020. The Syerston project, also in New South Wales, is under development, which contains 19,200 tonnes of scandium (300ppm). In Queensland, the Scandium-Cobalt-Nickel (SCONI) Project was finishing its economic feasibility study, which expects to obtain 3,000 tonnes of scandium from 12 million tonnes of mineral resource (162ppm) [22].

Associated with the availability of scandium, environmental issues related to the extraction processes has been concerning all stakeholders and put a focus on using the most sustainable techniques [26–31]. Due to the relatively low grades, a high

amount of waste material would be generated from a scandium ore if no other by-products are produced. Accordingly, the reuse of mining tailings is gaining importance.

Leading with all those aspects, the United Nations (the U.N.) released 17 Sustainable Development Goals (SDG) to be achieved by 2030 [32], which focuses on objectives on three dimensions of sustainable development which are to achieve global peace, justice, and international collaboration:

4) Economic development;
5) Social inclusion;
6) Environmental sustainability

The same approach can be applied in mining and metal processing industries, considering aspects of safe work, social issues, economics and the environment [33]. Nonetheless, it is well known that extractive activities are considered non-renewable. Thus, scientific and technical developments are carried out in order to make the processing more ecofriendly with respect to environmental issues such as tailings volume and toxicity; energy use and CO_2 emissions as well as the impacts of reagents in the extractive processing stages.

To facilitate future scientific and technical developments, the literature for scandium recovery from several sources is reviewed and presented with a discussion of future opportunities. The general processing route considered was using hydrometallurgy (aqueous media), due to the environmental benefits and costs when compared with pyrometallurgy for low grade ore. The review focused on research articles from scientific journals published between 2008 and 2020.

2.1.2. Review methodology

In the present work, a systematic review [33,56–59] is carried out based on a formulated research question: "*Is it possible to have an ecofriendly process for scandium extraction?*", in order to meet the following United Nations Sustainable Development Goals (SDG): number 7 (*affordable and clean energy*), 8 (*decent work and economic growth*), 9 (*industry, innovation, and infrastructure*) and 12 (*responsible, consumption and production*). As explained by Monteiro et al. (2019), SDGs can contribute to mitigating the negative impacts of mining activities [33]. The choice of

those SDGs is related to the economic and sustainable growth of industries by innovation with responsible consumption to minimize the waste generation or reuse.

The aim of this work is to evaluate the possibilities of scandium recovery routes focusing on sustainable and cleaner production. Insights into the extraction processes of scandium in light of clean technologies have been lacking, such as CO_2 emission, energy consumption, sustainable management of resources, economic growth, scientific innovation, safe work, sustainable production patterns, and hazardous chemicals pollution and contamination.

Processing from three different resources (topics) was evaluated: primary (as main source), secondary (as co-product) and possible opportunities (future commercial sources). The search for this review was focused on hydrometallurgical techniques: leaching, purification (precipitation) and separation (ion exchange techniques). Publications not considering any resource (such as ores, tailings, and residues) were also considered in a different section (no-classifications).

The research strategy was to search for relevant scientific papers published in journals using most recognized academic databases: ScienceDirect, Scopus, and Web of Knowledge, and Taylor and Francis online. Books, book chapters, patents and conference papers were considered to contextualize the topic, but not in research evaluation. The research was performed considering the period of publication from 2008 to 2020.

Six different combinations of keywords were used to achieve a number of publications to answer the question of the present work. The words used are related to scandium extraction in a sustainable approach from different sources. The following combinations of keywords were used:

i. “scandium” AND “waste”;
ii. “scandium” AND “residue”;
iii. “scandium” AND "recovery”;
iv. “scandium extraction” AND “green technology”;
v. “scandium extraction” AND “clean technology”;
vi. “scandium” AND “ecofriendly”.

The search was performed using the “advanced search”. The selection and classification of the processes were divided into three steps: search on the literature using keywords, selection of the extractive process for scandium obtaining from different sources, and the evaluation of processes. Then, the results were filtered by title and abstract, excluding duplicates.

Several criteria were adopted to evaluate the most relevant articles for full analysis: language (English), type of article (original or review) and agree to the theme. The theme must have been defined in title and/or abstract to be considered for full-text analysis. The literature review of all three topics followed the flowchart presented in Figure 3.

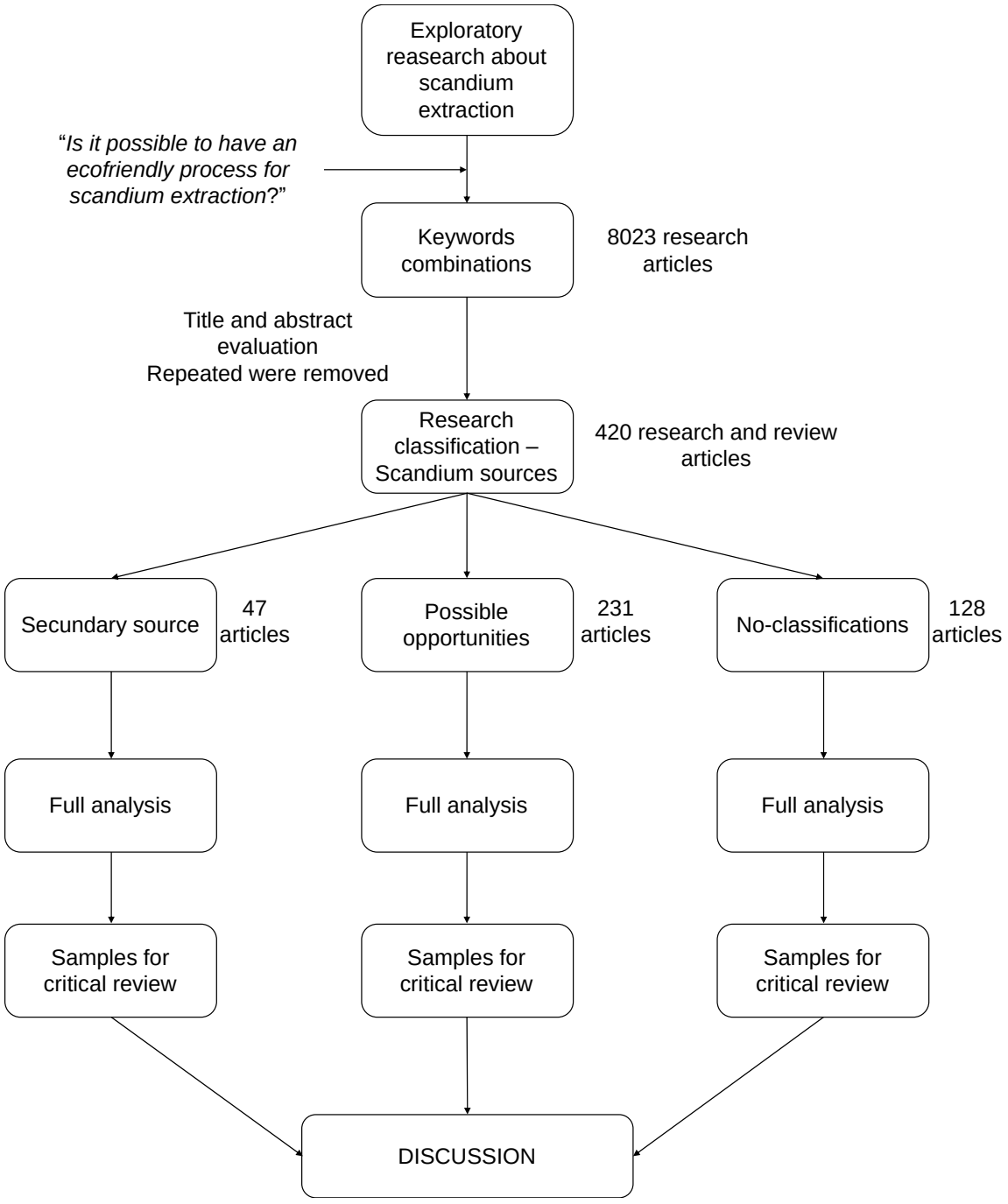

Figure 3: Flowchart of the literature review

An exploratory search was carried out using the listed combination of keywords. The classification was carried out filtering the articles according to the title and/or abstract. Results obtained were classified into three different groups: primary sources, secondary sources and possible opportunities. After that, the remaining articles were entirely evaluated. Those articles were classified considering processing

in aqueous media. Indeed, the articles were assessed if an ecofriendly process was the focus of the work. By to the methodology used in the present study, it was selected examples from each group of sources to be discussed.

2.1.3. Results and discussion

Figure 4 shows the number of publications for three keywords combination (i, ii and iii) from 2008 to 2020 in the databases ScienceDirect, Scopus, Web of Knowledge and Taylor and Francis online. ScienceDirect has the greatest number of publications, followed by Scopus, Web of Knowledge and Taylor and Francis online. It was observed an increase in the number of publications from ScienceDirect using those keywords after 2012. About the other databases, it was also observed a rise in the number of publications, mainly in Scopus and Web of Knowledge, after 2015. The launching of the 17 SDGs occurred in 2015, which contributed to the number of publications about the topic [32,33,60]. The rise of publications in 2011, may be explained due to the REE market crisis.

As for all REE production, China is the main scandium producer in the world, being the largest located in Inner Mongolia called as Bayan Obo with 90% of global scandium production, and it is the second largest deposit of niobium in the world. The main scandium-bearing mineral in Bayan Obo is Aegirine. Other minerals are columbite, Fe-rutile, parasite, tscheffkinite, hamartite, monazite, aeschynite, phlogopite, biotite [55,61].

Scandium is also obtained in Kazakhstan, the Philippines, Russia and Ukraine. New processes have been developed and under production in Australia, the Philippines, Russia and Dalur from different sources in pilot scale [3].

Due to the rise in their extraction allied to the increase in waste and pollution generation, the Chinese government executed policies to control the rare earth market (from exploration to sale). In 2010-2011, the government drastically reduced the export quota (40% less than in 2009). As a result, it impacted directly the relationships with other countries, for example 70% of the imports into the USA comes from China [62].

Later, the Chinese government abolished the quotas in 2015, however, an alert had already been sent about the risks of REE supply restrictions. After the market

crisis caused in 2011, the prices of rare earth elements spiked. Then, countries began to search for different sources of scandium to limit the reliance on China by developing several projects to obtain rare earth metals outside China [63]. As scandium is one of the most valuable REEs, it has been the focus of projects developed by many countries and companies.

The increased demand for metals for electronic equipment requires metals extraction to support it, which would be carried out by mining extraction and recycling process [64]. The extraction of REE will expand in the near future, and so will scandium demand [65].

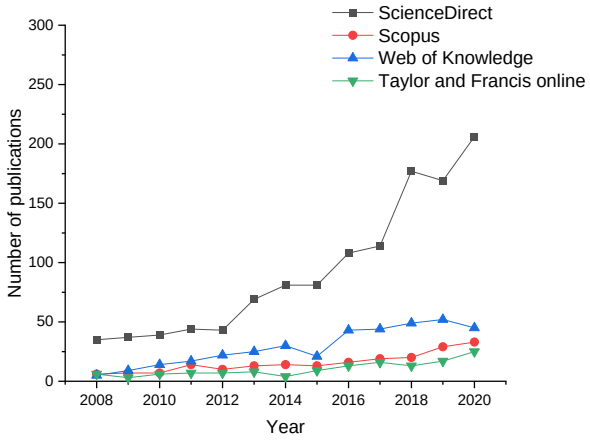

a)

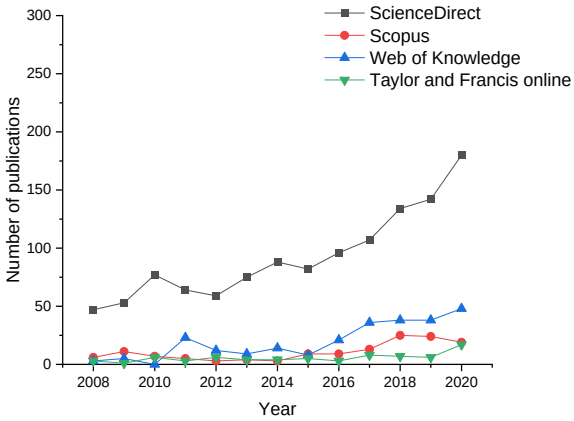

b)

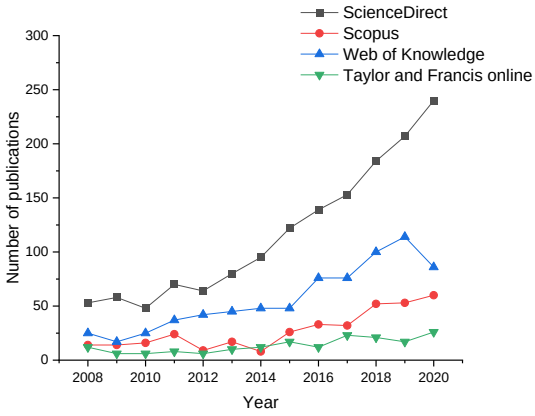

c)

Figure 4: Number of publications using the combinations of keywords i-iii from 2008 to 2020 in the databases ScienceDirect, Scopus, Web of Knowledge and Taylor and Francis online: a) "scandium" AND "waste"; b) "scandium" AND "residue"; c) "scandium" AND "recovery".

Figure 5 presents the number of publications from 2008 to 2020 using the keywords iv – vi from ScienceDirect database. Both combinations iv and v showed an increase in the number of publications after 2012, after a period of stabilization. The period 2013 – 2015 had no variation in the number of publications about those topics. Then, after 2015 the number rose. Those numbers corroborate with the analysis depicted before.

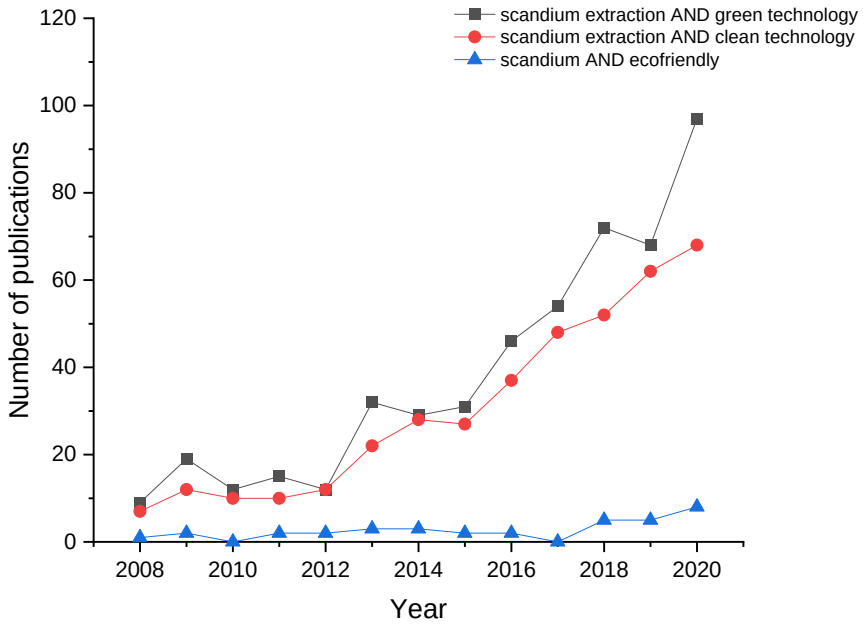

Figure 5: Number of publications using the combinations of keywords iv-vi from 2008 to 2020 in the databases ScienceDirect.

In the Taylor and Francis database, 147 articles were found using the combinations iv and v. The number of publications increased from 2010 to 2013 and then reached the plateau. No data was found using combination vi. The reason to not find publications specifically with the words “scandium extraction” and “green technology” / “clean technology” (using quotation marks) can be interpreted as low interest in extraction processes for scandium obtaining by green and/or clean technologies. Despite that, the articles found were evaluated. In Scopus and Web of Science, only 12 and 7 articles were found, respectively.

The combination of “scandium” and “ecofriendly” resulted in 28 research articles (Figure 5c), a lower number compared with other combinations. It demonstrated that there is an insignificant interest in researches associated with scandium and an eco-friendly process. The search showed, in all keyword combinations, a strong increase in the interest of scandium obtaining, even from waste and residue. Besides Chinese control in REE exportation and the 17 SDGs launched in 2015, global policies have been encouraged to reuse waste materials – not only storage –and to reduce materials losses.

Sustainable consumption and production were the main objectives of European Union Sustainable Development Strategy (EU-SDS). The objective of environmental protection is to safeguard the earth’s capacity to support life. The Action Plans of EU SDS are smarter consumption (to promote knowledge about environmental impacts of products and services), leaner production (to increase process efficiency to reduce material losses) and global action (to support global market for environmental goods and services) [66].

Moreover, the interest in residues from the mining process (tailings) has been growing due to the risks for humans and environmental [67]. Further, the discussion about scandium obtained from different sources is expressed in the following sections.

2.1.3.1. Primary sources

The main primary scandium resources are the thortveitite and lolbeckite ores ($(Sc,Y)_2Si_2O_7$), which contain up to 45% of Sc_2O_3. This scandium silicate-rich ore contains also yttrium, REEs, iron, aluminum, thorium, zirconium, and alkaline earths, which is restricted in quantity and sources. Mine processes from Madagascar and Norway produce scandium from thortveitite, and in the USA it is obtained from thortveitite tailings [19,20].

A process patented by Baptiste (1959) describes scandium extraction by fractionation sublimation in chloride medium, to obtain $ScCl_3$. The process consists of heating to 950°C the ore mixed with a carbon source. Then, dry chloride is passed over the mixture. The sublimation temperature of scandium and yttrium chloride are 967°C and 1507°C, respectively. In the case of cerium and lanthanum, both elements sublimes at 1500˚C and 1747˚C, respectively [21].

Silicon, titanium, aluminum, iron, and zirconium chlorides sublimation temperatures are, respectively, 57°C, 136°C, 180°C, 310°C, and 331°C. The gases go through a refractory tube where the temperature of its downstream does not fall below 400°C. According to the patent, scandium oxide can then be obtained by precipitation using ammonia into the oxide from anhydrous scandium chloride, as well as sodium, magnesium, calcium, or by direct electrolysis of the to molten chloride. In this case, the patents aims the production of metallic scandium [21]. Scandium can also be obtained from thotvellite using ammonia bifluoride at 400°C in a stream of dry air [19]

Minerals with appreciable concentrations scandium are rarely found which make its extraction as primary source limited. It is estimated that only 400kg of scandium is obtained from primary sources, and the remaining 2000kg is obtained as a secondary source [20]. As elucidated before, scandium extraction does not follow processing in aqueous media. Indeed, due to the scarcity of those minerals, the focus has been to identify resources that can be used as secondary resources of scandium. However, minerals containing scandium-grades that justify its extraction are rare, limited and do not found spread, but concentrated in a few parts of the ores.

Substantially, since the global market is currently small and predicted to increase in the coming years, there will be a greater need for primary production in the foreseeable future. As discussed before, new sources of scandium will be needed to meet the growing demand.

The keywords search did not yield publications about the primary scandium resources. For this reason, it can be inferred that scandium extraction from thortveitite and lolbeckite ores are not considered “sustainable” and “ecofriendly”. Also, the search focused on “waste” and “residue” in order to reach the SDGs 8, 9, and 12.

2.1.3.2. Secondary sources

Scandium production as a secondary source is currently carried out in China (iron ore, REE, titanium, and zirconium), Kazakhstan (uranium), Russia (apatite and uranium) and Ukraine (uranium). In India, a plant construction awaits environmental approval. Philippines, Russia, and Danur are expect to produce scandium from, respectively, nickel, aluminum, and uranium sources [3]. Studies involving the

scandium extraction from other resources have considered as possibilities, as explained below.

In the present review, publications involving the following as secondary sources were included: REE (and also from Bayan Obo mine), Fe, Ti, Fe-Ti, Zr, U, apatite, W, Th, and ferrocolumbite. It was considered from Bayan Obo which is discussed separately from other REE mines due to its importance. The search using all keywords has shown that, among the 47 publications classified, 83% were research articles and 15% were paper reviews. Only one publication was about economic/policy aspects.

Among the publications found about scandium recovery from secondary sources, 70% were related to ores and 30% about residues (where it is obtained as co-product). It was also classified the manuscripts into 6 groups: characterization (33%), in situ recovery (2%), leaching (16%), separation (28%), concentration (12%) and process (leaching+separation – 9%). The higher percentage of publications considering characterization may indicate the search for new secondary sources of scandium from mining processs, and separation techniques due to the challenges to separate from high concentration of impures and also to obtain a pure product.

Figure 6 shows the percentage of each resource found in the literature review considered as secondary. About 38% of publications evaluated the scandium extraction from REE source, as well as Bayan Obo (5%), the largest REE resource in the world [61] because scandium has found always associated with these elements. Moreover, studies of scandium extraction from uranium, titanium, iron, tungsten, thorium, and apatite, for instance, indicate that there is a great interest in these resources or wastes to supply the metal market.

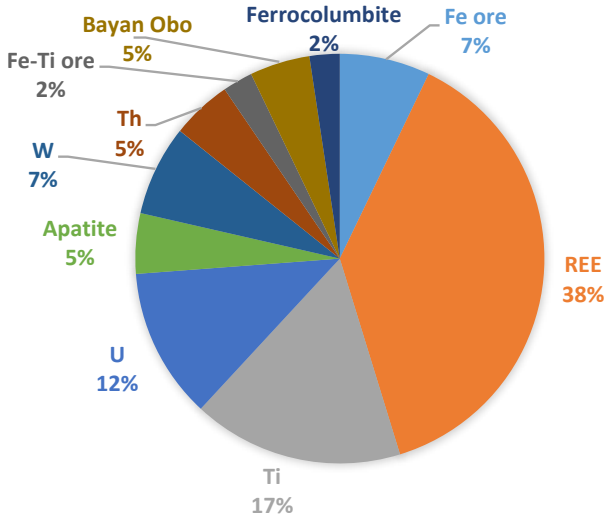

Figure 6: Percentage of publications found in literature review classified as secondary resources

Seredkin et al. (2016) studied the exploration, environmental problems and economic aspects of in situ recovery of several elements from uranium deposits, being one of them scandium (up to 3ppm). The authors have discussed both economic and extraction aspects of in situ extraction, and a deep discussion about scandium by itself was not performed [68]. Concentration steps can be carried out in order to upgrade or selective recover scandium after uranium extraction. Undoubtedly, this scandium content represents a challenge to recover cost-effectively, and for this reason its obtaining may not be considered.

The publications about secondary resources were divided into three parts: characterization, leaching and concentration, and solvent extraction/ion exchange resin studies. About the materials studied, 57% were about ores and 30% were about scandium extraction from residues. Further, 4 papers explored concentration techniques to increase scandium content. Characterization studies consisted of 36% of publications, 14% were about leaching, and 25% about separation using the ion-exchange technique (solvent extraction and ion exchange resins). Detailed information is presented in Table 4 and Table 5. Also, the SolvEx process would be used for scandium obtaining, but Izatt et al. (2009) states that the technology is very sensitive to scale up and operational control, and the process has not been proven on a large scale basis yet [69].

The data obtained showed that comparing the number of publications about leaching and ion exchange techniques, it can be inferred that there is more interest in obtaining a high-purity scandium solution through separation techniques than the leaching process itself. Scandium can be leached in acid conditions (pH below 4), as well as iron, titanium, aluminum, and several contaminants [70]. For this reason, while developing an innovative process for leaching of scandium-bearing material, a selective separation from a solution that supports high-contaminants content should be evaluated. As a result, the number of publications about separation is higher than leaching.

Table 4 summarises characterization studies from different resources containing scandium, which can range from 5ppm [71], in REE deposit, to 3.5wt% [72], in the Bayan Obo deposit, being the latter varying according to different mineral phases and which is not well distributed in the ore.

Comparing both REE deposits, scandium concentration is not even similar. Cui & Anderson (2017) described a deposit from the USA (Bear Lodge Project) with scandium-content up to 165ppm, while Smythe et al. (2013) reported a REE ore with 5-6ppm scandium. Thorium resources have scandium, but both publications didn’t mention the graded. In niobium ores, scandium content can vary from 0.022 - 0.032wt.% (Brazil) to 0.057wt% (Tomtor).

Table 4: Publications considering the characterization of secondary resources

	Resource	Sc concentration	Reference
In situ recovery	Uranium deposits	0.2–1mg/L in the pregnant leach solution; 2.5–3 ppm for cut-off grade	[68]
Characterization	REE - The Bear Lodge Project (EUA)	165ppm	[73]
	REE - Not informed	5 - 6ppm	[71]
	REE - Quebec	51ppm	[74]
	REE - alkali-carbonatite deposits	8-435ppm (Sc_2O_3)	[75]
	REE - allanite	24ppm	[76]
	REE - monazite	15ppm	[77]
	Apatite - Kovdor baddeleyite-apatite-magnetite deposit	up to 780ppm (Sc_2O_3)	[78,79]
	Bayan Obo	0.34 – 3.45wt% (Sc-bearing aegirine); 0.00 – 0.04wt% (Sc-free aegirine); 2.82 – 3.64wt% (“Perrierite-(Ce)); 0.20 – 0.25wt% (Sc-bearing ferrocolumbites (TS-16)	[72]
	Nb / Nb-Fe	Brazil: 0.0219 - 0.0322wt.% (Sc_2O_3); Tomtor deposit: 0.057wt.% (Sc2O3)	[80,81]
	Thorium	Not reported	[82,83]

Table 5 shows the scandium content, leaching parameters, and extraction efficiency of studies found in the literature review. Scandium concentration, as presented, varied from 40ppm (Fe-Ti residue) to 2.1wt% (U-REE). The leaching agents explored were sulfuric acid (H_2SO_4) and hydrochloric acid (HCl), being the first the most common for industrial applications. Moreover, according to Zhang et al. (2013), HCl is commonly used due to the scandium trichloride formation, which is easily separated from impurities throughout the leaching process [84].

Table 5: Publications considering scandium content and leaching of secondary resources

	Resource	Sc concentration	Leaching conditions explored	Leaching process with high-scandium extraction	Sc recovery (%)	Reference
Leaching	Fe-Ti residue	40 - 100ppm	H_2SO_4 300g/L, S/L = 1/7; 95°C for 5hr. Samples were machined in: AGO-2U planetary-centrifugal activator; Pulverisette 5 planetary ball mill; Aktiva-tor-2SL activator.	Pulverisette 5 planetary ball mill Leaching conditions as expressed before	85-95%	[85]
	REE - silicate	0.006wt%	H_2SO_4 dosage (0.125mL - 2.5mL/g ore); 15-24h; 70-300°C; S/L = 1/20 - 1/70	H_2SO_4 dosage 1.875mL; 15h; 200°C; 1/30	492µg/L	[86]
	Bayan Obo tailings	0.0085wt% and 0.03wt% (Sc_2O_3) before roasting-magnetic separation;	H_2SO_4: 6-18mol/L; 80-300°C; S/L = 1/1-1/8.	18mol/L; 245°C; S/L 1/4;	96%	[87]
	Nb ore concentrate	0.95wt%	HCl 33%; S/L = 1/1.8-1/2.2; 60-100°C;	S/L = 1/2.2; 100°C	97%	[88]
	Nb residue - non-magnetic	120ppm	H_2SO_4-SO_2; T = 95°C; 0-8g activated carbon; S/L = 1/3-1/4.6; 0-24hr; SO2: 10-65NL/hL and to reach 200mV;	6h; 4g activated carbon/kg of ore; 850g H_2SO_4/kg of ore;	Sc extraction was not reported: 10% REE losses (inclusion in geothite phase)	[89]
	U-REE and its tailings, Elliot Lake	1.5wt% - 2.1wt%	-	H_2SO_4 60-80g/L; 75°C; 48hr	>90% REE (Beneficiation)	[90,91]

Cont. of Table 5.

	Resource	Sc concentration	Technique	High scandium concentration	Increase in concentration	Reference
Concentrate	REE ore	48.9ppm	Magnetic separation - magnetic field: 72–900 kA/m; particle size: 70-90mm	particle size: 0.074mm; magnetic field: 1450kA/m	314.89ppm and 77.53% of recovery	[92]
	Fe ore	343.2ppm	particle size distribution (grindind) + magnetic separation: classification - 10-40µm; grinding time: 4-10min; magnetic field: 0.06-0.9T	grinding time: 6min; particle size: <74µm; 0.9T	71.3ppm and 55.62% of recovery	[93]
	Fe ore	55.72ppm (Sc_2O_3)	Shaking table + magnetic separation - feeding concentration: 15-23wt%; feeding quantity: 10-13L/min; stroke frequency: 250-325times/min; stroke: 13-19mm	feed concentrate: 18 wt%; feeding quantity: 11 L/min; stroke frequency: 275 times/min; stroke: 17mm.	83.1ppm and 79.5% of recovery	[94]

Li et al. (2019) reported that HCl leaching efficiency is higher than other inorganic acids, indicating the strong high solubility of HCl for hydroxides. The authors studied a precipitate from KOH sub-molten salt leaching cake of fergusonite [88], where the precipitation occurs in aqueous media [95]. Indeed, as shown by Shimazaki et al. (2008), scandium is presented in secondary resources mainly as silicate, and studies reported in the literature have shown that scandium extraction can reach more than 95% using H_2SO_4 or HCl by leaching process.

Both Stepanov et al. (2018) and Zhang et al. (2013) studied scandium extraction from Fe source (Fe-Ti residue and Fe ore, respectively), where scandium content ranged from 40 to 122ppm. Iron, silicon, and titanium concentrations were strictly similar - around 7%, 17%, and 0.4-1%, respectively. In both studies, the scandium recovery was almost the same using different leaching agents, reaching up to 95%.

A few concentration techniques were also explored, such as magnetic separation and shaking table followed by magnetic separation. Indeed, scandium content can increase due to the fact that it is associated with iron oxides [96], and high magnetic fields must be applied considering most of all these oxides which trapped scandium. Studies depicted in Table 5 have shown that magnetic separation concentrated scandium, achieving almost 80% of recovery.

2.1.3.3. Possible opportunities

In order to increase the possibilities for obtaining scandium, several new sources are considered in the present review. About 128 manuscripts were found in the search, where 82% of publications were research articles and 14% were review articles. Possible scandium sources were divided into the following groups: bauxite residue or red mud (RM); waste electrical and electronic equipment (WEEE); nickel laterite (Ni); municipal wastes (MUN); phosphogypsum and phosphate rocks (Pho); coals and fly ashes (Coal) and others (Others).

Figure 7 shows the percentage of each group considered as an opportunity. Indeed, the interest in scandium extraction from bauxite residue is greater than all groups. It occurs due to two main reasons: first, the volume of waste material produced in the world achieved 4 billion tonnes in 2015, which have been considered an

important source for many elements, not only scandium; second, the content of rare earth elements presented in bauxite residues are considered enough to deserve consideration for potential by-product recovery [20,34].

Nickel laterite ore is already known as a scandium source. Coal and fly ashes, phosphogypsum and phosphate rocks, and municipal wastes have also shown to be potential sources of scandium. In the group analyzed as others, there are the following sources: Russian Arctic, copper mining, Rödberg mining, petroleum/shales, tin mines, Tomtor deposit, and the Pacific Ocean. Excluding papers that evaluated pyro- + hydrometallurgical processing (Figure 8), 42% were considered as examples of materials characterization where scandium was determined.

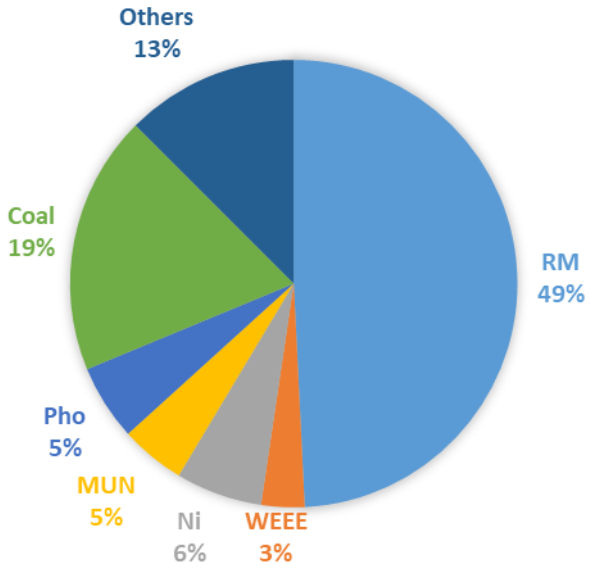

Figure 7: Percentage of publications found in literature review classified as opportunity. Pho = phosphogypsum and phosphate rocks; WEEE = waste electrical and electronic equipment; RM = bauxites, Bayer process and red mud/bauxite residue sources ; MUN = municipal wastes.

The literature review has shown that focus has been mainly about the characterization of materials focusing on metals recovery, followed by leaching (20%) and separation techniques – purification (5%), ion exchange resins (7%), solvent extraction (7%), ionic liquid (6%), and membranes (1%), as depicted in Figure 8. For this reason, further discussions are divided into areas.

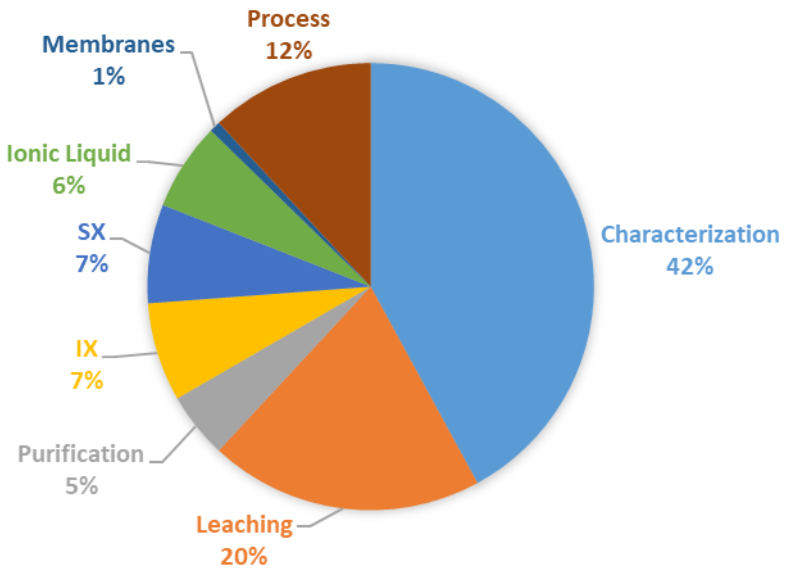

Figure 8: Breakdown of publications found in literature review classified as opportunity – excluding pyro and pyro+hydro processing. IX = ion exchange resins; SX = solvent extraction.

2.1.4. Scandium recycling opportunities and recovery from unconventional sources

It was observed in the literature review an increase interest in different options for scandium obtaining, from electronic devices to mining wastes unexplored. Table 6 presents examples of scandium content in WEEE, nickel laterite, municipal wastes, phosphogypsum and phosphate rocks, and coal and fly ashes.

Kohl & Gomes (2018) evaluated desktop computers without the screen, collected in a Brazilian university, for recycling potential study. Scandium was detected as trace element in motherboards and processor sockets, and all trace elements content is lower than 5% [97]. Priya & Hait (2018) studied sixteen printed circuit board (PCB) samples and scandium concentration ranged between 6 and 31ppm. According to the authors, information technology and telecommunication equipment PCBs were the most abundant in terms of scandium and REE content [98], where it is used in processor socket of motherboards [97].

Considering all the factors involved in scandium obtaining, those PCBs might be considered in the future a secondary resource of this element. However, the recycling process must consider other trace elements to make it feasible. For scandium and REE, maybe it would be possible obtaining an REE concentrate, not them separated, due to the low content. Moreover, mechanical separation (as well as manual separation) increases metal content and facilitates the processing [99].

Thejo Kalyani & Dhoble (2015) have shown that scandium and all REE are used in OLEDs because they have very sharp emission spectra and for this reason, ideal as red-light emitting materials and display devices, providing highly monochromatic light-emitting diodes and displays [100].

The main challenge with metal recovery from municipal waste is the collecting and segregating the post-consumer waste and inhomogeneity of metals content, which can be seen in Table 6, where scandium content varied from 0.1 to 20ppm, which may not be considered as a scandium source. As a matter of fact, metals recovery from urban mining may be carried out from WEEE associated with valuable metals recovery (e.g. copper, gold, silver, and tin).

Scandium can be also found also in nickel laterite resources from New Caledonia [101,102], Cuba and Dominican Republic [103]. In Ni-Co ores, scandium content is up to 100ppm, which might result in future exploration associated with nickel and cobalt extraction, making nickel laterites also a scandium resource.

Saadaoui et al. (2017) have shown that there is scandium in phosphogypsum and phosphate rocks [104]. Samples analyzed by Cánovas et al. (2018) from Spain have 15 – 386ppm of scandium [105]. However, their use as a scandium source is restricted by its scarcity and lack of reliable supply, as mentioned by Chen & Graedel (2015).

Furthermore, the search for new REE sources found coal and fly ashes as a future possibility. Scandium content on these sources varies from 0.5 to 297ppm; also, REE content might reach 1220ppm [106]. As most of the sources considered here as an opportunity, metal concentration is not homogeneous.

Table 6: Examples of scandium content from sources considered as an opportunity

Resources	Locality	Sc content	Observations	References
Waste Electrical and Electronic Equipment	Brazil; India	<5%; up to 33pm	- Brazil: WEEE discharged at university (Rio Grande do Sul) - India: 16 end-of-life EEE under WEEE categories as information technology and telecommunication equipment, large household equipment, consumer equipment, and lighting equipment.	[97,98,100]
Nickel laterite	Australia, New Caledonia, and Cuba and the Dominican Republic	1 - 1504ppm	- Scandium was found scattered in Australian laterites: 1 - 1504ppm - Ni-Co laterite in New Caledonia: up to 100ppm - Cuba and Dominican Republic: Moa Bay: 8 - 98ppm; Loma Caribe: 55.6 - 87ppm.	[101–103,107]
Municipal wastes	Italy; Switzerland; the Democratic Republic of the Congo; UK; Romania	0.1 - 19.7ppm	- Samples from waste incinerator plants - Landfills from the UK; - Ashes from power plants from Australia, Brazil, China, India, Bulgaria, Germany, the UK, and the USA.	[108–113]
Phosphogypsum and phosphate rocks	Spain	15 - 386ppm	-	[104,105,114]
Coal and fly ashes	USA; China; South Africa; Canada; Colombia; India; Russia; Korea; Turkey; and Finland	0.5 - 297ppm	Lower than 100ppm and not homogeneous	[106,115–123][124]

Table 7 shows examples of scandium content in bauxite residue. As previously established, bauxite residue is the main material where has been considered as possible scandium and REE future resource. Scandium content can reach more than 120mg/kg in the waste material. As sources with concentration range 20 – 50mg/kg are considered as resources of scandium, bauxite residue has shown as a strategic material for its obtaining.

For instance, scandium content in bauxite residue of BAZ (RUSAL) aluminum plant is 0.009% [125]. Gentzmann et al. (2021) also identified scandium in Russian bauxite residues: North Ural (102mg/kg) and North Timan (70mg/kg). Scandium content from Germany, Greece and Hungary were 57mg/kg, 99mg/kg and 94mg/kg, respectively [126]. Several REE is also presented in the bauxite residue, but scandium by itself represents 95% of economic value of all rare earth elements in the waste [127].

As stated by Wang et al. (2011), scandium is commonly associated with aluminum sources in nature, and after the Bayer Process for alumina extraction, scandium is almost doubly enriched in the bauxite residue [20]. Vind et al. (2018) showed that its concentration in the Bayer liquor is lower than <0.05mg/L In the process, the alkaline leaching of bauxite precipitates iron, which traps scandium, which is mainly hosted in hematite and goethite structures. Furthermore, the pH of the bauxite residue is up to 12-14, which causes a high acid consumption in the acid leaching process for metals recovery [54,96,128,129].

Additionally, the amount of bauxite residue around the world achieved 4 billion tonnes, and considering scandium content of 50-100mg/kg, it indicates that there are about 200,000 tonnes of scandium presented in this residue, where Sc_2O_3 may cost around US$ 3,800 per kilogram, but it needs US$ 500 per kilogram of production costs [3]. The literature review indicates that the scandium content in the bauxite residue is more homogeneous than all sources presented here as opportunities, making this source important and strategic. Many different resources have been considered as sources of scandium, such as tin ore (5.2 – 238mg/kg) [130], Tomtor deposits (0.05 - 0.14%wt.) [131,132], the Pacific Ocean (<130ppm) [133], and those were scandium content is up to 20 ppm or lower, in which there is no economic viability for its extraction [134–141].

Table 7: Examples of scandium content in bauxite residue

	Resource	Locality	Sc concentration	Observations	References
Characterization	Bauxite residue/bauxite /Bayer process	Greece	130mg/kg	Sample from Greece	[142]
		China, Brazil, and Ghana	7.0 - 97.6mg/kg	Samples from China, Brazil, and Ghana	[37,143]
		Italia	16-110mg/kg	Samples from southeast of Italy and from Sardinia	[144]
		Europe	43-60mg/kg	Samples disposed of different years in industries of Europe	[145]
		Greece	<0.05 mg/L	Scandium content in Bayer Liquor	[128]
		-	86-135mg/kg	Bauxite residue and non-mag material prepared by reductive roasting-magnetic separation process of bauxite ore residue	[146]
		-	100mg/kg	Samples from filter press	[147]
		Russia	30mg/kg and 102mg/kg	Metals content from bauxite residue after a previous treatment	[148]
		Turkey	No data for scandium	Sample from Turkey compared with the literature	[149]
		China	55mg/kg - 116mg/kg	Samples from China	[150,151]

2.1.4.1. Leaching

Table 8 shows examples of leaching studies for scandium recovery from bauxite residue. Pre-treatment using high temperatures (pyrometallurgy) were not considered. For instance, Deng et al. (2018) studied the scandium recovery from bauxite residue after iron, aluminum, and silicon removal, which occurred by reductive roasting at 1100°C with sodium salts and low-intensity magnetic separation with 0.1T. Leaching experiments were carried out using phosphoric acid (H_3PO_4) which reached 90% of scandium extraction [152]. The use of high-pressure leaching has also been considered from bauxite residue after iron removal using coke at 1500°C. Scandium extraction reached 95% [153]. Further studies here presented considered a direct leaching process of bauxite residue.

Before acid leaching for metals recovery, a hydrometallurgy approach for alkalinity reduction of bauxite residue has explored. Li et al. (2017) studied sodium removal from the residue using citric acid. The main goal was the alkalinity decreasing to reduce acid consumption on the leaching process. The authors showed that 95% of sodium was removed [154]. A similar achievement was obtained using different approaches where the sodium could be recycled to the bayer process in its alkaline form, NaOH [155].

It is possible als the used CO_2 to reduce the alkalinity of bauxite residue. Details are presented in Table 8. The results achieved by the authors showed that the pH of the residue decreased where hydroxide ions were converted to carbonate, but the neutralization process stabilizes silicate compounds. Moreover, the leaching of neutralized bauxite residue showed a decrease of 20% on aluminum, iron, and titanium leaching, and less acid consumption. However, scandium recovery was lower compared with raw bauxite residue, maybe due to its chemical association between iron and titanium [156].

Borra et al. (2015) studied alkalinity removal by water washing, resulting in 10-15% of sodium extraction after four steps. The low efficiency may be due to the fact that sodium is present as insoluble aluminosilicates, and it has been demonstrated not to be efficient [157]. For scandium leaching, several reagents were explored for bauxite residue, and HCl has shown the best leaching agent among all studied. It might occur

because it is more selective than H_2SO_4 as demonstrated by Zhu et al. (2018), where impurities extraction, mainly iron, is lower when compared with H_2SO_4 [158].

Zhou et al. (2018) evaluated EDTA on scandium recovery from bauxite residue with HCl, enhancing its extraction from 60% (without EDTA) to up to 80% (using EDTA). Moreover, it was possible to use less acid and increase scandium extraction efficiency. Leaching using 40% of HCl increased scandium extraction from less than 10% to 80% using ($HCl+H_2O$):bauxite residue:EDTA equals to 40mL:10g:2g, at 70˚C over 4h [159]. Likewise, EDTA may also be impractical for large scale on industrial applications due to reagent costs, even considering the reagent recycling.

For industrial applications, when compared with HCl, it can be preferable to work with H_2SO_4 due to the low price and safety due to: i) materials of construction possibilities are limited when HCl is used; and ii) at elevated temperature HCl vapour is released coming off the top of the vessesls causing general corrosion problems around the operation. Borra et al. (2015) evaluated different mineral and organic acids. The efficiency of using organic acids was lower than mineral acids, even at high temperatures [157]. Also, the REE leaching varies according to the mineral acid used, due to their association with the leaching agents, ionic radii of the elements, and possibly tendency for complexation stabilizing in solution or acid strength.

The use of H_2SO_4 resulted in high scandium recovery from bauxite residue, even at low temperatures, may be increased as the temperature increases; otherwise, it enhances iron extraction resulting in a non-selective process [160]. Ochsenkuehn-Petropoulou et al. (2018) evaluated multi-step leaching for scandium recovery from Greek bauxite residue. Despite the increase in scandium recovery, it caused great reduction in scandium concentration due to the use of fresh leaching agent to react with bauxite residue over and over. It must increase the costs of further separation process to recover low scandium content, which in this case may reach ppb concentration [161].

One of the most considerable challenges to be overcome is silica gel formation, which decreases scandium leaching efficiency trapping part of the liquor obtained in the leaching, as demonstrated by Alkan et al. (2018). A solution to be explored is the use of hydrogen peroxide (H_2O_2) for silica gel suppression favoring the quartz formation. Kinetic studies must be explored deeply to evaluate the mineral

phases formed during H_2SO_4 leaching with and without H_2O_2, in order to evaluate if any phase is still present that may incorporate scandium.

It was noticed that recently only bauxite residue from Greece and China have been studied for direct leaching. Many studies have considered the thermal pre-treatment using mainly for iron and silicon removal, due to high concentration and silica gel formation, respectively. A few examples are bauxite residues from Jamaica [162], Greece [163], and Canada [164].

Table 8: Examples of leaching studies for scandium recovery from bauxite residue

Resource	Location	Sc concentration in solution	Leaching agent	Conditions	Sc extraction	Reference	Observations
Bauxite Residue	Greece	105mg/kg	H_2SO_4	S/L ratio 1/50; 1h; 25˚C	60%	[160]	Leaching above 80°C increased iron extraction resulting in non-selective process
	China	100mg/kg	HCl	130% HCl dosage; S/L ratio = 1/4; 75°C; 3h	93.30%	[165]	Leaching + SX experiments
	China*	-	$C_6H_8O_7$			[154]	The main goal is the sodium removal to decrease the alkalinity and acid consumption on acid leaching - 95% of Na removal: citric acid dosage of 15%, L/S ratio 7 mL/g; 100°C, stirring speed 300 rpm; 120 min
	Greece	121mg/kg	HCl	HCl 6N; 24h; 25°C; S/L ratio 1/50	75-80%	[157]	Leaching agents studied: HCl, HNO_3, H_2SO_4, CH_3COOH, CH_3SO_3H and citric acid.
	Greece	121mg/kg	H_2SO_4 + H_2O_2	2.5M H_2SO_4; 2.5M H_2O_2; 90°C; 30min; S/L ratio 1/50	68%	[48]	For suppressed silica gel formation.
	Greece*	121mg/kg	CO_2 + H_2SO_4	35% H_2SO_4; S/L ratio 1/10; 25°C; 24h	35%	[156,166]	Use of CO_2 for bauxite residue neutralization: neutralised bauxite residue at ambient conditions (qCO2: 0.25 L/min, T: 25 °C, L/S: 5); high-pressure neutralised bauxite residue (PCO2: 30 bar, T: 25 °C, L/S: 5); high-pressure and high-temperature neutralised bauxite residue (PCO2: 30 bar, T: 150 °C, L/S: 5).

Cont. of Table 8.

Bauxite Residue	China	100mg/kg	HCl + EDTA	ratio of leaching agent ($HCl+H_2O$): bauxite residue; EDTA was 40 mL: 10 g: 2 g; HCl dosage 40%; 70 °C; 4.0h.	79.6%	[159]	Use of EDTA for selective scandium leaching
	Greece	98mg/kg	H_2SO_4	60min; S/L ratio 10%; 2M; 230˚C (under pressure)	60%	[161]	Multi-step leaching process. Low temperatures achieve better results due to low energy consumption
	Greece	100mg/kg	H_2SO_4	6M H_2SO_4; 85˚C; S/L ratio 30%; 4h	16.6mg/L	[167]	Use of Taguchi methodology to optimize scandium selective leaching.
	China	54.4 - 115.5mg/kg	-	-	37%	[150]	-

* pre-treatment previously leaching experiments

The number of publications found about scandium leaching from all other opportunities was lower compared those using bauxite residue as the feed. It may have occurred because scandium content in bauxite residues is higher and it's spread evenly, as presented previously in Table 7. From phosphogypsum and phosphate rocks, scandium content was lower than 10mg/kg. Cánovas et al. (2019) studied samples from Spain and scandium concentration was 1mg/kg, where its extraction achieved 99% using 0.5mol/L H_2SO_4 and 3mol/L HNO_3 [168]. Similar REE extraction was obtained by Abisheva et al. (2017) HNO_3 7.5 mol/L [169].

Scandium content in coal and fly ashes from the USA ranges from 2 to 35mg/kg [170–174]. Yang et al. (2019) analyzed a few samples where its content was 1144mg/kg, and leaching efficiency reached 80%. Önal & Topkaya (2014) studied the high-pressure leaching of Çaldağ lateritic nickel ore as an alternative of heap leaching. Nickel and cobalt extraction rise up to 94%. Scandium content was 0.0065wt.% and its leaching percentage was 90.9% (24mg/L in the liquor) [175].

A few studies considered a sulfation-roasting-leaching process, which was not considered in the present analysis. As an example, Anawati & Azimi (2019) explored the acid-baking process (25 - 400°C) of bauxite residue followed by water leaching. Scandium extraction reached maximum efficiency (80%) at 400°C, where it occurred as iron oxide is converted to sulfate [164]. Despite the fact that H_2SO_4 can be recovered and condensed for reuse on the acid-baking process, the acid consumption is still considered too high, mainly due to the alkalinity of the residue.

Studies have also explored the use of ionic liquid on the leaching process. The main advantage might be the selective extraction carried out by the organic leaching agent and also avoiding acid consumption. Bonomi et al. (2018) studied the ionic liquid 1-ethyl-3-methylimidazolium hydrogensulfate ([Emim][HSO_4]) for scandium and titanium extraction from Greek bauxite residue. Scandium extraction increased as iron and titanium leaching increases. The process efficiency reached 80% for scandium with almost all the iron extracted. Aluminum and sodium extraction extents were 40%. On the other hand, the ionic liquid is viscous and costs up to US$1,000 per kilogram. [176].

Davris et al. (2018) studied the ionic liquid HbetTf2N for REE extraction from ‘Rödberg’ ore of Fe carbonatite complex deposit. Scandium content in initial material was 90mg/kg and its extraction reached up to 60%. Other REE, calcium, and magnesium leaching were, respectively, 40-60% and 80-90% [177]. Furthermore, Davris (2016) evaluated the use of ionic liquid for metals leaching from bauxite residue. As before, calcium was the main contaminant extracted; on the other hand, iron leaching was lower than using mineral acids, but scandium extraction extent was limited to 40% [178].

Ionic liquids should be more selective in leaching reaction, but scandium extraction efficiency is lower comparing with mineral acids, such as H_2SO_4 and HCl. Moreover, the price of the ionic liquid is higher than typical leaching agents used in industrial applications and the high viscosity poses significant challenges which likely make the process less economically feasible compared to conventional aqueous acid solutions.

In all studies, scandium is presented in the liquor generated in trace concentration, while iron, silicon, and aluminum are commonly the main contaminants. Further steps must consider selective scandium separation, both contaminants removal or scandium recovery.

For instance, Zhang & Honaker (2018) explored the precipitation of solution varying the pH 4.85 - 6.11, containing 1.1% of REE, 18.4% Al, 1.7% Zn, 1.4% Cu, 1.14% Mn, 0.5% Ni and 0.2% Co. REE was precipitated using oxalic acid, which resulted in a product containing 94% of REE [170]. Despite that, the concentrate obtained has less economic value than a pure product. For this reason, it is preferable to use an ion-exchange technique for selective separation or contaminants removal from the liquor generated from leaching step.

2.1.4.2. Ion exchange techniques

The main techniques studied for selective scandium recovery are ion-exchange chelating resins and solvent extraction, being the last one well-explored due to the highly selective capacity and high contaminant content. Cyanex 272, D2EHPA, Ionquest 290, and Cyanex 923 are widely explored in sulfate solution, as shown in

Table 9. Despite that, commercial chelating resins are not explored from leaching process of possible scandium resources. Those resins tend to become more favorable economically as scandium content declines.

Zhu et al. tested several resins for vanadium recovery from leached of bauxite residue [179,180], while Zhang et al. (2017) synthesized a chelating resin with titanium phosphate functional group for scandium recovery from Greek bauxite residue, which achieved 91% of efficiency [181].

Zhou et al. and Roosen et al. also tested modified absorbent and synthesized chelating resin for scandium recovery [182,183]. For all, high selectivity for scandium was evaluated compared with iron, silicon, and titanium, the main contaminants from bauxite residue leached. Scandium recovery from H_3PO_4 using commercial chelating resins (DOWEX-50WX8 and DOWEX-50WX4) and from acid mine drainage (AMD) using synthesized chelating resin was also explored [184,185].

As Bao et al. (2018) evaluated, the kinetic of scandium adsorption onto chelating resins with the phosphonic acid functional group is higher than iminodiacetate [186]. These results, associated with the literature review showed in Table 9, demonstrated that scandium recovery by ion exchange technique is more efficient using phosphonic groups, both solvent extraction and chelating resins. As further explained, REE tend to have a strong affinity with the P=O functional group by coordinate reactions.

Moreover, the elution (resins) and stripping (solvent extraction) have not been extensively explored, which should improve scandium recovery and obtain a high purity product. Sodium carbonate and bicarbonate are highly selective for scandium elution, but fluorine compounds, such as ammonium and sodium, have shown better results than mineral acids.

Table 9: Solvent extraction and ion exchange resins application for scandium recovery

Resource	Location	Organic extractant / Chelating resin	Medium	Sc concentration	% recovery	Reference
Bauxite residue	China	P507: 2-ethyl hexyl phosphonic acid 2-ethyl hexyl ester; P204: Bis(2-ethylhexyl) phosphate; N1923: Primary amine	HCl	15mg/L	99.3%	[179]
	China	P507: 2-ethyl hexyl phosphonic acid 2-ethyl hexyl ester; P204: di-2-ethylhexyl phosphoric acid; Versatic 10: carboxylic acids	H_2SO_4	9mg/L	96.50%	[187]
	Australia	Cyanex 272: di-2,4,4-trimethylpentyl phosphinic acid; Ionquest 801: 2-ethylhexyl phosphonic acid mono-2-ethylhexyl ester; D2EHPA: di-2-ethylhexyl phosphoric acid; Versatic 10: 2-methyl-2-eth- ylheptanoic acid; Shellsol D70: 100% aliphatic diluent; Primene JMT: 1,1,3,3,5,5,7,7,9,9-decamethyl decyl amine; LIX 984N: un-modified 50:50 blend of aldoxime; LIX54-100: β-dike- tones.	H_2SO_4	5.53mg/L	> 99%	[188]
	India	D2EHPA: di-2-ethylhexyl phosphoric acid; Cyanex 272: di-2,4,4-trimethylpentyl phosphinic acid; Cyanex 301: dialky1dithiophosphinic acid	H_2SO_4	41mg/L	100%	[189]
	not informed	P507: 2-ethyl hexyl phosphonic acid 2-ethyl hexyl ester.	H_2SO_4	142mg/L	95.3%	[190]

Cont. of Table 9.

Ni laterite	not informed	Ionquest 290: bis(2,4,4-trimethylpenthyl) phosphonic acid; D2EHPA: di(2-ethylhexyl) phosphoric acid; Cyanex 272: bis(2,4,4-trimethylpentyl) phosphinic acid; Cyanex 923: Trialkyl phosphine oxide.	H_2SO_4	46mg/L	>95%	[191]
	not informed	D2EHPA: di(2-ethylhexyl) phosphoric acid;	H_2SO_4	20-30mg/kg	≈100%	[192]
	Brazil	Cyanex 923: mixture of four trialkylphosphine oxides R3PO (trioctylphosphine oxide), R'R2PO (dioctylmonohexylphosphine oxide), R'2RPO (dihexylmonooctylphosphine oxide), R'3PO (trihexylphosphine oxide) (R is n-octyl and R' is n-hexyland) Cyanex 272: di-2,4,4-trimethylpentyl phosphinic acid;	H_2SO_4	990mg/L	86.7%	[193]
Phosphogypsum and phosphate rocks	USA	D2EHPA: di(2-ethylhexyl) phosphoric acid;	H_3PO_4	1 – 15ppm		[184]
	-	Tributyl phosphate	HNO_3	198mg/L of ∑REMs	99.98%	[194]

In addition to traditional ion exchange techniques, the use of ionic liquid has increased, not only for selective leaching but also to separate scandium from leaching of mining wastes [195] and WEEE [196]. Avdibegovic et al. (2018) explored the use of ionic liquid for selective scandium recovery from Greece red mud, where its efficiency might reach up to 100%. Comparing ionic liquid with scandium precipitation as phosphate, its recovery from sulfuric medium using [Hbet-STFSI-PS-DVB] was only efficient after Fe(III) removal [197,198]. Indeed, several studies have been published about ionic liquid applications in recent years.

Considering all publications classified as opportunities, there are more about separation than leaching (28% and 21%, respectively). It indicates that there is more concern in obtaining a high-pure scandium solution. Leaching studies concerning is about acid consumption, mainly from bauxite residue. All scandium sources have high iron, aluminum, and silicon content, where a selective separation is required despite high-selective leaching reaction.

Indeed, the largest number of publications found were about chemical characterization from several sources, not only mineral but also municipal wastes and waste electrical and electronic equipment, which implies that there is an increased interest in metals recovery by urban mining, mainly REE. Moreover, the number of publications about these elements recovery from coal and fly ashes leads to achieving the conclusion that different sources are being studied.

2.1.4.3. Non-classifications

In the literature review, a considerable number of the manuscripts examined scandium separation from aqueous media using different techniques. The main goal of those publications is the selective separation or the removal of contaminants, focusing on application in real solutions from bauxite residue, nickel laterite, and wastewater from zirconium refinery, evaluating parameters such as pH, temperature, and contaminants. Figure 9 shows the percentage of techniques studied. Despite the high selectivity of the solvent extraction technique, there were more publications exploring chelating resins due to the low scandium content in those solutions.

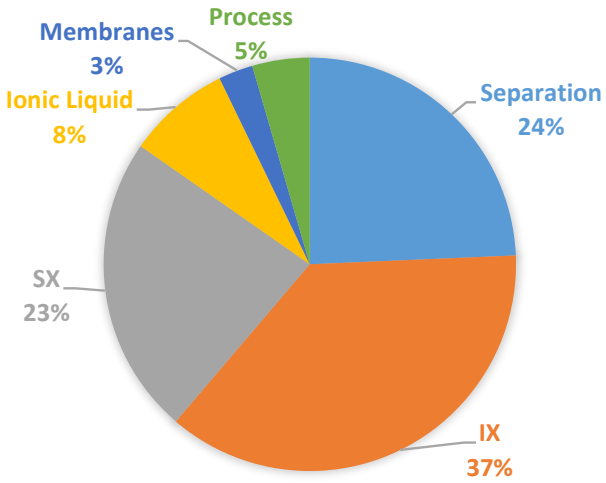

Figure 9: Percentage of publications found in literature review for each technique without classification. IX = ion exchange resins; SX = solvent extraction.

Table 10 presents the publications found that used the solvent extraction technique. Synthetic solutions were used for these studies in mineral acid medium, simulating the leaching process. Organic extractants tested have phosphorus-based functional groups, where Cyanex 272, D2EHPA, and Cyanex 923 presented separation efficiency up to 99%. Indeed, those are widely applied on extraction process from a varied source [199–202]. According to Li (2019) and Yudaev et al. (2021), organophosphorous extractants are important for rare earth elements, since they allow the separation from contaminants easily and to obtain a high-pure solution [203,204]. It demonstrates the reason for high scandium separation than other compounds.

The literature has also shown that the mixture of organic extractants (synergism) is being explored, as studied by Hu et al. (2020). The mixture of two extractants (binary system) increases the selective separation and efficiency when compared separated. Zhang et al. (2018) concluded that D2EHPA + TBP recovered 99.7% of scandium associated with high scandium separation when compared to iron. Zhao et al. (2016) and Sharaf et al. (2018) published similar results efficiency.

Table 10: Solvent extraction studies for scandium recovery or purification

Sc concentration	Medium	Organic extractant	% recovery	Reference
100mg/L	NaOH	Aliquat 336 - CH_3R_3NOH	95%	[205]
23.62mg/L	H_3PO_4	P204 - di-(2-ethylhexyl) phosphoric acid	95%	[206]
12mg/L	H_2SO_4	D2EHPA - di-2-ethylhexyl phosphoric acid; MTAA - methyltrialkylammonium	99%	[207]
45 – 450mg/L	H_2SO_4, HCl and HNO_3	Cextrant 230 - di-(2-ethylhexyl)[N-(2-ethylhexyl) amino methyl] phosphonate	-	[208]
10.21mg/L	H_2SO_4	D2EHPA - di-2-ethylhexyl phosphoric acid; N1923 - primary amine	98%	[209]
140mg/L	H_2SO_4	Cyanex272 - di-2,4,4-trimethylpentyl phosphinic acid; Cyanex923 - a mixture of four trialkylphosphine oxides	up to 95%	[210]
>2g/L	HNO_3, HCl, H_2SO_4	TRPO - isoamyldialkyl(C7-C9)phosphine oxide	up to 80%	[211]
4.5mg/L	H_2SO_4	HTTA - 2-thenoyltrifluoroacetone; TOPO - tri-n-octylphosphine Oxide	-	[212]
2g/L	Trichloroacetate solutions	B15C5 - benzo-15-crown-5	-	[213]
4.5mg/L	HNO_3	PC88A - 2-ethylhexylphosphonic acid mono-2-ethyl- hexyl ester; Versatic 10 - neodecanoic acid	up to 90%	[214]
20mg/L	H_2SO_4	D2EHPA - di-2-ethylhexyl phosphoric acid; TBP - tri-n-butyl phosphate	99.72%	[215]
1g/L	HCl	D2EHPA - di-2-ethylhexyl phosphoric acid; Cyanex 272 - di-2,4,4-trimethylpentyl phosphinic acid;	99%	[216]
0.30mg/L	HNO_3	TODGA - N,N,N',N' tetra-octyl-3-oxopentanediamide	>99%	[217]
45mg/L	HCl	Phoslex DT-8 - Oxidized di(2-ethylhexyl)dithiophoshate; Kelex 100, PC88A, and Cyanex 302	-	[218]
450mg/L	H_2SO_4	DEHAMP - di(2-ethylhexyl)-N-heptylaminomethylphosphonate	90%	[219]

Cont. of Table 10				
45mg/L	HCl	MSP-8 - O,O-bis(2-ethylhexyl) Hydrogen Thiophosphate	100% (extraction); 20% (1st stripping); 80% (2nd stripping)	[220]
4.5mg/L	H_2SO_4	D2EHAG - N-[N,N-di(2-ethylhexyl)aminocarbonylmethyl]- glycine; D2EHAF - N-[N,N-di(2-ethylhexyl)- aminocarbonylmethyl]phenylalanine	99%	[221]
-	H_2SO_4	PC-88A - 2-ethylhexyl phosphonic acid mono-2-ethylhexyl ester; Versatic 10 - neodecanoic acid; and XAD-7HP - acrylic ester co-polymer	99%	[222]

Yoshida et al. (2019) studied different organic extractants for scandium separation, being the most common D2EHPA (organo- phosphorus acid), Versatic 10 (carboxylic acid) and TOPO (a solvating extractant). Besides these, the authors also studied the D2EHAG, D2EHAS, and DE2HAF, which are amic acids. Results showed that D2EHPA separated scandium up to 100% in all pH range (0.5 – 3.0), while D2EHAG and D2EHAS achieved similar results in pH above 2.0. DE2HAF achieved 65% at pH 3.0, and the efficiency of scandium separation using Versatic 10 and TOPO was lower than 20%. As demonstrated by the authors, organic extractants are suitable for scandium separation.

Table 11 shows the developments in scandium recovery by ion exchange solid materials, such as chelating resins and new exchangers. Comparing such ion-exchange techniques, both positives and negatives aspects should be considered. Solvent extraction might obtain a high-pure product, faster and high separation degree but the operational cost is considered high and environmentally harmful. On the other hand, ion exchange resins have other operational challenges but they are more suitable for concentrations below 1g/L (until ppm or ppb), while solvent extraction is suitable for target metal concentration above 1g/L [223]. As scandium is presented in concentrations lower than 1g/L (nickel laterite) and 40mg/L – 5mg/L (bauxite residue), as shown in Table 9, solid-liquid separation by ion exchange must be proper in this case.

All those studies presented were carried out using a synthetic solution to simulate the real liquor from leaching step in order to evaluate the parameters of separation. For instance, Avdibegović et al. (2019) synthesized adsorbent material (α-zirconium phosphate - $Zr(HPO_4)_2 \cdot H_2O$) for scandium separation over iron, as it is the main contaminant in all processes discussed in Section 2.1.3.2. After batch experiments, column experiments were performed for both synthetic solution and real leaching liquor from Greek bauxite residue by HCl [224].

Commercial resins were widely explored, such as TP 260, TP 209, TP 272, Lewatit M500, Lewatit SP112 to obtain a high-concentrate and pure scandium solution. Indeed, all of them evaluate the effect of iron on scandium separation. Among those, TP 260 and TP 272 have shown more selective than iron and aluminum, and TP 272

achieved highest Sc-Fe separation, mainly for ferrous iron than ferric iron, which might be performed by a chemical reducing process [225].

Different materials were tested, as algae (*Posidonia oceanica*) for scandium separation as a low cost adsorbant. Ramasamya et al. (2019) simulated a acidic mine drainage for the separation of rare earth elements, where the material achieved better results for scandium than commercial resins due to the high concentration of contaminants [226].

By the same token, Hamza et al. (2020) prepared a adsorbant manufactured with algine and polyethyleneimine beads. Results depicted that the material is selective for scandium when compared with sodium, magnesium and samarium. Experiments with solution from leaching of bauxite residue demonstrated that even in acidic pH (1.24), the material was more selective for scandium than iron, aluminum, silicon, zirconium and titanium [227].

Moreover, several studies explored new materials synthesized focusing on scandium separation and chelating resins impregnated by organic extractants. Ramasamy et al. (2017) synthesized mesoporous silica for scandium and REE (yttrium and lanthanides group) adsorption. The exchanger materials have O– and N– donor ligands, such as amino and carboxylic groups, despite P–. Moreover, silica is a support material extensively studied for solid-liquid separation due to its high surface area in addition to thermal resistance [228], which justify the high amount of publications found in the literature for new ion exchange materials production focusing on REE separation.

Moon et al. (2020) impregnated a support resin with Cyanex 272 for separation of scandium from yttrium in hydrochloride medium. The solvent-impregnated resin effectively separated the rare earth elements, where scandium was adsorbed and yttrium remained in the solution [229].

Zhang et al. (2019) also studied a silica-polymer adsorbent impregnated with HDEHP (di(2-ethylhexyl) phosphonate) for scandium separation over REE. Both studies indicate that these exchangers can be used for scandium separation. Indeed, the development of new materials for the separation step would increase the number of exchanges and increasing the possibility of replacement of high-cost raw materials for purification step, as in the case with the solvent extraction.

Complementary to these techniques, precipitation and ionic liquid have also explored. Yagmurlu et al. (2018) explored different precipitant agents ($CaCO_3$, NaOH, NH_4OH, KOH, K_2HPO_4, $(NH_4)_2HPO_4$, Na_2HPO_4) for scandium separation from synthetic solution based on liquor from bauxite residue leaching in sulfuric, nitric, and hydrochloride acids media. The results have shown that NH_4OH was more selective with low scandium losses. Hydroxides and calcium carbonate precipitation experiments obtained highest scandium losses in both HCl and HNO_3 media. According to the authors, scandium concentrate solution obtaining can be performed through three steps: first, iron removal by NH_4OH; second, iron removal with scandium losses by NH_4OH, which returns to the beginning of the process; and finally, a concentrate solution by phosphate precipitation using Na_2HPO_4 [230].

In addition, da Silva et al. (2018) tested $CaCO_3$, $Ca(OH)_2$, NaOH, and MgO for impurities removal in H_2SO_4 media – calcium, magnesium, manganese, iron, aluminum, thorium, and uranium. Despite scandium losses were lower than 4%, it was obtained a high-pure mix of REE (high and light) after two precipitation steps. About 98% of impurities were removed using $CaCO_3$ at pH 3.5 followed by $Ca(CO_3)_2$ at pH 5.0 [231]. In another work, the authors tested sodium sulfate and disodium hydrogen phosphate for selective REE precipitation. As before, an REE concentrate was obtained [232]. The present literature review has shown that scandium separation cannot be performed by precipitation, but impurities removal previous ion-exchange technique is an opportunity to increase the selective separation.

Table 11: Chelating resins studies for scandium recovery or purification

Sc concentration	Medium	Resin	% recovery	Reference
90mg/L	HCl	SiAcP - silica composite.	99.9%	[233]
45mg/L	HCl	am- ZrP, am-TiP - amorphous zirconium and titanium; α-TiP - phosphate and crystalline titanium phosphate	60%	[224]
1-200mg/L	H_2SO_4	*Posidonia oceanica* - green marine algae	98%	[226]
25mg/L	H_2SO4	Activated carbon and silica composites	90%	[234]
30mg/L	-	APTES - 3-Aminopropyl triethoxysilane; APTMS - 3-Aminopropyl trimethoxysilane; MTM - Trimethoxymethylsilane; TMCS - Chlorotrimethylsilane	99%	[235]
18g/L	HCl	[D201][DEHP] - di(2-ethylhexyl) phosphonate; [D201][C272] - bis(2,4,4-trimethylpentyl) phosphonate	95%	[236]
45mg/L	HCl	Solvent-impregnated resin (SIR) containing Cyanex 272 - bis(2,4,4-trimethylpentyl)phosphinic acid	87%	[229]
10mg/L	H_2SO_4	Aminocarbonylmethylglycine	99%	[237]
4.6mg/L	HNO_3	SBA-15, KIT-6, silica gel, and β-zeolite	95%	[238]
20mg/L	HCl	y-AA-x@MIL-101s - Acrylic Acid-Functionalized Metal−Organic	90%	[239]
50mg/L	H_2SO_4	TP 260 - aminomethyl phosphonic; TP 209 - iminodiacetate; TP 272 - bis(2,4,4-trimethylpentyl) phosphinic acid	-	[186]
450mg/L	H_2SO_4	Macroporous TRPO/SiO2-P adsorbent	100%	[240]
-	HNO_3	Purolite A170 - dimethylamine; Lewatit M500 - tertiary amine; Lewatit SP112 - sulfo groups	99%	[241]
20mg/L	HCl	The newly synthesized resin containing glycol amic acid group for	-	[242]
0.5g/L	HCl	732-type resin - strongly acidic cation exchange resin used	21%	[243]
25mg/L	HCl	amino and non-amino functionalized silica gels	99%	[244]
-	H_2SO_4	HDEHP/SiO_2-P - di(2-ethylhexyl) phosphonate silica-polymer	-	[233]

Cont. of Table 11				
1-2mg/L	HCl and HNO_3	1-(2-pyridylazo)-2-napththol (PAN) and acetylacetone (acac) immobilized gels	-	[228]
0.18mg/L	HNO_3	silica sol-gel material doped with trioctylmethylammonium 1-phenyl-3-methyl-4-benzoyl-5-onate	-	[245]
49.5mg/L	HCl and HNO_3	Hbet–STFSI–PS–DVB - sulfonyl(trifluoromethanesulfonylimide) poly(styrene-co-divinylbenzene)	-	[246]
	H_2SO_4	PC-88A - 2-ethylhexyl phosphonic acid mono-2-ethylhexyl ester; Versatic 10 - neodecanoic acid; and XAD-7HP - acrylic ester co-polymer	99%	[222]

Finally, as demonstrated in Section 2.1.3.2, the use of ionic liquid for REE recovery is explored achieving up to 97% of scandium recovery [247–250]. As discussed by Makanyire et al. (2016), comparing with solvent extraction, the ionic liquids are water-soluble determining environmental and economic management related issues. According to the authors, ionic liquids are classified as green solvent due to the low vapor pressure, decreasing health impairments, environmental and security risks. However, the costs of these organic reagents are still considered too high, which makes the ionic liquids non-competitive with organic extractants [251].

Turanov et al. (2016) and Sun et al. (2011) studied ionic liquids for selective scandium separation over yttrium and REE. Results indicated that these compounds might be used for selective separation of REE. Considering the number of publications focusing on REE separation by the ionic liquid, the cost issues may be solved by designing a process that results in a high-pure product. So, the raw material cost would be paid in the process by itself. In the present review, it was realized that the interest on the ionic liquid in the last years has increased, mainly due to the importance of REE extraction and separation to obtain high-pure products caused by Chinese market control and raises on their consumption.

Liquid membrane have demonstrated an outline for scandium recovery. Parhi et al. (2019) studied the hollow fibre liquid membrane (HFLM) for scandium separation from manganese-containing solution (HCl). The ionic liquid (IL) R_4ND achieved better results than D2EHPA in chloride medium [252]. It was monstrated that process using liquid membranes benefits the process in light of sustainability since toxic and dangerous reagents are replaced [105,253,254].

2.1.5. Sustainable evaluation and challenges to be overcome

By the reason of Chinese control on the REEs market (95%) [17,23] countries around the world have searching for new sources of those elements. Indeed, Brazil has more REEs ores than China but still needs investment to explore these resources. North America, Africa, Asia, and Australia have REEs ores to be explored. As related by Chen (2011), even comparing the number of deposits (REEs resources) with reserves (resources for industrial applications), Brazil is the leader in REEs sources –

32% - followed by China (22%). There are almost 34 countries spread in the world, and the expectation is for growth [255].

The main discussion in the last years about mining activities is the depletion of natural resources. Many authors have argued that they will be exhausted, and to meet the sustainable development, the metals resources would change from natural to recycling (urban mining). Indeed, the scarcity of natural sources is more about economic viability issues, where the grade of the target metal (or metals) has decreased. In addition, the demand won't decrease or remain constant, leading us to search for new sources [18,256]. For this reason, a search on scandium extraction from many types of sources has been increased in the last years, as the present study showed.

New scandium sources may contribute to the circular economy, and industrial wastes (mining and coal ashes) and municipal wastes (i.e. WEEE) were widely investigated to achieve it. According to Binnemans et al., the investment in sustainable primary mining (from new REEs ores to reopening old mines) and urban mining will support the critical metals supply (as well as scandium) [257,258]. Nonetheless, scandium recycling rate is none, as shown by the European report [17]. In fact, the knowledge of new opportunities allied to the innovative extraction/recycling processing targeting circular economic must be invested.

Indeed, such REEs are partially used for green energy production. As it is expected an increase of 5% on production, it's also important a green extractive processing. Due to low REEs content in natural resources, sustainability must be led to reuse of mining tailings and recycling processing. Many strategies are available to be used to achieve other SDGs, as discussed by Monteiro et al. (2019).

2.1.6. Future strategy and process perspectives for scandium extraction

The present study discussed the current techniques for scandium recovery from primary and secondary sources; likewise, opportunities were also discussed. Indeed, the focus here was for processing in aqueous media (hydrometallurgy). Despite the present study did not consider pyrometallurgical processing as sustainable route, the combination of pyro + hydro could reach this goal for many reasons.

First, iron may be removed by thermal processing, which can be used as raw material for pig iron or steel production. However, the literature review has shown that this material contains high amount of impurities which decreases its added-value [51]. Surely, high energy is required for the process; on the other hand, industrial or urban wastes can be used for energy production, which must benefit the SDGs [32]. Considering the greenhouse gases released and energy consumption, hydrometallurgy processing is the may route to reach the goals proposed by U.N. [32,59,60].

The most important aspect of ecofriendly scandium processing is to promote its recycling and reuse minimizing the dependency of such natural resources. Furthermore, effective administrative policies to establish and implement recycling programs in governmental spheres is crucial [26]. For countries such as Brazil, the USA, and Australia - that have continental sizes - they will be benefited by aqueous processing, where small factories may be spread over the territory, in spite of one big thermal processing factory [64], mainly for urban mining where scandium can be obtained.

Sections 2.1.3.2 and 2.1.3.3 have shown that the main scandium sources to supply its future demand are mining tailings (mainly bauxite residue and nickel laterite). As WEE are rich in REEs, such as yttrium, lanthanum, cerium, and neodymium, and scandium is present in a few of them, urban mining focusing on the recovery of all of these elements, as well as other metals (as copper, zinc, gold and silver), the SDG would be achieved. The future of scandium production and supply can be considered as promising. Economics aspects of mine production allied to sustainability are all explored in the present literature review, which goes straight to the sustainable development goals for a green production [32,33,60]. Among the existing extractive routes and those at the beginning of development, the processing in aqueous media might achieve the goals for an ecofriendly process for scandium extraction

It is considered that scandium content over 20mg/kg – 50mg/kg can be explored due to the economic viability, and considering the aspects pointed by Chen (2011), and adopting for scandium supply, it is important to recognize that the literature review presents the characterization of different materials to be used as raw material for metals production, such as WEEE and mining tailings.

Despite scandium is the target element, many others can be extracted. For instance, bauxite residue may contain yttrium and elements from the lanthanide group to have prospected. Furthermore, the literature review has shown that titanium and zirconium can also be recovered. For sodium, it is extracted and recycled in the Bayer Process. Iron, aluminum, and silicon may be used for new product development, as Izidoro et al. (2019) demonstrated for zeolite A synthesis for industrial wastewater treatment [27]. However, acid consumption is still a challenge to be overcome. Despite that, it may achieve a circular economy.

From nickel laterite waste, scandium content is lower and its extraction may have the same problems as bauxite residues, and nickel and cobalt may be recovery with scandium. Considering coal ashes, the concentration is even lower and both technical and economic viability would not be achieved.

For scandium supply, urban mining would not be considered due to low content. Also, associated with the difficulty of REEs separation, mixed oxides of these elements would be produced instead of separated. Still, the recovery of such elements will increase the economic benefits of recycling, even more using a residue as raw material.

From urban mining, scandium concentration would be increased on the dismantling step, where parts, where it is found, may be separated, as the case of processor socket. Considering the studies were quantified scandium on WEEE, all of them it is presented in trace concentration. It indicates that it may be difficult to obtain scandium concentrated in recycling process. On the other hand, the recycling and the recovery of metals from wastes will reduce environmental impacts and improve efficiency. As a conclusion, despite those problems, it is a way to reach sustainability on the extraction of scandium.

Certainly, several issues must be solved, as to how far recycling is priceless than extractive processing from natural resources. It is well known that the separation of metals on recycling processing may be more expansive than from natural, due to the number of impurities found in these sources. In other words, a technical feasibility study must be taken into account. It is the key to sustainability: join the environment with the economic aspects.

3. OBJECTIVES

The goals of this thesis were: the characterization of the scandium sources; study the parameters of acid leaching, such as acid concentration, temperature, solid/liquid ratio and time; and the parameters of scandium and zirconium separation by solvent extraction, such as organic extractant, pH, temperature, TBP as modifier and A/O ratio.

4. MATERIALS AND METHODS

A Brazilian company supplied the bauxite residue. In contrast, the silicate-based ore was supplied by a Canadian company and sent to the University of Sao Paulo by the Hydrometallurgical group of the University of Queensland. The methodology is detailed in each article presented in Section 5.

Figure 10 shows the methodology for experiments with bauxite residue. The characterization and leaching experiments of bauxite residue were carried out at LAREX at the University of São Paulo. First, the sample was homogenized and then dried for characterization. Next, chemical and physical characterization was carried out by X-ray fluorescence, scanning electron microscopy coupled with energy dispersive spectroscopy, particle size distribution, X-ray diffraction, total organic carbon, and inductively coupled plasma optical emission spectrometry.

After chemical characterization, leaching experiments were carried out evaluating two inorganic acids: sulfuric acid (H_2SO_4) and phosphoric acid (H_3PO_4). Experiments were performed in a glass reactor under stirring and temperature control. It was evaluated the effect of time, solid-liquid ratio, H_2O_2 dosage, temperature, and acid concentration. In addition, such experiments were carried out to study the scandium extraction and co-extraction of other valuable elements and contaminants.

Solvent extraction experiments were carried out to separate scandium and zirconium from the bauxite residue leach solution. Two trialkylphosphine acids and one tertiary amine were studied, evaluating the effect of pH, temperature, organic extractant concentration, the synergism with TBP, and aqueous-organic ratio.

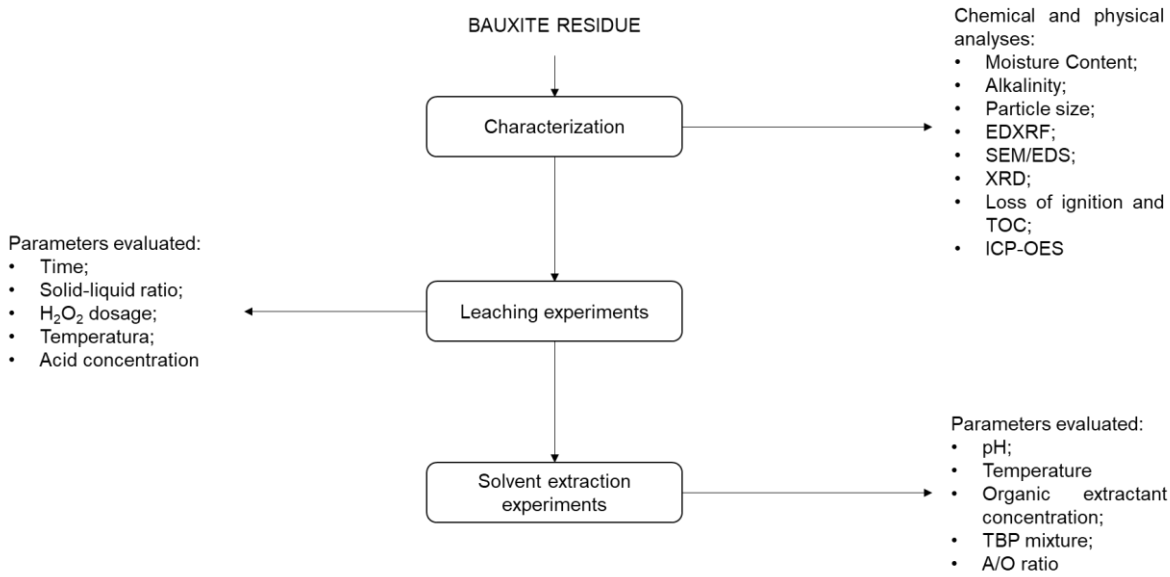

Figure 10: Schematic flowchart of the methodology used for characterization, leaching, and solvent extraction experiments of bauxite residue

The silicate-based material was characterized at the School of Chemical Engineering at the University of Queensland and LAREX at the University of São Paulo. Chemical characterization was carried out scanning electron microscopy coupled with energy dispersive spectroscopy, particle size distribution, X-ray diffraction, and inductively coupled plasma optical emission spectrometry. Figure 11 depicts the methodology used for experiments carried out using silicate-based material to extract scandium and valuable elements.

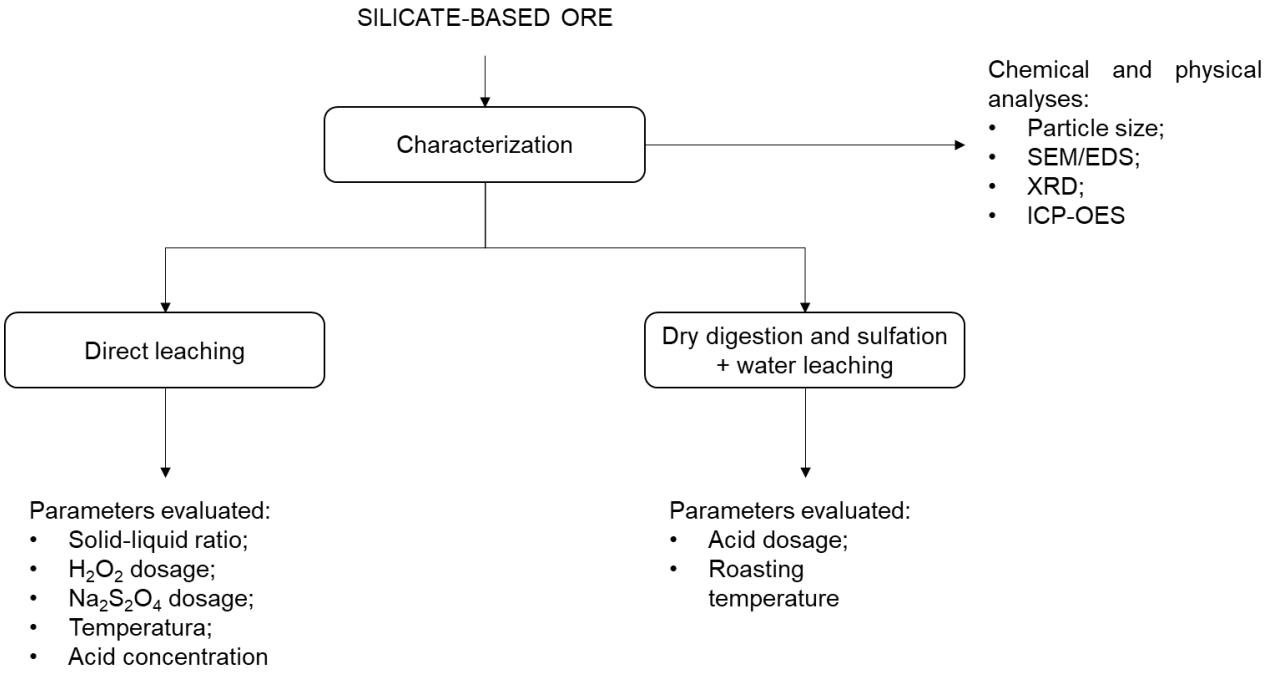

Figure 11: Schematic flowchart of the methodology used for characterization of silicate-based ore and extraction experiments.

Extraction experiments were carried out using H_2SO_4. Direct leaching, dry digestion, and acid baking followed by water leaching techniques were adopted to extract scandium and rare earth elements. First, direct leaching was studied, evaluating the effect of solid-liquid ratio, acid concentration, H_2O_2 and $Na_2S_2O_4$ dosage, and temperature. Then, dry and acid baking was studied, and the effect of acid dosage and roasting temperature were evaluated in-depth.

The aqueous solution of leaching and solvent extraction experiments was analyzed in ICP-OES to quantify trace elements (scandium and rare earth elements) and in EDXRF or AAS for chemical quantification of elements in high concentration, when specified.

5. RESULTS AND DISCUSSION

This section presents four manuscripts submitted and published in scientific journals. Chapter 5.1 shows the data of bauxite residue characterization comparing with the literature review. Moreover, a discussion of challenges and possibilities within different techniques to extract scandium and valuable elements is approached.

Chapter 5.2 depicts the results for acid leaching of bauxite residue aims the extraction of scandium. The inorganic acids H_2SO_4 and H_3PO_4 were studied in direct leaching experiments through different parameters: time (30min – 660min), solid-liquid ratio (1/10 – 1/50), H_2O_2 dosage (15g/L and 1-4mL/h), temperature (25°C – 90°C) and acid concentration (10% - 60%).

Chapter 5.3 shows the data for extraction of scandium and valuable elements from silicate-based ore by direct leaching and dry digestion/acid baking. First, the effect of solid-liquid ratio (1/5 – 1/50), H_2SO_4 concentration (0.5mol/L – 4.0mol/L), H_2O_2 and $Na_2S_2O_4$ dosage (1% - 10%) and temperature (25°C – 90°C) were evaluated considering the extraction yield of the target elements. Also, the dry digestion and acid baking were evaluated by studying the effect of acid dosage (0.6mL - 1.5mL) and roasting temperature (25°C – 400°C).

Finally, Chapter 5.4 brings forward results of scandium and zirconium separation from the bauxite leach solution. The organic extractants Alamine 336, D2EHPA, and Cyanex 923 were evaluated to obtain high separation factors of the target elements compared to the main contaminants (iron, aluminum, and titanium). The effect of pH (0.5 – 2.0), temperature (25°C – 60°C), concentration of organic extractant (5% - 25%), synergism with TBP (1% - 10%), and A/O ratio (5/1 – 1/5) were evaluated.

5.1. Characterization of bauxite residue from a press filter system: comparative study and challenges for scandium extraction

A.B. BOTELHO JUNIOR; D.C.R. ESPINOSA; J.A.S. TENÓRIO

Department of Chemical Engineering; Polytechnic School, University of Sao Paulo, Sao Paulo – Brazil.

Abstract

A new step in the Bayer Process has been used to recover NaOH and to decline its content from the red mud. After the digestion, the residue is separated from the Bayer liquor and goes through press filters, which enables to recover NaOH and decrease the moisture content. It is already known that the red mud is one of the most important resources of scandium. For this reason, the goal of this work was to characterize a Brazilian Red Mud for scandium recovery. The sample was collected after the press filter system. Analysis of EDXRF, SEM-EDS, and XRD were performed. Microwave digestion using acids mixture was carried out to determine the concentration of the main elements. Fe_2O_3 represents 40% of the BRM, and Sc concentration is 43mg/kg. The SiO_2 content is 22%, which is the highest found in the literature review. On the other hand, sodium concentration is the lowest. Literature review was carried out to compare with BRM, as well as the current studies to recover scandium by the leaching-ion exchange process. Scandium recovery using leaching-ion exchange process may be possible with efficiency higher than 90%. In addition, the most challenge is the silica gel formation during the leaching.

Keywords: Brazilian red mud; Bauxite residue; Critical metals

Graphical abstract

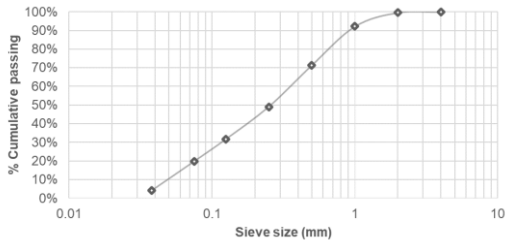

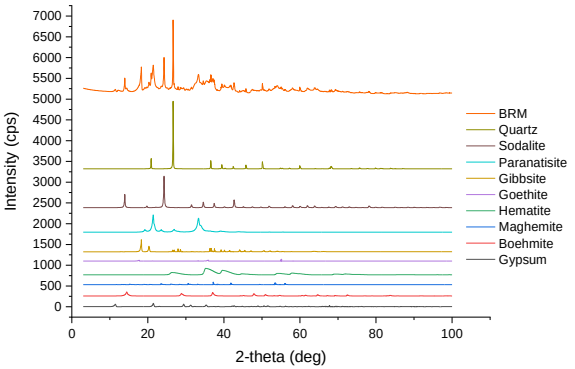

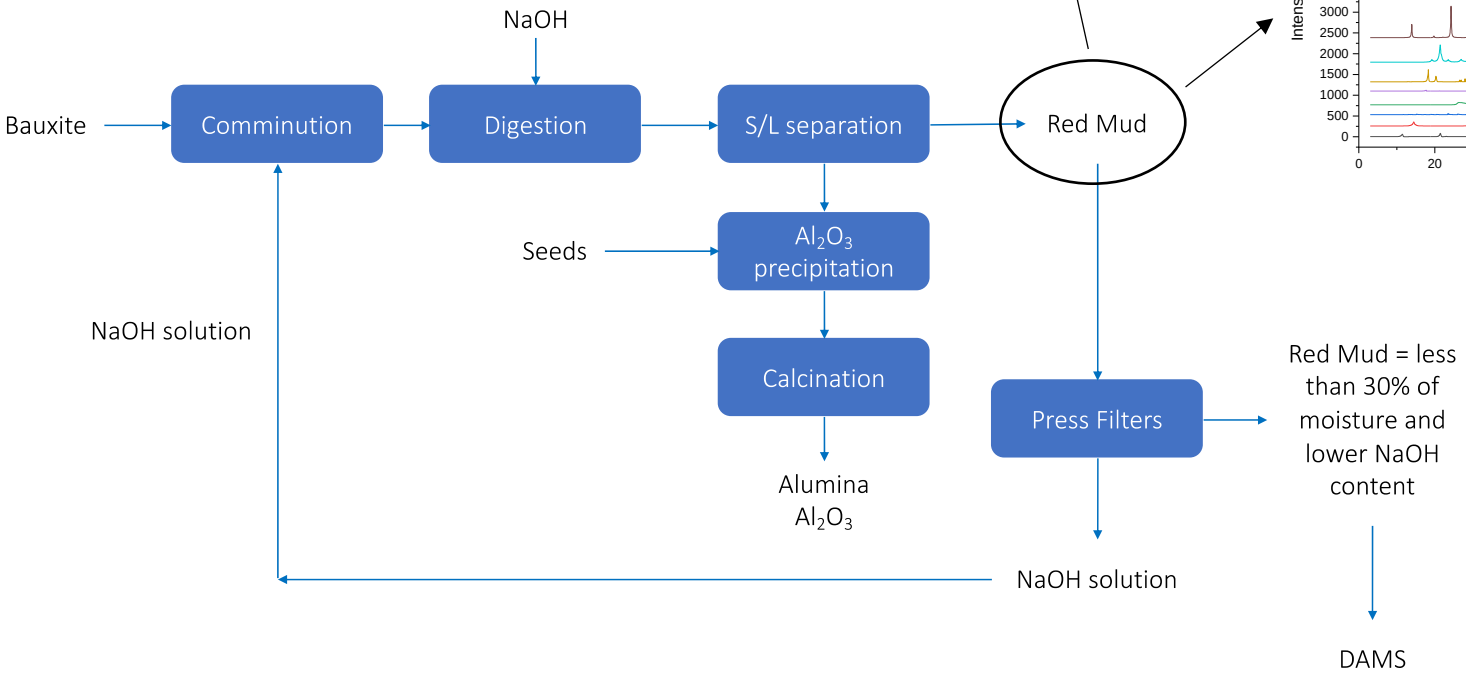

Statement of Novelty

A Brazilian Red Mud (or bauxite residue) has been fully characterized. Because its environmental risks and the huge amount stored in dams and due to the recent accidents occurred in Brazil caused by mine tailing dams collapse, it is important to give new reuse and applications for these residues. The literature review has demonstrated that bauxite residues may contain several rare earth elements, being scandium the most valuable and critical. However, there is a lack in the literature about the red muds from Brazil. Based on this situation, the characterization and the discussion about scandium recovery focusing on sustainable process by leaching-ion exchange presents the novelty of this work.

5.1.1. Introduction

Brazil is the third country in bauxite resources and production in the world [259,260]. This ore is the raw material for alumina production through the Bayer Process, where sodium hydroxide is used as leaching agent, which enables the selective leaching of alumina. After the leaching step, solid-liquid separation is required [261,262]. The solid phase (residue) is called *red mud*, or bauxite residue. For each tonne of alumina produced, around 1-1.5 ton of red mud is generated. An estimate indicates that, in 2015, 4 billons tonnes of bauxite residue were generated around the world, four times higher than in 1985. By now, it is stocked in tailings dams [263–265].

In an innovative process, after the solid-liquid separation, the red mud goes through a press filter equipment to recover NaOH solution and decline the moisture percentage of the residue. As a result, the dam that had previously been built for wet disposal increased its useful life for more 30 years. Figure 12 shows the flowchart of the Bayer Process. NaOH solution recovered might be sent to the comminution step, which helps to mill of bauxite to reach the particle size distribution desired. The desilication step is not shown in Figure 12.

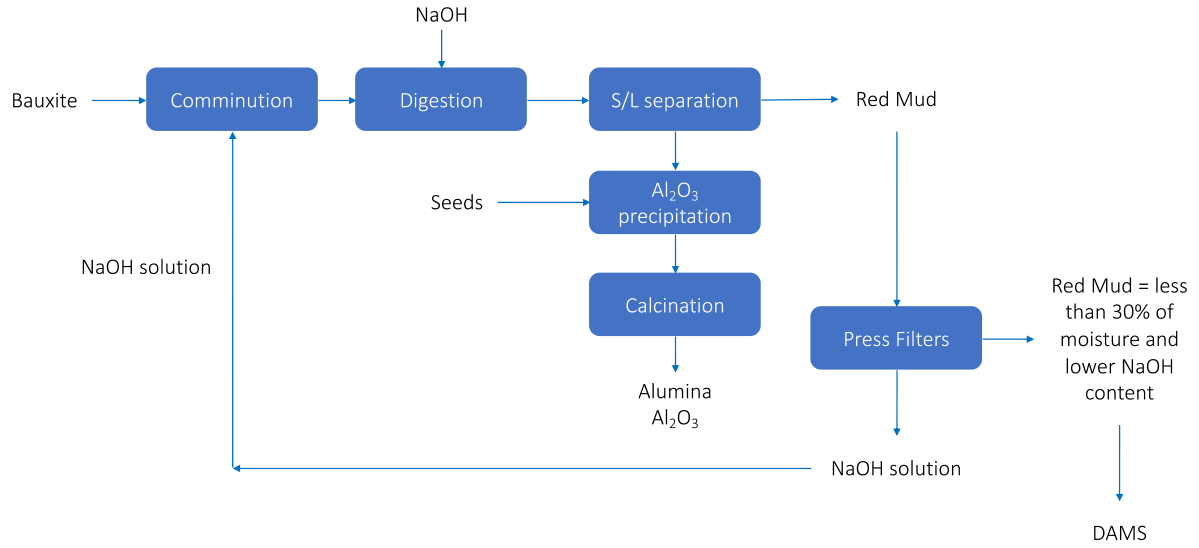

Figure 12: The flowchart of the Bayer Process, where the red mud goes through the press filter for NaOH solution recovery and to decline the moisture content

The major elements presented in a red mud are iron, aluminum, sodium (from digestion), silicon and titanium. Nonetheless, there is also the presence of several elements in a minor concentration, which can be cited scandium, yttrium, zirconium, and vanadium. Rare earth elements (REE) from the lanthanide group can also be found [263].

In light of the rare earth resources, almost 90% of world's production originates from China. By 2009, China's and world production increased 77% (129,000ton) and 45% (132,000ton), respectively [266]. Consequently, the Chinese government sets quotas for the rare earth exportation. In 2010, the exportation of rare earth elements was cut, causing an increase in market price [62,63,266]. For this reason, alternatives have been studied to obtain those elements from different resources to supply the demand.

The presence of those elements relies on the bauxite composition, which differs in any part of the world. Despite the presence of different REE, scandium is the most valuable element present in the red mud, representing 95% of the economic value of the residue [20,267].

To the best of our knowledge, scandium is obtained only as a by-product from the extraction of titanium and rare earth (China), uranium (Kazakhstan and Ukraine)

and apatite (Russia). China is responsible of 66% of the scandium global production. Resources of scandium are found in Australia, Canada, China, Kazakhstan, Madagascar, Norway, the Philippines, Russia, Ukraine and the USA [65]. However, about 70% of total scandium sources are in bauxites, and after the Bayer Process, it is sent to red mud [268,269].

The European Union considered scandium as critical due to the risk of supply interruption, strong control of a few countries on production and also its need in the manufacturing of modern life [270–272]. Today, these critical metals are in critically short supply, and it is important to prevent this list from continuing. Among these opportunities, the recovery of scandium from red mud has been considered. Several extraction process have been studied; however, it must be designed according to the characteristics of the residue. Despite the studies presented in the literature [273], none of them considered scandium extraction from a red mud from Brazil. A brief literature review is given to provide the state of art knowledge existing in scandium recovery from red mud.

5.1.2. A literature review of scandium recovery from red mud

There are a few routes that are being explored for scandium recovery from red mud. Some of them also considered the extraction of the main elements present in the residue, such as iron, aluminum, titanium, and sodium.

Borra *et.al.* (2016) studied the iron extraction by the smelting process for both iron recovery and to increase the scandium content. The red mud from Greece was mixed with graphite powder and wollastonite and heated at 1500ºC. Results showed that 85% of iron was removed, and the REE content increased in slag comparing with concentration in red mud. Leaching experiments in slag showed that all scandium, 70% of titanium and most of REE were recovered using HCl and HNO_3 at 90ºC [274].

Hodge et al. (2019) studied the recovery of aluminum and sodium by the bauxite residue sinter leach process (BRSLP). Iron and aluminum are the main metals presents in the red mud, followed by silica, sodium, and titanium. The process consists in to make $NaAlO_2$ soluble and insoluble Ca_2SiO_4 avoiding reactive silica to precipitate aluminum. The red mud was mixed with sodium and calcium carbonate and heated at

1000ºC. Results indicated sodium and aluminum recovery up to 50%, while silica recovery was lower than 10% [155].

Also, a combination of sulfation and water leaching can be used for REE recovery. The process consists in a reaction between sulfuric acid and red mud in an oven in temperatures above 200ºC. The reason for that is to form REE sulfate, which is soluble in water. Despite results indicated that the REE extraction reached 90%, scandium leaching by water might reach 60% [164,275].

Although iron, sodium and aluminum removal are extremely important for both concentrate the scandium and further to remove contaminant from the process, the use of pyrometallurgy to recover metals from red mud make it economically infeasible [263,268,276].

Using pyrometallurgy has been losing its competitiveness on REE recovery from low-grade resources, due to the high energy consumption and environmental pollutants [263,277–279]. In spite of the REE extraction reaches 90% by sulfation and water leaching, the efficiency on scandium extraction is lower when compared with direct leaching. For this reason, hydrometallurgical processing has been developed, mainly for the extraction from low-grade resources.

Studies have considered the use of ionic liquid for scandium extraction. Davris et al. (2016) studied the direct leaching of Greek red mud using functionalized hydrophobic ionic liquid, which is an organic solvent consisting solely of ions. These ionic liquids provide selective dissolution during the leaching reaction. The authors obtained 70-85% REE extraction, while results for scandium was did not exceed 45% [280].

Bonomi et al. (2018) studied the direct leaching of red mud with Brønsted acidic ionic liquid 1-ethyl-3-methylimidazolium hydrogensulfate. Scandium extraction reached 80%, while iron extraction was almost 100% at the same condition [176]. Despite the higher efficiency on scandium extraction, both high iron extraction and the price of ionic liquid might make the process infeasible. Comparing with mineral acids, ionic liquids are considered too expensive.

Pepper et al. (2016) studied the leaching of red mud by different mineral acids. Iron extraction is lower using phosphoric acid than sulfuric acid [281]. Borra *et.al.*

(2015) studied REE recovery by direct leaching using different inorganic and organic acids from Greek red mud. The authors showed that the scandium extraction is directly related with iron extraction, which might indicate that scandium is trapped by the iron phases. Scandium extraction reached 80% as well as iron extraction [54].

There are two main problems with the direct leaching of red mud. It will be necessary extremely acid conditions primarily due to the alkaline content of the red mud, which makes the acid consumption excessive and turn the process infeasible. The red mud is obtained from an alkaline process, and most of all elements are presented as hydroxide. Further, there is sodium hydroxide presented in the residue. The acid consumption can be decreased in high liquid/solid ratios, but the amount of solution to be treated also increases [48,54,273,282].

Another problem on the acid leaching process is the silica gel formation, as showed by Alkan *et.al.* (2018). This makes the solid-liquid separation difficult. In addition, the silica gel traps a part of the liquor generated during the acid leaching, which decreases the metals extraction, mainly rare earth elements [48].

Solvent extraction is commonly used for the separation of REE from the liquor generated on the leaching step [1,283]. The high concentration of iron as the major contaminant decreases the process efficiency. Ion exchange chelating resins can be used also for scandium recovery [19,284,285]. Parameters for the extraction process are established according to the composition of the red mud and its physicochemical characteristics. Consequently, an industrial process can be designed for scandium extraction and further elements with economic aspects.

For this reason, the aim of this work was the characterization of Brazilian Red Mud (BRM) for scandium recovery. The moisture content, alkalinity, and particle size distribution were analyzed. The X-ray fluorescence and X-ray diffraction analysis were performed to study the main elements and the mineral phases present in the residue. Analysis by SEM/EDS were carried out to study the residue morphology. Quantification analysis was performed in ICP-OES after acid digestion. All results were compared with red mud from different parts of the world. From these results, a critical overview was made to evaluate the hydrometallurgical process and challenges to obtain scandium and valuable metals from BRM.

5.1.3. Materials and methods

A sample of BRM (16kg) was received from a Brazilian company. Subsequently, the red mud was separated from Bayer liquor and went through the press filter. The sample was homogenized following the pile method and separated in 1kg packages. Then, the BRM was ground using mortar and pestle for the moisture content analysis. Samples used for alkalinity measurements, particle size analysis, XRD, SEM-EDS, EDXRF and digestion were first dried in an oven at 60°C for 24 hours.

5.1.3.1. Moisture Content

The analysis of moisture content were performed by infrared moisture analyzer (GEHAKA – IV2000) with a 1g of the sample. Two different methods were applied: Auto Dry, where the sample was heated until at 150°C and maintained until mass loss had been less than 0.05%; and drying time, where the sample was heated until at 150°C and maintained for 30min. All analysis were carried out in duplicate.

5.1.3.2. The pH Measurements

A 250g of the BRM dried was mixed with 1L of deionized water and left to stand for 7 days [286]. The pH was measured using a pHmeter HANNA and an electrode (Sensoglass) Ag/AgCl 3mol/L. The measurement was also performed by titration, where 10mL of the extract was mixed with 90mL of deionized water and methyl orange as indicator. Sulphuric acid 0.1mol/L was used, and the pH was quantified using Equation 1.

$$H_2SO_4 + 2OH^- \rightarrow {SO_4}^{-2} + 2H_2O \qquad \text{Equation 1}$$

5.1.3.3. Particle Size Analysis

The method of sieves was used for the particle size analysis. Eight sieves were used: 4mm, 2mm, 1mm, 0.5mm, 0.25mm, 0.125mm, 0.075mm, 0.038mm and the ground. The sieves were stirred for 15min. The linearized Gates-Gaudin-Schumann

(GGS) (Equation 2) and Rosin-Rammler-Bennet (RRB) (Equation 3) models were calculated, as presented in Table 12 [287–293].

Table 12: Distribution models. [288,289]

Model	Parameters	Equations
GGS	K, m	$X = \left(\frac{D}{k}\right)^{m}$
RRB	D', n	$X = 1 - e^{-(D/D')}$

$$\ln X = -m.\ln K + m.\ln D \qquad \text{Equation 2}$$

$$\ln\left(\ln\left(\frac{1}{1-X}\right)\right) = -n.\ln D' + n.\ln D \qquad \text{Equation 3}$$

Equation 4 was used to calculate the D10, D50 and D90, where x is 10, 50 and 90. Sauter Mean Diameter (SMD), d^2 and d^3 were calculated using Equations 5-7, respectively. The SMD is directly related to the surface area per unit of volume and the mean volumetric fraction [290,291,294].

$$Dx = \left[\left(\frac{D_2 - D_1}{\log \%_2 - \log \%_1} \times \log \%_x\right) - \log \%_1\right] + D_1 \qquad \text{Equation 4}$$

$$SMD = \frac{1}{\sum \frac{x}{D}} \qquad \text{Equation 5}$$

$$d^2 = \frac{\sum \frac{x}{D}}{\sum \frac{x}{D^3}} \qquad \text{Equation 6}$$

$$d^3 = \frac{1}{\sum \frac{x}{D^3}} \qquad \text{Equation 7}$$

5.1.3.4. Energy Dispersive X-Ray Fluorescence Analysis (EDXRF)

EDXRF analysis was carried out using the PANalytical Model Epsilon 3-XL equipment. A quantification is performed through energy dispersion that identifies the

elements contained in the sample from Sodium to Americium. The atoms of the sample generate a characteristic X-rays with irradiation of the X-ray beam. Omnian method was used to quantify elements according to the wavelengths and specific energy for each element. For this purpose, 3g of sample was added in a sample holder with 6µm polypropylene film.

5.1.3.5. Scanning Electron Microscopic Energy-Dispersive X-Ray Spectroscopy (SEM-EDS) Characterization

Analyses by micro-regions was a well-explored technique at the present study to define the chemical compositions of the main mineral phases. Through a microscope, coupled with quantitative analysis system, "in situ" analysis was carried out.

Scanning electron microscopy with backscattered electron detector and coupled with energy dispersion microanalysis was used to analyse the morphology, to identify the main elements presented in the residue and their distribution (Phenom model ProX). The microscope contains a Si (Li) detector with a resolution of 15kV.

Contrast by retro-scattered electrons makes the particles rich in elements with a higher atomic number are lighter in grayscale. Particles with darker tonality represent elements with lower atomic weight. The accuracy and reproducibility of the EDS analyses were evaluated several times through the standards provided.

5.1.3.6. X-Ray Diffraction (XRD) Characterization

A mineralogical assessment of BRM was performed by MiniFlex 300 (Rigaku) with incident CuKα radiation and equipped with graphite monochromator and nickel filter. The sample analyzed was pooled, which was scanned from 3° to 100° (2θ) with a 4°/min rate and 0.02 step.

A data containing diffraction peaks was obtained as a response. Knowing the wavelength of incident X-ray beam and with the aid of Bragg's law, it is possible to determine the interplanar spacings of reflections corresponding to the phases reached by the beam. Comparing these interplanar spacing values with the spacings listed on standard cards, it is possible to determine the presence of phases in the samples. The

PDXL software with the databases COD and ICDD were used to identify and quantify (Rietveld method) the phases that make up the BRM. It should be remembered that the X-ray diffraction technique has no resolution for present phases with a volume fraction less than 5%.

5.1.3.7. Loss On Ignition And Total Organic Carbon

The loss on ignition analyses were performed in two different temperatures: 900°C and 1100°C. In a porcelain crucible, 5g of BRM sample was placed in a muffle furnace [295]. The sample was then heated at a rate of 10°C/min until reaching the desired temperature, and then maintained for 2 hours.

The analysis of Total Organic Carbon was carried out using the TOC equipment solid module (Shimadzu). A sample of 0.05g was put on the porcelain crucible and heated until 900°C to quantify the total carbon. The equipment has, internally, an ozone atmosphere (made using oxygen ultrapure) to promote the carbon oxidation. To quantify the carbon inorganic, 0.05g of sample was mixed with 0.4mL of phosphoric acid in a porcelain crucible. Then, the mixture was heated until 200°C. The difference among these results is the total organic carbon.

5.1.3.8. Microwave Acid Digestion And ICP-OES Analysis

The acid digestion was performed in a microwave acid digester equipment (MARS 6 iWAVE CEM). A sample of BRM was dried at 60˚C for 24h, where 0.1g was mixture of acids: 2.5mL H_2SO_4 (P.A. 98%), 2.5mL H_3PO_4 (P.A. 85%), 2.0mL HNO_3 (P.A. 65%) and 2.0mL HF (P.A. 48%). The temperature of the vessel was increased until 200°C in 5min, and maintained for 60min; then, it was cooled for 15min until 70°C. After reaches the room temperature, 0.9g of boric acid (H_3BO_3) was added for HF neutralization. The sulfuric-phosphoric acids combination is used to react with alumina (Al_2O_3), while nitric acid is used to react with metals in general. Hydrofluoric acid is necessary to react mainly with silica, as well as other oxides.

5.1.4. Results and discussion

5.1.4.1. Analysis of moisture and pH measurements

Analysis of the moisture content of the BRM (fresh sample) were performed using infrared equipment by two different methods and the analysis were made in duplicate. Results obtained were very similar. AutoDry method showed that the moisture content was 23.1%, similarly with result obtained using drying time, which was 22.9%. Comparing with the literature, there are less moisture content than in other residues.

Kaußen & Friedrich (2018) studied a red mud from an old industrial landfill, where the sample contained 30.5% of moisture [296]. Pascual *et.al.* (2009) studied a red mud from Spain for thermal characterization. The moisture content of Spanish red mud was 33.3% [297].

As can be seen, the moisture content on BRM is lower, and it occurs because the red mud is filtrated for NaOH recovery, which decreases its moisture content. Furthermore, the NaOH removal might also declines the alkalinity. Literature review shows that the alkalinity on the red mud is considered high (pH $\geq$13) [263,264]. The pH value of the residue is different due to characteristics of bauxite, which impacts on the NaOH consumption in the process.

For the analysis, a sample of BRM was mixed with deionized water and left to stand for 7 days to obtain an extract of the residue. The alkalinity was measured using a pHmeter and titration. The results obtained were, respectively, 12.7 and 12.6.

As Borra *et.al.* (2015) showed, the extraction of REE from red mud increases when the concentration of acid increases, which is required due to the high alkalinity of the residue [54]. Knowing the pH value of the red mud is important for economic viability, to calculate the acid consumption in the leaching step.

Singh *et.al.* (2018) studied an Indian red mud for construction applications, where the pH of the residue was 11.0 [298]. Snars and Gilks (2009) evaluated red mud from different parts of the world for environmental applications. The pH values varied from 9.75 (Italy) to 12.6 (Worsley – England). In a Brazilian sample analyzed by the authors, the pH was 12.2 [299].

The alkalinity is not only due to the presence of NaOH, but also the presence of metal hydroxides in the red mud. Most of all metals precipitates as hydroxide in alkaline medium [70]. Different methodologies were studied to decline the alkalinity of red mud. Water can be used for NaOH removal, which can reaches 15% after several washes; however, the alkalinity still remains as same as before caused by the buffering activity of the metal hydroxides that are present in the red mud [54].

Panda *et.al*. (2017) characterized and studied a neutralization of a red mud from India using bio-neutralization. The bio-neutralization decreases the red mud alkalinity from pH 10.5 to 7.5 after eight days, and the reached equilibrium after four days [287]. Results obtained for BRM indicates that the use of filter press after the solid-liquid separation declines the moisture content in the BRM, and slightly decreases the alkalinity, the latter being similar to data found in the literature.

5.1.4.2. Particle Size Analysis

Figure 13 shows the particle size distribution of BRM. The value of D10 obtained was 0.06mm, which indicates that 10% of the particles have a diameter smaller than it. The values of D50 and D90 are, respectively, 0.26mm and 0.95mm. Literature review shows that the residue is composed of fine particles. Li et al. (2014) showed that the particles size was 50% lower than 0.15mm, and more than a half of the particles were in range of 0.15 – 0.4mm [300]. The particle size distribution of the red mud studied by Liu and Poon (2016) showed that the D50 and D90 values were, respectively, 0.02mm and 0.04mm [301].

Applying mathematical models is important to obtain statistical parameters used in industrial processes, that are representative of the particulate material residue. Figure 14 and Figure 15 present the GGS and RRB distribution models for BRM. The r^2 (*correlation coefficient*) showed that the residue fitted better to the RRB distribution - 0.9585 -, while r^2 for the GGS model was 0.8114.

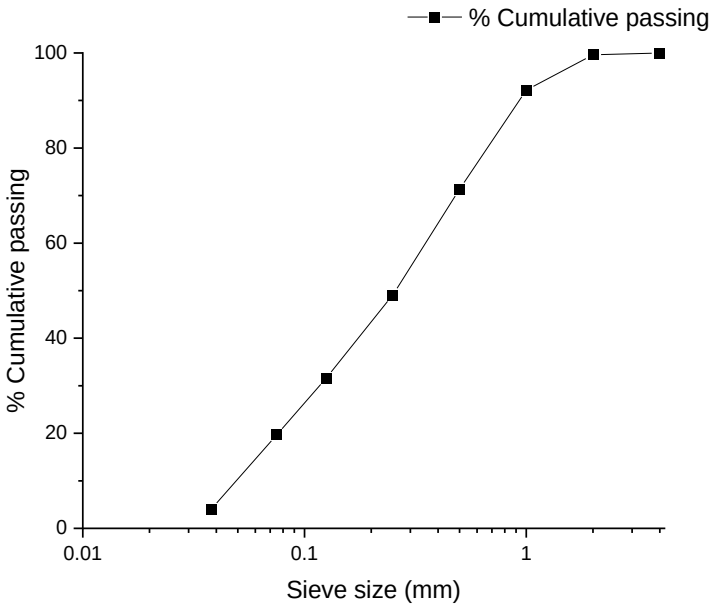

Figure 13: Particle size distribution of Brazilian Red Mud (BRM)

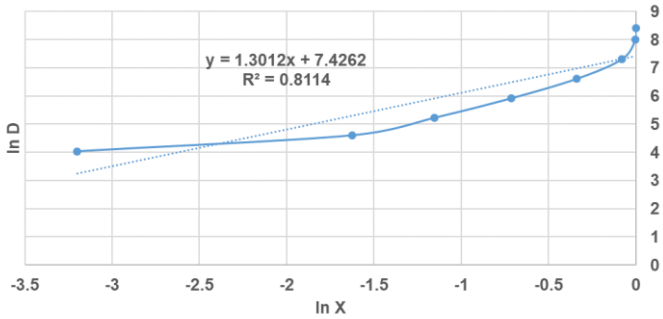

Figure 14: GGS distribution model for BRM

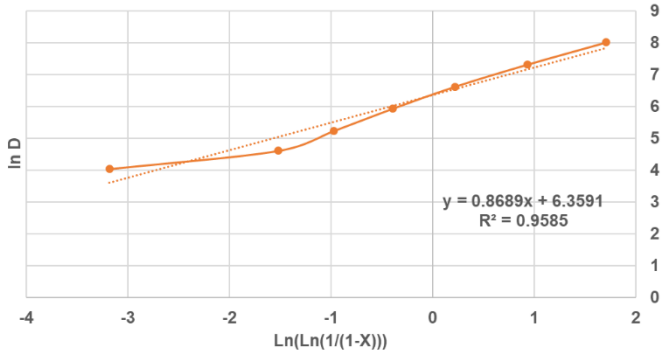

Figure 15: RRB distribution model for BRM

The Indian red mud studied by Singh *et.al.* (2018) were considered by the authors as ultrafine, where the D90 value was 0.075mm. According to the authors, the presence of aluminum and sodium minerals provide to the residue a characteristics fineness [298]. Finer red mud particles were also observed in the residue studied by Panda *et.al.* (2017), where the D10 value was less than 0.1mm [287].

5.1.4.3. Energy Dispersive X-Ray Fluorescence Analysis (EDXRF)

The EDXRF analysis was performed to know which elements are present in the sample. Also, it is helpful for the SEM-EDS and XRD analysis, as well as calibration curves for ICP-OES analysis.

Table 13 shows the concentration of major components (oxides) in BRM, and Table 14 shows the concentration of minor components. The main compound is iron (36.78% as oxide), followed by aluminum (11.65%) and silicon oxides (9.89%). Specifically, the sodium concentration is reduced when comparing with literature, which is a consequence of the press filter uses.

Table 13: Major components (oxides) in the Brazilian Red Mud analyzed in X-ray fluorescence, in percentage

Compound	Concentration (%)
Fe_2O_3	36.78
Al_2O_3	11.65
SiO_2	9.89
CaO	5.16
TiO_2	2.22
Na_2O	2.04
ZrO_2	0.37

Kauβen and Friedrich (2018) analysed a red mud for aluminum recovery by alkaline extraction. XRF analysis showed the presence of 29.5% Fe_2O_3, 27% Al_2O_3,

13.1% SiO_2 and 8% TiO_2. Na_2O content presented in BRM is lower than red mud studied by the authors – 7% -, as for the reasons discussed previously [296].

Mesgari Abbasi *et.al.* (2016) analysed an Iranian residue for the red mud/carbon nanotube composites synthesis. The composition of the sample was 28.78% Fe_2O_3, 21.35% CaO, 19.29% SiO_2 and 17.25% Al_2O_3. TiO_2, Na_2O, MgO and K_2O were also presented in the sample analyzed (7.36%, 1.79%, 1.75%, and 0.63%, respectively) [302].

Snars and Gilkes (2009) studied red mud samples from different countries and industries around the world. The residues with most iron oxide concentration were from Worsley (56.9%) and Brazil (45.6%) [299]. The hydrometallurgical process is harmed by the high iron concentration, which impacts directly the separation process [1,225,283].

Besides acid consumption for the leaching of iron (pH below 3.5), it will be necessary to remove it from the liquor to obtain the desired elements (i.e. precipitation), or use techniques that will recover the desire metal selectively (i.e. solvent extraction or ion exchange resins). Due to the differences in concentration between iron and scandium (more than 1,000 times), iron impacts directly on the costs of the process. For this reason, hydrometallurgical processing must consider these elements for economic feasibility studies.

Table 14: Minor components (oxides) in the Brazilian Red Mud analyzed in X-ray fluorescence, in percentage

Compound	Concentration (%)
V_2O_5	0.088
Cr_2O_3	0.061
MgO	0.056
Nb_2O_5	0.052
Rb_2O	0.039
Bi_2O_3	0.027
SrO	0.022
CuO	0.018
ZnO	0.015
Ga_2O_3	0.015
HgO	0.014
Sc_2O_3	0.012
As_2O_3	0.009

Scandium is the most important element among those presented in minor concentration. In red mud, it can represent more than 95% of economic value [268]. The concentration of scandium in the BRM might be 0.012% (oxide), as X-ray fluorescence analysis showed. Besides that, gallium (Ga_2O_3 – 0.015% in BRM) is also considered as a critical metal and it can be also recovered from red mud [116,303–305]. Gallium production is mainly as a by-product of the Bayer Process, and its amount in bauxite resources is more than 1 million tonne [56].

Scandium is also considered critical metal. Titanium might be considered in the near future, due to its unique proprieties and applications [48]. Major elements content in BRM is quite similar comparing with bauxite residues around the world, as EDXRF analysis showed.

5.1.4.4. Scanning Electron Microscopic Energy-Dispersive X-Ray Spectroscopy (SEM-EDS) Characterization

Figure 16 shows the image of backscattered electrons of the BRM and the EDS spectra (Figure 16a – 400x, b – 2500x, and c– 10000x). The elements presented

in the residue were: oxygen, iron, titanium, calcium, sodium, aluminum and silicon. The main element in the sample is oxygen, once the residue comes from a process to extract alumina from bauxite (oxide) using sodium hydroxide [264], which indicates that the main mineral phases can be oxides and hydroxides.

Iron is the main metal present in the BRM, giving its red coloration to the residue. The presence of silicon in bauxite causes losses of alumina and sodium hydroxide. Reactive silica is the most cause of aluminum and sodium losses, and the literature review indicates that bauxites containing 6-8% of reactive silica are not economical feasible for alumina extraction. In the Bayer Process, silica reacts forming sodium aluminum hydrosilicate and is removed from the Bayer liquor as part of red mud. Several studies and patents have discussed processes to remove reactive silica from the bauxite and to recover aluminum and sodium from red mud [155,306–308].

Scandium and other rare earth elements were not detected in SEM-EDS analyses due to their low concentration. According to Vind et al. (2018), scandium is hosted by hematite, goethite and zircon in a following proportion: 55%, 25% and 10%, respectively. Also, in acid leaching the extraction of scandium is dependent on iron extraction, which is first released from goethite and then from hematite. A reason to explain the main presence of scandium in hematite phase may be it substitutes ferric iron, while in the goethite phase hosts scandium in its particles surface [20,96,129,268].

As it can see, BRM particles can be considered as thin, as shown in Figure 13; in addition, SEM/EDS analysis showed that the smallest particles are composed mainly for iron (82.6%wt), followed by oxygen (7.5%wt) and aluminum (3.1%wt) (Figure 16a). It might indicate the high presence of iron mineral phase, such as hematite or goethite.

In the meantime, the same image showed the biggest particle size is mainly composed of iron (48.7%wt), titanium (36.9%wt) and oxygen (11.8%wt). It can indicates the presence of ilmenite ($FeTiO_3$). Pontikes & Angelopoulos (2013) showed that titanium can be present in the red mud as oxide (rutile and anatase), calcium titanium oxide and iron-titanium oxide. As scandium is present in iron mineral phases, magnetic separation can concentrate scandium but also resulting in metal losses.

Nevertheless, further analysis showed different composition for a same particle size. Figure 16b and Figure 16c show the SEM image in 2500x and 10,000x, respectively and their EDS analysis. Several points were investigated and no separation among the metals were identified, i.e. iron, aluminum and titanium were always presented in the sample with a small difference in their composition among the particles analysed. As a conclusion, a scandium concentration by mechanical separation is rejected.

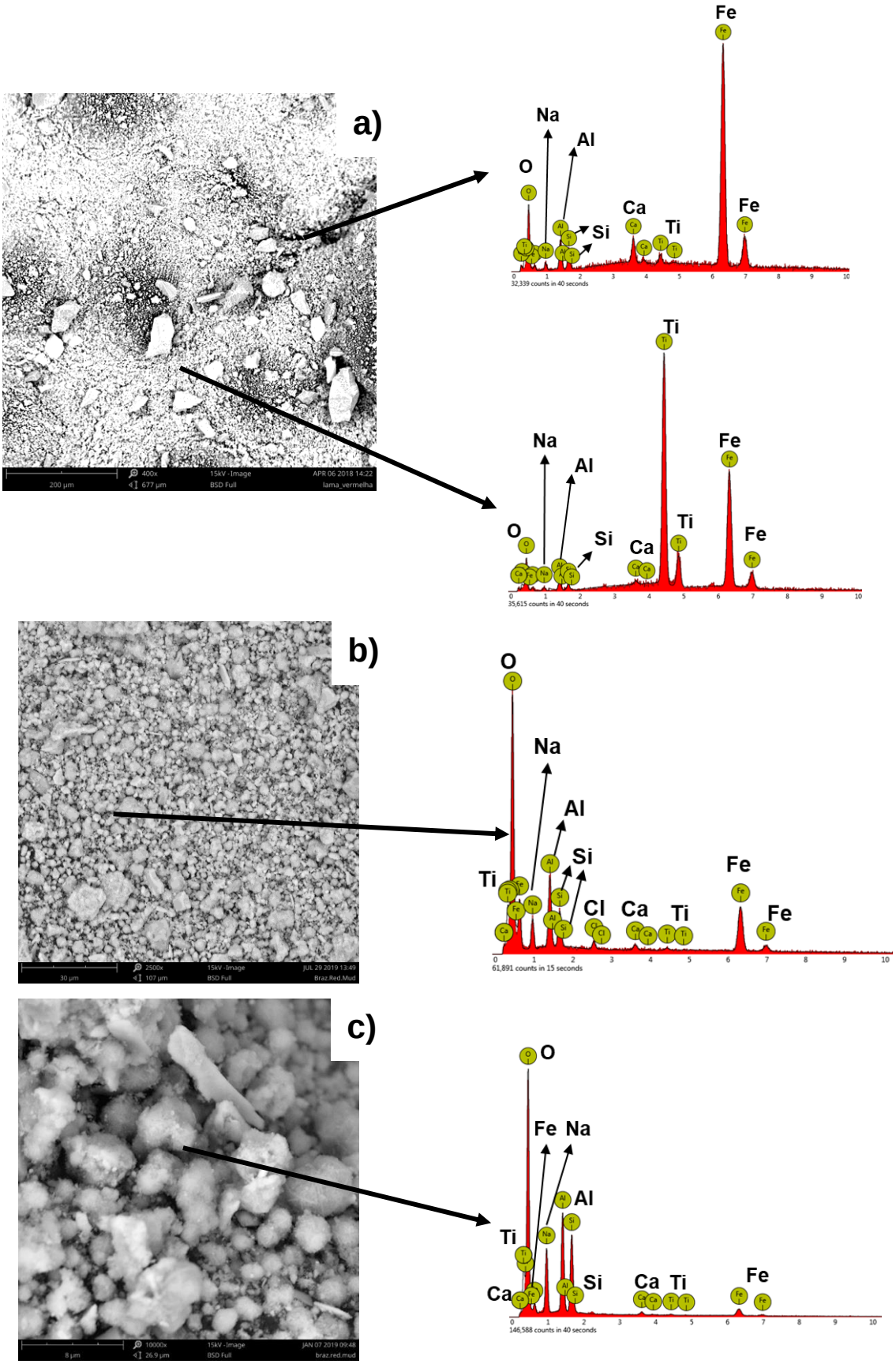

Figure 16: The image of backscattered electrons of the BRM and EDS spectra of the analyzed point (SEM-EDS) a) 400x, b) 2500x and c) 10000x

5.1.4.5. X-Ray Diffraction (XRD) Characterization

The diffractogram of the BRM is shown in Figure 17, as well as the phases identified. Table 15 shows the formula of these phases. The main phase presented in the BRM is hematite, followed by gibbsite, sodalite, and quartz. The results obtained are in accordance with the literature review. Moreover, the results agree with EDXRF and SEM/EDS analyses, which identified as the main elements iron, aluminum, sodium and silicon.

As it was observed in SEM/EDS analysis, titanium can be present in the BRM in different oxides, such as calcium-titanium and iron-titanium oxides, as well as titanium oxide. The XRD showed also the presence of paranatisite (sodium and titanium silicate). It shows that a portion of titanium is also presented as silicate, not only as oxide. The residue studied by Kauβen and Friedrich (2018) has as the main phases hematite (44%), gibbsite (15%), boehmite (13%) and sodalite (7%) [296].

The red mud studied by Abhilash *et.al.* (2014) had different phase proportions. The Indian red mud analyzed by the authors has as major phases gibbsite, quartz, boehmite, calcite, and anatase. Afterward, minor phases presented in the sample were hematite, sodium aluminum titanium silicate, calcium oxide allanite-La and dissakisite-Ce [309]. The Indian red mud studied by Singh *et.al.* (2018) has sharper peaks of Hematite. Peaks of Quartz and Gibbsite were detected, as well as Goethite and Calcite [298]. The Chinese red mud studied by Liu *et.al.* (2009) had as the mineral phases quartz, hematite, limonite, cancrinite, calcite, and illite. Most of the iron in the sample was presented as hematite and limonite (98.41%) [310].

Table 15: The main phases, their formulas and percentage detected in the BRM sample

Phase	Formula
Quartz	SiO_2
Sodalite	$Na_4(Al_3Si_3O_{12})Cl$
Gibbsite	$Al(OH)_3$
Goethite	FeO(OH)
Hematite	Fe_2O_3
Boehmite	AlO(OH)
Gypsum	$CaSO_4.2H_2O$

In study developed by Snars and Gilkes (2009), red mud samples from different parts of the world were analyzed and distinct phases were identified. In general, major phases presented in red mud were hematite, goethite, quartz, gibbsite, boehmite, anatase and calcite. Red mud from Italy had Halite (NaCl) as the main substance, due to the previous treatment with seawater before its disposal. Sample from Brazil analyzed by the authors had hematite and goethite as the main mineral phase, and a small quantity of gibbsite. Peaks of quartz were not identified [299].

The red mud studied by Panda *et.al.* (2017) has predominantly gibbsite, hematite, and quartz. Vanadium oxide was also detected [287]. Liu *et.al.* (2017) studied the scandium recovery from high alkali Chinese red mud, which the main phases identified by the authors were goethite (25.52%), hematite (14.63%), gibbsite (11.90%), zeolite (6.33%) and quartz (6.28%) [311].

The difference between mineral phases of the residue is not only their composition, but also the mineral phases of bauxite processed on the Bayer process. Still, as each process is adapted to process a specific mineral, it affects the residue generated. The main phases found in red muds are composed by iron (Hematite and Goethite), aluminum (Boehmite and Gibbsite) and silicon (Quartz), and also calcium (Calcite and Gypsum) and titanium (Anatase).

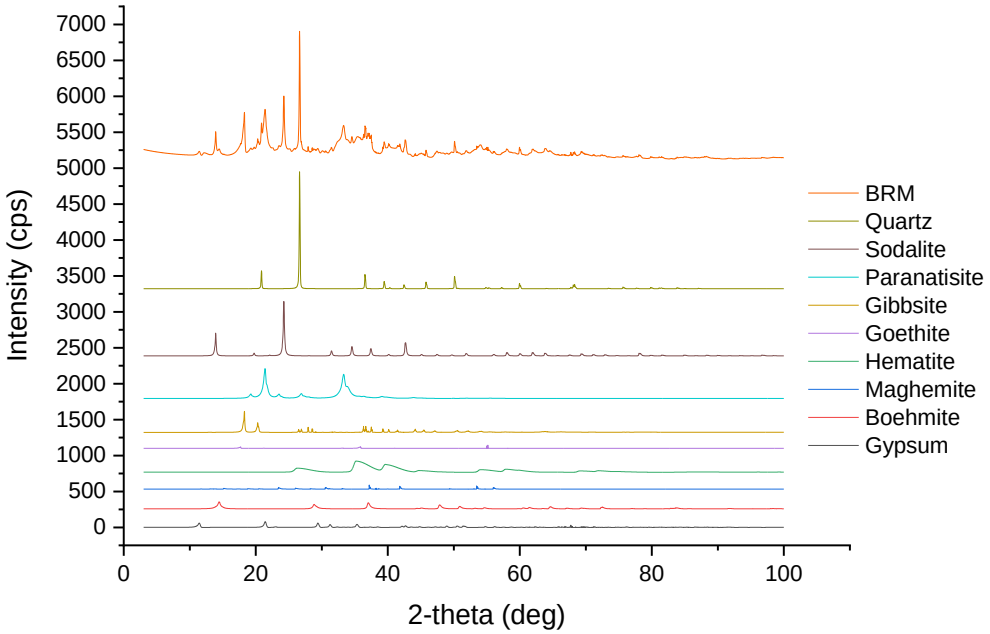

Figure 17: X-ray diffractogram of the BRM sample and the main phases detected

5.1.4.6. Loss On Ignition And Total Organic Carbon

Experiments of loss on ignition were performed in two different temperatures: 900°C and 1100°C. It represents the organic and inorganic carbon, and water which is chemically bound in the minerals [298,312]. Results were 14.5% and 14.8% for temperatures of 900°C and 1100°C, respectively. It is possible to confirm that the results were pretty much similar.

The loss on ignition of the red mud studied by Liu and Poon (2016) was 8.14% [301]. Gräfe *et.al.* (2011) examined different samples of red mud, where the loss on ignition varied from 4.4% (Arkansas) to 14% (Suriname) [295].

The organic carbon analysis were carried out in two parts: the first is the total carbon analysis, where a sample is heated until 900°C and the sensor makes the quantification; the second part is the inorganic carbon quantification, where the sample is mixed with phosphoric acid and heated until 200°C. It was not found any data in literature review reporting the presence of organic carbon in red mud. In the same way, Power & Loh (2010) discuss the origins and chemistry of organic compounds in the Bayer process. According to the authors, the presence of organic matter raise the costs

for alumina production, which are composed of humic substances, lignins and cellulose. Furthermore, the organic carbon distribution in bauxite residue is different comparing with the raw material, incorporated during the bauxite leaching as both precipitate and by adsorption. The organic matter differs also in concentration and types of compounds [313].

Results showed that the total carbon presented in the BRM is 0.6%, while the inorganic carbon is 0.32%. Therefore, the total organic carbon is 0.28%. As pointed before, analysis of organic carbon in red mud were not found in the literature. Power *et al.* (2010) evaluated bauxite samples from Guinee, Australia, Brazil, Suriname and India. The authors reported that the organic carbon percentage were, respectively, 0.25%, 0.03%, 0.18%, 0.47% and 0.18% [313].

5.1.4.7. Microwave acid digestion and characterization using inductively-coupled plasma (ICP-OES)

The digestion in the microwave was performed using 2.5mL of sulfuric acid, 2.5mL of phosphoric acid, 2mL of hydrofluoric acid and 2mL of nitric acid for each 0.1g of BRM. The liquor obtained was filtrated, but no solid phase was detected. Then, it was analyzed for the main elements: Fe, Al, Si, Ca, Na, Ti, Nb, Sc, Y and Zr. Besides yttrium was not detected in the EDXRF analysis, it is in most cases found with scandium. Still, this REE is considered a critical metal. Its applications are in lasers, phosphors, alloys, medical devices, superconductors, wind turbine additive and other sustainable technologies [283,314].

Results are shown in Table 16. Iron is the main element in the sample – 189.4kg/tonne, which represents 46.45% of all elements analyzed. The concentration of aluminum, silicon and titanium are 91.8kg/tonne (22.52%), 75.2kg/tonne (18.53%) and 14.1kg/tonne (3.47%), respectively. Among the elements presented in minor concentration, there are niobium, zirconium, scandium and yttrium in the concentration of 1356.2mg/kg, 1320.3mg/kg, and 42.21mg/kg and 24mg/kg, respectively.

The Table 16 also compares the composition of BRM with red mud samples from different parts of the world. The goal of this part is to study the differences between the bauxite residue from Brazil and other countries. All those studies evaluated scandium and REE recovery using techniques discussed in Introduction. The

concentration of those metals are presented in the literature in a different ways, as concentration or percentage which is indicated.

Zirconium was detected in the sample from Jamaica, where the concentration found is 6.5mg/kg. The presence of yttrium was detected in samples from India (0.005%), Greece (76mg/kg and 0.01%) and from Jamaica, being the last one with the highest concentration among all – 373mg/kg. Scandium, which represents 95% of the economic value of the rare earth elements, was detected in the samples from India (0.005%), China (76mg/kg), Greece (121mg/kg and 0.02%), Canada (47mg/kg) and Jamaica (55mg/kg).

Among the elements present as majority, the BRM has the highest silicon concentration of all (23.7%). As Alkan *et.al.* (2018) showed, acid leaching of the red mud causes a silica gel formation, which difficult the hydrometallurgical problematic [48]. For this reason, the recovery of scandium from BRM has technical viability to be overcome.

Aluminum oxide content in the BRM is also higher than the red mud samples verified in the literature, which may be caused by the elevated reactive silica content in bauxite, which resulted in high aluminum and silicon concentration in the residue. Sodium oxide content in the BRM is the lowest among them, due to the use of the press filter to recover NaOH solution during the process. As a result, acid consumption can be lower than other red muds given in Table 16.

Narayanan *et al.* 2018 showed that it is also possible to recover elements such as lanthanum, cerium and praseodymium from red mud. On the other hand, separation of those rare earth elements has technical feasibility to come through due to its chemical characteristics [162]. Zirconium could be a sub-product of the process of scandium recovery from BRM. Nevertheless, scandium is still the most valuable element in the residue to be recovered. Rare earth elements such as lanthanum and cerium were not identified in the BRM sample.

Table 16: Composition of the BRM and data reported from other red muds. The values are presented in percentage of oxides, except when mg/kg or in elementary is indicated

Country	Brazil	India	China	China	China	Greece	Greece	Australia	Spain	Canada	Jamaica
	BRM	[309]	[311]	[300]	[116]	[51]	[315]	[281]	[297]	[316]	[162]
Fe_2O_3	36.4	37.03	27.2[2]	48.2[2]	20.74	44.6	42.34	29.82	47.85	44[2]	20[2]
Al_2O_3	23.3	19.87	11.87[2]	7.3	20.73	23.6	16.26	21.69	20.2	18.2[2]	16[2]
SiO_2	21.6	10.23	9.44[2]	8	17.19	10.2	6.97	12.28	7.5	14.3[2]	[1]
CaO	5.9	[1]	2.24[2]	0.9	15.85	11.2	11.64	1.79	6.22	4.4[2]	2[2]
Na_2O	9.0	[1]	7.31[2]	1.4	6.39	2.5	3.83	5.19	8.4	6.2[2]	
TiO_2	3.2	11.98	2.16[2]	1.4	5.29	5.7	4.27	6.88	9.91	9.3[2]	18[2]
Sc_2O_3	0.0097	0.005[2]	76[3]	[1]	[1]	121[3]	0.02	[1]	[1]	47[3]	55[3]
Y_2O_3	0.0041	0.001	[1]	[1]	[1]	76[3]	0.01	[1]	[1]	[1]	373[3]
ZrO_2	0.2399	[1]	[1]	[1]	[1]	[1]	[1]	[1]	[1]	[1]	6.5[3]
V_2O_5	0.0310	[1]	[1]	[1]	[1]	[1]	[1]	[1]	[1]	[1]	[1]
La_2O_3	0.016	[1]	[1]	[1]	[1]	[1]	[1]	[1]	[1]	[1]	[1]
CeO_2	0.0664	[1]	[1]	[1]	[1]	[1]	[1]	[1]	[1]	[1]	[1]
Nd_2O_5	0.0109	[1]	[1]	[1]	[1]	[1]	[1]	[1]	[1]	[1]	[1]

[1] not analyzed

[2] elementary (%)

[3] elementary (mg/kg)

5.1.5. Discussion about the scandium extraction from Brazilian red mud by leaching-ion exchange process

Paramguru et al. (2005) published a review paper about the many uses for red mud, not only for scandium extraction [317]. Akcil et al. (2018) discussed a several techniques for scandium extraction from red mud by hydrometallurgical processing [49]. However, a thorough characterization of Brazilian red mud was never been carried out, which showed important to design a process that overcomes the challenges of scandium extraction from BRM. As discussed previously in Introduction, it will be discussed the scandium extraction from BRM, techniques well explored and the challenges to be overcome.

From a complete characterization of the residue, mainly quantifying the scandium concentration, an extraction process can be designed. The BRM contains the lowest sodium content; in other hand, silicon concentration is the highest. Both considerations represents positives and negatives aspects, respectively.

A hydrometallurgical route comprises the steps of leaching (acid or alkaline), purification (i.e. precipitation) and followed by selective separation (i.e. solvent extraction of ion exchange resins) [318]. In the leaching step, direct leaching is advantageous because it is not necessary to prepare the material, which would increase process costs [48,176,268]. In a few cases, magnetic separation can concentrate the desire metals in non-magnetic or magnetic fractions [49,317,319,320].

However, in our literature review, magnetic separation was not applied for red mud without pre-treatment. Deng et al. (2017) concentrated scandium and titanium by magnetic separation. Previously, the bauxite residue was mixed with sodium salts and the non-magnetic material concentrated in scandium and titanium was obtained after a carbothermal reductive roasting [321]. Despite the high scandium separation, the temperature reaches at 1050°C,[300] which result in high energy consumption.

The leaching of the scandium, as well as yttrium, titanium, zirconium and gallium, is possible in an acid medium at pH below 4.0. Yttrium can be leached in pH below 6.5. Meanwhile, the leaching of zirconium is possible in pH below 0 [70].

In an acid medium, iron and aluminum are also leached. Both elements are the main metals presented in the BRM. The liquor generated in the leaching would have a high amount of those elements. Studies indicated that the iron extraction in acidic medium can reaches 50% depending on leaching conditions, but most of the best results for scandium extraction reports at least 5% of iron extraction [281]. In general, iron concentration in the liquor might reaches 300pm, while REE content reaches 9ppm [54].

Equation 1 shows the leaching of metal hydroxides in acidic medium (*Me* = metal). Iron is mainly presented as hematite (Equation 8 and 9), where its leaching can generate both ferrous iron and ferric iron, depending on the redox potential.

Titanium and zirconium leaching are represented in Equation 10. The leaching of scandium by sulfuric acid is shown in Equation 11. A thermodynamic simulation was carried out on FactSage 7.2 software, which showed that the main presence of Sc^{+3} in the liquor, and low quantity of $Sc(OH)^{+2}$ (Equation 11) The use of other leaching agents, such as nitric, hydrochloride or phosphoric acid, also obtain scandium as +3. The use of computational thermodynamic can be a useful tool on leaching studies.

$$Me(OH)_x + 2x\ H^+ \leftrightarrow Me^{+x} + x\ H_2O \qquad \text{Equation 8}$$

$$Fe_2O_3 + 6\ H^+ \leftrightarrow\ 2Fe^{+3} + 3\ H_2O \qquad \text{Equation 9}$$

$$(Ti\ or\ Zr)O_2 +\ 4\ H^+ \leftrightarrow\ (Ti\ or\ Zr)^{+4} + 2\ H_2O \qquad \text{Equation 10}$$

$$2\ Sc(OH)_3 + 3\ H_2SO_4 \leftrightarrow 2\ Sc^{+3} + 6\ H_2O + 3\ {SO_4}^{-2} \qquad \text{Equation 11}$$

As can be observed in Table 16, scandium content in the BRM is pretty similar with red muds around the world, as well as iron and aluminum. There are two main differences: sodium and silicon content. As explained before, the low concentration of sodium is due to the filter press process for sodium hydroxide recovery. Its removal can benefit the leaching process, where the acid consumption must be lower than other red muds.

Due to the alkalinity of the residue, it is necessary high concentrations of acid for both neutralize the residue and to extract scandium. The acid consumption can reaches 70% during the process [322]. The extraction of metals increases as the acid concentration increased. Pepper et al. (2016) showed that the iron extraction increased from 5% using 1M of sulfuric acid to 50% using 5M [281]. The authors do not evaluate the leaching of scandium, but the scandium extraction is directly related to iron leaching.

Despite the advantage on acid consumption that BRM has comparing with the literature, on the other hand, the high silicon content is a problem on leaching step, which causes the silica gel formation. The gel formed make the solid/liquid separation difficult and trap a part of liquor generated. Equation 12 shows the monosilicic acid ($Si(OH)_4$) formation, which polymerizes producing polysilicic acid (Figure 18) [323]. The silica gel formation can be avoided using high liquid/solid ratio (up to 1/25), which can also increases the scandium extraction. In spite of that, high amount of solution would be treated for selective scandium separation.

In order to solve this problem, Alkan *et.al.* (2018) studied the leaching process for scandium and titanium extraction with sulfuric acid and hydrogen peroxide. The use of H_2SO_4+H_2O_2 avoided silica gel formation. Leaching experiments without hydrogen peroxide showed dissolution of silicon, while experiments with oxidant agent showed no silicon dissolution, where all silicon precipitates forming Quartz [48].

However, there are two main points about it. First, there is no study on the literature about the kinetics of silica gel formation during the acid leaching of red mud, which can be used to evaluate different routes to depress or to avoid its formation. Allied to that, the study presented by Alkan et al. also didn’t explored the kinetics of H_2SO_4+H_2O_2 reaction. Secondly, most of the studies considered the leaching in solid-liquid ratio equals to 1/50, which increases the costs of the process with the quantity of solution used to extract the metals and also to be separated. The BRM sample can be used in a future study to explore the kinetics on silica gel formation and investigate different possibilities to avoid it. Moreover, the use of thermodynamic simulation on leaching may be used to study the scandium extraction avoiding the silica gel forming [41].

$$n\,SiO_{2_{(s)}} + 2n\,H_2O \rightarrow n\,Si(OH)_{4_{(aq)}}$$ Equation 12

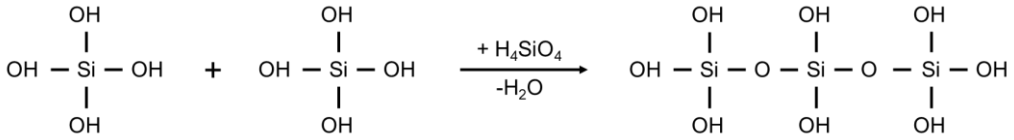

Figure 18: Silica gel polymerization during the acid leaching producing polysilicic acid

After the leaching, a precipitation is required to purify the liquor to remove contaminants such as iron and aluminum. However, the precipitation technique through pH variation can present disadvantages due to the high acid concentration. Nonetheless, the iron precipitation causes the co-precipitation of several metals presented in the solution, primarily in minor concentration, which might result in scandium losses [324,325].

The separation can be carried out using an ion exchange technique, both ion exchange resins as well as solvent extraction. The advantage of chelating resins is the selectivity for ions present in solution [326,327], which is important to remove scandium from the liquor.

Literature review showed that iron concentration must be at least 1,000 times higher than scandium. Bao *et.al.* (2018) studied two chelating resins, aminomethyl-phosphonic (TP 260) and iminodiacetate (TP 209), and one solvent impregnated resin, bis(2,4,4-trimethylpentyl) phosphinic (TP 272), for scandium adsorption. The scandium-iron separation was 56 times higher for Fe(II) than Fe(III), due to the order of resin selectivity [284]. Iron and aluminum are the main contaminants present in the liquor, and both are partially adsorbed by the resin.

Li *et.al.* (2018) studied the scandium recovery by solvent extraction. The organic extractant used was D2EHPA with di-(2-ethylhexyl) phosphate. The effect of pH was studied and scandium separation increased as the pH increased. The main contaminant which decreased scandium extraction efficiency was calcium. The process efficiency was 98% using 2% DEHPA at pH 1.8 as aqueous/organic (A/O) ratio 3:1.[328] According to the authors' knowledge and literature review, both chelating resin and solvent extraction can separate selectively scandium, but iron and

aluminum would be also adsorbed. An elution/stripping will carry out also those elements. Synergism can also benefit the selective separation.

This discussion comparing with the literature shows that the main challenges to be overcome on scandium extraction from BRM are: i) to avoid the silica gel formation; ii) selective elution/stripping from ion exchange separation. The acid consumption might not be a problem due to the low sodium content resulting in higher scandium extraction and economic feasibility. The literature review also showed that the selective scandium separation should be further explored.

5.2. Extraction of scandium from critical elements-bearing mining waste: silica gel avoiding in leaching reaction

A.B. BOTELHO JUNIOR; D.C.R. ESPINOSA; J.A.S. TENÓRIO

Department of Chemical Engineering; Polytechnic School, University of Sao Paulo, Sao Paulo – Brazil.

ABSTRACT

Scandium is one of the most valuable rare earth elements, and its extraction is centralized in China. For this reason, the search of new scandium sources is required to supply the demand. Bauxite residue is considered a secondary scandium resource. It has estimated around 4 billion tonnes of bauxite residue worldwide with 20–200mg/kg of scandium. Hydrometallurgical route is considered advantageous due to its low content. However, the acid leaching generates silica gel reducing the extraction rate and making the solid/liquid separation difficult. H_2O_2 can be used to avoid its synthesis, and the parameters during the leaching must be explored. Despite the studies in the literature about scandium extraction from bauxite residue, there is a lack of investigation about suppressing the synthesis of silica gel in the acid reaction. For this, the present study aimed the scandium extraction from bauxite residue by H_2SO_4 and H_3PO_4 leaching. The use of H_2O_2 was evaluated to avoid silica gel formation. The effect of time, temperature and acid concentration was evaluated. Results showed that scandium extraction is directly related to iron extraction. The H_2O_2 contributed to silicon oxide formation during the acid reaction but declined scandium extraction by half. The leaching rate increased from 25°C to 90°C achieving 99% for iron and aluminum and 91% for scandium. The increase of H_2SO_4 concentration increased the titanium leaching. Leaching of metals using H_3PO_4 was similar to H_2SO_4 leaching. Moreover, the extractive process focused on near-zero-waste generation is essential to avoid waste stored in dams.

Keywords: Leaching; bauxite residue; red mud; sustainability.

5.2.1. Introduction

In 2020, the European Union updated the list of critical materials, those at risk of interruption in the short and medium-term. At the same, these elements in the list are supplied for a few countries, which results in market control. In the new list, bauxite, lithium, titanium, and strontium were added, totalizing 30 critical materials. There is also niobium in the list mainly supplied by Brazil, lithium by Chile, and the rare earth elements, where China controls around 95% of the market [329]. For this reason, the search for new sources of critical materials (both primary or secondary) is necessary to be independent of other countries, and there is no risk of interruption in supply.

Among the list elements, the main critical could be the rare earth elements (scandium, yttrium, and the lanthanide group elements) since up to 98% of global production is from China [62,329]. Scandium is one of the most valuable (US$ 3,800 per kg of the oxide 99.99% purity), and it's not usually found in rare-earth minerals, except in the Bayan Obo reserve (China) with 0.006% - 0.016% of Sc_2O_3 [1,3]. It is worth mentioning that scandium is not traded as a commodity, and for this reason its price can vary significantly.

Scandium is mainly applied in solid-oxide fuel cells as well as heat exchangers. Also, its use for optical, electronic, aeronautical, automotive, and transportation industries is due to its alloy characteristics, mainly for military applications. Moreover, its consumption has increased due to the specific mechanical and chemical properties over other metals [20].

Scandium extraction is restricted to a uranium extraction (0.1% of Sc_2O_3). China, the Philippines, and Russia are the leaders in global production. New recovery processes have been developed, as in the case of Canada (Sorel-Tracy, Quebec) and Australia (the Owendale and Sunrise projects in New South Wales and the SCONI project in Queensland). In the Philippines, scandium oxalate was produced from high-pressure leaching of nickel operation. In Russia, scandium recovery from bauxite residue is ongoing (Ural Mountains). There is a development of process for scandium recovery uranium production in Dalur (Kurgan region). In Turkey, ammonium-scandium-hexafluoride was produced as by-product from nickel and cobalt production [1,3,20].

Moreover, slags from blast furnaces used in the production cast iron and tin smelting [1], nickel laterite residue [20], and bauxite residues [330] are also sources of scandium.

Nickel laterite ores in Australia and Brazil may contain high scandium-content – up to 400mg/kg; however, scandium is found only in a few nickel reserves [20,331]. Bauxites worldwide, on the other hand, are rich in scandium – from 7mg/kg to 53mg/kg in the ore. After the Bayer Process for alumina production, the scandium is trapped by the bauxite residue (also called *red mud*) and sent to dams. Scandium concentration may vary from 134mg/kg (Greece) and 121mg/kg (Jamaica) to 43mg/kg (Brazil) [37,129,176]. Russian bauxite residue contains from 50 to more than 300mg/kg of scandium [125,126].

It has calculated up to 4 billion tonnes of bauxite residue stored worldwide, whose value in scandium oxide can vary between US$400 – 4,500billion. Thus, and due to the problems that mining tailings in dams have been caused [27,332,333], different strategies have been explored for scandium extraction from the residue: pyro+hydrometallurgical routes and hydrometallurgical.

Borra et al. (2016) studied the pyro+hydrometallurgical processing for scandium obtaining. First, an alkali fusion (950°C – 1500°C) followed by water leaching was used for aluminum recovery. Further, the solid phase's smelting is used for pig iron obtaining, and the slag is leached by acid for rare earth elements (including scandium) and titanium recovery [51]. Besides, the flowchart results in different products, energy consumption could make the process expensive, and the slag with high silicate content could result in a silica gel formation during the acid leaching.

Different hydrometallurgical processing has been explored for scandium recovery from the bauxite residue, as depicted in Table 17. Anawati & Azimi (2019) studied the acid baking using sulfuric acid (H_2SO_4) followed by water leaching, where the efficiency achieved up to 80%. In this case, as most of the scandium is trapped in iron mineral phases, the process focused on converting the iron compounds into a soluble one in water and rare earth elements [164].

Rivera et al. (2018) studied the dry digestion of bauxite residue comparing with direct leaching to avoid the silica gel formation. In direct leaching, silicon leaching increased as the acid concentration increased. On the other hand, dry digestion

avoided silicon dissolution due to the silica hydrolysis depletion, and the leaching of scandium and iron achieved 40% and 25%, respectively [127].

Reid et al. (2017) [316], Rychkov et al. (2021) [125], and Alkan et al. (2018) [48] studied the direct leaching of bauxite residue by H_2SO_4, and Borra et al. (2015) [54] studied the hydrochloride acid (HCl) as leaching agent comparing with minerals acids and results indicated that the scandium leaching rate was similar among them. The scandium extraction by different leaching agents could be useful for industrial applications. Furthermore, Bonomi et al. (2018) [176] studied an ionic liquid for scandium recovery in temperatures above 150°C as an option for industrial approach.

The biggest challenge for direct leaching of bauxite residue is the silica gel formation. Alkan et al. (2018) demonstrated that its synthesis could be avoided using hydrogen peroxide (H_2O_2), but scandium leaching efficiency decreased since iron oxides were not leached [48]. Nevertheless, the acid leaching of bauxite residue suppressing silica gel formation avoids the liquor being trapped during its synthesis, increasing the process efficiency. In other work, Alkan et al. (2019) studied the scandium leaching from bauxite slag leaching after iron removal under oxidizing medium (H_2O_2). In direct leaching experiments, the scandium extraction achieved similar results than direct leaching, but silicon leaching was close to 0% [334]. As observed, the use of H_2O_2 can avoid the silicon leaching and consequent silica gel formation.

Table 17: An overview of previous studies for scandium extraction from bauxite residue by different hydrometallurgical routes

Reference	Bauxite residue source	Scandium content	Process	Extracting agent	Leaching agent concentration	Solid/Liquid ratio	Temperature	Time	Efficiency
Ochsenkuehn-Petropoulou et al. (2018) [161]	Greece	98-127.9mg/kg	Direct leaching	H_2SO_4	3M	1/5	90°C	60min	50%
Rychkov et al. (2021) [125]	Russia	0.009%	Carbonization method + Direct leaching	CO_2 H_2SO_4	pH 0	1/3	30°C	6h	50%
Wei et al. (2020) [335]	China	0.012% (oxide)	Roasting and magnetic separation before direct leaching	HCl	20%	1/6	80°C	5h	80%
Anawati & Azimi (2019) [164]	Canada	31.1mg/kg	Acid baking + water leaching	H_2SO_4 H_2O	0.95mL H_2SO_4/g BR	9.5mL H_2O/g BR	200°C	2h	80%
Alkan et al. (2018) [48]	Greece	120mg/kg	Direct leaching	H_2SO_4 + H_2O_2	2.5 M H_2SO_4 : 2.5 M H_2O_2	1/10	90°C	30min	68%
Bonomi et al. (2018) [176]	Greece	134mg/kg	Direct leaching	1-ethyl-3-methylimidazolium hydrogensulfate (Brønsted acidic ionic liquid)	-	2.5%	200°C	12h	80%

Cont. Table 17

Zhu et al. (2020) [53]	China	0.015%	Direct leaching	H_2SO_4 + CaF_2	7mol/L H_2SO_4 + 5% CaF_2	1/5	90°C	75min	95%
Rivera et al. (2018) [127]	Greece	121mg/kg	Dry digestion followed by water leaching	H_2SO_4	98%	1/1 (dry digestion); 1/20 (water leaching)	25°C	24h	40%

Furthermore, the study of different leaching agents can benefit industrial applications. The leaching residue's composition must be studied to focus on a new application or use, preventing more waste in dams and contributing to the circular economy. For this reason, the goal of the present study was the extraction of scandium from bauxite residue in aqueous media. The present study contributes to the 17 sustainable development goals, mainly the targets 8.2, 8.4, 12.4, and 12.6 [42].

There is no study in the literature of scandium extraction from a Brazilian bauxite residue. Sulfuric and phosphoric acid were studied as leaching agents. The effect of solid-liquid ratio, acid concentration, time, and temperature were evaluated. Hydrogen peroxide (H_2O_2) was tested to avoid silica gel formation, and its concentration was studied.

Besides the efficiency rates, the solid phase (leaching residue) was also analyzed to explore future applications for the waste generated during the extractive step. The residue formed in oxidative acid leaching (acid + H_2O_2) was also analyzed to study the silica gel formation.

5.2.2. Materials and methods

5.2.2.1. Materials

A Brazilian company provided the bauxite residue used in the present study. The material was dried at 60˚C for 24h before chemical characterization. The chemical composition was carried out by complete dissolution of the residue by acid mixture (H_3PO_4, HF, HNO_3, and H_2SO_4) and further neutralization by boric acid (H_3BO_3) in a microwave acid digestion system (CEM MARS 6 iWAVE) followed by Inductively Coupled Plasma Optical Emission Spectrometer (ICP-OES – Agilent Technologies 70 series).

Particle size distribution was analyzed in eight different sieves (4, 2, 1, 0.5, 0.25, 0.125, 0.075, and 0.038mm). The mineralogical assessment of the bauxite residue was investigated using MiniFlex 300 X-ray diffractometer (Rigaku) from 3° to 100° (2θ) at a rate of 4°/min in steps of 0.02°. Loss of ignition was tested at 900˚C and 1100˚C at a rate of 10°C/min for 2h. The chemical characterization of the bauxite residue used in leaching experiments has already been reported elsewhere [37].

All reagents used in leaching experiments were of analytical grade: H_3PO_4 (85%), H_2SO_4 (98%), and H_2O_2 (27%). Ultrapure water was used to prepare the acid solutions. For the leaching experiments, the bauxite residue was dried at 60°C for 24h. Then, the material was ground using a mortar and pestle.

5.2.2.2. Methodology

Leaching experiments were performed in an automated 1L batch-glass reactor (Atlas Sodium) under stirring (800rpm) with a reflux condenser and temperature control. Acid solution (500mL) was added into the reactor until reaching the desired temperature before adding the dry material. After the leaching procedure, the solid-liquid mixture was collected from the reactor, and the separation was first performed in ultracentrifuge (3,000rpm during 10min). Then, the liquor was filtered from the leaching residue using a glass fiber filter paper (0.7μm). The leaching residue was washed using ultrapure water. Both liquor and washing water were analyzed.

The experimental error was determined using acid concentration equals 20%, and the leaching experiment performed at 25°C, 800rpm, solid-liquid ratio equals 1/10 during 8 hours. The experiment was carried out in triplicate [40]. The standard variation was equal to 2.4%, and it was applied in all experiments performed in the present study.

Table 18 shows the experimental conditions for scandium extraction in an acidic medium. Samples were analyzed in ICP-OES and EDXRF (PANalytical Epsilon 3 XL) (leaching liquor). The mineralogy of the leaching residue was analyzed in XRD. Samples were diluted in HNO_3 4% for chemical analyzes in ICP-OES. Iron, titanium, and aluminum were analyzed in EDXRF, and scandium was analyzed in ICP-OES. The leaching residue was washed using ultrapure water and dried at 60˚C for 24h before XRD analysis. Achieving the best conditions, the final liquor was characterized by ICP-OES.

Table 18: Conditions of leaching experiments for scandium extraction from bauxite residue

Time	30 – 660min
Solid-liquid ratio (S/L)	1/10 – 1/50
H_2O_2	15g/L (0.44mol/L) and 1 – 4mL/h (0.35 – 1.40mol/L)
Temperature	25 – 90˚C
Concentration	20% (3.8mol/L) - 60% (11.5mol/L)

5.2.3. Results and discussion

5.2.3.1. Characterization of the critical elements-bearing mining waste

The characterization of the bauxite residue is presented in Table 19. The main element is iron, followed by aluminum, silicon, sodium, calcium, and titanium. Among the element in low concentration, there are five rare earth elements, vanadium, and zirconium. Considering the most valuable elements in the bauxite residue, scandium represents 93% of economic value, followed by zirconium (5.3%) and cerium (1.4%). For this reason, the focus on leaching experiments was on scandium leaching as the target element, as well as aluminum and iron as the primary contaminants.

XRD's principal mineral phases were: Quartz, Sodalite, Paranatisite, Gibbsite, Goethite, Hematite, Boehmite, and Gypsum (see Figure 24). The moisture content was 23.1%, and the D10, D50, and D90 were 0.06mm, 0.26mm, and 0.95mm, respectively. The losses on ignition analyses carried out at 900°C, and 1100°C achieved similar results: 14.5% and 14.8%, respectively. The total carbon content was 0.6%, the inorganic carbon was 0.32%, and the total organic carbon was 0.28%.

Table 19: Characterization of bauxite residue

%	**Fe_2O_3**	36.4
	Al_2O_3	23.3
	SiO_2	21.6
	Cao	5.9
	Na_2O	9.0
	TiO_2	3.2
g/tonne	**Sc**	43.5
	Y	24.2
	Zr	1329.8
	V	130.3
	La	103.7
	Ce	405.1
	Nd	77.6

5.2.3.2. Kinetic modeling of scandium extraction

The leaching of scandium, iron, aluminum, silicon, and zirconium were evaluated overtime at 25°C, 800rpm, H_2SO_4 concentration equals to 20% solid-liquid ratio equals to 1/10 for 10 hours (600min). Figure 19a shows the leaching rate of aluminum, iron, titanium, zirconium, and silicon over time. The acid leaching is first for neutralization of the alkali residue and dissolution of aluminosilicates [54].

The extraction of scandium and iron increases over time, while aluminum and zirconium slightly decreased after 4h. Titanium leaching remained constant. The leaching of silicon remained constant between 1-4h and then declined after 4h of the experiment. It occurs due to the silica gel formation (Figure 20), which traps the liquor as the chain increases. For this reason, the leaching rate declined for silicon over time.

Equation 13 depicts the silica gel formation from the sodalite mineral phase. The synthesis occurs in extremely acid conditions, where each mol of sodalite reacting with 24mol of H^+ ions generate 6mol of silica gel. The leaching of silicon is related to the sodalite decomposition, and as the silica gel is formed, the silicon extraction declined over time [281]. The synthesis of silica gel was observed in the samples took

until 6 hours of leaching reaction. The results indicated that after 8h of the leaching process, the leaching of silicon achieved the equilibrium, indicating the silica gel synthesis achieved the equilibrium. The main point was observed between 4h and 6h of leaching reaction.

Figure 19b shows the relation of scandium over iron leaching. As observed, the extraction of scandium is closed related to iron leaching – the recovery of scandium increases as iron extraction increases. In the bauxite, iron compounds host scandium ions during the mineral formation. After the Bayer process, the bauxite residue host such compounds [20,96,305]. In the case of Greek bauxite residue, Vind et al. (2018) stated that hematite, goethite, and zircon might host 55%, 25%, and 10% of the total Sc in the bauxite residue, respectively. So, only iron compounds are responsible for hosting around 80% of scandium ions [129]. For this reason, scandium extraction from bauxite residue is strictly connected to iron and zirconium leaching.

The effect of S/L ratio was studied. No difference was observed in the finds. The leaching of iron and scandium increased from 2.5% and 47% (S/L ratio equals to 1/10) to 4.1% and 58% (S/L equals to 1/50), respectively. The same behaviour was observed for aluminum (from 20% to 32%), titanium (from 5% to 9%) and zirconium (from 17% to 25%). As reported by Borra et al. (2015), the increase of the amount of acid rose the leaching of metals [54]. There is no economic advantageous to use S/L ratio equals to 1/50 to achieve the same scandium extraction rate. For this reason, further experiments were carried out in S/L ratio equals to 1/10.

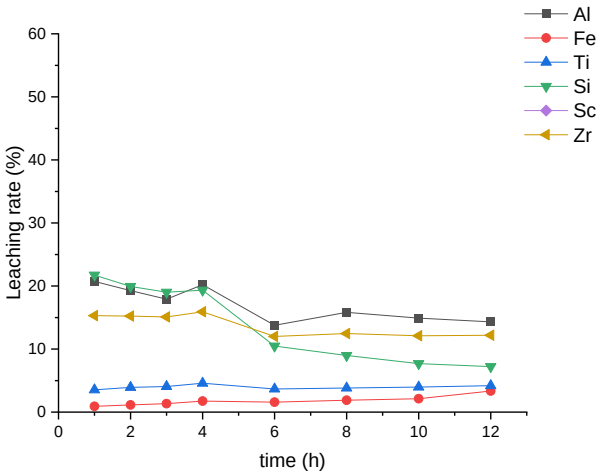

(a)

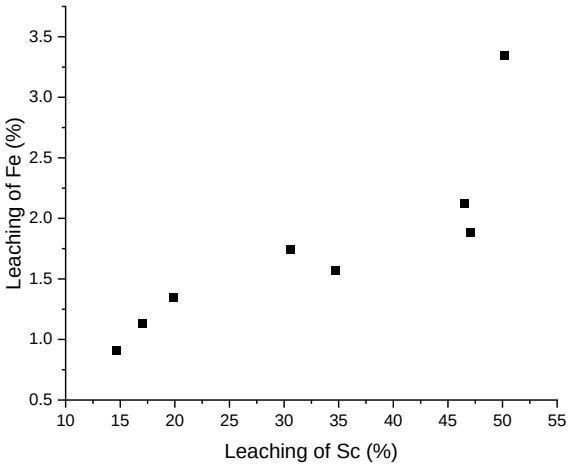

(b)

Figure 19: (a) Leaching of aluminum, iron, titanium, zirconium and silicon over time; and b) Leaching of iron and scandium correlation. Experimental conditions: T = 25°C, 8000rpm, H_2SO_4 concentration = 20%, S/L = 1/10.

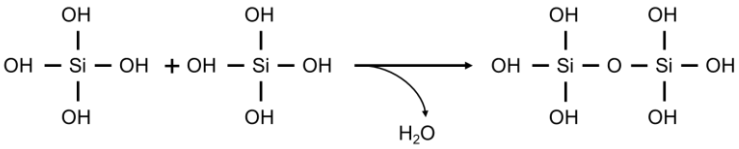

Figure 20: Reaction of silica gel formation during the acid leaching of bauxite residue [48]

$$Na_8(Al_6Si_6O_{24})Cl_{2(s)} + 24H^+_{(aq)} \rightarrow 6Al^{+3}{}_{(aq)} + 6H_4SiO_{4(s)} + 8Na^+{}_{(aq.)} + 2Cl^-{}_{(aq)}$$

Equation 13 [281]

Four kinetic models were tested for iron and scandium leaching through the shrinking core model: a) diffusion control through the fluid film (**Equation 14**); b) solid product diffusion control (**Equation 15**); c) surface chemical reaction control (**Equation 16**) [316,336]; and d) porous product layer (**Equation 17**) [337–339]. In the equations, k_1, k_2, k_3, and k_4 (min^{-1}) are the rate constants, *t* is the time reaction (min), and *x* the fractional conversion of scandium and iron.

$$1 - (1 - x)^{\frac{2}{3}} = k_1 \times t \qquad \text{Equation 14}$$

$$1 - 3(1 - x)^{\frac{2}{3}} + 2(1 - x) = k_2 \times t \qquad \text{Equation 15}$$

$$1 - (1 - x)^{\frac{1}{3}} = k_3 \times t \qquad \text{Equation 16}$$

$$1 - \frac{2}{3}x - (1 - x)^{\frac{2}{3}} = k_4 \times t \qquad \text{Equation 17}$$

The kinetic modeling for iron and scandium following the **Equations 14-17** is presented in Figure 21, where the equations were plotted versus the reaction time. The rate constants (*k*) were calculated from the slopes, and their correlation coefficients are also given in Figure 21 and Table 20. The results indicated that the solid product diffusion control controls the iron leaching and scandium leaching best fitted by the surface chemical reaction control.

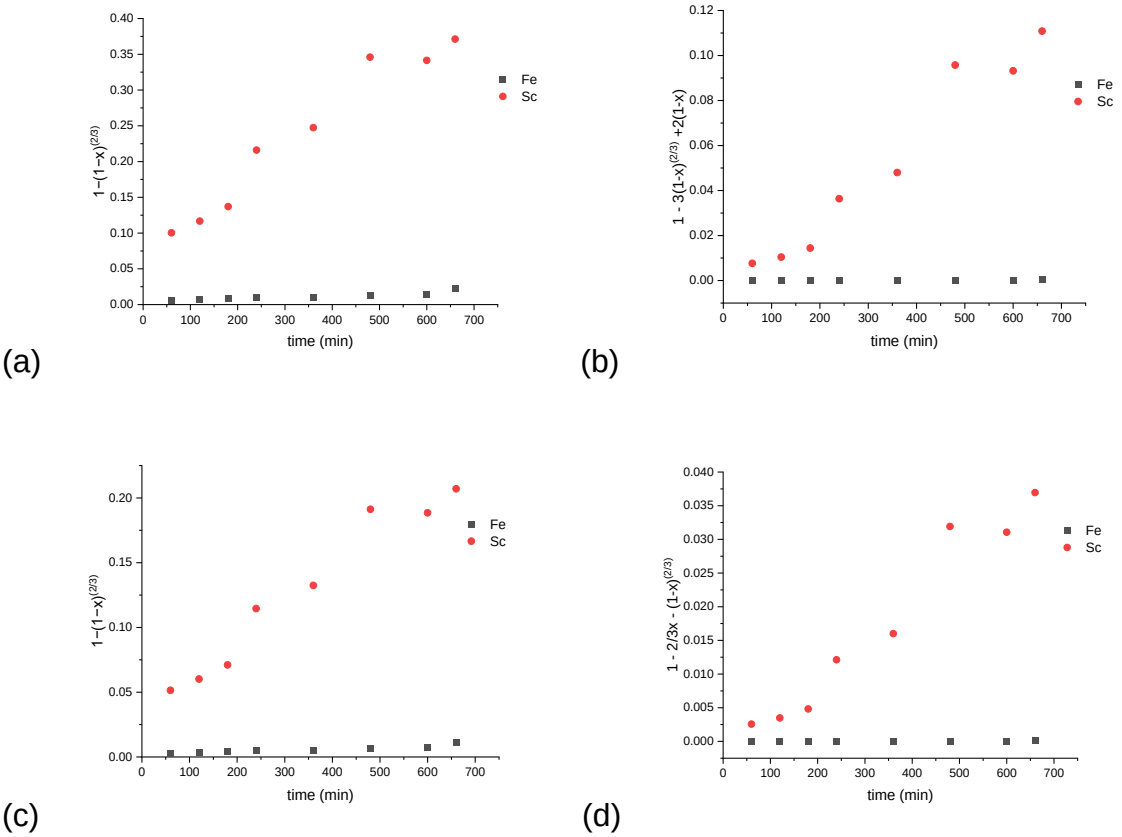

Figure 21: Kinetic modeling of scandium and iron leaching from bauxite residue: a) diffusion control through the fluid film; b) solid product diffusion control; c) surface chemical reaction control; d) porous product layer. T = 25°C, 8000rpm, H_2SO_4 concentration = 20%, S/L = 1/10, t = 10h.

Reid et al. (2017) studied the leaching of scandium from bauxite residue under microwave treatment by sulfuric acid 1.5mol/L. Kinetic modeling at 25-90˚C within 12min was controlled by the diffusion step and scandium leaching achieved 64% [316]. Anawati & Azimi (2019) studied the water leaching kinetic of scandium after acid baking (200˚C), where the results suggests the diffusion control due to the treatment with sulfucic acid concentrated before leaching step [164].

Wei et al. (2020) studied the scandium leaching from bauxite residue using HCl, where the efficiency achieved up to 84% using 20% of acid concentration, 80°C for 3 h and solid-liquid ratio equals to 1/10, and the kinetic modelling reached the Avrami model [335]. Basturkcu (2020) studied the leaching of rare earth elements from

bauxite residue. In the case of yttrium, the kinetic modelling fitted better for product diffusion control [340].

Table 20: Rate constant for iron and scandium extraction for different kinetic models and their respective correlation coefficient values.

	diffusion control through the fluid film		**solid product diffusion control**		**surface chemical reaction control**		**porous product layer**	
	k_1 (min^{-1})	R^2	k_2 (min^{-1})	R^2	k_3 (min^{-1})	R^2	k_4 (min^{-1})	R^2
Fe	$1x10^{-5}$	0.9804	$2x10^{-7}$	0.9824	$7x10^{-6}$	0.9805	$7x10^{-8}$	0.9747
Sc	0.0005	0.9448	0.0002	0.9351	0.0003	0.9459	$7x10^{-5}$	0.9239

5.2.3.3. Acid leaching of bauxite residue supported by hydrogen peroxide

Silica gel polymerization during the acid leaching of bauxite residue is one of the biggest challenges to be overcome since a part of the liquor is trapped inside the silica gel, resulting in losses of extraction efficiency rate. Moreover, iron sulfates as rhomboclase compounds result in co-precipitation of scandium in the leaching residue.

Anawati and Azimi (2019) explored the acid baking-water leaching, where the bauxite residue was mixed with H_2SO_4 concentrated (98%) and further baked in a furnace 400°C. The solid material is then leached with water. It converts scandium into a soluble sulfate salt. Results indicated high scandium recovery (up to 80%) and no silica gel formation. On the other hand, industrial-scale challenges are related to mixing H_2SO_4 concentrated and bauxite residue and handling it (worker safety and corrosion-resistant equipment) and the acid recovery from the off-gas of the acid-baking kiln [164].

Indeed, direct leaching consumes less energy than acid baking. For this reason, different approaches might be explored. Alkan et al. (2018) studied silica gel suppression on H_2SO_4 leaching with hydrogen peroxide (H_2O_2). In direct acid leaching, the rhomboclase phase is formed during acid leaching and co-precipitate scandium. The authors stated that the leaching of silicon and, consequently, silica gel formation declined as the concentration of H_2O_2 increased due to the oxidizing medium. On the other hand, the extraction of scandium decreased. It might be occurred due to the non-

leaching of the goethite phase from the bauxite residue since scandium is trapped inside this phase [48,129].

For the present study, it was explored the oxidizing leaching in order to avoid silica gel formation. First, a solution with H_2SO_4 20%v/v was prepared with H_2O_2 15g/L (0.44mol/L) right before the leaching experiment. Due to the fast decomposition in acidic medium, experiments were carried out adding H_2O_2 over the leaching reaction – 1mL (0.35mol/L), 2mL (0.70mol/L), and 4mL/h (1.40mol/L).

Results are presented in Figure 22. A slight increase in leaching rate was observed when compared with non-oxidizing leaching. However, the scandium leaching dropped as the H_2O_2 was applied in the reaction. As Alkan et al. (2018) observed, the leaching efficiency of scandium decreased as the H_2O_2 concentration increased. It might indicate most of the scandium is trapped in the goethite phase of the bauxite residue since iron oxide was still identified in the leaching residue (Figure 24).

In extremely acid conditions, the reaction of sodalite avoiding silica gel formation by H_2O_2 is proposed in **Equation 18**. As H_2O_2 is present in the solution, silicon from sodalite forms silicon oxide. However, at the same conditions, H_2O_2 decomposes fast in $H_{2(g)}$ and $O_{2(g)}$.

$$Na_8(Al_6Si_6O_{24})Cl_{2_{(s)}} + 24H^+_{(aq)} + H_2O_2 \rightarrow 6Al^{+3}{}_{(aq)} + 6SiO_{2_{(s)}} + 8Na^+{}_{(aq.)} + 2Cl^-{}_{(aq)} + 13H_2O + {}^1/_2\, O_2 \qquad \text{Equation 18}$$

According to Alkan et al. (2018), H_2O_2 benefits titanium leaching. **Equation 19** shows the reaction of titanium oxide and H_2SO_4, which forms $TiOSO_4$. In oxidizing leaching (**Equation 8**), it reacts with H_2O_2 forming TiO-OSO_4 - titanium peroxo sulfate, soluble during leaching reaction. However, as presented in Figure 22, in the present study, H_2O_2 had almost no effect in titanium leaching.

Figure 23 shows the redox potential of the leaching liquor in mV. As the oxidizing agent is added, the redox potential increased, mainly when the H_2O_2 was added during the experiment. At these conditions, Fe(II) is stable [225]. It occurs due

to the decomposition in an acidic medium. As a fresh oxidizing agent is added over the experiment, the silica gel formation is avoided. Moreover, as observed in **Equation 20**, titanium leaching increases as H_2O_2 is added during the process.

$$TiO_{2(s)} + H_2SO_{4(aq)} \rightarrow [TiO]SO_{4(aq)} + H_2O \qquad \text{Equation 19}$$

$$[TiO]SO_{4(aq)} + H_2O_2 \rightarrow [TiO-O]SO_{4(aq)} + H_2O \qquad \text{Equation 20}$$

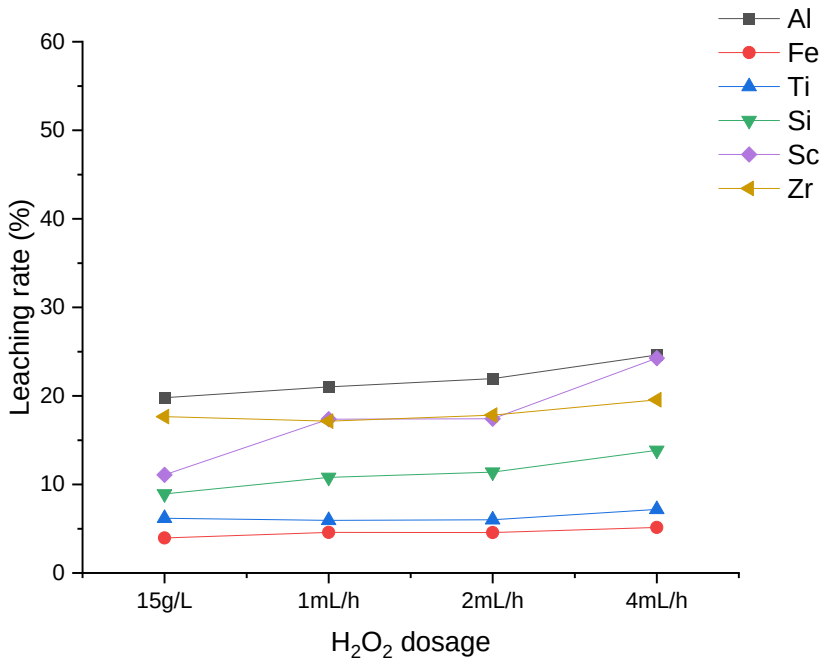

Figure 22: The effect of H_2O_2 on the leaching rate of aluminum, iron, titanium, silicon, scandium, and zirconium from the bauxite residue. Experimental conditions: T = 25°C, 8000rpm, H_2SO_4 concentration = 20%, S/L = 1/10, t = 8h. H_2O_2: 15g/L = 0.44mol/L; 1mL/h = 0.35mol/L; 2mL/h = 0.70mol/L; 4mL/h = 1.40mol/L.

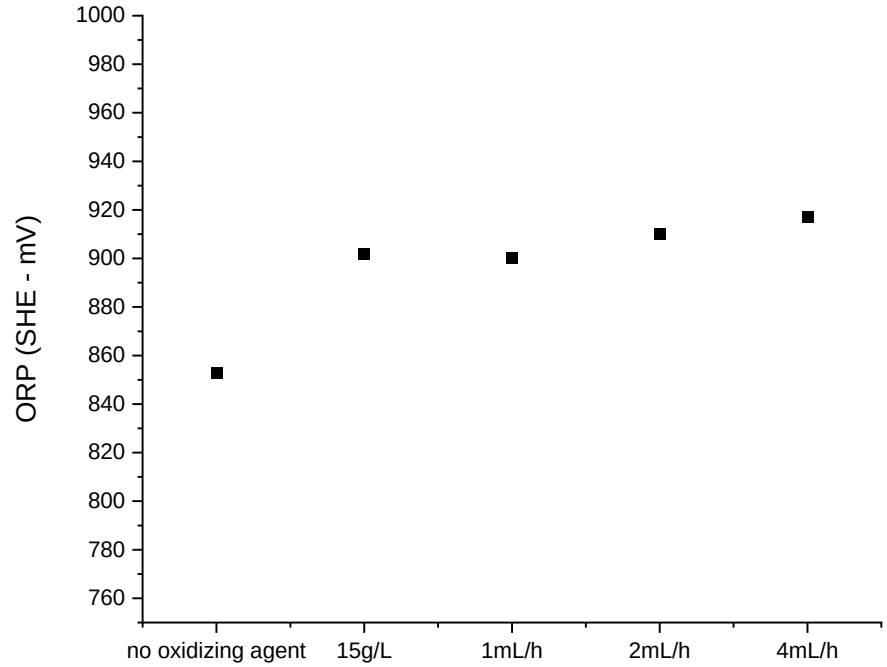

Figure 23: Redox potential (ORP) of experiments varying the H_2O_2 adding. Experimental conditions: T = 25°C, 8000rpm, H_2SO_4 concentration = 20%, S/L = 1/10, t = 8h.

Figure 24 shows the XRD of the bauxite residue and leaching residues. It is possible to see that gypsum peaks were identified in the leaching residues formed an oxidizing reaction. Peaks of iron oxide were identified in all samples, as well as quartz and iron sulfate. Similar results were presented in the literature [48,315].

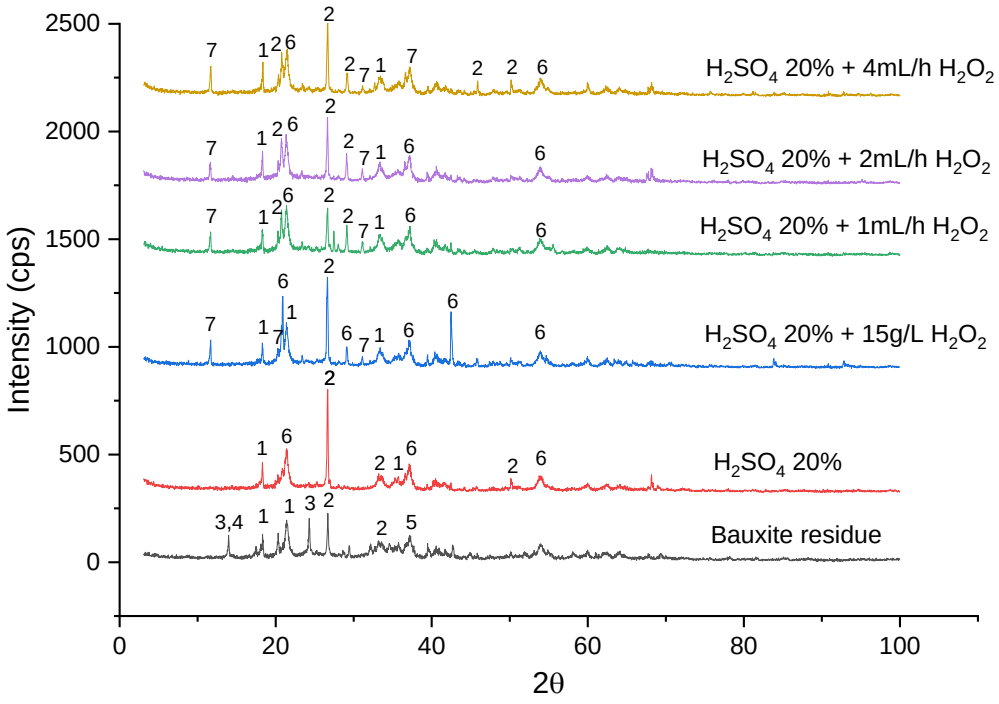

Figure 24: XRD of bauxite residue and leaching residues of experiments performed using H_2SO_4 20% and oxidizing media: 1 - Iron oxide; 2 – Quartz; 3 – Sodalite; 4 – Gibbsite; 5 – Boehmite; 6 - Iron sulfate; 7 – Gypsum.

5.2.3.4. Effect of temperature on leaching rates

The effect of temperature was evaluated with and without H_2O_2 (1.40mol/L) in a solid-liquid ratio equals to 1/10, 800rpm during 8h. The temperatures studies were 25°C, 45°C, 60°C, and 90°C. The results are presented in Figure 25, where it is observed that the temperature enhances the extraction of scandium, iron, and aluminum, achieving up to 90% in both cases. Titanium and zirconium leaching slightly increased from 5% to 26% and from 17% to 26%, respectively. Also, titanium extraction had almost no difference under H_2O_2 effect.

For silicon, the opposite was observed. As the temperature increased, the leaching of silicon declined. It may have occurred due to the decomposition of silica gel at high temperatures. At 25°C and 45°C, a similar leaching rate was observed. At 60°C and 90°C, the extraction efficiency declined to almost 0%. Furthermore, no differences were observed in acid leaching with and without H_2O_2 during 8h of reaction. The scandium extraction in oxidizing medium is lower at 25˚C and 45˚C, as well as

iron. At high ORP values, iron precipitates [341]. As the leaching occurred under H_2O_2 effect, probably the leaching of iron is lower, and less scandium was released.

Also, the use of H_2O_2 was not necessary to avoid silicon leaching and further silica gel formation. Comparing the methodology and used by Alkan et al. (2018) [48], the silicon leaching was close to 0% after 8h of reaction time and at 90˚C in the present study (scandium leaching up to 90%), while Alkan et al. studied the scandium leaching during 30min at 75˚C (scandium leaching up to 65%). Moreover, it was observed that as the silicon leaching declined, the solid-liquid separation was facilitated, which may indicate that SiO2 is formed instead of silica gel.

Figure 26 shows the XRD of leaching residue for each temperature studied. At 25°C and 45°C, the solid phase comprises quartz, iron sulfate, iron oxide, and gypsum. As the temperature increases, the leaching residue becomes more concentrated in quartz and gypsum, corroborating iron's leaching rate. At 90°C, the residue is composed of quartz and gypsum.

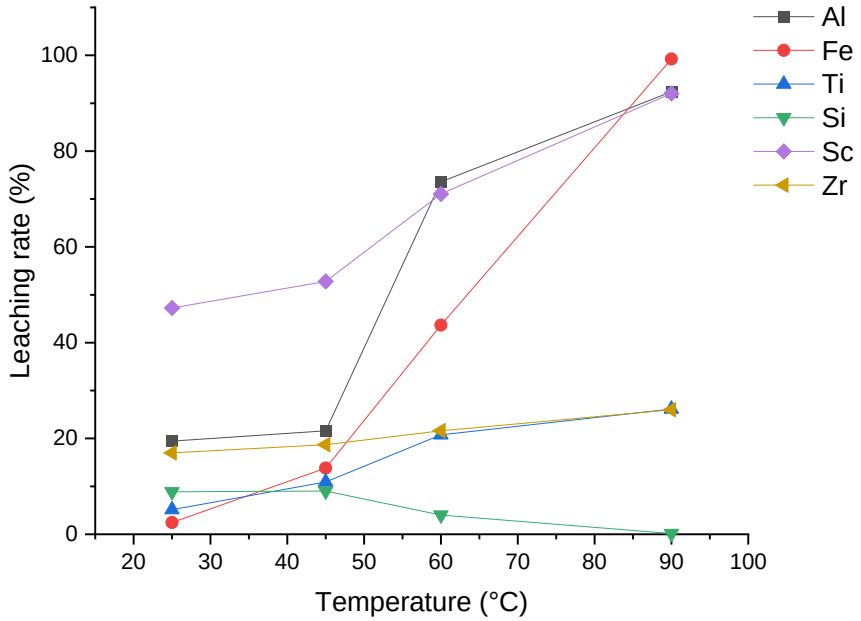

(a)

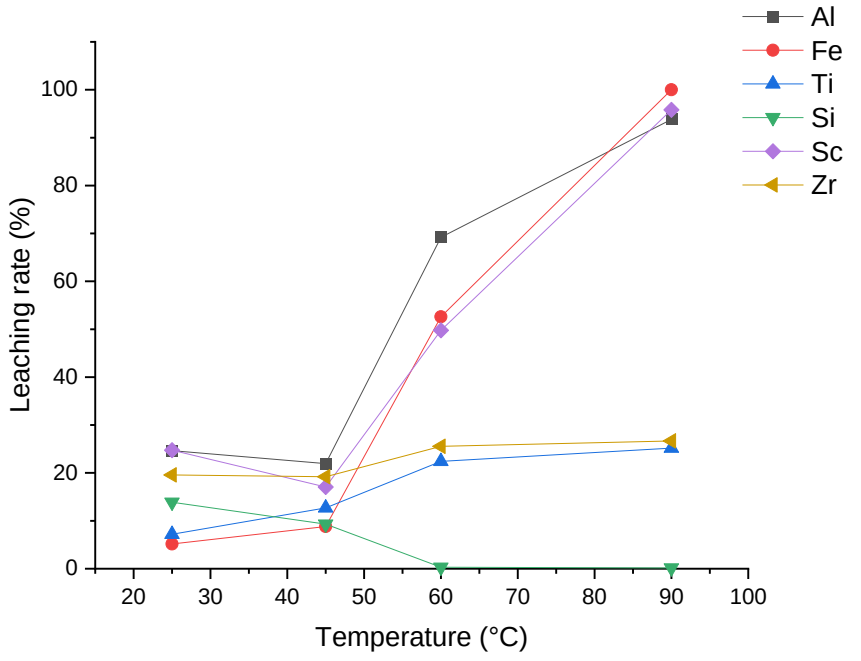

(b)

Figure 25: The effect of temperature on the leaching rate of aluminum, iron, titanium, silicon, scandium, and zirconium from the bauxite residue. Experimental conditions: 800rpm, H_2SO_4 concentration = 20%, S/L = 1/10, t = 8h, (a) without and (b) with H_2O_2 (1.40mol/L).

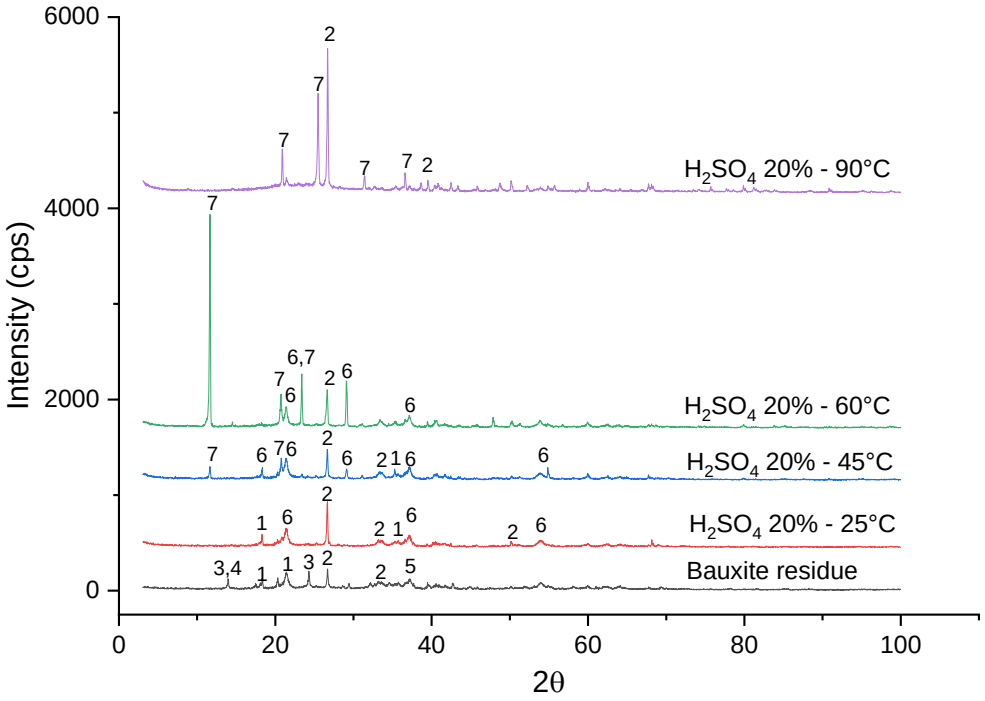

Figure 26: XRD of bauxite residue and leaching residues of experiments performed using H_2SO_4 20% and oxidizing media: 1 - Iron oxide; 2 – Quartz; 3 – Sodalite; 4 – Gibbsite; 5 – Boehmite; 6 - Iron sulfate; 7 – Gypsum.

Additionally, the leaching of bauxite residue directly depends on the activation energy. The Arrhenius equation, which express the rate constant and temperature relationship assuming the reaction mechanism is unchanged as the temperature varies [342,343], is used to calculate the activation energy. The equation also allows the determination of apparent activation energy for leaching of the elements from the bauxite residue [164]. It is shown in **Equation 21**, where *A* is the frequency factor, *E* is the activation energy (J/mol), and *R* is the gas constant (for the present study, it is equals to 8.31J/(mol.K)) [318,336,343]. The linear form is depicted in **Equation 22**. Results are presented in Table 21 for both systems (with and without an oxidizing agent).

$$k = Ae^{-\frac{E}{R.T}} \qquad \text{Equation 21}$$

$$\ln k = \ln A - \frac{E}{R.T} \qquad \text{Equation 22}$$

Table 21: Values of activation energies calculated and frequency factor for the leaching of aluminum, iron, titanium, silicon, scandium, and zirconium from the bauxite residue by H_2SO_4 20%.

		Al	**Fe**	**Ti**	**Si**	**Sc**	**Zr**
without oxidizing agent	The activation energy (J/mol)	24.23	51.62	23.06	-56.40	9.72	6.05
	Frequency factor	3.2×10^{-4}	2.8×10^{-8}	1.5×10^{-3}	3.9×10^{10}	4.4×10^{-2}	5.2×10^{-1}
with oxidizing agent	The activation energy (J/mol)	21.22	44.39	17.98	-69.11	21.46	4.95
	Frequency factor	9.3×10^{-4}	3.6×10^{-7}	8.8×10^{-3}	7.2×10^{12}	9.8×10^{-4}	7.2×10^{-1}

5.2.3.5. Effect of sulfuric acid concentration on leaching of bauxite residue

The effect of H_2SO_4 concentration was studied from 10% to 60% at 90°C, solid-liquid ratio equals to 1/10, 800rpm during 8h. The use of H_2O_2 was also evaluated. The leaching rate is presented in Figure 27. Alkan et al. (2018) studied the effect of H_2SO_4 concentration in the leaching rate of Greek bauxite residue. As the acid concentration increased, the silicon leaching decreased. According to the authors, it occurs due to the increase in ionic strength. At 75°C during 2h in a solid-liquid ratio equals to 1/10, the silicon leaching decreased from 60°C to close to zero as the H_2SO_4 concentration increased from 1M to 4M [48]. As data presented in Figure 27, almost no silicon was leached in all acid concentrations.

As depicted by Voßenkaul et al. (2017), acid concentration increases, leading to a fast silicon liberation with high ionic strengths. As a result, silicon precipitates as oxide and releases the main elements [344]. Indeed, as observed in Figure 25, the temperature has a similar effect. For this reason, no difference was observed in silicon leaching as the H_2SO_4 concentration increased from 10% to 60%.

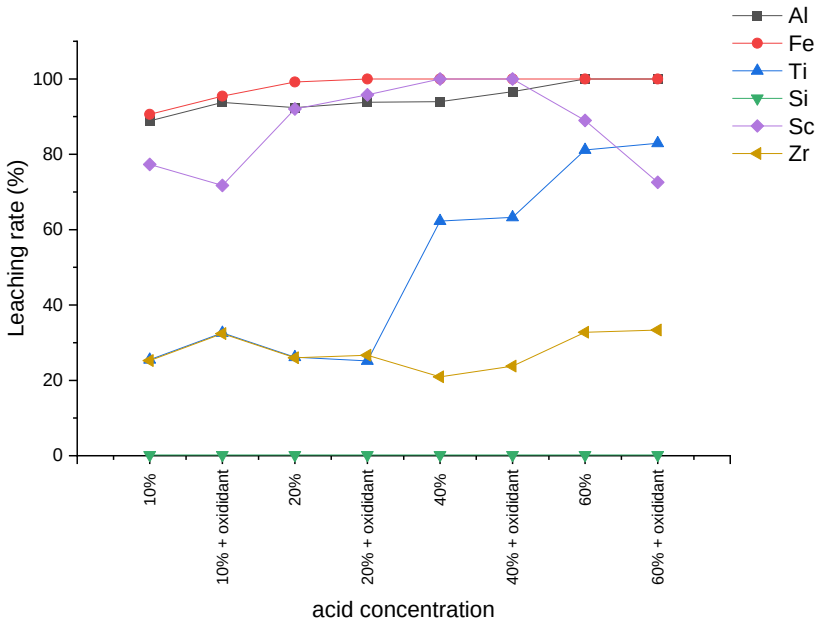

Figure 27: The effect of H_2SO_4 concentration on the leaching rate of aluminum, iron, titanium, silicon, scandium, and zirconium from the bauxite residue. Experimental conditions: 800rpm, S/L = 1/10, t = 8h, T = 90°C. Oxidizing agent = H_2O_2 (1.40mol/L)

Zirconium leaching had almost no difference – from 25% (10% of H_2SO_4) to 33% (60% of H_2SO_4). The oxidizing leaching increased the leaching rate only in H_2SO_4 concentration equals to 10%, where the zirconium leaching was 32% under the H_2O_2 effect. On the other hand, as the acid concentration increased, no difference was observed in the leaching rate. It might be due to the H_2O_2 degradation since the acid conditions facilitate the process.

Aluminium and iron leaching increased from ~90% to ~100% as the acid concentration increased from 10% to 20% and remained constant. In the case of titanium, it is clearly shown that the increase in H_2SO_4 concentration benefits the leaching rate. As shown in **Equation 19**, the increase of acid concentration benefits the generation of $[TiO]SO_{4(aq)}$ and consequently the titanium leaching. The oxidant leaching had effect in titanium leaching for 10% of H_2SO_4 (**Equation 20**); on the other hand, comparing acid concentration 20-60%, the H_2O_2 had no effect probably due to its faster decomposition in extremely acid conditions.

For scandium leaching, it is observed in Figure 27 that the efficiency rate increased from 77% to 92% as the acid concentration increased from 10% to 20%. At 60% of H_2SO_4 concentration, the scandium extraction decreased to 89%. It occurs due to the excess of sulfate ions (SO_4^{-2}) in the media compared to scandium ions [345]. The XRD of leaching residues obtained in experiments varying the acid concentration were similar to those presented in Figure 26.

Figure 28 depicts the redox potential of the leaching liquor in each acid concentration with and without an oxidizing agent. As the H_2SO_4 concentration increased from 10% to 60%, the redox potential decreased even after H_2O_2 addition. It indicates that a part of H_2O_2 decomposes with the increase of the H^+ ions in solution. **Equation 23** shows the direct hydrogen peroxide decomposition pathway in an acidic medium (E_0 = 1.77V). As the concentration of H^+ ions increased, the water generation increases. Moreover, it has formed hydroxyl radicals (OH•) at the same conditions, as depicted in **Equation 24**, which has higher electrochemical oxidation potential (E_0 = 2.8V). To avoid silica gel formation, the H_2O_2 is the main reagent and not the redox potential (**Equation 18**).

$$H_2O_2 + 2H^+ + 2e^- \rightarrow 2\,H_2O$$ Equation 23 [346,347]

$$H_2O_2 + e^- \rightarrow \mathrm{OH}\bullet + OH^-$$ Equation 24 [348]

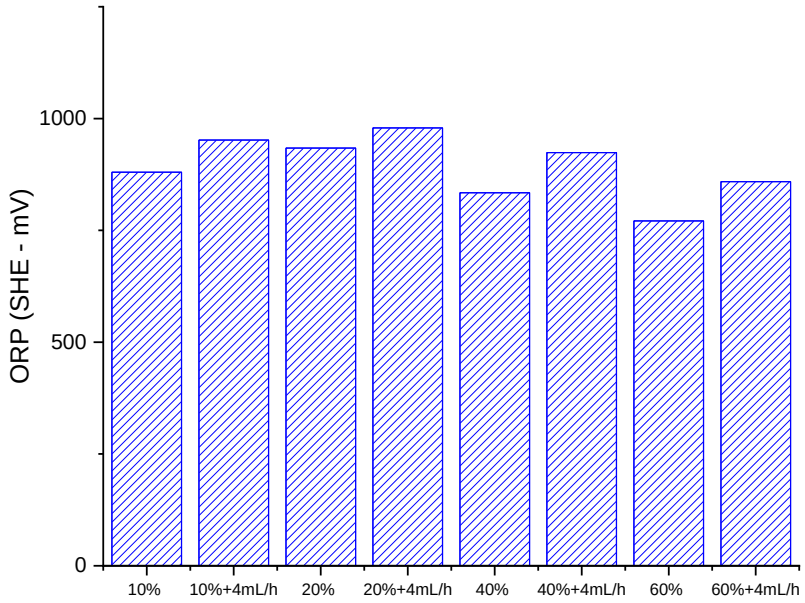

Figure 28: Redox potential (ORP) of experiments varying the H_2SO_4 concentration. Experimental conditions: 800rpm, S/L = 1/10, t = 8h, T = 90°C. Oxidizing agent = H_2O_2.

5.2.3.6. Comparative on leaching efficiencies on sulfuric and phosphoric acid

The experiments with H_3PO_4 were performed varying the acid concentration and temperature. As previously demonstrated, the oxidizing leaching has almost no effect on extraction rate, mainly scandium, and silica gel was avoided as the temperature increased, where H_2O_2 is quickly degraded. For this reason, experiments for H_3PO_4 leaching were carried out without an oxidant agent.

Figure 29 shows the leaching rate for temperature varying from 25°C to 90°C. As observed for H_2SO_4 leaching, the temperature increased the extraction efficiency of the main elements. Iron and aluminum leaching increased from 8% and 28% (25°C) to 95% and 91% (90°C), respectively. Scandium efficiency achieved similar results.

Zirconium extraction slightly increased from 24% to 37% as the temperature increased from 25°C to 90°C. In the case of silicon, the leaching rate decreased as the temperature increases. Similar results were observed for the H_2SO_4 reaction. However, at 90°C, the percentage of silicon extracted from the bauxite residue was 13% compared to 0.2% of the leaching rate using H_2SO_4 (Figure 25). By the same

token, titanium extraction at 90°C was 36% using 20% H_3PO_4, in contrast to 26% using 20% H_2SO_4.

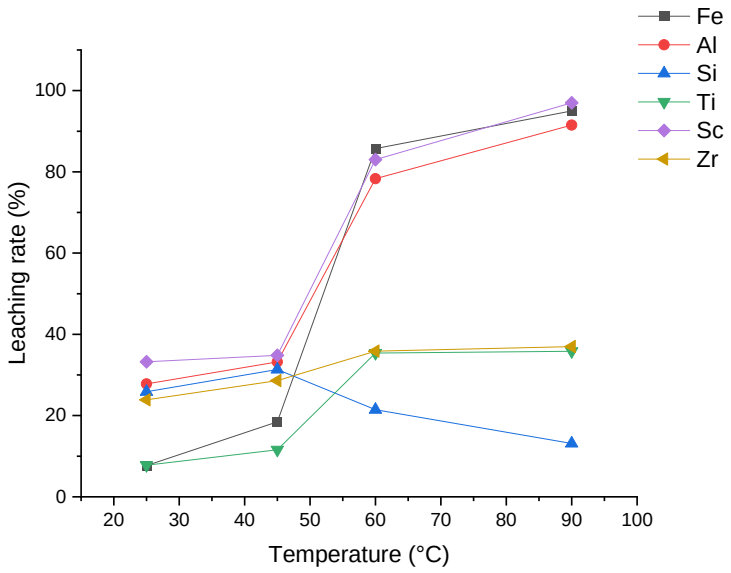

Figure 29: The effect of temperature on the leaching rate of aluminum, iron, titanium, silicon, scandium, and zirconium from the bauxite residue. Experimental conditions: 800rpm, H_3PO_4 concentration = 20%, S/L = 1/10, t = 8h.

Table 22: Values of activation energies calculated and frequency factor for the leaching of aluminum, iron, titanium, silicon, scandium, and zirconium from the bauxite residue H_3PO_4 20%.

	Al	**Fe**	**Ti**	**Si**	**Sc**	**Zr**
The activation energy (J/mol)	18.25	37.37	23.29	-10.33	16.75	6.38
Frequency factor	2.4×10^{-3}	3.2×10^{-6}	1.0×10^{-3}	2.1×10^{2}	3.8×10^{-3}	3.1×10^{-1}

The effect of H_3PO_4 concentration was evaluated from 10% to 60%, and the leaching rate is shown in Figure 30 for experiments performed at 25°C (a) and 90°C (b). In both cases, the silicon leaching decreased as the acid concentration increase. As depicted in H_2SO_4 experiments, the silicon release from the sodalite phase

increased with high ionic strengths and then precipitated as oxide [344]. Also, the temperature contributes to the silicon precipitation. For experiments carried out with 20% H_3PO_4 at 25°C, the leaching rate was 26%, while at 90°C and same acid concentration, the extraction of silicon was 13%.

The aluminum, iron, and scandium extraction were similarly achieving up to 100% at 90°C for H_3PO_4 above 20%. Titanium extraction increased as the temperature and acid concentration increased. Figure 31 shows the XRD of leaching residues of the experiment performed at 90°C in different H_3PO_4 concentrations. In contrast to H_2SO_4 experiments where calcium sulfate ($CaSO_4$) and silicon oxide were detected (Quartz), the leaching residues are rich in silicon oxide.

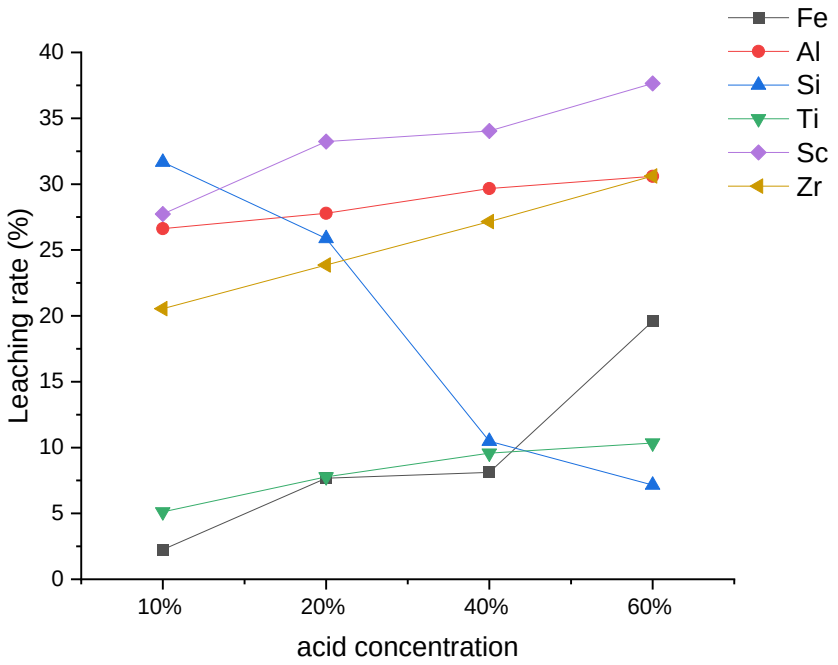

(a)

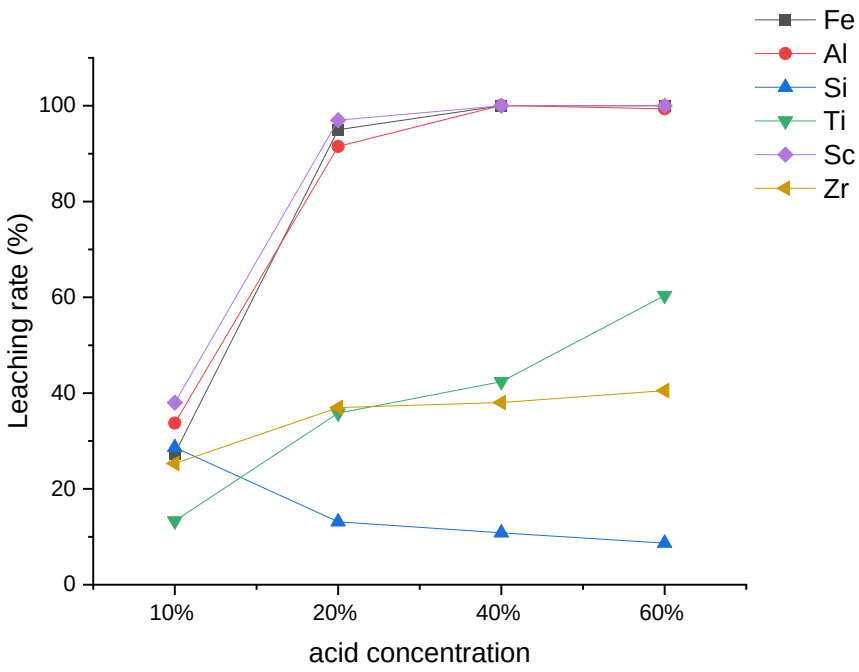

(b)

Figure 30: The effect of H_3PO_4 concentration on the leaching rate of aluminum, iron, titanium, silicon, scandium, and zirconium from the bauxite residue. Experimental conditions: 800rpm, S/L = 1/10, t = 8h, T = (a) 25°C and (b) 90°C.

Pepper et al. (2016) depicted titanium tends to be more stable in the bauxite residue than other mineral phases, such as those with iron and aluminum. The increase of titanium leaching with more concentrated acid contributes to the higher concentration of protons facilitating the extraction rate [281]. As observed in Figure 30, the temperature also benefits the process.

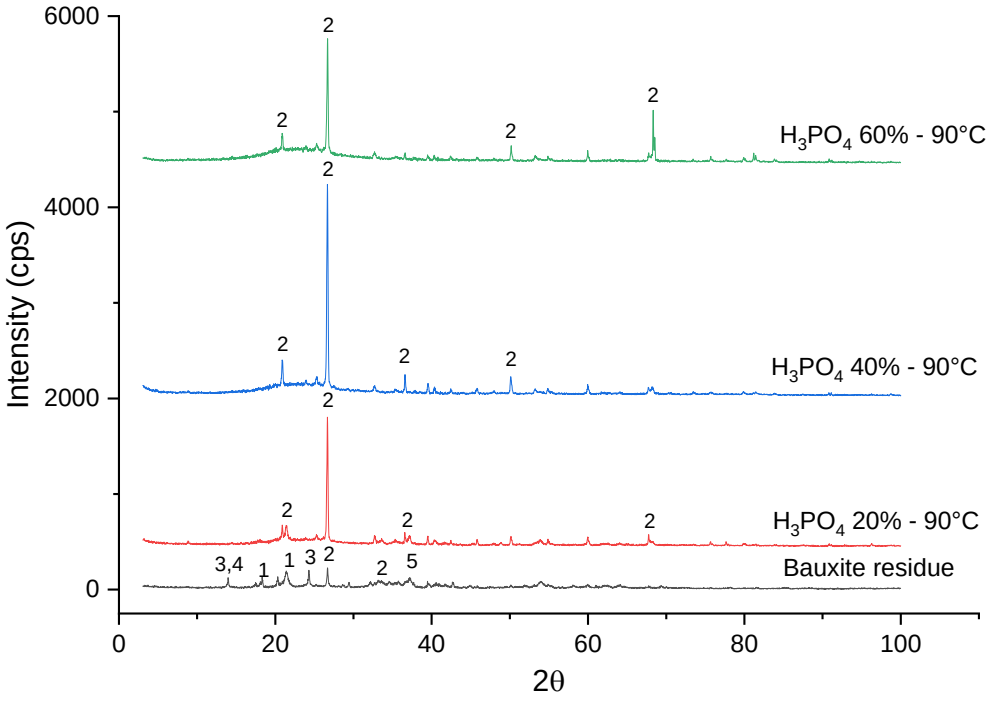

Figure 31: XRD of bauxite residue and leaching residues of experiments performed at 90°C using H_3PO_4 in different concentrations: 1 - Iron oxide; 2 – Quartz; 3 – Sodalite; 4 – Gibbsite; 5 – Boehmite.

5.2.4. Discussion on leaching of bauxite residue into a near-zero-waste generation

According to the results presented before, the best conditions for scandium extraction in both H_2SO_4 and H_3PO_4 leaching was: 20% of acid concentration, solid-liquid ratio equals to 1/10, 90°C and 8h. For this, the composition of the liquor was characterized and depicted in Table 23. The rare earth content varies from 2.4mg/L (scandium) to 27.6mg/L (cerium). The main elements in the solution are iron (up to 11,000mg/L) aluminum (up to 6,000mg/L) and sodium (up to 3,100mg/L). Calcium

content differs according to the leaching agent, as a part of the element precipitates in the H_2SO_4 leaching as sulfate (Figure 29). The H_3PO_4 leached more silicon than H_2SO_4 – 454mg/L and 7.4mg/L, respectively – as well as titanium – 312mg/L and 200mg/L.

It's worth mentioning that scandium extraction achieved 50% at 25˚C for 8h with low iron leaching (up to 3.5%), where the Fe/Sc ratio was up to 180. Indeed, the amount of iron may impact the recovery of scandium by ion exchange technique. Comparing with all scandium, and consequently iron, extraction (Fe/Sc ratios equals to 4,000), it generates a liquor with low concentration of contaminants, which can be more feasible for separation steps than the highest scandium extraction and, consequently, contaminants leaching. As a matter of fact, the Fe/Sc ratio is the potential showstopper for scandium extraction from bauxite residue.

The economic analysis is presented in Figure 32, considering the most valuable elements in the leaching liquor. Scandium is responsible for at least 95% of the solution's economic value, followed by zirconium and neodymium. Comparing the costs of leaching agents, which are similar [47], the leaching with H_2SO_4 achieved the most valuable solution. Also, the leaching of contaminants such as aluminum, calcium, and silicon was lower, facilitating further separation steps.

Table 23: Composition of the liquor in mg/L after leaching by H_2SO_4 and H_3PO_4. Experimental conditions: acid concentration = 20%, 800rpm, S/L = 1/10, t = 8h, T = 90˚C.

	Al	**Fe**	**Ca**	**Na**	**Sc**	**Si**	**Ti**	**V**	**Zr**	**La**	**Ce**	**Nd**	**Y**
H_2SO_4	5059.8	11804.3	480.1	3104.5	2.7	7.4	200.4	8.6	43.4	5.9	27.6	2.2	1.5
H_3PO_4	6147.1	11812.5	2157.3	3300.4	2.4	454.7	312.2	8.0	52.1	6.0	27.0	2.0	1.4

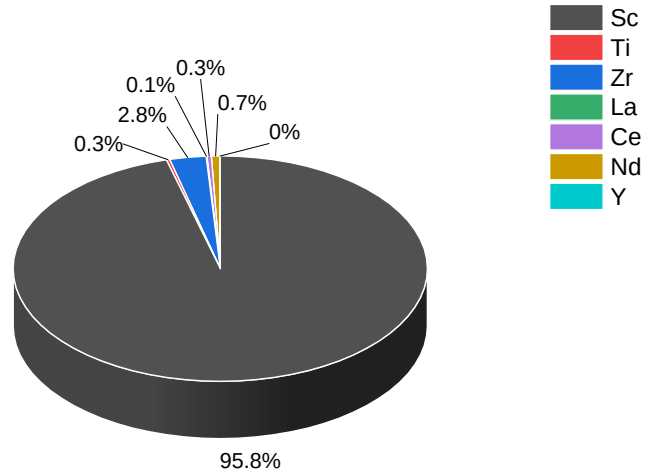

(a)

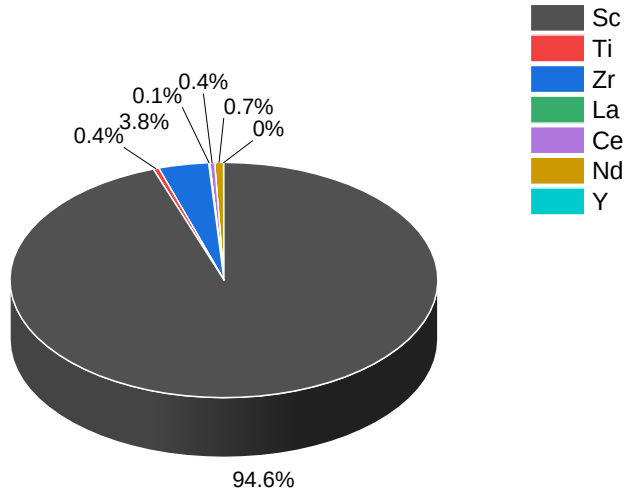

(b)

Figure 32: Economic value of the liquor obtained after leaching process by (a) H_2SO_4 and (b) H_3PO_4. Experimental conditions: acid concentration = 20%, 800rpm, S/L = 1/10, t = 8h, T = 90˚C.

Considering the residue, the H_2SO_4 leaching generated a residue composed mainly of silicon dioxide, titanium oxide, and calcium sulfate (Figure 29), while the H_3PO_4 leaching generated a residue mainly composed of silicon dioxide and titanium oxide (Figure 30). In both cases, the leaching residue may be used for titanium

extraction by HCl. Haverkamp et al. (2016) studied the leaching rate process of titanium-rich ore at 80˚C. If the goal is TiO_2 production, titanium hydrolysis can be avoided during leaching, but favored for selective separation after extraction step [45].

In contrast to ilmenite ores, in which the reaction occurs with 10.3mol/L of HCl, the residue's leaching from the bauxite processing might occur in lower acid concentration. For both H_2SO_4 and H_3PO_4, as results demonstrated (Figure 27 and Figure 30), the leaching rate of bauxite residue for titanium achieved up to 60% and 80% using 60% of H_3PO_4 and H_2SO_4, respectively. Pepper et al. (2016) compared common minerals acids (H_2SO_4, H_3PO_4, HNO_3, and HCl) and concluded that for leaching reaction using 5mol/L is: H_3PO_4 > HCl > H_2SO_4 > HNO_3 [281]. For H_3PO_4, the number of H^+ ions in solution is three times higher than HCl. At the same time, the H_2SO_4 solution has two times H^+ ions and achieved lower efficiency.

Also, the leach residue can be used for construction industry, due to the composition (high calcium and silicon content). Bauxite residue has been studied by different authors to be used for cement production [43,44,349,350]. However, due to the presence of scandium and other rare earth elements, as well as titanium, the extraction of these valuable elements before cement production. As a result, a near-zero-waste process is designed for the recovery of different elements and the application of the wastes generated throughout the process.

Comparing the amount of solid phase before and after acid extraction, the H_2SO_4 leaching residue was 34% of the input process, while H_3PO_4 leaching residue was 25%. It’s worth mentioning that residues containing phosphorous required attention, due to negative impact on aquatic life and soils triggering eutrophication processes, causing proliferation of algae and macrophytes [351–353].

Considering that the current process sent the bauxite residue to the dams, the proposed process results in less residue to be stored. Due to the characteristics of the leaching residue in both acid processes, the material can be used for construction [310,354–356]. It results in a near-zero-waste process.

5.3. Extraction of rare earth elements from silicate-based ore through hydrometallurgical route

A.B. BOTELHO JUNIOR[1]*; D.C.R. ESPINOSA[1]; J. VAUGHAN[2]; J.A.S. TENÓRIO[1]

[1] Department of Chemical Engineering; Polytechnic School, University of Sao Paulo, Sao Paulo – Brazil.

[2] School of Chemical Engineering; The University of Queensland, Brisbane, Queensland – Australia.

ABSTRACT

The European Union and several countries/regions classified the rare earth elements (REE) as critical due to the risk of supply interruption. For this reason, the growing demand for REE makes forgotten reserves gain economic interest. So, the search of new sources and the development of chemical process is important, as silicate-based ore. Since there is almost no literature for extraction of REE from this source, a new approach has been developed at the present study. Direct leaching and acid baking were studied using sulfuric acid. The effect of acid concentration, temperature, solid-liquid ratio, oxidizing/reducing medium, and acid dosage were studied. Results showed that the extraction of REE achieved up to 80% at 90˚C in oxidizing medium, and scandium and iron achieved 13.5% and 65.0%, respectively. For acid baking experiments, the results were better than direct leaching for REE - over 85%. Scandium leaching rate was lower than direct leaching. On the other hand, the extraction of iron was lower in acid baking than direct leaching. Iron and scandium extraction rates were higher in lower temperatures (< 200˚C) and acid dosage achieving 50% and 6.3%, respectively. Future studies may explore the thermal treatment before acid leaching.

Keywords: lanthanum; scandium; leaching; acid baking; critical metals.

5.3.1. Introduction

The rare earth elements denote a group of 17 elements that includes scandium, yttrium, and lanthanides (elements with atomic numbers 57 – 71). The term is not because they are rare, since their concentration in the Earth's crust ranges

around 150-220ppm (copper is 55ppm and zinc is 70ppm, for instance), but due to their chemical similarity. Despite that, these elements are rarely concentrated into minable ore deposits, making the extraction of rare earth elements an economic and technical challenge [1,357].

The market is controlled by China. As a result, the European Union classified the rare earth elements as *critical materials* and the risk of supply interruption in the middle term [329]. For this reason, the search for new sources of rare earth elements is necessary to serve the growing market. For this reason, several researches are focused in new rare earth elements source to supply the market [41,358,359].

On the other hand, extraction from primary resources (e.g. ores) are still necessary [55,258,360–362]. The main minerals of rare earth elements in the world are Monazite (phosphate - $(Ce,La,Nd,Th)PO_4$), Xenotime (phosphate - YPO_4), and Bastnasite (carbonate - $(Ce,La,Y)CO_3F$) [35]. China is the largest producer (140,000 tons), followed by the USA (38,000 tons), Burma (30,000 tons), and Australia (17,000 tons). Moreover, the reserves are concentrated in China (44 million tons), Vietnam (22 million tons), Brazil (21 million tons), and Russia (12 million tons). In 2015, the global production was 130,000 tons; in 2021, it is expected up to 240,000 tons [5].

Among the extractive routes currently adopted, the hydrometallurgical has the advantage of producing high-pure products even in low concentrations, as in the case of rare earth elements. The processing route can vary according to the rare-earth mineral. Monazite extraction, for instance, a phosphate mineral, can occur by sulfuric acid digestion (200-220˚C) and further purification steps, such as precipitation and solvent extraction; alkali treatment at 140-150˚C with sodium hydroxide 70% is also used. Bastnasite ore ($REECO_3F$, where REE = rare earth elements) can be processed by hydrochloric acid 10%, sulfuric acid concentrated at 480˚C, or by calcination before leaching. Further steps are also precipitation and solvent extraction [1].

In all cases above mentioned, different rare earth elements can be obtained. In the case of scandium, the most valuable among them is rarely found, and its extraction is commonly limited to uranium, thorium, niobium, and rare earth elements production as a by-product. Different extractive approaches can be used, such as alkali fusion, acid leaching under pressure, and chlorination (hydrochloric acid in high temperatures) [357].

A hydrometallurgical route has explored the extraction of rare earth elements from bauxite residue and nickel laterite waste since these elements' concentration is up to 100mg/kg or lower [20,54,363]. Borra et al. (2015) studied the direct leaching of bauxite residue to extract rare earth elements achieving up to 80% of extraction efficiency [54].

Moreover, the acid baking has been explored for extraction of rare earth elements due to low acid consumption and faster kinetics. Anawati & Azimi (2019) studied the acid baking of bauxite residue to extract rare earth elements. Sulfuric acid concentrated was mixed to the material and heated at 200-400˚C. Then, the material resulted was leached with water for extraction of rare earth elements, where achieved the equilibrium within 2h at 90˚C [164]. Kim & Azimi (2020) studied the extraction of slag rich in rare earth elements by acid baking, and the authors also stated that the water leaching achieved the plateau after 120min in all cases, and the kinetic rate is faster at 90˚C than lower temperatures [364]. Zou et al. (2021) demonstrated that lanthanum and cerium extraction also achieved the plateau after 120min from rare earth polishing powder wastes after the baking process [365].

Due to the increasing interest in such elements and control of fewer countries of their extraction, new resources search makes necessary. Among the potential resources of rare earth elements there are silicates and oxides. In the case of silicate-based ores, there is a lack in the literature due to scarcity. However, due to the growing demand for rare earth elements, these reserves have been considered even with lower rare earth elements than recognized minerals [35].

There are only a few works in the literature about direct leaching or acid baking of rare earth elements from silicate-based ores, probably because such minerals are less common than phosphates (Monazite and Xenotime) and carbonates (Bastnasite) [35]. However, since these elements' consumption has grown over the years, it is necessary to search for new potential resources of rare earth elements.

For this, the present study's goal was the extraction of rare earth elements from a silicate-based ore by the hydrometallurgical route. Sulfuric acid was used as a leaching agent. First, direct leaching experiments were carried out in an acid medium for 8 hours. The effect of solid-liquid ratio, concentration, and temperature were studied. The use of sodium dithionite and hydrogen peroxide were evaluated as

reducing and oxidizing agents, respectively. Secondly, acid baking was studied, varying the sulfuric acid/ore ratio and temperature. To compare with acid baking, dry digestion was carried out at room temperature (25˚C). After the sulfation process, the water leaching was carried out at 90˚C for 2 hours. The samples were characterized in XRD, SEM/EDS, and ICP-OES.

5.3.2. Materials and methods

5.3.2.1. Materials

The silicate-based ore rich in rare earth elements was supplied from a Canadian site (primary ore). The particle size distribution was measured. The quantification of the main elements was carried out in XRF. Minor elements were determined by alkali fusion by mixing 0.5g of the ore with 1.5 g of sodium carbonate and 1.5 g of sodium tetraborate decahydrate at 1100˚C for 30min followed by dissolution in HCl media.

The mineralogical assessment was carried out by X-ray diffraction technique (XRD, Rigaku MiniFlex 300). The sample analyzed was pooled and scanned from 3° to 100° (2θ) with a 4°/min rate and 0.02 step. The powder morphology was studied by scanning electron microscopy with a backscattered electron detector and coupled with energy dispersion (Phenom model ProX).

Sulfuric acid (95-98%, Química Moderna), nitric acid (65%, Neon), hydrogen peroxide (29%, Synth), and sodium dithionite (99%, MetaQuímica) were of analytical grade. Acid solutions and calibration curves were elaborated with ultra-pure water.

5.3.2.2. Experimental design

Before extraction experiments, the samples were ground into -0.5mm of particle sizes using a motorized pestle/mortar mill (Marconi) to ensure sample homogeneity and dried at 60˚C for 24 hours. Before experiments, the experimental error was calculated, as previously depicted [40]. The leaching experiment was carried out at 25˚C, solid-liquid ratio equals 1/10, 4mol/L of sulfuric acid, 200rpm of stirring speed during 8h. The standard deviation calculated was 3.2%.

5.3.2.3. Direct leaching

The experiments to evaluate the effect of acid concentration, solid-liquid ratio, reducing and oxidizing agent, and temperature were carried out in sealed Erlenmeyer flasks (250mL) under stirring (200rpm) and temperature control (25˚C). To study the effect of temperature, the experiments were performed in glass reactors (200mL) fitted with a reflux condenser and placed on a hot plate with a magnetic stirring system.

The parameters explored in the present study are depicted in Table 24. The effect of solid-liquid ratio was studied for 1/5, 1/10, 1/25, and 1/50, and further, the sulfuric acid concentration was evaluated for the values of 0.5mol/L, 1.0mol/L, 2.0mol/L, and 4.0mol/L. The oxidizing and reducing leaching was studied using hydrogen peroxide (H_2O_2) and sodium dithionite ($Na_2S_2O_4$), considering the concentrations of 1%, 2.5%, 5%, and 10% ($v_{H_2O_2}/v_{alid\ solution}$ and $v_{Na_2S_2O_4}/v_{acid\ solution}$, respectively). The effect of temperature was studied at 25˚C, 45˚C, 60˚C, and 90˚C.

Table 24: Parameters studied in direct leaching experiments for the extraction of rare earth elements from silicate-based ore

Variables	Conditions
Solid-liquid ratio (S/L)	1/5 – 1/50
Concentration	0.5mol/L – 4.0mol/L
$Na_2S_2O_4$	1% - 10%
H_2O_2	1% - 10%
Temperature	25 – 90˚C

After the leaching procedure, the mixture was first centrifuged at 3,000rpm for 10min and then filtered with a quantitative filter paper 2μm. The leaching residue was washed using ultra-pure water and dried at 60˚C for 24h for XRD analyses. The leach solution and the washing water were diluted in HNO_3 4% for chemical analyzes in Inductively Coupled Plasma Optical Emission Spectrometer (ICP-OES – Agilent Technologies 70 series). Iron concentration was analyzed in AAS (Shimadzu AA-7000)

5.3.2.4. Dry and acid baking

Crushed samples were mixed with 0.6mL-1.5mL of sulfuric acid 98% in a porcelain crucible with a glass rod homogenizing the mixture. The temperatures studied were 25˚C (dry digestion), 200˚C, 300˚C, and 400˚C. Further, the water leaching was studied at 90˚C for 2h and the solid/liquid ratio equals 1/10.

5.3.3. Results and discussion

5.3.3.1. Characterization and economic analysis of silicate-based ore

The chemical composition of the ore was analyzed to provide a basis for extraction efficiency calculations. The major elements in the form of oxides are shown in Table 25. Silicon is the main element in the ore, followed by iron, calcium, aluminum, and titanium. Sodium, magnesium, potassium, manganese, and phosphorous oxides are concentrated above 0.4%.

The concentration of zirconium and rare earth elements is presented in Table 26, as well as the economic importance of each element in the silicate-based ore. From the characterization, it is evident that the ore is rich in zirconium and both heavy and light rare earth elements. Also, it is rich in scandium (191mg/kg). Among the minor concentration elements, lanthanum, cerium, neodymium, and yttrium are the main rare earth elements where the total is 1.1wt%. On the other hand, the most valuable element is scandium (76.8%), followed by neodymium and zirconium.

Table 25: Major chemical components in the ore

Compounds	wt%
SiO_2	39.4
Fe_2O_3	36.3
Cao	8.79
Al_2O_3	4.61
TiO_2	2.32
Na_2O	1.64
MgO	1.44
K_2O	1.42
MnO	1.09
P_2O_5	0.43

Table 26: Zirconium and rare earth elements composition of the ore sample and their economic value in the silicate-based ore

Elements	Concentration (mg/kg)	Economic value (in US$)
Zr	8,090	6.0%
Ce	5,420	0.8%
La	2,330	0.3%
Nd	2,140	7.3%
Y	1,100	0.2%
Pr	626	3.2%
Th	375	1.7%
Sm	358	0.1%
Gd	268	0.4%
Dy	238	2.8%
Sc	191	76.8%

The cumulative particle size distribution is shown in Figure 33. In the silicate-based ore, 90% of the particles are smaller than 1412.9µm, and 50% are smaller than 348.5µm. Since the particle size distribution of the sample is considered high, and due

to the fact that the study of its effect in acid leaching was not explored in the present study, the ore sample was ground into -0.5mm.

Scanning electron microscopy (SEM) was used to study the sample's surface morphology, as presented in Figure 34. The EDS spectrum shows the distribution of the chemical elements. As shown, the sample matrix is mainly composed of silicon and oxygen, indicating the presence of silicates as main compounds. Calcium and iron were also identified. Among the minor elements presented in Table 26, it was identified zirconium, lanthanum, cerium, neodymium, and yttrium. These results are in line with the chemical characterization.

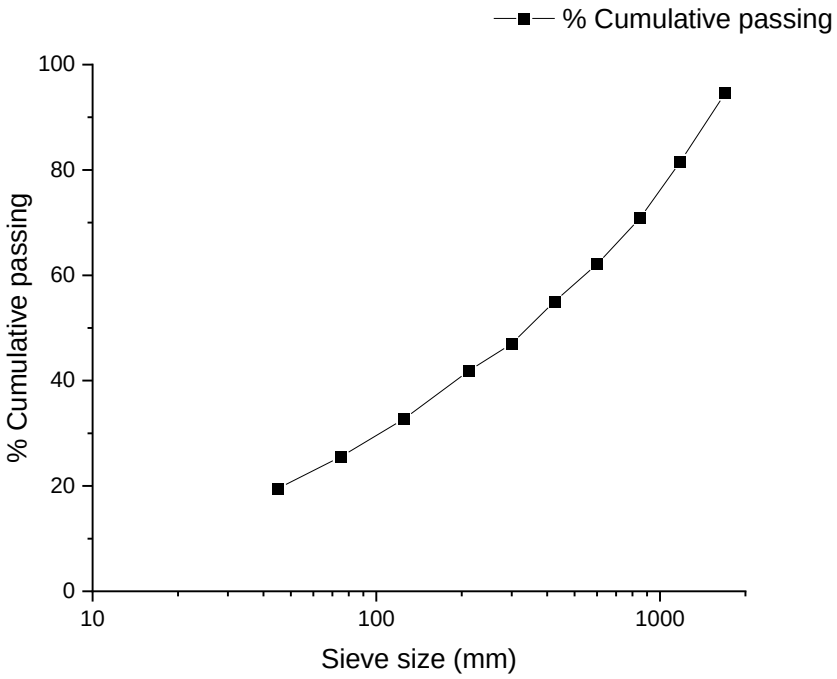

Figure 33: Particle size distribution of the silicate-based ore

Figure 35 shows the X-ray diffractogram of the sample. The main phases identified were Dickite ($Al_2Si_2O_5(OH)_4$), Ferrohornblende ($(Na,K)Ca_2(Fe,Mg)_5(Al,Si)_8O_{22}(OH)_2$), Fayalite ($Fe_2(SiO_4)$), Hedenbergite ($CaFeSi_2O_6$), and Albite ($(Na,Ca)Al(Si,Al)_3O_8$). As previously observed in the SEM/EDS analyses, the main mineral phases identified were silicates. It was

impossible to confirm the rare earth elements' mineral phases due to the low concentration in the ore.

The common silicate minerals of rare earth elements are: Allanite ($(Ce,Ca,Y)_2(Al,Fe^{2+},Fe^{3+})_3(SiO_4)_3(OH)$), Gadolinite ($Y_2Fe^{2+}Be_2Si_2O_{10}$), Zircon ($(Zr,REE)SiO_4$), Thortveitite ($(Sc,Y)_2Si_2O_7$), Cascandite ($Ca(Sc,Fe^{3+})HSi_3O_9$), Gadolinite ($Y_2Fe^{2+}Be_2Si_2O_{10}$) or Jervisite ($(Na,Ca,Fe^{2+})(Sc,Mg,Fe^{2+})Si_2O_6$) [357]. For this reason, it is worth concluding that the rare earth elements could be in the ore as silicates.

Preliminary magnetic separation was carried out and the mineral phases and their respective percentage are presented in Table 27. Results demonstrated that 80-90% of rare earth elements and 90% of scandium, 90% of silicon and 88% of zirconium, which shows that the main valuable elements are hosted in silicates and zircon mineral phases. Only 20% of iron is magnetic (mainly as ilmenite) is presented in the magnetic fraction. As a conclusion, the magnetic separation did not concentrate the rare earth element or removed impurities, and leaching experiments were carried out using the raw material.

Table 27: Mineral phases of the magnetic and non-magnetic fraction of the silicate-based ore

Magnetic fraction		**Non-mag fraction**	
Hedenbergite	14.28%	Phlogopite	9.14%
Hilairite	1.49%	Hedenbergite	15.20%
Ilmenite	14.91%	Zirconia	4.73%
Zirconia	1.45%	Fayalite	11.81%
Fayalite	10.87%	Diopside	21.20%
Diopside	31.46%	Hastingsite	1.65%
Ferrohornblende	10.94%	Albite	22.02%
Magnetite	14.60%	Ferrohornblende	14.25%

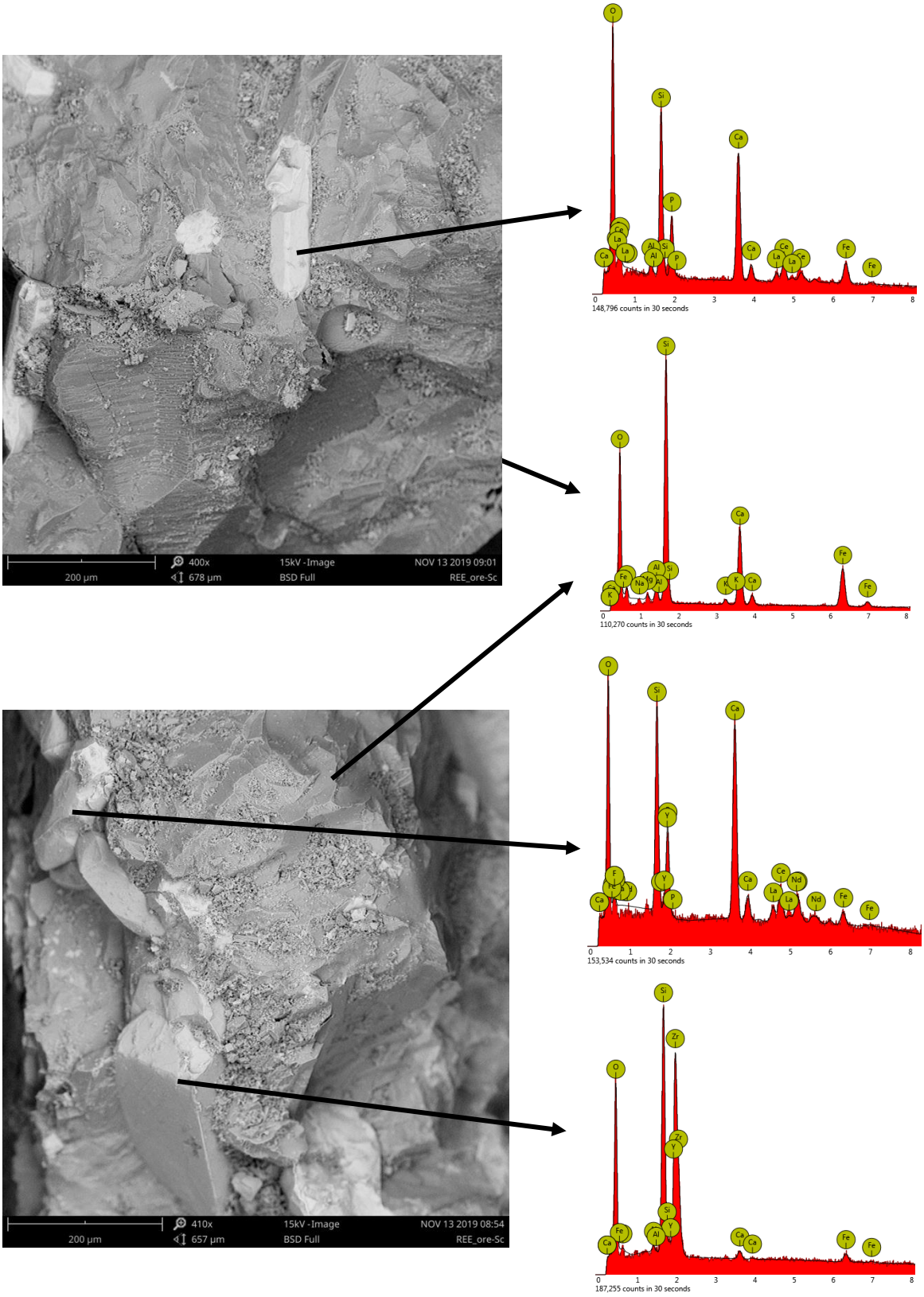

Figure 34: The image of backscattered electrons of the ore and EDS spectra of the particles

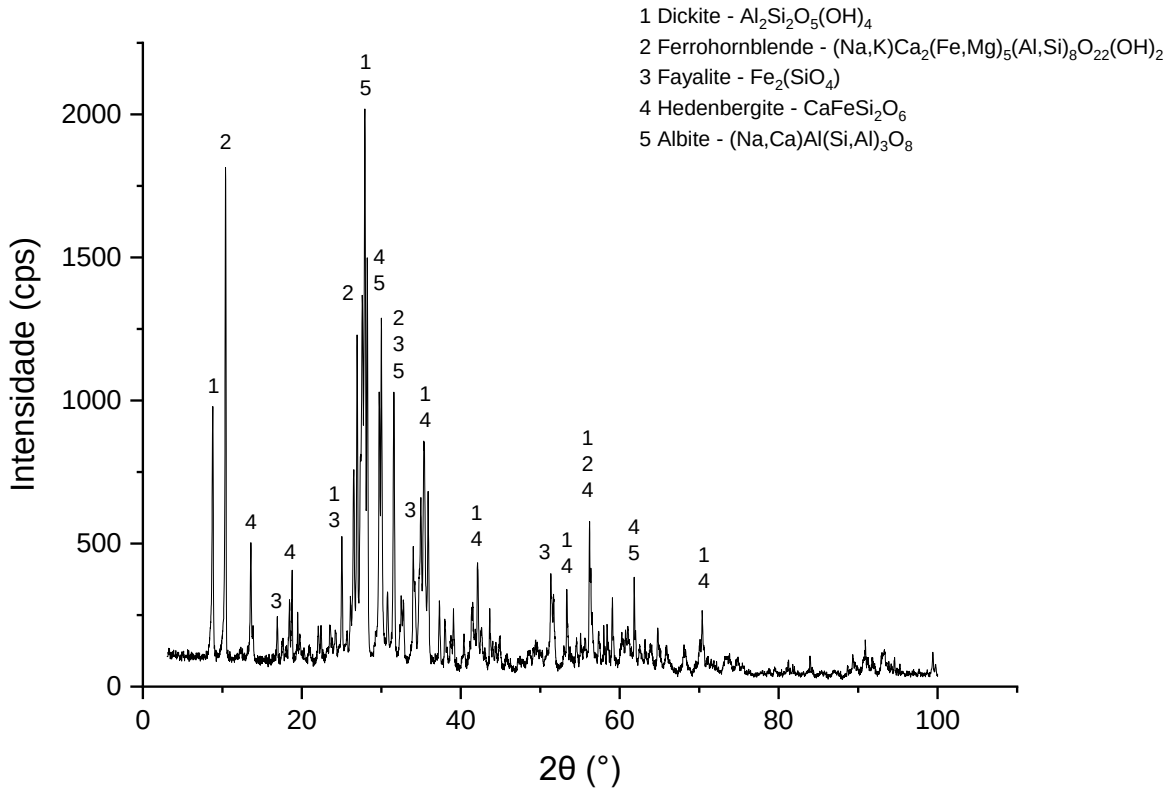

Figure 35: X-ray diffractogram of the silicate-based ore and the main phases detected

The extractive process of rare earth elements from silicate ores can be accomplished through different approaches. In the case of Gadolinite, for instance, it can be performed by a) alkali fusion + water leaching; b) chlorination; and c) acid leaching (H_2SO_4, HCl, or HNO_3) and further precipitation as oxalate [1]. The disadvantages of alkali fusion are the high sodium hydroxide consumption, difficulty to wash and filter due to the high viscosity, and a large amount of water to recover the excessive sodium hydroxide [357]. Moreover, as in the case of scandium extraction where the alkali fusion step is used and further acid leaching, the consumption of acid for both neutralizes the alkali and extract the elements can make the process economically unfeasible. It can be observed in scandium extraction from bauxite residue [37,54,164].

For this reason, in the present study it was explored direct leaching and acid baking. The elements analyzed were iron, zirconium, titanium and the rare earth

elements. All the rare earth elements can be extracted in an acid medium, as proposed in the acid leaching. In the case of dry digestion or acid baking using sulfuric acid, the purpose is to convert the rare earth elements into sulfate salts, water-soluble. The same can occur in direct leaching by sulfuric acid. In the case of nitric or hydrochloric acids, they have been replaced due to the leaching efficiency, costs and cause industrial problems related to corrosion.

Reid et al. (2017) demonstrated that the extraction rate of rare earth elements by mineral acids from bauxite residue might achieve similar results. Scandium leaching rate was 32%, 45%, and 40% using nitric, hydrochloric, and sulfuric acid 1.5mol/L at 90˚C for 30min. Similar results were obtained for neodymium [316]. Zhang et al. (2020) demonstrated that sulfuric acid could be used for scandium extraction silicate ore [86]. Nevertheless, there is a lack of literature about sulfuric acid leaching of rare earth elements from silicate-based ore.

5.3.3.2. Direct leaching

Effect of solid-liquid ratio and acid concentration

The experiments were performed in Erlenmeyer flasks at 25˚C for 8h and stirring speed 200rpm. The experiments were carried out with 100mL of sulfuric acid 4mol/L, varying the mass of the ore. The leaching rate of iron, zirconium, lanthanum, cerium, neodymium, and scandium are shown in Figure 36. Titanium content was lower than the detection limit of the equipment. The redox potential of the leaching liquor was measured at 630mV.

The leaching rate of zirconium was lower than 0.5% - it was 0.4% for solid-liquid ratio equals to 1/5 and slightly increased to 0.5% for 1/50. For iron, the leaching rate increased from 33.2% to 53.3% as the solid-liquid ratio increased from 1/5 to 1/50. It occurs since the increase in the solid-liquid ratio increases the amount of acid for each part of the ore's leaching reaction.

In the rare earth elements, there was virtually no difference in the increase of the solid-liquid ratio. In the case of lanthanum, cerium, and yttrium, for instance, the leaching rate increased from 61.0%, 57.7% and 47.7% (1/5) to 64.9%, 61.0% and 52.0% (1/50), respectively. Scandium extraction achieved up to 3%.

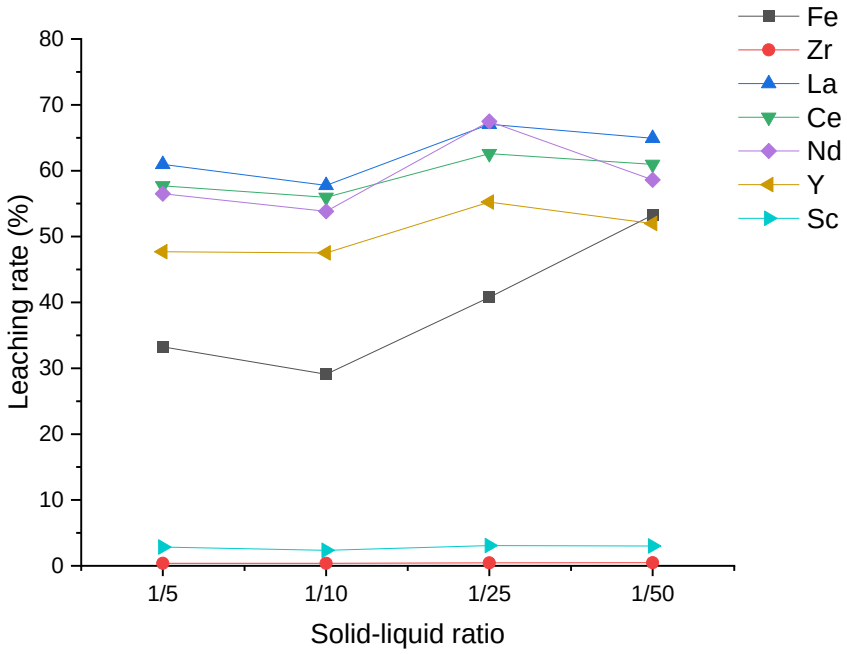

Figure 36: Leaching rate of iron, zirconium, lanthanum, cerium, neodymium, yttrium, and scandium varying the solid-liquid ratio. Experimental conditions: 100mL of sulfuric acid 4mol/L; T = 25˚C; t = 8h; stirring speed = 200rpm.

Figure 37 shows the effect of acid concentration in the leaching of silicate-based ore. The iron extraction increased from 19.7% (0.5mol/L) to 24.8% (1.0mol/L) and then remained constant as the concentration of H^+ increased. It might occur due to the reaction of iron oxides present in the ore, which are easier leached than other iron compounds [366] than ilmenite [367], for instance. In this case, hydrochloric acid with sodium bifluoride and metallic iron is used as a reducing agent for titanium extraction [45].

The leaching of scandium slightly increased as the acid concentration increased until 2.4%. Zirconium leaching remained the same (up to 0.45%). The extraction of lanthanum, cerium, neodymium, and yttrium decreased as sulfuric acid concentration increased. The concept of salvation can explain the decrease in leaching efficiency. As the concentration of electrolyte increases, the proportion of

water/electrolyte decreases, resulting in fewer water molecules for the leaching reaction because cations and anions tightly hold them in the solution [316,368].

As shown in Equations 25 and 25, the leaching of rare earth elements by sulfuric acid generates their ions in sulfate media. As the concentration of sulfate anions increases, the rare earth elements precipitate as sulfate salts [345]. It may explain why the leaching of rare earth elements declined.

$$REE_2O_3 + H_2SO_{4(aq)} \rightarrow REE^{+3} + {SO_4}^{-2} + H_2O \qquad \text{Equation 25}$$

$$REE^{+3} + {SO_4}^{-2} \rightarrow REE_2(SO_4)_3 \qquad \text{Equation 26}$$

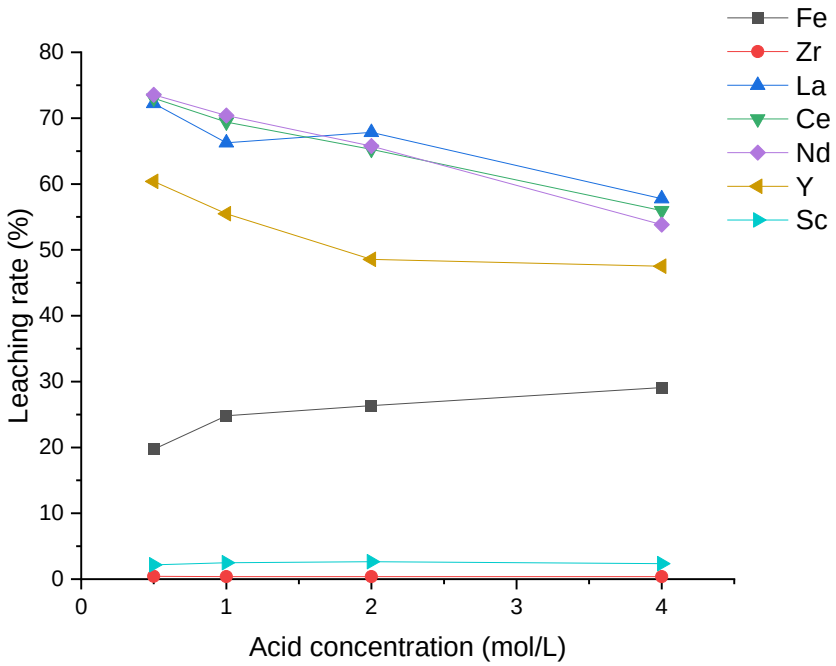

Figure 37: Leaching rate of iron, zirconium, lanthanum, cerium, neodymium, yttrium and scandium varying the acid concentration. Experimental conditions: 100mL of sulfuric acid; solid-liquid ratio = 1/10; T = 25˚C; t = 8h; stirring speed = 200rpm.

Oxidizing and reducing leaching experiments

Hydrogen peroxide and sodium dithionite were used as oxidants and reducing agents, respectively, in the leaching process. In the case of hydrogen peroxide, it was studied due to the silica gel synthesis during silicates' leaching. Alkan et al. (2018) studied the oxidizing leaching of bauxite residue to avoid silica gel formation. As stated by the authors, the compound is formed during the acid leaching of silicates, and its synthesis decreases the leaching rate since a part of the liquor generated in the leaching is trapped. By the same token, H^+ are consumed during the silica gel synthesis. Also, the silica gel causes practical process problems due to the difficulty in the solid-liquid separation step [48].

In the case of sodium dithionite as a reducing agent, it was used to reduce the redox potential during the reaction. Figure 38 shows the Pourbaix diagram of Fe-S-H_2O system, where is highlighted the pH of the leach solution and initial redox potential and the decrease as the sodium dithionite is used in the reaction. According to Luo et al. (2015), and as demonstrated in the Pourbaix Diagram, in reducing medium the leaching of iron could be benefited and the target metals present in these compounds will be released [366].

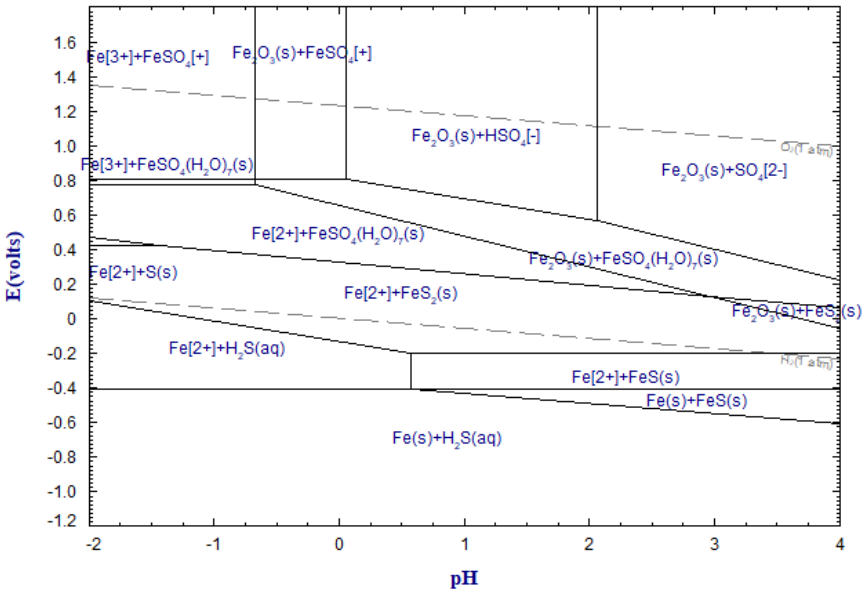

Figure 38: Pourbaix Diagram of Fe-S-H_2O system elaborated with the FactSage 8.0 software.

Since the same rare earth elements can be found in iron compounds, as scandium [164], the conversion into ferrous iron and thereby release the elements, reducing agent to lower the potential of the leaching reaction can be highly beneficial. Luo et al. (2015) stated that the use of a reducing agent in the leaching of nickel laterite increased the leaching of iron and nickel from 40% to up to 60% [366].

Figure 39 shows the leaching rate of iron, titanium, zirconium, and rare earth elements adding hydrogen peroxide and sodium dithionite into the reaction. The extraction efficiency in oxidizing leaching increased as the hydrogen peroxide was added into the system until 2.5% in all cases and then slightly decreased. The exception was iron, where declined from 29.3% (2.5v/v% of hydrogen peroxide) to 9.3% (10.0v/v% of hydrogen peroxide). As depicted in Figure 38, for sulfuric acid 2.0mol/L without oxidant agent, the iron can be presented in the solution as ferrous iron and in the solid phase as iron sulfate, where it occurs after the leaching reaction. However, in the oxidizing leaching reaction where the redox potential increased to 1,000mV, iron oxide is not leached totally, and only a part generates iron sulfate ions.

The leaching of lanthanum, cerium, and neodymium increased from up to 65% (without hydrogen peroxide) to 85% (5.0v/v% of hydrogen peroxide). In the case of scandium, its efficient rate increased from 2.6% (without hydrogen peroxide) to 4% (5.0v/v% of hydrogen peroxide). The leaching of titanium increased in the oxidizing leaching. The H_2SO_4-H_2O_2 system contributes to the formation of titanium peroxo sulfate, which is soluble during leaching, as shown in Equation 27 and Equation 28 [48].

$$TiO_2 + H_2SO_4 \rightarrow [TiO]SO_4 \qquad \text{Equation 27}$$

$$[TiO]SO_4 + H_2O_2 \rightarrow [TiO-O]SO_4 + H_2O \qquad \text{Equation 28}$$

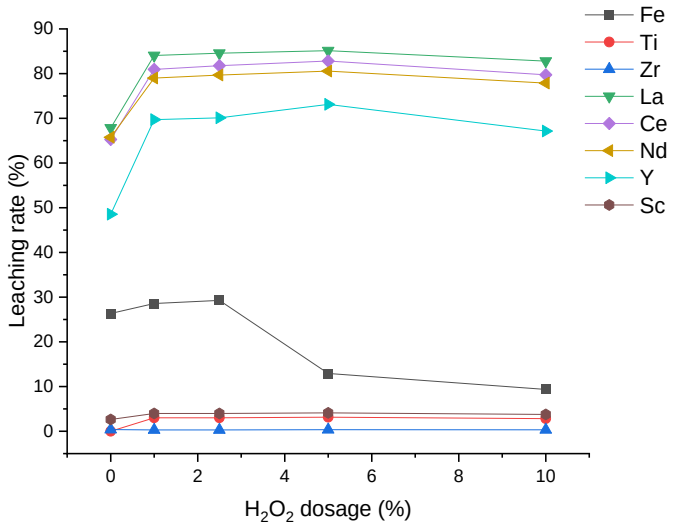

(a)

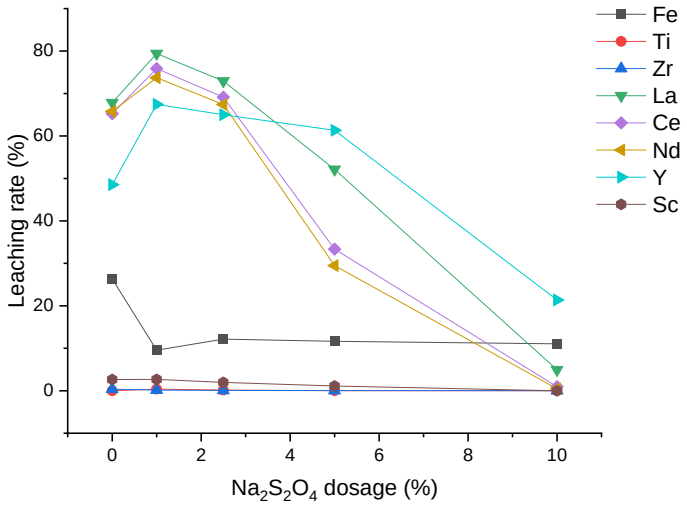

(b)

Figure 39: Leaching rate of iron, zirconium, lanthanum, cerium, neodymium, yttrium and scandium varying the percentage of (a) hydrogen peroxide (H_2O_2) and (b) sodium dithionite ($Na_2S_2O_4$). Experimental conditions: 100mL of sulfuric acid 2.0mol/L; solid-liquid ratio = 1/10; T = 25˚C; t = 8h; stirring speed = 200rpm.

The leaching rate in reducing medium is presented in Figure 39b. As observed, the H_2SO_4-$Na_2S_2O_4$ system increased the leaching of rare earth elements from around 60% (without sodium dithionite) to 80% (1.0wt% of sodium dithionite) and 70% (2.5wt% of sodium dithionite). The same behavior was observed for the other elements. The decrease in leaching efficiency above 2.5wt% of sodium dithionite. This is not because

of reducing redox potential but due to the acid consumption by sodium dithionite. As previously reported, in an acid medium, sodium dithionite reacts with H^+ and releases H_2S [225,369–371]. For this reason, as more reduction is added into the leaching process, the extraction rate decreased, and consequently, the pH of the solution grew (until 3.0). As a result, the leaching efficiency achieved lower values for 10wt% of sodium dithionite than 2.5wt%.

Comparing the oxidizing and reducing leaching reaction, the H_2SO_4-H_2O_2 system has more benefit to the leaching of rare earth elements than the H_2SO_4-$Na_2S_2O_4$ system, where the extraction of lanthanum, cerium, and neodymium achieved up to 80%. The concentration of yttrium and scandium in the solution increased more than 17%, adding 1wt% hydrogen peroxide into the reaction. For 1wt% of sodium dithionite, yttrium content increased 12%, and no difference was observed for scandium.

Thermodynamic experiments

The effect of temperature in the oxidizing leaching of silicate-based ore was studied from 25˚C to 90˚C. Results are presented in Figure 40, which shows that the increase in temperature benefited rare earth elements' leaching. Lanthanum, cerium, neodymium, and yttrium extraction slightly increase in the function of temperature. In iron, titanium, zirconium, and scandium, the extraction was even more accentuated – 65.0%, 31.1%, 3.1%, and 13.5% at 90˚C, 4.0mol/L of sulfuric acid, and 1v/v% of hydrogen peroxide, respectively.

As observed in experiments carried out with 2.0mol/L of sulfuric acid and 1v/v% of hydrogen peroxide (Figure 40b), the extraction of lanthanum, cerium, and neodymium slightly decreased as the temperature increased from 25˚C to 90˚C. It might be occurred due to the decomposition of hydrogen peroxide as the temperature increased. At 25˚C, the oxidant agent acts with the acid in the leaching reaction; however, hydrogen peroxide decomposes faster with increasing temperature, which is ever more favorable in an acid medium [48].

On the other hand, the leaching of iron, zirconium, titanium, and scandium increased as the temperature increases. It may indicate that scandium, the most valuable rare earth element in silicate-based ore, is strongly related to their minerals.

Due to its low concentration, scandium was not detected in SEM/EDS and XRD analyses. Moreover, it is already known that it is spread out in different minerals and not concentrated in a few compounds. Scandium occurs in trace concentration is up to 800 minerals, also because it substitutes the major elements, like iron and aluminum, in the ores [20,357]. It difficult its extract from primary resources.

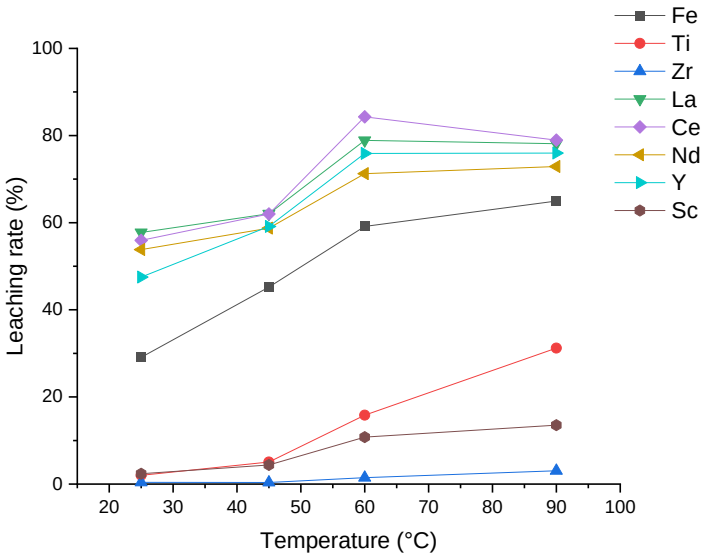

(a)

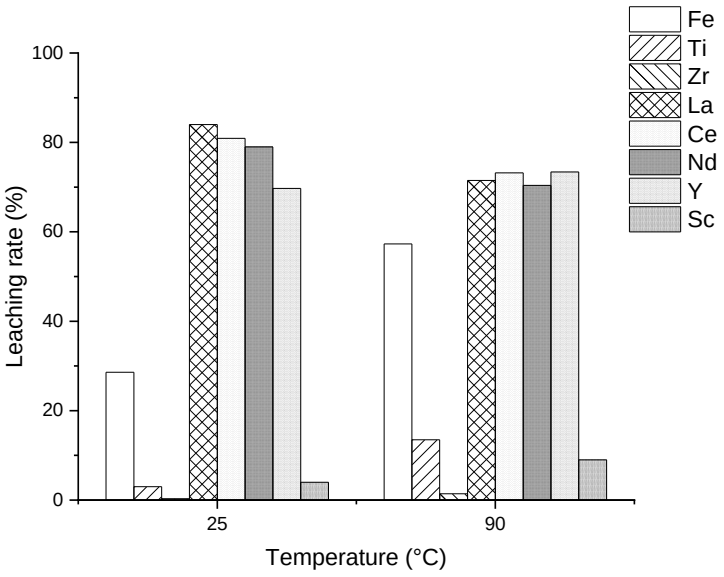

(b)

Figure 40: Leaching rate of iron, zirconium, lanthanum, cerium, neodymium, yttrium and scandium varying the temperature. Experimental conditions: 100mL of sulfuric acid (a) 4.0mol/L and (b) 2mol/L; 1v/v% H_2O_2; solid-liquid ratio = 1/10; t = 8h; under magnetic stirring.

Figure 41 shows the correlation between the scandium leaching and iron, zirconium, and rare earth elements. Low linear correlation $r^2 < 0.9$ was observed for zirconium and cerium. It shows that scandium is spread out in different minerals in the silicate-based ore. The linear correlation (r^2) between lanthanum and cerium was equaled to 0.98 and up to 0.9 between iron and rare earth elements. It indicates that the rare earth elements might be in the same minerals containing iron. As the iron leaching increased from 30% (25˚C) to 65% (90˚C) and the rare earth elements increased from up to 60% (25˚C) to 80˚C (90˚C), it shows that not all iron compounds contain rare earth elements.

The effect of temperature can be expressed by the Arrhenius equation as depicted in **Equation 29** and **Equation 30**, where ***K*** is the reaction rate, ***A*** is the frequency factor, ***Ea*** is the activation energy, R is the gas constant (8.3145J/(mol.K)) and ***T*** is the temperature [86,343]. Results are shown in Table 28. The activation energy for iron, titanium, zirconium, and scandium was 11.3, 39.4, 31.6, and 25.4kJ/mol, respectively. For lanthanum, cerium, neodymium, and yttrium, the activation energy was 4.7, 5.4, 6.8, and 4.5kJ/mol, respectively.

$$K = Ae^{\frac{-Ea}{RT}} \qquad \text{Equation 29}$$

$$\ln K = \ln A - \frac{Ea}{R.T} \qquad \text{Equation 30}$$

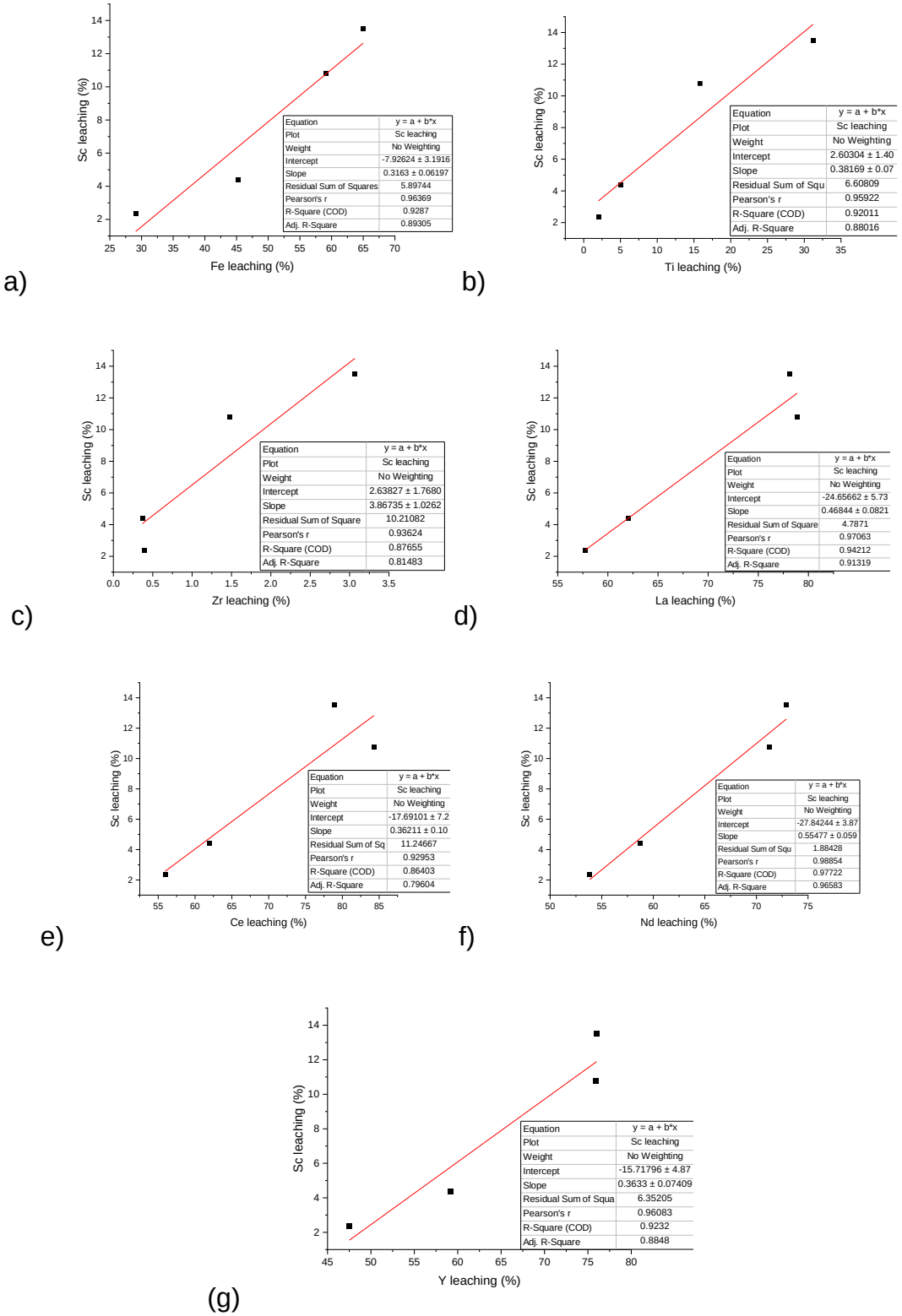

Figure 41: Correlation between leaching rates of scandium and (a) iron, (b) titanium (c) zirconium, (d) lanthanum, (e) cerium, (f) neodymium and (g) yttrium rates in different temperatures. Experimental conditions: 100mL of sulfuric acid 4.0mol/L; 1v/v% H_2O_2; solid-liquid ratio = 1/10; t = 8h; stirring speed = 200rpm.

Table 28: Arrhenius data for the leaching of iron, zirconium, lanthanum, cerium, neodymium, yttrium and scandium varying the temperature. Experimental conditions: 100mL of sulfuric acid 4.0mol/L; 1v/v% H_2O_2; solid-liquid ratio = 1/10; t = 8h; stirring speed = 200rpm.

	Fe	**Ti**	**Zr**	**La**	**Ce**	**Nd**	**Y**	**Sc**
Activation energy (J/mol)	11,217.87	39,404.73	31,617.41	4,661.09	5,387.19	6,830.66	4,541.61	25,448.91
Frequency factor (x 10^{-2})	3.38	5.90 x 10^{-4}	9.73 x 10^{-2}	26.19	19.83	12.73	29.48	0.14
linear correlation (r^2)	0.8911	0.9639	0.8492	0.788	0.7051	0.8401	0.8663	0.9098

Dry digestion and acid baking experiments

Despite the direct leaching achieved extraction rate of rare earth elements, there are different leaching methods studied. Dry digestion and acid baking are a few of them studied in the literature to extract rare earth elements. One of the reasons is the recovery of sulfuric acid in the process. Rivera et al. (2018) reported that the dry digestion for extraction of rare earth elements the economic benefits than direct leaching [127]. In acid baking, where the source is mixed with sulfuric acid and heated at 200-400˚C, SO_2 released from the pyrometallurgical step can be recovered for sulfuric acid production and then recycled. Nevertheless, direct leaching consumes less energy than acid baking [164].

Moreover, the main problem of direct leaching of silicate ores by sulfuric acid is the silica gel formation. According to Terry (1983), the following results the action of acids in the silicate [86,372]:

a) Complete destruction of silicate structure and cations release, generating silica gel;

b) Partial dissolution of silicate structure and cations release, which leads the silica compound in the solid phase; and
c) The acid does not react with the silicate.

Anawati & Azimi (2019) studied the acid baking of bauxite residue to extract rare earth elements. The authors state that the water leaching achieved equilibrium within 2h of the process. Moreover, water leaching at 90˚C achieves a faster kinetic reaction than at lower temperatures [164]. Kim & Azimi (2020) studied the extraction of slag rich in rare earth elements by acid baking, and the authors also stated that the water leaching achieved the plateau after 120min in all cases, and the kinetic rate is faster at 90˚C than lower temperatures [364].

Zou et al. (2021) demonstrated that lanthanum and cerium extraction also achieved the plateau after 120min in leaching after the baking process from rare earth polishing powder wastes [365]. As depicted by Demol et al. (2019), the reaction time of water leaching after acid baking of rare earth concentrates varies between 0.08 - 3h [35]. For this reason, for the present study, it was adopted as leaching time as 2h.

Effect of acid dosage

The experiments were performed at 400˚C, and the acid dosage studied were: 0.6mL, 1.0mL, 1.3mL, and 1.5mL for each gram of ore. The mixture was homogenized at room temperature and then heated to the desired temperature for 2 hours. The water leaching was carried out using ultra-pure water in a solid-liquid ratio equals to 1/10 at 90˚C for 2h.

The effect of resin dosage is shown in Figure 42. The extraction of cerium achieved 92% for 0.6mL of acid dosage for each gram of sample. It is higher than direct leaching experiments, where its extraction achieved up to 80%. Similar results were observed for lanthanum and neodymium.

Yttrium extraction was higher indirect leaching than acid baking at 400˚C. The same was observed for iron and scandium. During heating, iron compounds are converted to iron sulfate, which is soluble in water. Equations 7-8 show the reaction of iron with sulfuric acid concentrated at 150-250˚C generating iron sulfates. In

temperatures up to 400˚C (**Equation 33-34**), iron oxide (hematite) is formed, releasing sulfur oxide. Basic iron sulfate can also be formed. In both cases, the iron compound is insoluble [35].

According to the equations, the increase in sulfuric acid dosage growth the generation of insoluble iron compounds. As these compounds bearer scandium and its release during water leaching are directly related to iron extraction, the leaching of scandium is declined. Moreover, it is reported in the literature that, at high temperatures, the rare earth elements compounds formed in the acid baking are insoluble in the water leaching [35].

Moreover, after the water leaching, the leach solution's pH was up to 1.5, which indicates that most of the sulfuric acid was released as gas in the baking step. As shown in **Equation 31-34**, the same might occur in the leaching of rare earth elements: first, sulfate compounds were formed; and due to the temperature, a decomposition occurs, forming oxides.

Figure 43 shows the X-ray diffractogram of the samples after acid baking. Iron sulfate was identified in samples after acid baking. However, hematite was also identified. As depicted, the mineral phase Fayalite was decomposed; on the other hand, other silicate phases did not fully react with sulfuric acid concentrated.

$$Fe_2O_{3(s)} + 3H_2SO_{4(l)} \rightarrow Fe_2(SO_4)_{3(s)} + 3H_2O_{(g)} \quad \text{Equation 31}$$

$$Fe_3O_{4(s)}(s) + 4H_2SO_{4(l)} \rightarrow Fe_2(SO_4)_{3(s)} + FeSO_{4(s)}(s) + 4H_2O_{(g)} \quad \text{Equation 32}$$

$$Fe_2(SO_4)_{3(s)} \rightleftarrows Fe_2O_{3(s)} + 3SO_{3(g)} \quad \text{Equation 33}$$

$$Fe_2(SO_4)_{3(s)} \rightarrow Fe_2O(SO_4)_2 + SO_{3(g)} \quad \text{Equation 34}$$

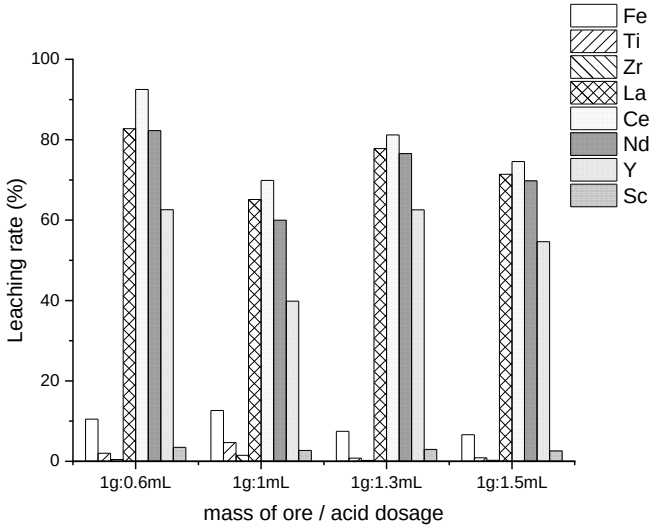

Figure 42: Leaching rate of iron, zirconium, lanthanum, cerium, neodymium, yttrium, and scandium varying the acid dosage. Experimental conditions for baking: 1g of ore; T = 400˚C; 2h. Experimental conditions for water leaching: solid-liquid ratio = 1/10; t = 2h; under magnetic stirring.

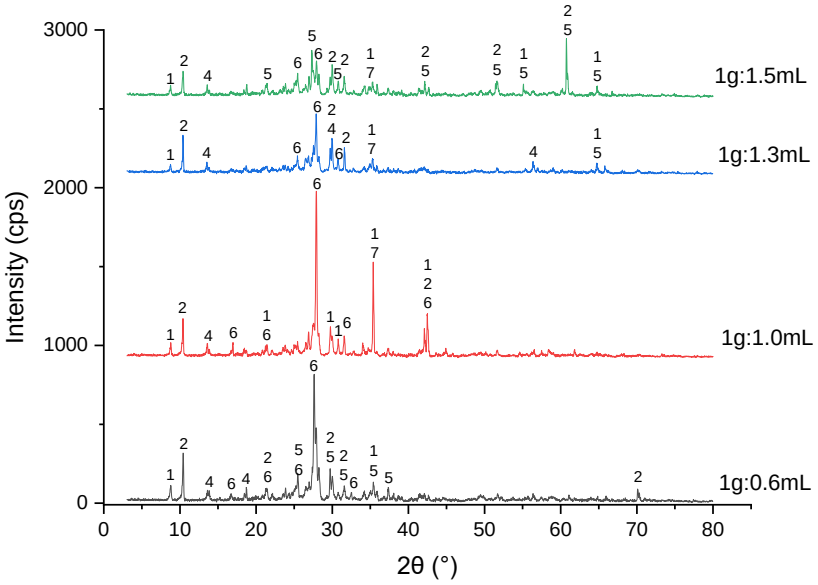

Figure 43: X-ray diffractogram of the samples and the main phases detected varying the acid dosage. Experimental conditions for baking: 1g of ore; T = 400˚C; 2h. Peaks: 1- Dickite; 2- Ferrohornblende; 3- Fayalite; 4- Hedenbergite; 5- Albite; 6- Iron sulphate; 7- Hematite.

Effect of temperature

The baking process temperature was evaluated between 200-400˚C using a proportion 1g or ore / 0.6mL of sulfuric acid. Dry digestion (25˚C) was also tested for the same proportion. Ultra-pure water was used for leaching at 90˚C for 2h. Results are shown in Figure 44. The pH of the liquor of water leaching increased from 0.2 (25˚C) to 1.5 (300˚C and 400˚C). **Equation 35** depicts the decomposition reaction of sulfuric acid in the baking process. As the temperature increases, there will be less acid to react with the ore, and sulfur oxide and water will be released as gases [35].

$$H_2SO_{4(l)} \rightarrow SO_{3(g)} + H_2O_{(g)} \qquad \text{Equation 35}$$

For cerium extraction, the highest extraction occurred at 400˚C. Indeed, the acid baking at 400˚C releases more sulfur oxides than in lower temperatures, which explains low leaching rates.

There was almost no effect in neodymium and yttrium extraction as the temperature in acid baking increased. At 200˚C of process, lanthanum achieved the highest extraction rate (87.0%), as well as zirconium (4.9%)

Comparing to direct leaching, acid baking increased the extraction of rare earth elements. For iron extraction, the extraction rate was higher in lower temperatures (25˚C and 200˚C). In the case of scandium, the highest extraction rate was obtained in dry digestion and acid baking at 200˚C (6.3% and 5.7%, respectively), lower than obtained in direct leaching at 90˚C (13.5%).

Varying the acid dosage (0.6mL and 1.5mL) for the baking process at 200˚C, presented in Figure 44b, the extraction of rare earth elements slightly increased. According to the results presented here, it is concluded that dry digestion or acid baking could partially destroy the silicate structures.

As observed, the extraction rate of lanthanum, cerium, and neodymium was higher than direct leaching. On the other hand, scandium, titanium, zirconium, and

yttrium rates were lower. For iron, no difference was observed between direct leaching and dry digestion or acid baking.

(a)

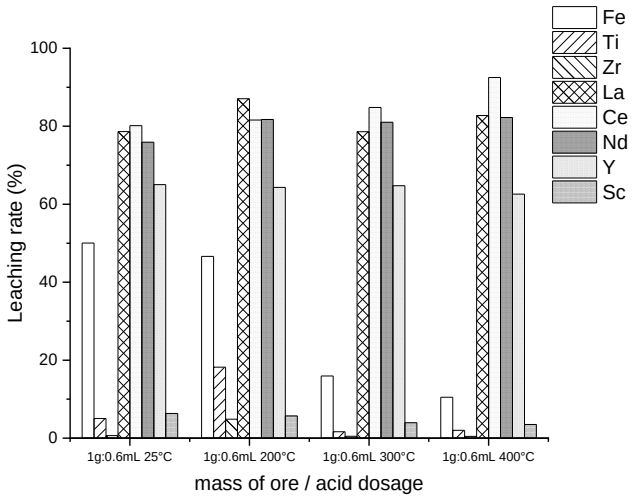

(b)

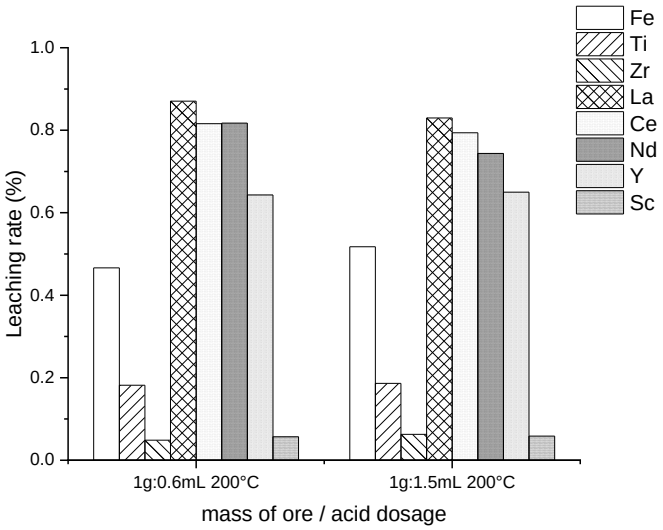

Figure 44: Leaching rate of iron, zirconium, lanthanum, cerium, neodymium, yttrium, and scandium (a) varying the temperature and (b) varying the acid dosage at 200˚C. Experimental conditions for baking: 1g of ore; 2h. Experimental conditions for water leaching: solid-liquid ratio = 1/10; t = 2h; under magnetic stirring.

5.4. Selective separation of Sc(III) and Zr(IV) from the leaching of bauxite residue using trialkylphosphine acids, tertiary amine, tri-butyl phosphate and their mixtures

A.B. BOTELHO JUNIOR; D.C.R. ESPINOSA; J.A.S. TENÓRIO

Department of Chemical Engineering; Polytechnic School, University of Sao Paulo, Sao Paulo – Brazil.

ABSTRACT

The separation of scandium from the solution generated in acid leaching is one of the main challenges for the hydrometallurgical processing of bauxite residue. Several organic extractants were evaluated, being the most prominent phosphine acids, while amine-based compounds have shown great results for separating metallic ions. The present study aims at the separation of scandium and zirconium from the Brazilian bauxite residue. The acid leaching was carried out using 20% of H_2SO_4, S/L ratio equals 1/10, for 8h at 90°C. Further, solvent extraction experiments were carried out using D2EHPA, Cyanex 923, and Alamine 336 diluted in kerosene, evaluating the effect of pH, temperature, extractant concentration, synergism with TBP and A/O ratio. After optimizing various process parameters, Alamine 336 has obtained separation factors of Zr/Al, Zr/Fe, and Zr/Ti equal to 15150, 45054, and 19713, respectively, at pH 1.0, A/O ratio equals to 1:1 and 25°C. The stripping rate achieved 92% using Na_2CO_3 0.25mol/L. The scandium separation ratio reached higher values for Cyanex 10% than D2EHPA 10% + TBP 5%. Scrubbing for contaminants removal may be carried out using HCl 5mol/L with 0.1% of scandium losses, and all scandium was stripped by H_3PO_4 5mol/L. Despite the works reported in the literature, none explored the recovery of scandium and zirconium by the leaching-solvent extraction process. The flowchart proposed is strictly connected to the sustainable development goals 7, 8, 9, and 12.

Keywords: solvent extraction; Cyanex 923; Alamine 336; scandium

Graphical abstract

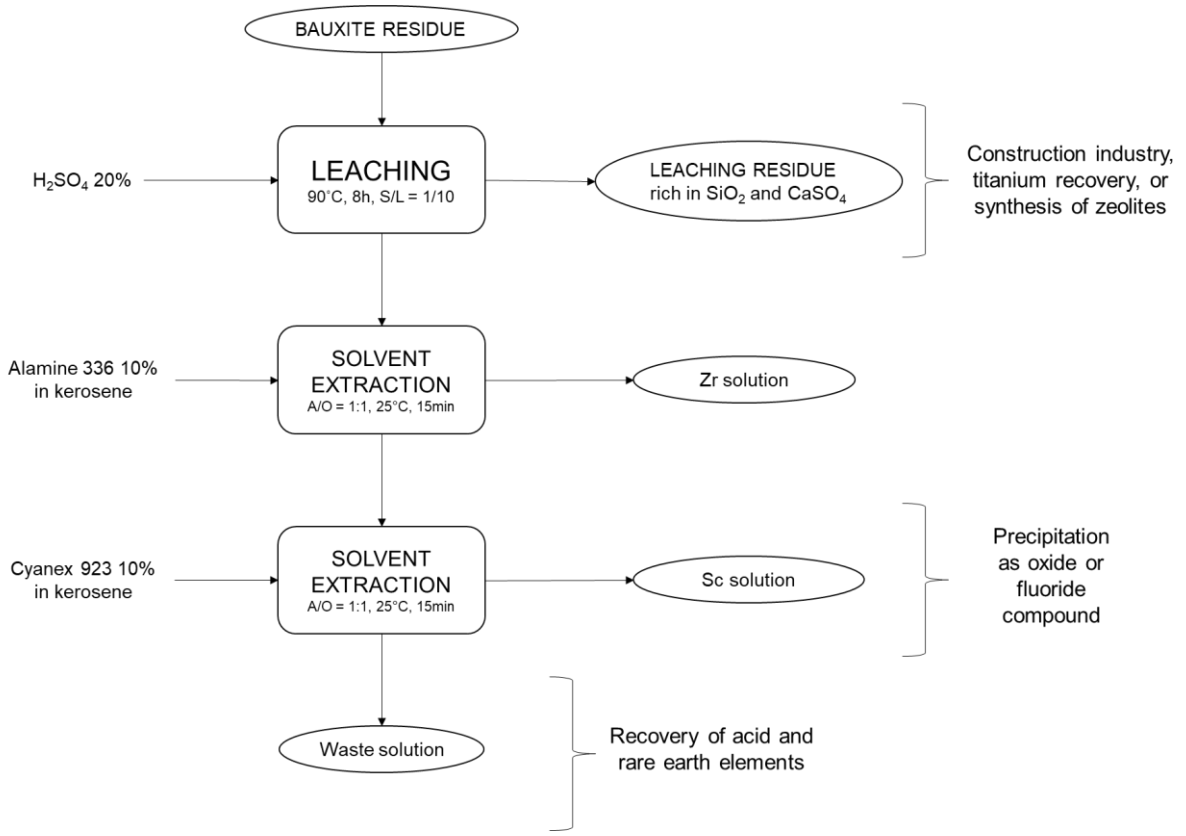

5.4.1. Introduction

The biggest challenge of the current process development is to design a process approaching the circular economy, where all the residues and wastes may be used for other applications [26]. Also, such materials would support the supply chain of critical materials, which has supply risk in the short and medium-term [329]. In this context, the extraction of critical metals from bauxite residue, a waste material produced in the Bayer process for alumina production, may represent a significant advance for sustainable development [373].

The residue contain as main elements iron (15-46%), aluminum (5-24%), titanium (2.1-11%), silicon (3-30%) and sodium (2.1-11.7%), and in trace concentration there are rare earth elements and zirconium [273]. In 2020, the European Union updated the list of critical raw materials [374], where it is present titanium, zirconium, and rare earth elements, in special scandium, which represents up to 95% of the economic value of the bauxite residue [20]. It is because scandium is dispersed in the

Earth's crust and is rarely found in concentration which makes its extraction economically feasible [55].

Several studies have been developed in the last years on scandium extraction from the residue, and pyrometallurgical and hydrometallurgical routes have been explored. For instance, Borra et al. (2016) studied the alkali roasting for aluminum removal followed by smelting for iron removal. The slag generated is then leached to recover rare earth elements and titanium with up to 80% [51]. Also, the combination of sulfation, roasting, and water leaching was previously explored, but the kinetic of scandium dissolution is low (2 days under stirring) [275]. In both situations, the scandium extraction yield is around 60%.

Furthermore, as depicted by Liu & Naidu (2014), pyrometallurgical requires high energy consumption, and it is not suitable for the extraction of elements in trace concentrations [20]. Direct leaching of bauxite residue may achieve up to 90% of the scandium extraction rate using mineral acids, where sulfuric acid (H_2SO_4) is the most common for industrial purposes. Also, the literature review reports high extraction of contaminants requiring separation steps [48,54,159,160].

Precipitation, ion exchange resins, and solvent extraction are some techniques that have been explored [19]. Membranes supported with organic extractants have demonstrated promising results but require more development for industrial feasibility [214,252]. The removal of contaminants or separation of target metals by precipitation is widely applied, but it would cause losses of scandium due to the high concentration of iron in the solution (over 10,000 times) [375]. Ion exchange resins have been demonstrated a separation yield of 90% for scandium; however, as depicted by Bao et al. (2018), the separation factor of Sc/Fe(III) and Sc/Fe(II) systems were 0.16-29.4 and 55-409, respectively. Thus, it shows that the separation of scandium and iron is low [284].

Solvent extraction is an established technique for the separation of purification of an aqueous solution by a mixture of the organic and aqueous phases, where the organic extraction removes the target element. The separation of the phases occurs by density difference [284]. Table 29 shows the literature review for scandium and zirconium separation by solvent extraction. Phosphinic and phosphoric acids (Cyanex 272, and D2EHPA) are frequently used to extract scandium due to the interaction

between the ions and the functional group. At the same time, amine-based extractants (Aliquat 336, Alamine 336, Alamine 300, and TEHA) are most suitable for zirconium extraction.

Table 29: A literature review of scandium and zirconium separation by solvent extraction

Sc content	Medium	Organic extractant	% recovery	Reference
24mg/L	H_3PO_4	P204 - di-(2-Ethylhexyl) phosphoric acid	95%	[206]
140mg/L	H_2SO_4	Cyanex 272 - di-2,4,4-trimethylpentyl phosphinic acid; Cyanex923 - a mixture of four trialkyl phosphine oxides	95%	[210]
>2g/L	HNO_3, HCl, and H_2SO_4	TRPO - isoamyldialkyl(C7-C9)phosphine oxide	80%	[211]
4.5mg/L	HNO_3	PC88A - 2-ethylhexylphosphonic acid mono-2-ethyl- hexyl ester; Versatic 10 - neodecanoic acid	up to 90%	[376]
20mg/L	H_2SO_4	D2EHPA - di-2-ethylhexyl phosphoric acid; TBP - tri-n-butyl phosphate	99.72%	[215]

Zr content	Medium	Organic extractant	% recovery	Reference
0.2g/L	H_2SO_4	Aliquat 336 - tricaprylmethylammonium chloride, a quaternary ammonium salt; Alamine 308 - tri-isooctyl amine; Alamine 336 - mixture of tri-octyl/decyl amine; Alamine 300 - tri-n-octyl amine; and TEHA - tri-2-ethylhexyl amine	90%	[377]
0.2g/L	H_2SO_4	D2EHPA - di-2-ethylhexyl phosphoric acid; Cyanex 272 - di-2,4,4-trimethylpentyl phosphinic acid; and LIX 63 - 5,8-diethyl-7-hydroxy-6-dodecanone oxime	90%	[378]
0.2g/L	HNO_3	LIX 63 - 5,8-diethyl-7-hydroxy-6-dodecanone oxime; PC 88A - 2-ethylhexylphosphonic acid mono-2-ethyl- hexyl ester	> 95%	[379]

There is little literature reporting the recovery of both scandium and zirconium from the bauxite residue. Wang et al. (2013) propose separating zirconium using a primary amine extractant Primene JMT and scandium extraction by D2EHPA. However, the authors stated that scandium is co-extracted by the amine-based extractant, which declines the process efficiency [50]. For this reason, it is necessary to study to achieve a high separation rate of the Zr/Sc system and then obtain a scandium solution.

The present study aims to recover scandium and zirconium from leach solution of bauxite residue by solvent extraction. Leaching experiments were carried out with

dry bauxite residue with H_2SO_4. The leach solution was characterized before solvent extraction experiments. Cyanex 923, D2EHPA, and Alamine 336 in kerosene were tested for selective separation. The effect of pH, temperature, extractant concentration, and the synergism with TBP. Experiments were carried under magnetic stirring and temperature control for 15min in a beaker. The aqueous phase was separated from organic was performed in a glass separatory funnel and filtered for removal of organic remained.

5.4.2. Materials and methods

The present study proposes separating scandium and zirconium from bauxite residue, as depicted in Figure 45. First, the leaching of bauxite residue was carried to extract metals by sulfuric acid (H_2SO_4). Leaching parameters were evaluated. Then, separation steps were necessary to obtain high pure solutions containing scandium and zirconium. Solvent extraction was the technique chosen owing to its high selectivity than others. Three different organic extractants were studied: trialkylphosphine acid, tertiary amine, and their mixture with tri-butyl phosphate.

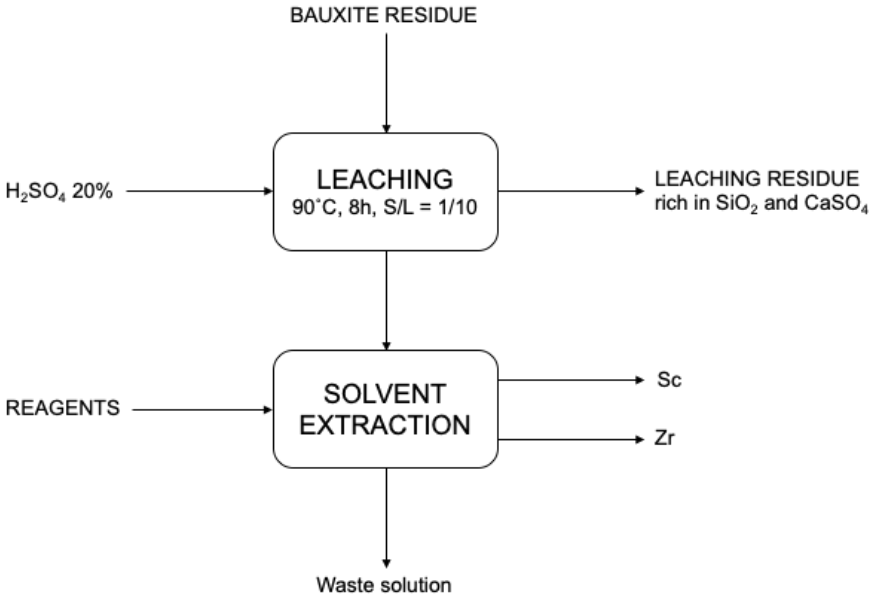

Figure 45: Initial process design for scandium and zirconium separation from bauxite residue

5.4.2.1. Materials

A Brazilian company supplied the bauxite residue sample. The chemical characterization is presented in Table 30. The main mineral phases were quartz, sodalite, gibbsite, goethite, hematite, boehmite, and gypsum. The moisture content and losses on ignition at 1100˚C were 23.1% and 14.8%, respectively. The total organic carbon and inorganic carbon content were 0.6% and 0.32%, respectively [37].

Cyanex 923 (mixture of four trialkylphosphine acids - TRPO), D2EHPA (di-2-ethylhexyl phosphoric acid), TBP (tributylphosphate), and Alamine 336 (tertiary amine) with purity ≥95% were used as the reagents without purification. Table 31 shows the physicochemical properties of the extractants used and the chemical structures. The extractants were dissolved in kerosene before experiments. The reagents H_2SO_4, NaOH, NaCl, $NaCO_3$, HNO_3, HCl, and H_3PO_4 were of analytical grade. The stock solution was prepared using the following reagents: $Fe_2(SO_4)_3.8H_2O$, $Al_2(SO_4)_3.17H_2O$, La_2O_3, Y_2O_3, and Nd_2O_5 previously dissolved and Sc, Ce(IV), Zr(IV), and Ti(IV) solutions (1,000mg/L). Ultra-pure water was used to prepare the solutions.

Table 30: Chemical characterization of bauxite residue used in the present study [37]

%	**Fe_2O_3**	**Al_2O_3**	**SiO_2**	**Cao**	**Na_2O**	**TiO_2**	
	36.4	23.3	21.6	5.9	9	3.2	
g/tonne	**Sc**	**Y**	**Zr**	**V**	**La**	**Ce**	**Nd**
	43.5	24.2	1329.8	130.3	103.7	405.1	77.6

Table 31: Properties and structure of organic extractants used in the current study [380–383]

Type	Structure		Properties
Cyanex 923	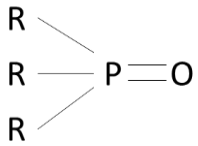	phosphine oxides as follows: $R_3P(O)$, $R_2R'P(O)$, $RR'_2P(O)$, $R'_3P(0)$ Where R = $[CH_3(CH_2)_7]$ - normal octyl R'= $[CH_3(CH_2)_7]$ - normal hexyl	Molecular weight – 348 Flash point (°C) – 182 Specific gravity (at 20°C) - 0.88g/cm^3 Viscosity at 25°C (C.P.) – 40 Solubility (g/100g solvent) - 0.001
D2EHPA	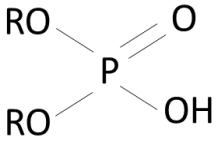	R: $C_4H_9CH(C_2H_5)CH_2$,$C_{16}H_{35}O_4P$	Molecular weight - 322.43 Flash point (°C) – 233 Specific gravity (at 20°C) - 0.970g/cm^3 Viscosity at 25°C (C.P.) - 0.42 Solubility (g/100g solvent) - 0.012
Alamine 336	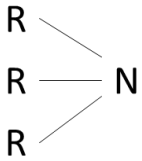	R: C_8H_{17},$C_{24}H_{51}N$	Molecular weight - 353.67 Flash point (°C) – 226 Specific gravity (at 20°C) - 0.8153g/cm^3 Viscosity at 25°C (C.P.) - 10.4 Solubility (g/100g solvent) - 0.01
TBP	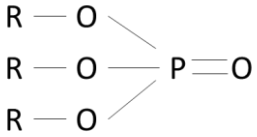	$CH_3(CH_2)_3O)_3PO$	Molecular weight - 266.31 Flash point (°C) – 400 Specific gravity (at 20°C) - 0.966g/cm^3 Viscosity at 25°C (C.P.) - 3.5 - 4.0 Solubility (g/100g solvent) - 0.042

5.4.2.2. Analytical procedure

Samples from solvent extraction experiments were analyzed in energy dispersive X-ray fluorescence (EDXRF - PANalytical Epsilon 3 XL) to determine Fe, Al, Ti, and Zr, and an inductively coupled plasma optical emission spectrometry (ICP-OES - Agilent Technologies 70 series) for the determination of rare earth elements. The mineral assessment was carried out in X-ray diffraction equipment (MiniFlex 300 - Rigaku). Samples were diluted when necessary using HNO_3 4%. The conditions of operation of the equipment followed the manufacturer's protocol. The pH was measured using Ag/AgCl electrode 3mol/L (Sensoglass).

5.4.2.3. Methodology

Leaching procedure

The bauxite residue sample was dried at 60˚C for 24 hours before leaching extraction. Experiments were carried out in a glass reactor (Atlas Sodium) at 800rpm using H_2SO_4. The temperature was controlled throughout the experiment. The effect of acid concentration, temperature, time, and solid-liquid ratio were evaluated. After the process, the solid-liquid separation was performed in the Büchner funnel and coupled to the vacuum pump. Liquid samples were analyzed in ICP-OES for chemical quantification, and the solid phase was analyzed in XRD.

Solvent extraction procedure

The extraction experiments were performed by mixing 10mL of the organic phase and 10mL of the synthetic solution of bauxite residue leaching. The volumes changed when required. Experiments were carried out for 15min under magnetic stirring. The pH was controlled using H_2SO_4 concentrated and NaOH 8mol/L as necessary. The effect of pH was studied using aqueous/organic ratio (A/O) equals to 1:1 and concentration of organic extractant 10% at 25˚C and 60˚C. Effect of organic extractant concentration and the synergic effect of TBP as modifier in extraction efficiency was explored (5% - 25%v/v and 1% - 10%v/v, respectively). The effect of the A/O ratio was also studied.

Stripping experiments were carried out using inorganic acids (H_2SO_4, HCl, HNO_3, and H_3PO_4) and salts (NaCl and N_2CO_3). Experiments were carried out under magnetic stirring for 15, and the A/O ratio equals 1:1 if different was used. The effect of stripping agent concentration was evaluated from 0.1mol/L to 5mol/L.

In extraction/stripping experiments, the aqueous phase was separated from organic by a separatory funnel in stand-by for 5min. Then, the aqueous solution was removed from the funnel and filtered for all organic solution removal. The experimental error was calculated by repeating experiments where the values were lower than 5% [40]. EDXRF determined the metallic ions concentration for significant elements and ICP-OES for trace elements.

The extraction efficiency (E), distribution ratio (D), stripping ratio (S), and separation factor (β) were calculated as depicted in the following equations, where: M_t and M_a are the initial and final concentrations of the metallic ions in the aqueous phase; M_{aq} and M_{org} are the concentration of metallic ions in the stripping solution and the loaded organic phase; and D_1 and D_2 are the distribution ratio of metallic elements 1 and 2. The concentration of metallic ions elements in the organic phase was calculated by mass balance.

$$E = \frac{M_t - M_a}{M_t} \qquad \text{Equation 36}$$

$$D = \frac{M_t - M_a}{M_a} \qquad \text{Equation 37}$$

$$S = \frac{M_{aq}}{M_{org}} \qquad \text{Equation 38}$$

$$\beta = \frac{D_1}{D_2} \qquad \text{Equation 39}$$

5.4.3. Results and discussion

5.4.3.1. Leaching experiments

The extraction of scandium was carried out with 500mL of the acid solution, and the dry bauxite residue was added into the reactor after the solution reached the

desired temperature. The leaching time was studied at 25˚C, the S/L ratio equals 1/10, and the acid concentration equals 20%. Results have shown that the scandium extraction achieved the plateau after 8h (47%). The leaching of scandium was related to the dissolution of iron since the element is mainly hosted in hematite and goethite mineral phases [129].

One of the main problem in direct leaching of bauxite residue is the synthesis of silica gel, which increase the acid consumption, decline scandium extraction and difficult the solid-liquid separation [48]. In the current study, it was also observed that the leaching of silicon from the sodalite mineral phase declined over time due to the compound formation until 8h. No difference was observed varying the S/L ratio for the extraction of scandium.

The temperature improved the extraction of the elements from bauxite residue. The extraction of scandium increased from 47% at 25˚C to 92% at 90˚C. However, the same leaching rate was observed for aluminum and iron. The extraction of zirconium increased from 17% (25˚C) to 26% (90˚C), while silicon leaching achieved 0% at 90˚C.

The effect of acid concentration was evaluated from 10% to 60% at 90˚C for 8h, and the S/L ratio equals 1/10. The extraction of scandium increased from 77% to 92% as the acid concentration increased from 10% to 20-40%. At 60% of H_2SO_4, the scandium extraction declined to 69% due to the excess of SO_4^{-2} ions compared to scandium ions [345]. The leaching efficiency for zirconium has no difference as the acid concentration increased.

As a result, the best conditions for scandium extraction from bauxite residue were 20% of H_2SO_4, S/L ratio equals 1/10, and 8h of leaching reaction at 90˚C. The chemical characterization of the leach solution is presented in Table 23. The primary contaminants are aluminum and iron, while the most valuable elements are scandium (>95% of the economic value) and zirconium (around 3% of the economic value). For this reason, the present study focused on the extraction of scandium and zirconium. According to the data presented in Table 23, a synthetic solution was prepared for extraction experiments considering the metallic elements Al, Fe, Sc, Ti, Zr, La, Ce, Nd, and Y at pH 0.5, as the real leach solution.

Table 32: Composition of the liquor in mg/L after leaching by H_2SO_4. Experimental conditions: acid concentration = 20%, 800rpm, S/L = 1/10, t = 8h, T = 90˚C.

	Al	Fe	Ca	Na	Sc	Si	Ti	V	Zr	La	Ce	Nd	Y
mg/L	5059.8	11804.3	480.1	3104.5	2.7	7.4	200.4	8.6	43.4	5.9	27.6	2.2	1.5

5.4.3.2. Solvent extraction experiments

Effect of extractants (D2EHPA, Cyanex 923 and Alamine 336)

The investigation of three different organic extractants was carried out focus on the extraction of scandium and zirconium with low extraction of contaminants (such as iron and aluminum). The most common extractants used for extraction of rare earth elements and zirconium are phosphorus [50], carboxylic acids [384], solvating [385], and anion exchangers [386]. The present study tested D2EHPA and Cyanex 923, both organophosphorus extractants, and Alamine 336, anion exchanger, diluted in kerosene (10% of organic extractant) and A/O ratio 1:1 for 15min under magnetic stirring.

First, the effect of pH was studied from 0.5 to 2.0 in different temperatures (25˚C and 60˚C) from the synthetic solution based on acid leaching of bauxite residue. Then, the pH was measured and controlled in all experiments, adding NaOH or H_2SO_4 to maintain the desired value.

At pH above 2.0, iron precipitates and carries scandium and other elements to the solid phase [387]. Losses of scandium were observed by Yagmurlu et al. (2017) in the precipitation of leach solution from bauxite residue using NaOH, KOH, limestone, and NH_3 as the pH of the solution increased. Phosphate precipitation showed similar results, where there was precipitation of iron and scandium over 50% at pH above 1.5 [375]. Similar achievements were found in the hydrometallurgy of nickel laterite, where the iron precipitation occurs and co-precipitates the targets metals due to the interaction between ferric or ferrous iron and other metallic ions present solution [225,325,387,388]. For this reason, the experiments were limited to pH 2.0.

Results of extraction yield at 25˚C are shown in Figure 46. The extraction order for zirconium can be given as follows: Alamine 336 >>> Cyanex 923 > D2EHPA. In the case of scandium, the extraction order was D2EHPA > Cyanex 923 >>> Alamine 336.

It followed the common extraction behavior varying the pH value, where the extraction yield increased until the plateau and then declined [389]. It is clearly shown that zirconium separation was more selective using Alamine 336 than D2EHPA and Cyanex 923. In H_2SO_4 media, the extraction of zirconium is possible by two reactions: adduct formation reaction and anion exchange reaction.

Equations 40-42 illustrate the extraction of zirconium in H_2SO_4 media by Alamine 336. First, the amines from the extractant are protonated by the acid (**Equation 40**). Then, in low pH, the zirconium extraction occurs by adduct formation as represented in **Equation 41**, representing the reaction that occurred in the present study. Finally, the extraction of zirconium in higher acidity may be represented as depicted in **Equation 42** [377].

$$R_3N_{(org)} + H_2SO_{4(aq)} \rightarrow R_3NH_2SO_{4(org)}$$

Equation 40 [377]

$$Zr(SO_4)_{2(aq)} + 2R_3NH_2SO_{4(org)} \rightarrow (R_3NH_2SO_4)_2Zr(SO_4)_{2(org)}$$

Equation 41 [377]

$$Zr(SO_4)_2{}^{2-}{}_{(aq)} + 2R_3NH_2SO_{4(org)} \rightarrow (R_3NH)_2Zr(SO_4)_{2(org)} + 2HSO_4{}^{-}{}_{(aq)}$$

Equation 42 [377]

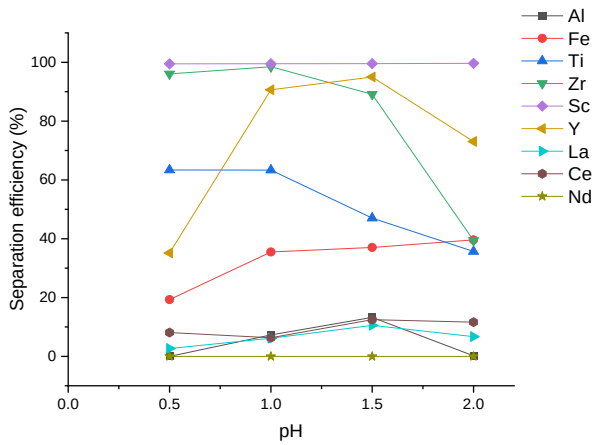

(a)

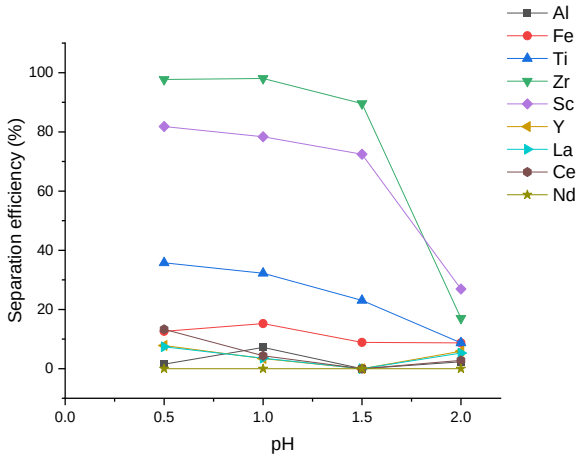

(b)

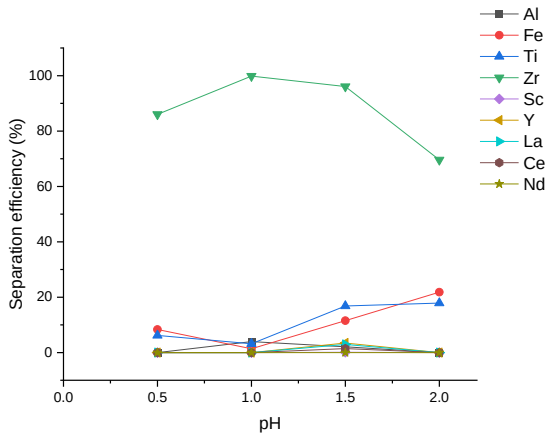

(c)

Figure 46: Effect of pH on extraction of metals from synthetic solution of bauxite residue leaching by (a) D2EHPA, (b) Cyanex 923, and (c) Alamine 336. Experimental conditions: A/O ratio = 1:1; organic extractant concentration = 10%; 15min; 25˚C

According to the present data, the extraction of zirconium was higher in pH below 1.5. Iron and titanium extraction achieved the maximum value at pH 2.0 by Alamine 336 (20%). Similar results were found by Wang & Lee (2015). The declined in zirconium extraction as the pH increased from 1.5 to 2.0 may be explained due to the salting out of sulfuric acid. However, as the solution becomes more acidic (below pH 0.5), low extraction of zirconium is expected due to the competition of metallic ions complexes and bisulfate to react with amines [377]. For this reason, the extraction of zirconium was selective at pH 1.0 using Alamine 336 with low co-extraction of iron (1.4%) and aluminum (4%). About 3% of titanium was co-extracted as well.

The extraction of scandium was closed to 100% in all pH values using D2EHPA with only one contact, as reported by the literature [50]. On the other hand, the extraction was not selective over other elements. For example, the extraction of yttrium increased from 40% (pH 0.5) to 95% (pH 1.5), while the other rare earth elements were lower than 15%. **Equation 43** shows the generic reaction between the rare earth elements (represented as REE) and the organic extractant. Zirconium was also all extracted in pH between 0.5 and 1.5. Iron extraction increased as the solution become less acidic, while titanium extraction declined from 60% to 40%.

$$(REE)^{+3}{}_{(aq)} + 3(\mathrm{HX})_{2(org)} \rightarrow (REE)X_3 3HX_{(org)} + 3H^{+}{}_{(aq)} \qquad \text{Equation 43 [201]}$$

Scandium in acid media reacts with sulfate and bisulfate ions forming a complex (**Equation 44**), which reacts with the organic extractant Cyanex 923, as Souza et al. (2019) depicted in **Equation 45**.

Despite the data reported in the literature, the extraction of scandium was lower than 80% in experiments with Cyanex 923. Due to the presence of zirconium in the solution, the extraction yield was over 90% in pH values between 0.5 and 1.5. The data presented have demonstrated that the extraction of scandium would be more selective than other elements if zirconium is first removed from the solution.

$$Sc^{+3}{}_{(aq)} + SO_4{}^{-2}{}_{(aq)} + HSO_4{}^{-}{}_{(aq)} \rightarrow HSc(SO_4)_{2(aq)} \qquad \text{Equation 44 [331]}$$

$$HSc(SO_4)_{2(aq)} + (HX)_{2(org)} \rightarrow HSc(SO_4)_2.(HX)_{2(org)} \qquad \text{Equation 45 [331]}$$

Table 33 shows the distribution coefficient for iron, titanium, zirconium, and scandium in pH varying from 0.5 to 2.0 at 25˚C and 60˚C. In general, the extraction of metallic ions had no difference as the temperature increased. In most cases, the coefficient value was lower than 1 for the rare earth elements, except for yttrium extraction at pH over 1.0 and 25˚C, and yttrium, lanthanum, and cerium at pH 2.0 and

60˚C by D2EHPA. It shows that Cyanex 923 was more selective for scandium than other rare earth elements. Therefore, it is essential to design a separation process to obtain high pure scandium products.

In the zirconium case, the distribution coefficient achieved the maximum value at pH 1.0 and 25˚C by Alamine 336, while for iron and titanium, the value was pretty much close to 0. Results obtained for experiments performed with Cyanex 923 demonstrated the selective for zirconium than rare earth elements. For scandium, the best results were obtained at 25˚C, mainly in an acidic solution (pH 0.5).

As Souza et al. (2019) observed, the extraction of scandium by Cyanex 923 declined as the temperature increased. According to the authors, it occurs due to the exothermic reaction between scandium ions and the organophosphorus extractant [331]. Also, the increase of temperature rose the extraction of iron and aluminum. As a result, further experiments for the extraction of zirconium were carried out using Alamine 336 at pH 1.0 and 25˚C. In the case of scandium, both D2EHPA and Cyanex 923 at pH 0.5 and 25˚C were tested.

Table 33: Distribution coefficient of iron, titanium, zirconium, and scandium in pH from 0.5 to 2.0 at 25˚C and 60˚C

			Fe	Ti	Zr	Sc
25˚C	D2EHPA	pH 0.5	0.2	1.7	24.2	188.2
		pH 1.0	0.6	1.7	64.5	198.1
		pH 1.5	0.6	0.9	8.2	225.5
		pH 2.0	0.7	0.6	0.7	280.9
	CYANEX 923	pH 0.5	0.1	0.6	42.6	4.5
		pH 1.0	0.2	0.5	49.9	3.6
		pH 1.5	0.1	0.3	8.6	2.6
		pH 2.0	0.1	0.1	0.2	0.4
	ALAMINE 336	pH 0.5	0.1	0.1	6.2	0.0
		pH 1.0	0.0	0.0	625.4	0.0
		pH 1.5	0.1	0.2	24.5	0.0
		pH 2.0	0.3	0.2	2.3	0.0
60˚C	D2EHPA	pH 0.5	0.5	1.8	32.4	20.0
		pH 1.0	1.4	4.0	22.5	142.8
		pH 1.5	1.4	4.1	11.1	151.0
		pH 2.0	1.3	1.2	0.8	117.1
	CYANEX 923	pH 0.5	0.0	0.4	40.6	1.1
		pH 1.0	0.0	0.4	18.4	0.3
		pH 1.5	0.0	0.1	3.1	0.3
		pH 2.0	20.7	8.0	10.4	0.0
	ALAMINE 336	pH 0.5	0.0	0.0	13.7	0.0
		pH 1.0	0.0	0.1	27.0	0.0
		pH 1.5	0.0	0.0	19.8	0.0
		pH 2.0	0.0	0.0	1.0	0.4

Extraction of zirconium

As previously reported, zirconium was highly separated by all organic extractants here studied, but Alamine 336 had demonstrated a high separation factor. For this reason, it was studied its extraction before the recovery of scandium. In experiments using the amine extractant, the effect of organic extraction concentration was evaluated from 5% to 25%v/v. The same solution composition of previous experiments was used, and the results are depicted in Figure 47. In all conditions, the extraction of zirconium was over 96%, and the coefficient distribution achieved the maximum value for an experiment using 10% of Alamine 336 - 625.4 (Table 34).

Table 34 shows the separation factor of zirconium compared to aluminum, iron, and titanium, where it is demonstrated that the separation was highly selective. The plot of log D vs. log [Alamine 336] determined the number of molecules of the extractant interacting with zirconium, and results indicated that at least one molecule

of organic extractant reacts with the metallic ion. As shown by Wang & Lee (2015), the extraction of zirconium by Alamine 336 may be represented as **Equation 46**. The difference may be related to the concentration, where the authors studied the extraction from 0.2g/L of zirconium.

$$Zr(SO_4)_{2(aq)} + R_3NH_2SO_{4(org)} \rightarrow R_3NH_2SO_4.Zr(SO_4)_{2(org)} \quad \text{Equation 46}$$

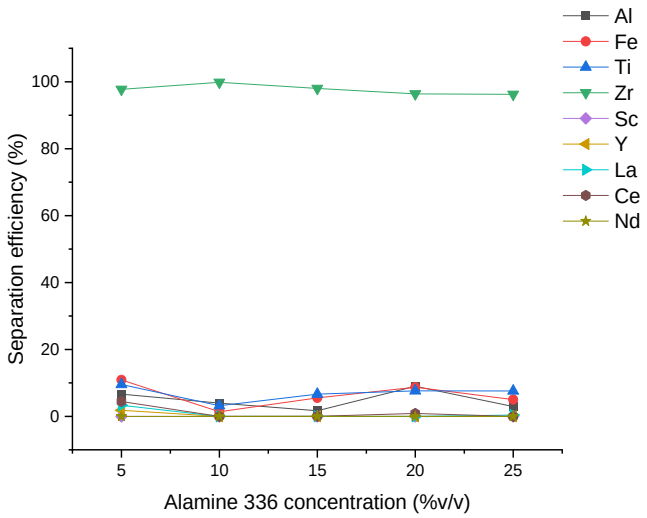

Figure 47: Effect of Alamine 336 concentration on extraction of metals from the synthetic solution of bauxite residue leaching. Experimental conditions: A/O ratio = 1:1; pH 1.0; 15min; 25˚C

Table 34: Separation factor for the zirconium in comparison to aluminum, iron, and titanium

	Alamine 336 concentration				
	5%	**10%**	**15%**	**20%**	**25%**
Zr/Al	612.2	15150.6	2899.5	270.1	848.7
Zr/Fe	356.3	45054.6	839.4	278.3	483.6
Zr/Ti	414.4	19173.2	690.6	322.3	312.1
D_{Zr}	43.5	625.4	49.2	26.6	25.6

The synergic effect between Alamine 336 and TBP was explored, and the extraction results are presented in Figure 48. The presence of solvation extractant had no benefit to zirconium extraction or improvement on selective extraction. As an opposite effect, the extraction of iron increased as TBP was used. In conclusion, TBP has no benefits in the extraction of zirconium by Alamine 336.

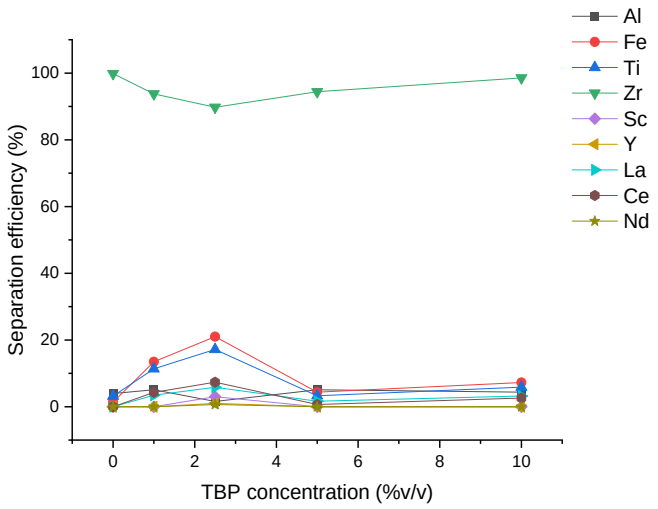

Figure 48: Effect of TBP concentration on extraction of metals from synthetic solution of bauxite residue leaching. Experimental conditions: A/O ratio = 1:1; pH 1.0; Alamine 336 concentration = 10%; 15min; 25˚C.

The effect of the A/O ratio was studied at 25˚C, for 15min, Alamine 10% in different A/O ratios. The extraction of zirconium increased as the amount of organic phase increases. The extraction of iron and aluminum remained up to 10% in all A/O ratios tested. The $\beta_{Zr/Al}$ and $\beta_{Zr/Fe}$ achieved the maximum value for A/O ratio equals to 1:1. If more mixer–settler plates are used in A/O ratios between 5/1 and 2/1, the extraction of iron and aluminum would increase, and the stripping step might be compromised. The use of only one contact would result in an economic advantage to the process.

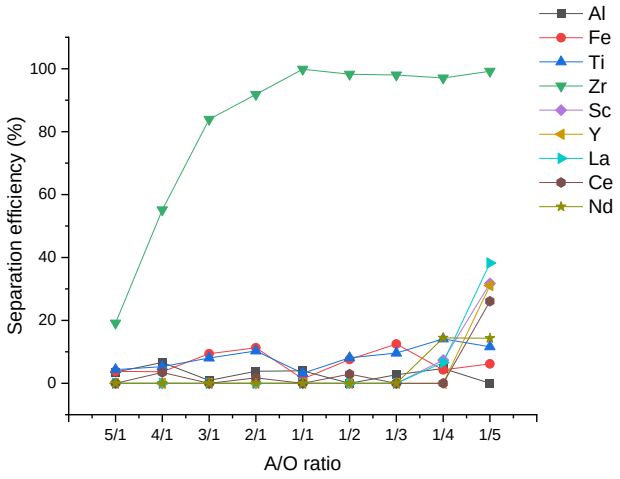

Figure 49: Effect of A/O ratio on the extraction of metals from the synthetic solution of bauxite residue leaching. Experimental conditions: pH 1.0; Alamine 336 concentration = 10%; 15min; 25˚C.

Extraction of scandium

The extraction of zirconium from bauxite residue leach solution was carried out with Alamine 336 10%, A/O 1:1, for 15min at 25˚C. About 4% of iron and 1.4% of aluminum were co-extracted. As a result, a synthetic solution without zirconium and considering the extraction of iron and aluminum was prepared for scandium separation experiments. The organic extractants tested were D2EHPA and Cyanex 923 in different concentrations and the effect of TBP as modifier and A/O ratio.

The effect of organic extractant concentration was evaluated at pH 0.5, A/O 1:1, for 15min at 25˚C. Results are shown in Figure 50. In the case of D2EHPA, no significant variation in the extraction of scandium in the intervals investigated was observed, which indicates that only one molecule reacts with scandium ions. Furthermore, the coefficient distribution for iron, titanium, yttrium, and lanthanum has demonstrated the same behavior as scandium.

The extraction efficiency for titanium and yttrium increased as the D2EHPA concentration increased, reaching 80% and 60%, respectively. Iron and lanthanum extraction achieved up to 40%. Although all scandium was extracted, iron and titanium in the organic phase may represent a problem for the final scandium solution in the stripping step. As observed by Saratale et al. (2020), iron was extracted and the rare

earth elements by phosphonic acid extractants. As mentioned by the authors, it must be considered the highest extraction efficiency of target metals and the lowest extraction of impurities [380]. Gao et al. (2019) also observed high selective for scandium by D2EHPA in H_2SO_4 media, as well as iron and titanium [209].

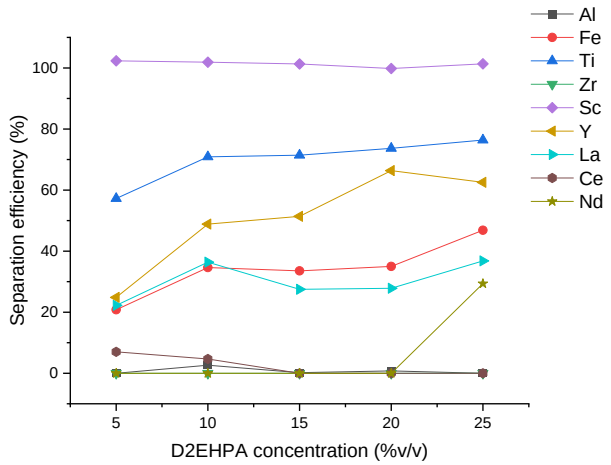

(a)

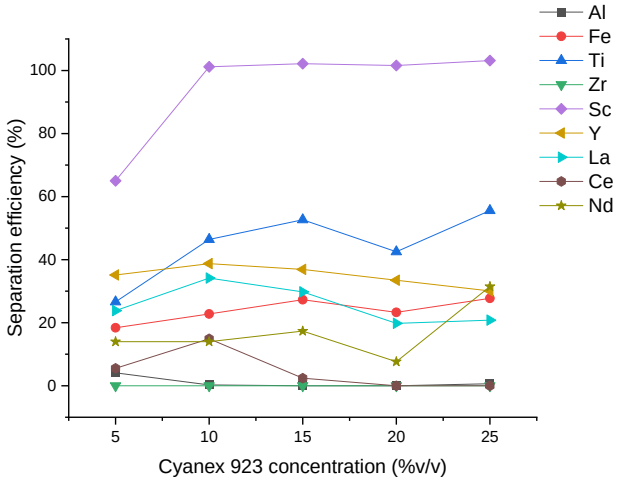

(b)

Figure 50: Effect of (a) D2EHPA and (b) Cyanex 923 concentration on extraction of metals from synthetic solution of bauxite residue leaching. Experimental conditions: A/O ratio = 1:1; pH 0.5; 15min; 25˚C

Comparing to data presented in Figure 50b, the scandium separation was more selective over titanium (<56%), iron (<28%), and other rare earth elements (<30%). The extraction rate for scandium increased from 65% (Cyanex 923 5%) to

100% (Cyanex 923 10-20%), while other elements remained constant. Titanium extraction increased from 27% to 56% as the extractant concentration increased. The coefficient distribution for iron, titanium, scandium, yttrium, and lanthanum in different concentrations of D2EHPA and Cyanex 923 is depicted in Table 35. The slope for scandium using Cyanex 923 (1.7) has demonstrated that two organic molecules react with the ions, which is depicted in **Equation 46**.

Table 35: Coefficient distribution for iron, titanium, scandium, yttrium, and lanthanum in different concentrations of D2EHPA and Cyanex 923

		Fe	**Ti**	**Sc**	**Y**	**La**
	log [extractant concentration]	log D	log D	log D	log D	log D
D2EHPA	-1.3	-0.6	0.1	1.6	-0.5	-0.5
	-1.0	-0.3	0.4	1.7	0.0	-0.2
	-0.8	-0.3	0.4	1.9	0.0	-0.4
	-0.7	-0.3	0.4	2.7	0.3	-0.4
	-0.6	-0.1	0.5	1.9	0.2	-0.2
Cyanex 923	-1.3	-0.6	-0.4	0.3	-0.3	-0.5
	-1.0	-0.5	-0.1	1.9	-0.2	-0.3
	-0.8	-0.4	0.0	1.7	-0.2	-0.4
	-0.7	-0.5	-0.1	1.8	-0.3	-0.6
	-0.6	-0.4	0.1	1.5	-0.4	-0.6

The synergism between organophosphorus extractants and TBP was studied, and the results are presented in Table 36. The modifier showed beneficial for selective separation of scandium as the extraction of contaminants by D2EHPA. The extraction of iron, titanium, yttrium, and lanthanum declined under modifier effect until up to 40%, which is the same separation efficiency of Cyanex 923 without TBP.

Zhang et al. (2018) found that up to 95% of scandium was extracted with the D2EHPA + TBP mixture; on the other hand, the increase in TBP concentration declined the separation of scandium and slightly increased iron extraction. According to the authors, the TBP is also a neutral extractant and reacts with D2EHPA forming a neutral molecule. Therefore, it decreases the effective concentration of D2EHPA in the solvent and has a lower scandium extraction rate [215].

Despite the data reported by Zhang et al. (2018), the extraction of iron declined as the TBP was used. It may be related to the acidity of the solution. The experiments performed by the authors occurred at pH -0.4, while the data presented in Table 36

was carried out at pH 0.5. According to Wang et al. (2013), the extraction of iron by D2EHPA + TBP mixture is improved in pH above 0.4 achieving 10% of yield from a solution with 1.6g/L of iron [50].

Table 36: Effect of TBP concentration on extraction of metals from synthetic solution of bauxite residue leaching by (a) D2EHPA and (b) Cyanex 923. Experimental conditions: A/O ratio = 1:1; pH 0.5; organophosphorus extractants concentration = 10%; 15min; 25˚C.

	TBP	Sc/Fe	Sc/Ti	Sc/Y	Sc/La	Sc/Ce
D2EHPA	0	99.1	21.5	55.0	91.7	1071.2
	1	136.2	38.5	55.4	84.0	40455.8
	2.5	88.6	21.4	64.5	83.4	-
	5	171.4	29.8	108.8	259.0	-
	10	115.3	52.9	72.8	88.5	-
Cyanex 923	0	288.2	98.0	134.4	163.8	485.1
	1	231.8	103.0	115.7	176.4	544.1
	2.5	700.7	295.5	380.7	605.2	1358.4
	5	293.3	115.6	181.8	254.7	769.5
	10	218.3	117.8	121.2	182.8	2376.0

Cyanex 923 demonstrated that there is no difference as TBP was used, neither to increase the extraction of rare earth metals nor to make the reaction more selective for scandium. Comparing the results depicted in Table 36, D2EHPA 10%v/v + TBP 10%v/v (**Equation 47**) achieved the same selective rate than Cyanex 923 10%v/v without modifier (**Equation 45**). Moreover, Cyanex 923 extracted more rare earth elements than D2EHPA, which may be used to obtain a mixture of rare earth elements as the final product.

$$HSc(SO_4)_{2(aq)} + HX_{(org)} + TBP_{(org)} \rightarrow HSc(SO_4)_2.HX.TBP_{(org)} \quad \text{Equation}$$

The effect of the A/O ratio was evaluated for both organophosphorus extractants at pH 0.5, 25˚C, and 15min without TBP. Results are shown in Figure 51. The extraction of scandium achieved 100% at A/O 1:1 and remained constant as the organic fraction increased. The extraction of iron and titanium was constant between 5/1 and 1/3 and then increased, achieving 52% and 80% in A/O equals 1/2. The same behavior was observed for yttrium extraction. No difference was observed in all experiments considering the separation factor for Sc/Fe and Sc/Ti.

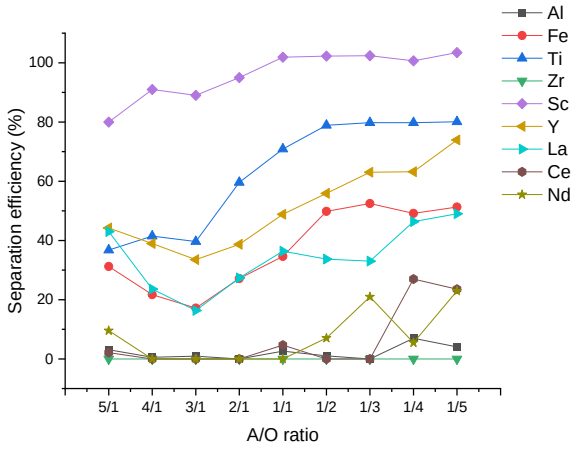

(a)

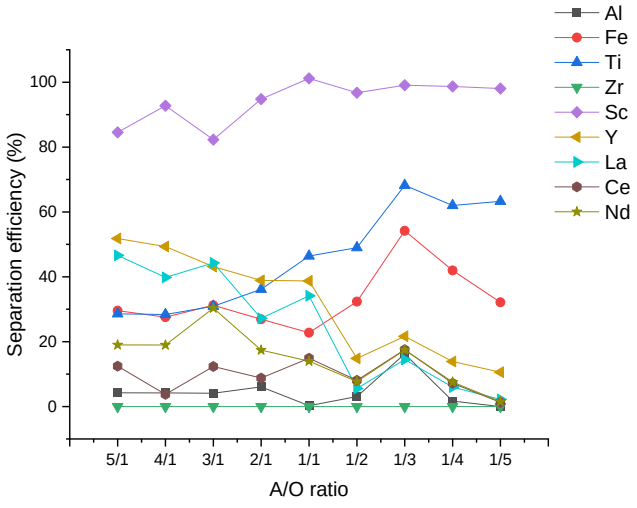

(b)

Figure 51: Effect of A/O ratio on extraction of metals from synthetic solution of bauxite residue leaching by (a) D2EHPA and (b) Cyanex 923. Experimental conditions: pH 0.5; organophosphorus extractant concentration = 10%; 15min; 25˚C.

The same may be inferred for Cyanex 923. As the amount of organic extractant increased, the process becomes more selective for scandium than other rare earth elements, and the separation factor for Sc/Fe and Sc/Ti was kept constant. Thus, considering the selective extraction, Cyanex 923 has demonstrated highly selective for scandium than other elements compared to D2EHPA. For this reason, further experiments were carried out with Cyanex 923.

5.4.3.3. Stripping experiments

Zirconium stripping

The results previously presented demonstrated that all zirconium ions were removed according to the following conditions: Alamine 336 concentration 10%, A/O ratio 1:1, 25˚C, and 15min of only one aqueous-organic contact. The stripping experiments were carried out using NaCl and Na_2CO_3 in different concentrations. The literature review has shown that different solutions may be used as stripping agents from amine-based extractants, such as diluted acid [390], water [391], diluted alkaline and saline solutions [377,378].

Banda et al. (2012) evaluated HCl and H_2SO_4 to strip zirconium and hafnium from Alamine 336 in different concentrations. The recovery of zirconium from the organic phase increased as the acid concentration increased, achieving 21.1% for H_2SO_4 and 100% for HCl [378]. However, stripping using alkaline solutions may generate turbidity and making impossible the aqueous-organic separation [377].

Wang & Lee (2015) has demonstrated that the stripping of zirconium from amine-based extractant (Alamine 308) is highly effective using NaCl and Na_2CO_3 even in low concentrations (<0.2mol/L). According to the authors, saline solutions above 0.05mol/L achieved over 90% of efficiency [377]. From extraction of zirconium in low acidity by one molecule of Alamine 336, the stripping process may be represented by **Equation 48** for NaCl and **Equation 49** for Na_2CO_3, where amine salt is deprotonated in the process.

$$R_3NH_2SO_4.Zr(SO_4)_{2(org)} + NaCl \rightarrow R_3NHCl_{(org)} + Na_2Zr(SO_4)_{2(aq)} + HSO_4^-{}_{(aq)}$$

Equation 48

$$R_3NH_2SO_4.Zr(SO_4)_{2(org)} + Na_2CO_{3(aq)} \rightarrow 2R_3N_{(org)} + Na_2Zr(SO_4)_{2(aq)} + H_2SO_4 + CO_2 + \frac{1}{2}O_2$$

Equation 49

For this reason, the present study explored the use of NaCl and Na_2CO_3 for zirconium stripping in different concentrations (mol/L). Experiments were performed at 25˚C, A/O ratio equals 1:1 for 15min, and the results are shown in Table 37. In all cases, neither iron nor aluminum previously co-extracted were stripped, which resulted in a highly pure solution of zirconium sulfate. The stripping achieved up to 91% in all concentrations of Na_2CO_3, while the same efficiency was possible using 1 and 2mol/L of NaCl, despite the results obtained by Wang & Lee (2015). There are only a few publications related to saline solutions as stripping agents for zirconium from amine extractants.

Table 37: Stripping of Zr from loaded Alamine 336 10% by NaCl and Na_2CO_3 at A/O 1:1, for 25min at 25˚C.

	Zr stripping	
	NaCl	Na_2CO_3
0.25	10%	92%
0.5	70%	94%
1	91%	91%
2	93%	92%

Scandium stripping

According to data obtained previously, the extraction of scandium was highly selective using Cyanex 923 10%, A/O ratio 1:1, 25˚C, and 15min of only one aqueous-organic contact. The inorganic acids H_2SO_4, HNO_3, HCl, and H_3PO_4, were evaluated for scandium stripping in concentrations from 0.1mol/L to 5mol/L, 25˚C, and 15min. The effect of rare earth elements stripping was also evaluated. Results are shown in Table 38. As reported by the literature, the use of most inorganic acids has low

efficiency for scandium stripping. Souza et al. (2019) evaluated the use of H_2SO_4, HNO_3, and HCl 5mol/L, which stripping rate was 2.4%, 7.5%, and 1%, respectively. The difference may be related to the scandium and contaminants concentration in the organic phase [331].

Experiments with H_2SO_4 showed that the stripping of scandium declined as the acid concentration increased in both A/O ratios, probably due to the high concentration of sulfate ions. Even using H_2SO_4 at A/O ratio equals to 2:1, the stripping of scandium was lower than 72%. The stripping of iron and titanium achieved 34% and 51%, respectively, for H_2SO_4 0.5mol/L and A/O ratio equals to 1:1, and declined as the acid concentration increased. Data obtained for the A/O ratio equals to 2:1 demonstrated that 62% and 50% of iron and titanium were stripped - concentration was lower than 220mg/L and 60mg/L, respectively. The increase of HCl concentration also declined the stripping of scandium but observed losses in all acid conditions, 5mol/L the lowest value (0.1%). The literature reports similar results for both acids [392].

In the case of HNO_3, the scandium recovery reached 15.5% in acid concentration 5mol/L. Despite all inorganic acids, H_3PO_4 has demonstrated a higher scandium stripping rate achieving 100% (5mol/L). In general, the stripping of other rare earth elements was lower than 1%, which shows the separation process is highly selective for scandium.

Das et al. (2018) showed that scandium could be entirely stripped from organophosphorus extractants by NaOH, which may be more selective than inorganic acids considering the presence of iron [216]. Otherwise, Ye et al. (2019) have demonstrated that impurities such as iron and aluminum may be co-extracted into the solution using alkaline solution [206]. Moreover, Wang et al. (2013) stated that precipitate is formed in the scandium stripping by NaOH from D2EHPA extractant [50]. Therefore, it would make the process unfeasible on an industrial scale.

Souza et al. (2019) has depicted that oxalic acid may be used for scandium stripping, but the authors achieved a lower percentage than the current study. According to the authors, 4% oxalic acid stripped up to 85% of scandium, while H_3PO_4 5mol/L recovered all scandium from the organic phase [331]. Thus, considering

scandium and all other rare earth elements stripping, H_3PO_4 5mol/L has demonstrated high selective for scandium.

Table 38: Stripping Sc and rare earth elements from loaded Cyanex 923 10% by inorganic acids for 25min at 25˚C.

		H_2SO_4 A/O = 1:1	HNO_3 A/O = 1:1	HCl A/O = 1:1	H_3PO_4 A/O = 1:1	H_2SO_4 A/O = 2:1
Sc	0.1	41.1%	3.4%	7.2%	0.0%	72.4%
	0.5	33.6%	2.0%	0.7%	38.5%	46.4%
	1	22.7%	2.9%	2.8%	60.2%	31.0%
	2	5.6%	7.1%	1.3%	95.1%	8.2%
	5	0.5%	15.5%	0.1%	100.0%	0.9%
Y	0.1	0.06%	0.08%	0.05%	0%	0.40%
	0.5	0.19%	0.18%	0.05%	0.20%	0.30%
	1	0.14%	0.23%	0.02%	0.20%	0.30%
	2	0.20%	0.15%	0.09%	0.18%	0.33%
	5	0.22%	0.14%	0.07%	0.22%	0.43%
La	0.1	0.21%	0.09%	0.32%	0.00%	0.28%
	0.5	0.21%	0.06%	0.17%	0.36%	0.23%
	1	0.16%	0.15%	0.16%	0.38%	0.22%
	2	0.12%	0.16%	0.07%	0.41%	0.17%
	5	0.13%	0.21%	0.13%	0.42%	0.10%
Ce	0.1	0.11%	0.04%	0.14%	0%	0.05%
	0.5	0.06%	0.02%	0.13%	0.08%	0.06%
	1	0.07%	0.04%	0.15%	0.05%	0.07%
	2	0.06%	0.09%	0.18%	0.05%	0.02%
	5	0.04%	0.08%	0.22%	0.03%	0.06%
Nd	0.1	0.70%	0.05%	0.97%	0%	1.35%
	0.5	1.00%	0%	0.50%	1.28%	0.82%
	1	0.68%	0.31%	0.49%	1.26%	0.37%
	2	0.61%	0.45%	0.31%	1.12%	0.57%
	5	0.50%	0.73%	0.08%	0.75%	0.17%

5.4.3.4. Conceptual flow-sheet for recovery of zirconium and scandium from bauxite residue

Figure 52 shows the flowchart of scandium and zirconium recovery from bauxite residue. Despite the works reported in the literature, none explored the recovery of scandium and zirconium by the leaching-solvent extraction process. The rare earth element is the most valuable, representing up to 95% of the economic value

in the residue [49,393]. After the acid leaching of the bauxite residue, zirconium is the second most valuable element, more than the other rare earth elements present in the leaching solution. Also, preliminary experiments evaluating D2EHPA, Cyanex 923, and Alamine 336 depicted that organic extractants were more selective for zirconium than scandium, and its removal is beneficial for scandium separation.

The leaching rate of scandium and zirconium by 20% H_2SO_4, at 90˚C, S/L ratio equals 1/10 for 8h, was 92% and 26%. The separation of zirconium was carried out by Alamine 336 10% in kerosene, pH 1.0, A/O ratio equals 1 with a single theoretical contact at 25°C for 25min. As a result, all zirconium was extracted with low co-extraction of aluminum and iron. The stripping was highly efficient (92%) using Na_2CO_3, obtaining high-pure zirconium solution without impurities. Then, another stripping is required for iron and aluminum removal from the organic phase before Alamine 336 regeneration for its reuse in the process.

In scandium recovery, Cyanex 923 was selective for the element after zirconium separation at pH 0.5, 10% of organic extractant in kerosene, A/O ratio equals to 1 with a single theoretical contact at 25°C for 25min. All scandium was separated with co-extraction of aluminum, titanium, iron, and rare earth elements. Stripping experiments has demonstrated that HCl 5mol/L may be used for contaminants removal with negligible losses of scandium (0.1%). Then, a final solution may be obtained by H_3PO_4 5mol/L. From the organic phase, rare earth elements may be stripped before Cyanex 923 reuse.

Considering the leaching and separation steps, the mass balance achieved an efficiency rate of 92% for scandium and up to 25% for zirconium as a co-product. Such flowchart designed may be advantageous considering the recovery of two valuable elements from the bauxite residue, which is currently stored in dams.

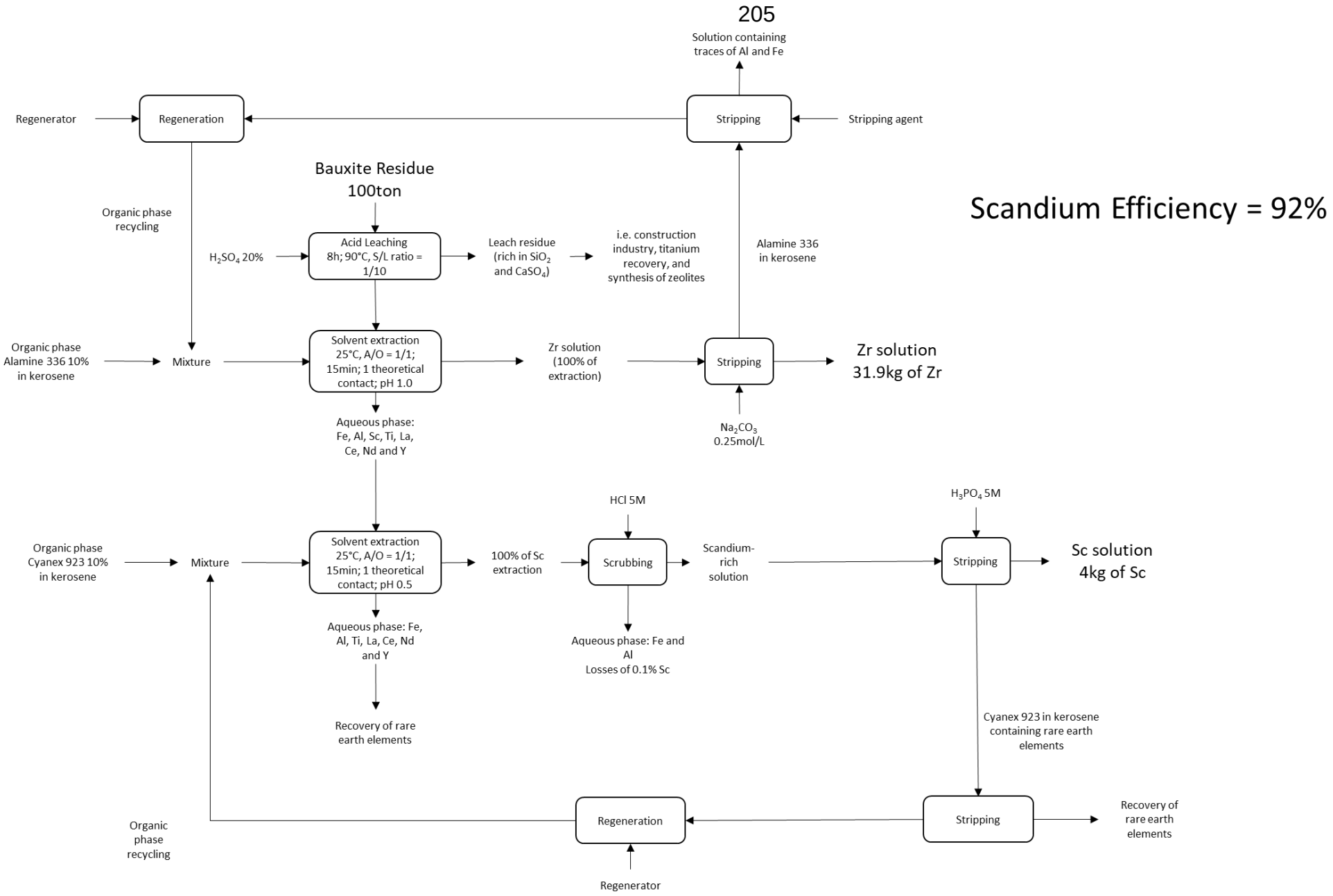

Figure 52: Flowchart proposed for scandium and zirconium recovery from bauxite residue by leaching-solvent extraction

Moreover, the leaching residue is rich in silicon oxide and calcium sulfate. The literature review has shown that this material may be used for the construction sector [43,44], titanium recovery [45], or production of zeolites for wastewater treatment [27,46]. In addition, there are several studies in the literature that report the use of bauxite residue as raw material for cement [349,350,354]. Due to rare earth elements in the residue, in special scandium, it might be economically feasible to extract these valuable elements and then use leaching residue for cement production. Moreover, the material has titanium in its composition, and an extraction step by HCl concentrated may be performed [45].

According to studies developed by Fungaro et al., the synthesis of zeolites was carried out with wastes with a similar composition of the leaching residue of the current study, where a high concentration of calcium and silicon produces zeolites for adsorption of cadmium and cesium, for instance [394,395].

Considering the process designed in this work, the goal is to recover scandium as the main product and zirconium as a co-product. Indeed, the current process proposes the reuse of bauxite residue for different applications for the wastes generated throughout the process in addition to the final products. As a result, the flowchart described in Figure 52 achieves the SGDs presented in Table 39. However, considering the production of scandium from the primary source, only the targets 7.2, 7a, 8.2, and 9.5 are achieved. For this reason, the present work is strictly connected to sustainable development.

Table 39: The Sustainable Development Goals related to the scandium production from bauxite residue.

SDGs	targets	
7	7.2	By 2030, increase substantially the share of renewable energy in the global energy mix 7.2.1 Renewable energy share in the total final energy consumption
	7a	By 2030, enhance international cooperation to facilitate access to clean energy research and technology, including renewable energy, energy efficiency and advanced and cleaner fossil-fuel technology, and promote investment in energy infrastructure and clean energy technology
8	8.2	Achieve higher levels of economic productivity through diversification, technological upgrading and innovation, including through a focus on high-value added and labour-intensive sectors
	8.4	Improve progressively, through 2030, global resource efficiency in consumption and production and endeavour to decouple economic growth from environmental degradation, in accordance with the 10-Year Framework of Programmes on Sustainable Consumption and Production, with developed countries taking the lead
9	9.2	Promote inclusive and sustainable industrialization and, by 2030, significantly raise industry's share of employment and gross domestic product, in line with national circumstances, and double its share in least developed countries
	9.4	By 2030, upgrade infrastructure and retrofit industries to make them sustainable, with increased resource-use efficiency and greater adoption of clean and environmentally sound technologies and industrial processes, with all countries taking action in accordance with their respective capabilities
	9.5	Enhance scientific research, upgrade the technological capabilities of industrial sectors in all countries, in particular developing countries, including, by 2030, encouraging innovation and substantially increasing the number of research and development workers per 1 million people and public and private research and development spending
	9b	Support domestic technology development, research and innovation in developing countries, including by ensuring a conducive policy environment for, inter alia, industrial diversification and value addition to commodities
12	12.2	By 2030, achieve the sustainable management and efficient use of natural resources
	12.4	By 2020, achieve the environmentally sound management of chemicals and all wastes throughout their life cycle, in accordance with agreed international frameworks, and significantly reduce their release to air, water and soil in order to minimize their adverse impacts on human health and the environment
	12.5	By 2030, substantially reduce waste generation through prevention, reduction, recycling and reuse
	12.6	Encourage companies, especially large and transnational companies, to adopt sustainable practices and to integrate sustainability information into their reporting cycle
	12a	Support developing countries to strengthen their scientific and technological capacity to move towards more sustainable patterns of consumption and production

6. CONCLUSIONS

From the results obtained for scandium extraction, the main conclusions were:

1. The bauxite residue contains 43.5mg/kg of scandium, 1329.8mg/kg of zirconium, 36.4% of Fe_2O_3, 23.3% of Al_2O_3 and 21.6% of SiO_2;
2. The main mineral phases of the residue were quartz, sodalite, gibbsite, goethite, hematite, boehmite, and gypsum;
3. The moisture content was 23.1%, and the D10, D50, and D90 were 0.06mm, 0.26mm, and 0.95mm, respectively;
4. The losses on ignition analyses were 14.5% (900°C) and 14.8% (1,100°C), respectively. The total carbon content was 0.6%, the inorganic carbon was 0.32%, and the total organic carbon was 0.28%;
5. Scandium and zirconium content in the silicate-based ore were 191mg/kg and 8,090mg/kg. The material has 36.3% of Fe_2O_3, 4.61% of Al_2O_3 and 39.4% of SiO_2;
6. The main mineral phases of the silicate-based ore were dickite, ferrohornblende, fayalite, hedenbergite, and albite;
7. The H_2O_2 little contributed to silicon oxide formation during the acid leaching of bauxite residue; on the other hand, the extraction rate for scandium declined due to low iron oxide leaching;
8. The leaching rate of iron, aluminum, titanium, and zirconium increased from 25°C (3%, 20%, 5%, and 17%, respectively) to 90°C (99%, 92%, 26%, and 26%, respectively) with and without an oxidizing agent;
9. At 25˚C, 20% of H_2SO_4 and 8h of reaction time, scandium and iron leaching achieved up to 50% and 3.5%, respectively, which can be more feasible for separation steps than at 90˚C due to high concentration of contaminants;
10. In the case of scandium, the leaching rate achieved 92%. No effect of H_2O_2 was observed for experiments carried out at 90°C;
11. Silicon leaching decreased from 9% to almost 0% as the temperature increased in both oxidizing and non-oxidizing medium, indicating that it accelerates precipitation as oxide;

12. The leaching residues of experiments carried out at 90°C are mainly composed of quartz (silicon dioxide) and gypsum (calcium sulfate);
13. As the acid concentration increased, the leaching rate of titanium increased from 25% (10% of H_2SO_4) to 83% (60% of H_2SO_4). On the other hand, scandium leaching declined from 92% to 73%, since it precipitates due to the high sulfate ions concentration;
14. The extraction rates in H_3PO_4 leaching were similar to H_2SO_4 leaching, where the efficiency for scandium, aluminum, and iron achieved up to 90%, and the leaching residue were composed mainly by quartz;
15. The leaching of silicon from sodalite mineral phase achieved 13% and concentration 61 times higher than in H_2SO_4 leaching solution;
16. Analysis of the leaching solution in both cases demonstrated that scandium is responsible for 95% of economic value. Yttrium, neodymium, lanthanum and cerium have also economic interest;
17. In the direct leaching of silicate-based ore, the solid-liquid ratio has almost no effect on the extraction of rare earth elements. As the amount of acid solution increased, the extraction of iron also increased. The same was observed varying the sulfuric acid concentration;
18. The use of hydrogen peroxide was beneficial to the extraction of rare earth elements. The leaching of lanthanum, cerium, and neodymium increased from up to 65% (without hydrogen peroxide) to 85% (5.0v/v% of hydrogen peroxide).
19. In the case of scandium, its efficient rate increased from 2.6% (without hydrogen peroxide) to 4% (5.0v/v% of hydrogen peroxide). The exception was iron, where declined from 29.3% (2.5v/v% of hydrogen peroxide) to 9.3% (10.0v/v% of hydrogen peroxide);
20. The H_2SO_4-$Na_2S_2O_4$ system increased the leaching of rare earth elements from around 60% (without sodium dithionite) to 80% (1.0wt% of sodium dithionite) and 70% (2.5wt% of sodium dithionite);
21. Comparing the oxidizing and reducing leaching reaction, the H_2SO_4-H_2O_2 system has more benefit to the leaching of rare earth elements than the H_2SO_4-$Na_2S_2O_4$ system, where the extraction of lanthanum, cerium, and neodymium achieved up to 80%;
22. The extraction of the valuable elements from the silicate-based ore by direct leaching increased from 40% (25°C) to 80% (90°C);

23. The extraction of rare earth elements by acid baking achieved up to 80% at 200°C of roasting temperature for 2h and 1g of ore : 0.6mL of H_2SO_4 concentrated. Scandium leaching rate was lower than direct leaching (5.6%);
24. Scandium extraction from bauxite residue achieves more SDGs than from silicate-based ore, which are: 7, 8, 9, and 12;
25. The solution was obtained after the leaching of 20% H_2SO_4, S/L ratio equals to 1/10, for 8h at 90°C, where 92% of scandium and 26% of zirconium were extracted;
26. Cyanex 923 and Alamine 336 were more selective for zirconium than scandium in all pH values. D2EHPA was more selective for scandium at pH 1.5 and 2.0, where 89% and 40% of zirconium was extracted, respectively;
27. No difference was observed for the extraction of metals, increasing the temperature from 25°C to 60°C;
28. All zirconium was separated from the solution using Alamine 336 10%, A/O ratio equals 1:1, at pH 1.0 for 15min at 25°C. No synergic effect was observed between amine extractant and TBP;
29. Cyanex 923 was more selective for scandium than D2EHPA, where the separation factor for Sc/Fe was 288 and 99, and Sc/Ti was 98 and 21.5, respectively, considering 10% of organic extractant, A/O ratio equals to 1:1 at 25°C for 15min;
30. The D2EHPA + TBP mixture reached the same selective separation of scandium as Cyanex 923 without the modifier;
31. Stripping of zirconium achieved 92% using Na_2CO_3 for concentrations from 0.25mol/L to 2mol/L;
32. The increase in NaCl concentration increased the stripping from 10% (0.25mol/L) to 93% (2mol/L);
33. Scrubbing of Cyanex 923 for contaminants removal may be carried out with HCl 5mol/L with losses of 0.1% of scandium. All remained scandium may be stripped using H_3PO_4 5mol/L;
34. The mass balance process design from bauxite residue demonstrated that scandium extraction reached 92% of efficiency, while zirconium was 25% as co-product;
35. Considering 100 tons of bauxite residue, an amount of 4kg of scandium and 31.9kg of zirconium may be produced. Considering the production of scandium

oxide or fluoride, the process would generate up to US$ 46,626 or US$ 1,940,980, respectively;

36. The process design is strictly connected to the sustainable development goals number 7 (7.2 and 7a), 8 (8.2 and 8.4), 9 (9.2, 9.4, 9.5 and 9b), and 12 (12.2, 12.4, 12.5, 12.6, and 12a).

REFERENCES

[1] Krishnamurthy N, Gupta CK. Extractive Metallurgy of Rare Earths. 2nd ed. Boca Raton: CRC Press; 2016.

[2] Kuchi R, Kim D. Rare-Earth Metal Recovery for Green Technologies. Cham: Springer International Publishing; 2020. https://doi.org/10.1007/978-3-030-38106-6.

[3] Gambogi J. Scandium. USGS 2021:2. https://pubs.usgs.gov/periodicals/mcs2021/mcs2021-scandium.pdf (accessed March 21, 2021).

[4] Ivers-Tiffée E, Weber A, Herbstritt D. Materials and technologies for SOFC-components. J Eur Ceram Soc 2001;21:1805–11. https://doi.org/10.1016/S0955-2219(01)00120-0.

[5] Gambogi J. Rare Earths. USGS 2021:2. https://pubs.usgs.gov/periodicals/mcs2021/mcs2021-rare-earths.pdf (accessed March 21, 2021).

[6] Gambogi J. Yttrium. USGS 2021:2. https://pubs.usgs.gov/periodicals/mcs2021/mcs2021-yttrium.pdf (accessed March 21, 2021).

[7] USGS. Interior Releases 2018 ' s Final List of 35 Minerals Deemed Critical to U. S. National Security and the Economy 2018:3. https://www.usgs.gov/news/interior-releases-2018-s-final-list-35-minerals-deemed-critical-us-national-security-and (accessed August 25, 2020).

[8] MCTIC. Plano de ciência, tecnologia e inovação para minerais estratéticos 2018:50. https://www.inova.rs.gov.br/upload/arquivos/202006/16181825-plano-de-ciencia-tecnologia-e-inovacao-para-minerais-estrategicos.pdf (accessed August 25, 2020).

[9] Martins LS, Guimarães LF, Botelho Junior AB, Tenório JAS, Espinosa DCR. Electric car battery: An overview on global demand, recycling and future approaches towards sustainability. J Environ Manage 2021;295:113091. https://doi.org/10.1016/j.jenvman.2021.113091.

[10] Takahashi VCI, Botelho Junior AB, Espinosa DCR, Tenório JAS. Enhancing cobalt recovery from Li-ion batteries using grinding treatment prior to the leaching and solvent extraction process. J Environ Chem Eng 2020;8:103801. https://doi.org/10.1016/j.jece.2020.103801.

[11] Savvilotidou V, Gidarakos E. Pre-concentration and recovery of silver and indium from crystalline silicon and copper indium selenide photovoltaic panels. J Clean Prod 2020;250:119440. https://doi.org/10.1016/j.jclepro.2019.119440.

[12] Dias PR, Benevit MG, Veit HM. Photovoltaic solar panels of crystalline silicon: Characterization and separation. Waste Manag Res 2016;34:235–45. https://doi.org/10.1177/0734242X15622812.

[13] European Commision. Critical Raw Materials Resilience: Charting a Path

towards greater Security and Sustainability 2020:1–24. https://ec.europa.eu/docsroom/documents/42849 (accessed October 7, 2020).

[14] European Union. Critical Raw Material list 2020. EU Sci HUB 2021:4. https://rmis.jrc.ec.europa.eu/?page=crm-list-2020-e294f6 (accessed July 30, 2021).

[15] Bobba S, Carrara S, Huisman J, Mathieux F, Pavel C. Critical Raw Materials for Strategic Technologies and Sectors in the EU - a Foresight Study. 2020. https://doi.org/10.2873/58081.

[16] Bobba S, Carrara S, Huisman J, Mathieux F, Pavel C. Critical Raw Materials for Strategic Technologies and Sectors in the EU - a Foresight Study. 2020. https://doi.org/10.2873/58081.

[17] European Commission. 2017 list of critical raw materials for the EU. Brussels: 2017.

[18] Sykes JP, Wright JP, Trench A, Miller P. An assessment of the potential for transformational market growth amongst the critical metals. Trans Institutions Min Metall Sect B Appl Earth Sci 2016;125:21–56. https://doi.org/10.1080/03717453.2015.1104055.

[19] Pyrzyńska K, Kilian K, Pęgier M. Separation and purification of scandium: From industry to medicine. Sep Purif Rev 2019;48:65–77. https://doi.org/10.1080/15422119.2018.1430589.

[20] Wang W, Pranolo Y, Cheng CY. Metallurgical processes for scandium recovery from various resources: A review. Hydrometallurgy 2011;108:100–8. https://doi.org/10.1016/j.hydromet.2011.03.001.

[21] Baptiste PEJ. Extraction of scandium from its ores. 2874039, 1959.

[22] Gambogi J. Scandium. 2019. https://doi.org/10.3133/70170140.

[23] Fernandez V. Rare-earth elements market: A historical and financial perspective. Resour Policy 2017;53:26–45. https://doi.org/10.1016/j.resourpol.2017.05.010.

[24] Hayes-Labruto L, Schillebeeckx SJD, Workman M, Shah N. Contrasting perspectives on China's rare earths policies: Reframing the debate through a stakeholder lens. Energy Policy 2013;63:55–68. https://doi.org/10.1016/j.enpol.2013.07.121.

[25] Ting MH, Seaman J. Rare Earths: Future Elements of Conflict in Asia? Asian Stud Rev 2013;37:234–52. https://doi.org/10.1080/10357823.2013.767313.

[26] Dutta T, Kim K-H, Uchimiya M, Kwon EE, Jeon B-H, Deep A, et al. Global demand for rare earth resources and strategies for green mining. Environ Res 2016;150:182–90. https://doi.org/10.1016/j.envres.2016.05.052.

[27] Izidoro JC, Kim MC, Bellelli VF, Pane MC, Botelho Junior AB, Espinosa DCR, et al. Synthesis of zeolite A using the waste of iron mine tailings dam and its application for industrial effluent treatment. J Sustain Min 2019;18:277–86. https://doi.org/10.1016/j.jsm.2019.11.001.

[28] Santamarina JC, Torres-Cruz LA, Bachus RC. Why coal ash and tailings dam disasters occur. Science (80-) 2019;364:526–8.

https://doi.org/10.1126/science.aax1927.

[29] Andrade GF, Paniz FP, Martins AC, Rocha BA, da Silva Lobato AK, Rodrigues JL, et al. Agricultural use of Samarco's spilled mud assessed by rice cultivation: A promising residue use? Chemosphere 2018;193:892–902. https://doi.org/10.1016/j.chemosphere.2017.11.099.

[30] Garcia LC, Ribeiro DB, De Oliveira Roque F, Ochoa-Quintero JM, Laurance WF, Grande C, et al. Brazil's worst mining disaster: Corporations must be compelled to pay the actual environmental costs: Corporations. Ecol Appl 2017;27:5–9. https://doi.org/10.1002/eap.1461.

[31] Almeida IM de, Jackson Filho JM, Vilela RA de G. Razões para investigar a dimensão organizacional nas origens da catástrofe industrial da Vale em Brumadinho, Minas Gerais, Brasil. Cad Saude Publica 2019;35. https://doi.org/10.1590/0102-311x00027319.

[32] Gigliotti M, Schmidt-Traub G, Bastianoni S. The Sustainable Development Goals. Encycl. Ecol. 2nd ed., Elsevier; 2019, p. 426–31. https://doi.org/10.1016/B978-0-12-409548-9.10986-8.

[33] Monteiro NBR, da Silva EA, Moita Neto JM. Sustainable development goals in mining. J Clean Prod 2019;228:509–20. https://doi.org/10.1016/j.jclepro.2019.04.332.

[34] King JF, Taggart RK, Smith RC, Hower JC, Hsu-Kim H. Aqueous acid and alkaline extraction of rare earth elements from coal combustion ash. Int J Coal Geol 2018;195:75–83. https://doi.org/10.1016/j.coal.2018.05.009.

[35] Demol J, Ho E, Soldenhoff K, Senanayake G. The sulfuric acid bake and leach route for processing of rare earth ores and concentrates: A review. Hydrometallurgy 2019;188:123–39. https://doi.org/10.1016/j.hydromet.2019.05.015.

[36] Botelho Junior AB, Espinosa DCR, Vaughan J, Tenório JAS. Recovery of scandium from various sources: A critical review of the state of the art and future prospects. Miner Eng 2021;172:107148. https://doi.org/10.1016/j.mineng.2021.107148.

[37] Botelho Junior AB, Espinosa DCR, Tenório JAS. Characterization of Bauxite Residue from a Press Filter System: Comparative Study and Challenges for Scandium Extraction. Mining, Metall Explor 2020. https://doi.org/10.1007/s42461-020-00333-3.

[38] Botelho Junior AB, Espinosa DCR, Tenório JAS. Extraction of Scandium from Critical Elements-Bearing Mining Waste: Silica Gel Avoiding in Leaching Reaction of Bauxite Residue. J Sustain Metall 2021. https://doi.org/10.1007/s40831-021-00434-3.

[39] Botelho Junior AB, Espinosa DCR, Tenório JAS. Selective separation of Sc(III) and Zr(IV) from the leaching of bauxite residue using trialkylphosphine acids, tertiary amine, tri-butyl phosphate and their mixtures. Sep Purif Technol 2021;279:119798. https://doi.org/10.1016/j.seppur.2021.119798.

[40] Botelho Junior AB, Pinheiro ÉF, Espinosa DCR, Tenório JAS, Baltazar M dos

PG. Adsorption of lanthanum and cerium on chelating ion exchange resins: kinetic and thermodynamic studies. Sep Sci Technol 2021;00:1–10. https://doi.org/10.1080/01496395.2021.1884720.

[41] Botelho Junior AB, Espinosa DCR, Tenório JAS. The use of computational thermodynamic for yttrium recovery from rare earth elements-bearing residue. J Rare Earths 2021;39:201–7. https://doi.org/10.1016/j.jre.2020.02.019.

[42] United Nations. Global indicator framework for the Sustainable Development Goals and targets of the 2030 Agenda for Sustainable Development 2020:21. https://unstats.un.org/sdgs/indicators/Global Indicator Framework after 2019 refinement_Eng.pdf%0Ahttps://unstats.un.org/sdgs/indicators/Global Indicator Framework_A.RES.71.313 Annex.pdf (accessed January 8, 2021).

[43] Hertel T, Pontikes Y. Geopolymers, inorganic polymers, alkali-activated materials and hybrid binders from bauxite residue (red mud) – Putting things in perspective. J Clean Prod 2020;258:120610. https://doi.org/10.1016/j.jclepro.2020.120610.

[44] Spooren J, Binnemans K, Björkmalm J, Breemersch K, Dams Y, Folens K, et al. Near-zero-waste processing of low-grade, complex primary ores and secondary raw materials in Europe: technology development trends. Resour Conserv Recycl 2020;160:104919. https://doi.org/10.1016/j.resconrec.2020.104919.

[45] Haverkamp RG, Kruger D, Rajashekar R. The digestion of New Zealand ilmenite by hydrochloric acid. Hydrometallurgy 2016;163:198–203. https://doi.org/10.1016/j.hydromet.2016.04.015.

[46] Izidoro JDC, Fungaro DA, Abbott JE, Wang S. Synthesis of zeolites X and A from fly ashes for cadmium and zinc removal from aqueous solutions in single and binary ion systems. Fuel 2013;103:827–34. https://doi.org/10.1016/j.fuel.2012.07.060.

[47] Sigma Aldrich 2021:2. https://bit.ly/3e2o17s (accessed March 2, 2021).

[48] Alkan G, Yagmurlu B, Cakmakoglu S, Hertel T, Kaya Ş, Gronen L, et al. Novel Approach for Enhanced Scandium and Titanium Leaching Efficiency from Bauxite Residue with Suppressed Silica Gel Formation. Sci Rep 2018;8:5676. https://doi.org/10.1038/s41598-018-24077-9.

[49] Akcil A, Akhmadiyeva N, Abdulvaliyev R, Abhilash, Meshram P. Overview On Extraction and Separation of Rare Earth Elements from Red Mud: Focus on Scandium. Miner Process Extr Metall Rev 2018;39:145–51. https://doi.org/10.1080/08827508.2017.1288116.

[50] Wang W, Pranolo Y, Cheng CY. Recovery of scandium from synthetic red mud leach solutions by solvent extraction with D2EHPA. Sep Purif Technol 2013;108:96–102. https://doi.org/10.1016/j.seppur.2013.02.001.

[51] Borra CR, Blanpain B, Pontikes Y, Binnemans K, Van Gerven T. Recovery of Rare Earths and Major Metals from Bauxite Residue (Red Mud) by Alkali Roasting, Smelting, and Leaching. J Sustain Metall 2016;3:393–404. https://doi.org/10.1007/s40831-016-0103-3.

[52] Botelho Junior AB. Recuperação de níquel e cobalto a partir de lixiviado de

níquel laterí-tico utilizando resinas quelantes e processo de pré-redução. Universidade de São Paulo, 2019. https://doi.org/10.11606/D.3.2019.tde-25032019-091140.

[53] Zhu X, Li W, Xing B, Zhang Y. Extraction of scandium from red mud by acid leaching with CaF2 and solvent extraction with P507. J Rare Earths 2020;38:1003–8. https://doi.org/10.1016/j.jre.2019.12.001.

[54] Borra CR, Pontikes Y, Binnemans K, Van Gerven T. Leaching of rare earths from bauxite residue (red mud). Miner Eng 2015;76:20–7. https://doi.org/10.1016/j.mineng.2015.01.005.

[55] Wang Z, Li MYH, Liu ZRR, Zhou MF. Scandium: Ore deposits, the pivotal role of magmatic enrichment and future exploration. Ore Geol Rev 2021;128:103906. https://doi.org/10.1016/j.oregeorev.2020.103906.

[56] Zhang L, Xu Z. A critical review of material flow, recycling technologies, challenges and future strategy for scattered metals from minerals to wastes. J Clean Prod 2018;202:1001–25. https://doi.org/10.1016/j.jclepro.2018.08.073.

[57] Scarazzato T, Panossian Z, Tenório JAS, Pérez-Herranz V, Espinosa DCR. A review of cleaner production in electroplating industries using electrodialysis. J Clean Prod 2016;168:1590–602. https://doi.org/10.1016/j.jclepro.2017.03.152.

[58] Moran CJ, Lodhia S, Kunz NC, Huisingh D. Sustainability in mining, minerals and energy: New processes, pathways and human interactions for a cautiously optimistic future. J Clean Prod 2014;84:1–15. https://doi.org/10.1016/j.jclepro.2014.09.016.

[59] Zhang L, Xu Z. A review of current progress of recycling technologies for metals from waste electrical and electronic equipment. J Clean Prod 2016;127:19–36. https://doi.org/10.1016/j.jclepro.2016.04.004.

[60] Pavez P, Honores J, Millán D, Isaacs M. UN sustainable development goals: How can sustainable/green chemistry contribute? Curr Opin Green Sustain Chem 2018;13:154–7. https://doi.org/10.1016/j.cogsc.2018.06.013.

[61] Fan H-R, Yang K-F, Hu F-F, Liu S, Wang K-Y. The giant Bayan Obo REE-Nb-Fe deposit, China: Controversy and ore genesis. Geosci Front 2016;7:335–44. https://doi.org/10.1016/j.gsf.2015.11.005.

[62] Han A, Ge J, Lei Y. An adjustment in regulation policies and its effects on market supply: Game analysis for China's rare earths. Resour Policy 2015;46:30–42. https://doi.org/10.1016/j.resourpol.2015.07.007.

[63] Victoria M, García R, Krzemie A, Ángel M, Menéndez M, Richard M, et al. Rare earth elements mining investment: It is not all about China. Resour Policy 2017;53:66–76. https://doi.org/10.1016/j.resourpol.2017.05.004.

[64] Kumar A, Holuszko M, Espinosa DCR. E-waste: An overview on generation, collection, legislation and recycling practices. Resour Conserv Recycl 2017;122:32–42. https://doi.org/10.1016/j.resconrec.2017.01.018.

[65] Gambogi J. Scandium. 2018.

[66] Nash HA. The European Commission's sustainable consumption and production

and sustainable industrial policy action plan. J Clean Prod 2009;17:496–8. https://doi.org/10.1016/j.jclepro.2008.08.020.

[67] Adiansyah JS, Rosano M, Vink S, Keir G. A framework for a sustainable approach to mine tailings management: Disposal strategies. J Clean Prod 2015;108:1050–62. https://doi.org/10.1016/j.jclepro.2015.07.139.

[68] Seredkin M, Zabolotsky A, Jeffress G. In situ recovery, an alternative to conventional methods of mining: Exploration, resource estimation, environmental issues, project evaluation and economics. Ore Geol Rev 2016;79:500–14. https://doi.org/10.1016/j.oregeorev.2016.06.016.

[69] Izatt SR, Bruening RL, Izatt NE, Dale JB. A Review of the Application of Molecular Recognition Technology (MRT) for Ni / Cu / Co Hydrometallurgical Process Separations and for the Purification of Cobalt Streams. South African Inst Min Metall Base Met Conf 2009 2009:323–40.

[70] Pourbaix M. Atlas of Electrochemical Equilibria in Aqueous Solutions. Second. Houston: National Association of Corrosion Engineers; 1974.

[71] Smythe DM, Lombard A, Coetzee LL. Rare Earth Element deportment studies utilising QEMSCAN technology. Miner Eng 2013;52:52–61. https://doi.org/10.1016/j.mineng.2013.03.010.

[72] Shimazaki H, Yang Z, Miyawaki R, Shigeoka M. Scandium-bearing minerals in the Bayan Obo Nb-REE-Fe Deposit, Inner Mongolia, China. Resour Geol 2008;58:80–6. https://doi.org/10.1111/j.1751-3928.2007.00045.x.

[73] Cui H, Anderson CG. Alternative flowsheet for rare earth beneficiation of Bear Lodge ore. Miner Eng 2017;110:166–78. https://doi.org/10.1016/j.mineng.2017.04.016.

[74] Costis S, Coudert L, Mueller KK, Cecchi E, Neculita CM, Blais JF. Assessment of the leaching potential of flotation tailings from rare earth mineral extraction in cold climates. Sci Total Environ 2020;732:139225. https://doi.org/10.1016/j.scitotenv.2020.139225.

[75] Antoniassi JL, Uliana D, Contessotto R, Kahn H, Ulsen C. Process mineralogy of rare earths from deeply weathered alkali-carbonatite deposits in Brazil. J Mater Res Technol 2020;9:8842–53. https://doi.org/10.1016/j.jmrt.2020.05.128.

[76] Kursun I, Terzi M, Ozdemir O. Determination of surface chemistry and flotation properties of rare earth mineral allanite. Miner Eng 2019;132:113–20. https://doi.org/10.1016/j.mineng.2018.11.044.

[77] Geneyton A, Filippov LO, Heinig T, Buaron N, Menad NE. Towards the efficient flotation of monazite from silicate-rich tailings with fatty acids collectors using a lanthanum salt as a selective phosphate activator. Miner Eng 2021;160:106704. https://doi.org/10.1016/j.mineng.2020.106704.

[78] Kalashnikov AO, Yakovenchuk VN, Pakhomovsky YA, Bazai A V., Sokharev VA, Konopleva NG, et al. Scandium of the Kovdor baddeleyite-apatite-magnetite deposit (Murmansk Region, Russia): Mineralogy, spatial distribution, and potential resource. Ore Geol Rev 2016;72:532–7. https://doi.org/10.1016/j.oregeorev.2015.08.017.

[79] Ivanyuk GY, Kalashnikov AO, Pakhomovsky YA, Mikhailova JA, Yakovenchuk VN, Konopleva NG, et al. Economic minerals of the Kovdor baddeleyite-apatite-magnetite deposit, Russia: Mineralogy, spatial distribution and ore processing optimization. Ore Geol Rev 2016;77:279–311. https://doi.org/10.1016/j.oregeorev.2016.02.008.

[80] Neumann R, Medeiros EB. Comprehensive mineralogical and technological characterisation of the Araxá (SE Brazil) complex REE (Nb-P) ore, and the fate of its processing. Int J Miner Process 2015;144:1–10. https://doi.org/10.1016/j.minpro.2015.08.009.

[81] Kuzmin VI, Flett DS, Kuzmina VN, Zhizhaev AM, Gudkova N V., Kuzmin D V., et al. The composition, chemical properties, and processing of the unique niobium–rare earth ores of the Tomtor deposit. Chem Pap 2019;73:1437–46. https://doi.org/10.1007/s11696-019-00695-z.

[82] Ault T, Krahn S, Croff A. Assessment of the potential of by-product recovery of thorium to satisfy demands of a future thorium fuel cycle. Nucl Technol 2015;189:152–62. https://doi.org/10.13182/NT14-19.

[83] Ault T, Van Gosen B, Krahn S, Croff A. Natural thorium resources and recovery: Options and impacts. Nucl Technol 2016;194:136–51. https://doi.org/10.13182/NT15-83.

[84] Zhang GF, Yan P, Yang QR. Experimental study on concentrating scandium by leaching from associated scandium ore. Adv Mater Res 2013;734–737:1033–6. https://doi.org/10.4028/www.scientific.net/AMR.734-737.1033.

[85] Stepanov SI, P'ei K, Boyarintsev A V., Giganov VG, Chekmarev AM, Aung MM. Use of Machining to Increase the Recovery of Scandium from Refractory Silicate Raw Material. Theor Found Chem Eng 2018;52:898–902. https://doi.org/10.1134/S0040579518050275.

[86] Zhang Y, Zhao H, Sun M, Zhang Y, Meng X, Zhang L, et al. Scandium extraction from silicates by hydrometallurgical process at normal pressure and temperature. J Mater Res Technol 2020;9:709–17. https://doi.org/10.1016/j.jmrt.2019.11.012.

[87] Zhang B, Xue X, Huang X, Yang H, Chen G. Study on recycling and leaching valuable elements from Bayan Obo tailings. Metall Res Technol 2019;116. https://doi.org/10.1051/metal/2018040.

[88] Li SC, Kim SC, Kang CS. Recovery of scandium from KOH sub-molten salt leaching cake of fergusonite. Miner Eng 2019;137:200–6. https://doi.org/10.1016/j.mineng.2018.11.052.

[89] Ribagnac P, Deblonde GJP, Blancher SB, Lengagne L, Donati L, Malimba C, et al. Leaching of niobium- and REE-bearing iron ores: Significant reduction of H2SO4 consumption using SO2 and activated carbon. Sep Purif Technol 2017;189:1–10. https://doi.org/10.1016/j.seppur.2017.07.073.

[90] Yu B, Aghamirian M. REO mineral separation from silicates and carbonate gangue minerals. Can Metall Q 2015;54:377–87. https://doi.org/10.1179/1879139514Y.0000000179.

[91] Goode JR. Thorium and rare earth recovery in Canada: The first 30 years. Can Metall Q 2013;52:234–42. https://doi.org/10.1179/1879139513Y.0000000074.

[92] Gao L, Chen Y. A study on the rare earth ore containing scandium by high gradient magnetic separation. J Rare Earths 2010;28:622–6. https://doi.org/10.1016/S1002-0721(09)60167-8.

[93] Yan P, Zhang G, Yang Y, Mclean A. Characterization and Pre-concentration of Scandium in Low-Grade Magnetite Ore. Jom 2019;71:4666–73. https://doi.org/10.1007/s11837-019-03541-5.

[94] Yan P, Zhang GF, Gao L, Shi BH, Shi Z, Yang YD. Applied research of shaking table for scandium concentration from a silicate ore. IOP Conf Ser Earth Environ Sci 2018;128. https://doi.org/10.1088/1755-1315/128/1/012143.

[95] Liu H Bin, Du H, Wang DW, Wang SN, Zheng SL, Zhang Y. Kinetics analysis of decomposition of vanadium slag by KOH sub-molten salt method. Trans Nonferrous Met Soc China (English Ed 2013;23:1489–500. https://doi.org/10.1016/S1003-6326(13)62621-7.

[96] Levard C, Borschneck D, Grauby O, Rose J, Ambrosi J-P. Goethite, a tailor-made host for the critical metal scandium: The FexSc(1-x)OOH solid solution. Geochemical Perspect Lett 2018:16–20. https://doi.org/10.7185/geochemlet.1832.

[97] Kohl CA, Gomes LP. Physical and chemical characterization and recycling potential of desktop computer waste, without screen. J Clean Prod 2018;184:1041–51. https://doi.org/10.1016/j.jclepro.2018.02.221.

[98] Priya A, Hait S. Comprehensive characterization of printed circuit boards of various end-of-life electrical and electronic equipment for beneficiation investigation. Waste Manag 2018;75:103–23. https://doi.org/10.1016/j.wasman.2018.02.014.

[99] Ziegler O. Waste electrical and electronic equipment (WEEE) handbook. 2012.

[100] Thejo Kalyani N, Dhoble SJ. Novel materials for fabrication and encapsulation of OLEDs. Renew Sustain Energy Rev 2015;44:319–47. https://doi.org/10.1016/j.rser.2014.11.070.

[101] Teitler Y, Cathelineau M, Ulrich M, Ambrosi JP, Munoz M, Sevin B. Petrology and geochemistry of scandium in New Caledonian Ni-Co laterites. J Geochemical Explor 2019;196:131–55. https://doi.org/10.1016/j.gexplo.2018.10.009.

[102] Ulrich M, Cathelineau M, Muñoz M, Boiron MC, Teitler Y, Karpoff AM. The relative distribution of critical (Sc, REE) and transition metals (Ni, Co, Cr, Mn, V) in some Ni-laterite deposits of New Caledonia. J Geochemical Explor 2019;197:93–113. https://doi.org/10.1016/j.gexplo.2018.11.017.

[103] Aiglsperger T, Proenza JA, Lewis JF, Labrador M, Svojtka M, Rojas-Purón A, et al. Critical metals (REE, Sc, PGE) in Ni laterites from Cuba and the Dominican Republic. Ore Geol Rev 2016;73:127–47. https://doi.org/10.1016/j.oregeorev.2015.10.010.

[104] Saadaoui E, Ghazel N, Ben Romdhane C, Massoudi N. Phosphogypsum:

potential uses and problems–a review. Int J Environ Stud 2017;74:558–67. https://doi.org/10.1080/00207233.2017.1330582.

[105] Cánovas CR, Macías F, Pérez López R, Nieto JM. Mobility of rare earth elements, yttrium and scandium from a phosphogypsum stack: Environmental and economic implications. Sci Total Environ 2018;618:847–57. https://doi.org/10.1016/j.scitotenv.2017.08.220.

[106] Taggart RK, Hower JC, Dwyer GS, Hsu-Kim H. Trends in the Rare Earth Element Content of U.S.-Based Coal Combustion Fly Ashes. Environ Sci Technol 2016;50:5919–26. https://doi.org/10.1021/acs.est.6b00085.

[107] Chassé M, Griffin WL, O'Reilly SY, Calas G. Australian laterites reveal mechanisms governing scandium dynamics in the critical zone. Geochim Cosmochim Acta 2019;260:292–310. https://doi.org/10.1016/j.gca.2019.06.036.

[108] Funari V, Braga R, Bokhari SNH, Dinelli E, Meisel T. Solid residues from Italian municipal solid waste incinerators: A source for "'critical'" raw materials. Waste Manag 2015;45:206–16. https://doi.org/10.1016/j.wasman.2014.11.005.

[109] Morf LS, Gloor R, Haag O, Haupt M, Skutan S, Lorenzo F Di, et al. Precious metals and rare earth elements in municipal solid waste - Sources and fate in a Swiss incineration plant. Waste Manag 2013;33:634–44. https://doi.org/10.1016/j.wasman.2012.09.010.

[110] Mavakala BK, Le Faucheur S, Mulaji CK, Laffite A, Devarajan N, Biey EM, et al. Leachates draining from controlled municipal solid waste landfill: Detailed geochemical characterization and toxicity tests. Waste Manag 2016;55:238–48. https://doi.org/10.1016/j.wasman.2016.04.028.

[111] Funari V, Bokhari SNH, Vigliotti L, Meisel T, Braga R. The rare earth elements in municipal solid waste incinerators ash and promising tools for their prospecting. J Hazard Mater 2016;301:471–9. https://doi.org/10.1016/j.jhazmat.2015.09.015.

[112] Gutiérrez-Gutiérrez SC, Coulon F, Jiang Y, Wagland S. Rare earth elements and critical metal content of extracted landfilled material and potential recovery opportunities. Waste Manag 2015;42:128–36. https://doi.org/10.1016/j.wasman.2015.04.024.

[113] Valentim B, Abagiu AT, Anghelescu L, Flores D, French D, Gonçalves P, et al. Assessment of bottom ash landfilled at Ceplea Valley (Romania) as a source of rare earth elements. Int J Coal Geol 2019;201:109–26. https://doi.org/10.1016/j.coal.2018.11.019.

[114] Chen M, Graedel TE. The potential for mining trace elements from phosphate rock. J Clean Prod 2015;91:337–46. https://doi.org/10.1016/j.jclepro.2014.12.042.

[115] Wagner NJ, Matiane A. Rare earth elements in select Main Karoo Basin (South Africa) coal and coal ash samples. Int J Coal Geol 2018;196:82–92. https://doi.org/10.1016/j.coal.2018.06.020.

[116] Lu F, Xiao T, Lin J, Li A, Long Q, Huang F, et al. Recovery of gallium from Bayer red mud through acidic-leaching-ion-exchange process under normal

atmospheric pressure. Hydrometallurgy 2018;175:124–32. https://doi.org/10.1016/j.hydromet.2017.10.032.

[117] Arbuzov SI, Volostnov A V., Mezhibor AM, Rybalko VI, Ilenok SS. Scandium (Sc) geochemistry in coals (Siberia, Russian Far East, Mongolia, Kazakhstan, and Iran). Int J Coal Geol 2014;125:22–35. https://doi.org/10.1016/j.coal.2014.01.008.

[118] Folgueras MB, Alonso M, Fernández FJ. Coal and sewage sludge ashes as sources of rare earth elements. Fuel 2017;192:128–39. https://doi.org/10.1016/j.fuel.2016.12.019.

[119] Wu S, Wang L, Zhang P, El-Shall H, Moudgil B, Huang X, et al. Simultaneous recovery of rare earths and uranium from wet process phosphoric acid using solvent extraction with D2EHPA. Hydrometallurgy 2018;175:109–16. https://doi.org/10.1016/j.hydromet.2017.10.025.

[120] Kuppusamy VK, Holuszko M. Rare earth elements in flotation products of coals from East Kootenay coalfields, British Columbia. J Rare Earths 2019;37:1366–72. https://doi.org/10.1016/j.jre.2018.12.016.

[121] Huang Q, Talan D, Restrepo JH, Baena OJR, Kecojevic V, Noble A. Characterization study of rare earths, yttrium, and scandium from various Colombian coal samples and non-coal lithologies. Int J Coal Geol 2019;209:14–26. https://doi.org/10.1016/j.coal.2019.04.008.

[122] Zhang P, Han Z, Jia J, Wei C, Liu Q, Wang X, et al. Occurrence and Distribution of Gallium, Scandium, and Rare Earth Elements in Coal Gangue Collected from Junggar Basin, China. Int J Coal Prep Util 2019;39:389–402. https://doi.org/10.1080/19392699.2017.1334645.

[123] Zhang W, Rezaee M, Bhagavatula A, Li Y, Groppo J, Honaker R. A review of the occurrence and promising recovery methods of rare earth elements from coal and coal by-products. Int J Coal Prep Util 2015;35:281–94. https://doi.org/10.1080/19392699.2015.1033097.

[124] Hodgkinson JH, Grigorescu M. Strategic elements in the Fort Cooper Coal Measures: potential rare earth elements and other multi-product targets. Aust J Earth Sci 2020;67:305–19. https://doi.org/10.1080/08120099.2019.1660712.

[125] Rychkov V, Botalov M, Kirillov E, Kirillov S, Semenishchev V, Bunkov G, et al. Intensification of carbonate scandium leaching from red mud (bauxite residue). Hydrometallurgy 2021;199:105524. https://doi.org/10.1016/j.hydromet.2020.105524.

[126] Gentzmann MC, Schraut K, Vogel C, Gäbler H-E, Huthwelker T, Adam C. Investigation of scandium in bauxite residues of different origin. Appl Geochemistry 2021;126:104898. https://doi.org/10.1016/j.apgeochem.2021.104898.

[127] Rivera RM, Ulenaers B, Ounoughene G, Binnemans K, Van Gerven T, Marin R, et al. Extraction of rare earths from bauxite residue (red mud) by dry digestion followed by water leaching. Miner Eng 2018;119:82–92. https://doi.org/10.1016/j.mineng.2018.01.023.

[128] Vind J, Alexandri A, Vassiliadou V, Panias D. Distribution of selected trace elements in the bayer process. Metals (Basel) 2018;8:1–21. https://doi.org/10.3390/met8050327.

[129] Vind J, Malfliet A, Bonomi C, Paiste P, Sajó IE, Blanpain B, et al. Modes of occurrences of scandium in Greek bauxite and bauxite residue. Miner Eng 2018;123:35–48. https://doi.org/10.1016/j.mineng.2018.04.025.

[130] Purwadi I, van der Werff H, Lievens C. Reflectance spectroscopy and geochemical analysis of rare earth element-bearing tailings: A case study of two abandoned tin mine sites in Bangka Island, Indonesia. Int J Appl Earth Obs Geoinf 2019;74:239–47. https://doi.org/10.1016/j.jag.2018.09.006.

[131] Samsonov NY, Tolstov A V., Pokhilenko NP, Krykov VA, Khalimova SR. Possibilities of Russian hi-tech rare earth products to meet industrial needs of BRICS countries. African J Sci Technol Innov Dev 2017;9:637–44. https://doi.org/10.1080/20421338.2017.1327922.

[132] Dobretsov NL, Pokhilenko NP. Mineral resources and development in the Russian Arctic. Russ Geol Geophys 2010;51:98–111. https://doi.org/10.1016/j.rgg.2009.12.009.

[133] Yasukawa K, Ohta J, Mimura K, Tanaka E, Takaya Y, Usui Y, et al. A new and prospective resource for scandium: Evidence from the geochemistry of deep-sea sediment in the western North Pacific Ocean. Ore Geol Rev 2018;102:260–7. https://doi.org/10.1016/j.oregeorev.2018.09.001.

[134] Smith DB, Woodruff LG, O'Leary RM, Cannon WF, Garrett RG, Kilburn JE, et al. Pilot studies for the North American Soil Geochemical Landscapes Project - Site selection, sampling protocols, analytical methods, and quality control protocols. Appl Geochemistry 2009;24:1357–68. https://doi.org/10.1016/j.apgeochem.2009.04.008.

[135] Sako A, Nimi M. Environmental geochemistry and ecological risk assessment of potentially harmful elements in tropical semi-arid soils around the Bagassi South artisanal gold mining site, Burkina Faso. Cogent Environ Sci 2018;4:1–23. https://doi.org/10.1080/23311843.2018.1543565.

[136] Budakoglu M, Abdelnasser A, Karaman M, Kumral M. The rare earth element geochemistry on surface sediments, shallow cores and lithological units of Lake Acigöl basin, Denizli, Turkey. J Asian Earth Sci 2015;111:632–62. https://doi.org/10.1016/j.jseaes.2015.05.016.

[137] Chermak JA, Schreiber ME. Mineralogy and trace element geochemistry of gas shales in the United States: Environmental implications. Int J Coal Geol 2014;126:32–44. https://doi.org/10.1016/j.coal.2013.12.005.

[138] Jaireth S, Hoatson DM, Miezitis Y. Geological setting and resources of the major rare-earth-element deposits in Australia. Ore Geol Rev 2014;62:72–128. https://doi.org/10.1016/j.oregeorev.2014.02.008.

[139] Sjöberg S, Allard B, Rattray JE, Callac N, Grawunder A, Ivarsson M, et al. Rare earth element enriched birnessite in water-bearing fractures, the Ytterby mine, Sweden. Appl Geochemistry 2017;78:158–71. https://doi.org/10.1016/j.apgeochem.2016.12.021.

[140] Hein JR, Mizell K, Koschinsky A, Conrad TA. Deep-ocean mineral deposits as a source of critical metals for high- and green-technology applications: Comparison with land-based resources. Ore Geol Rev 2013;51:1–14. https://doi.org/10.1016/j.oregeorev.2012.12.001.

[141] Andersson M, Finne TE, Jensen LK, Eggen OA. Geochemistry of a copper mine tailings deposit in Repparfjorden, northern Norway. Sci Total Environ 2018;644:1219–31. https://doi.org/10.1016/j.scitotenv.2018.06.385.

[142] Klauber C, Gräfe M, Power G. Bauxite residue issues: II. options for residue utilization. Hydrometallurgy 2011;108:11–32. https://doi.org/10.1016/j.hydromet.2011.02.007.

[143] Vind J, Malfliet A, Bonomi C, Paiste P, Sajó IE, Blanpain B, et al. Modes of occurrences of scandium in Greek bauxite and bauxite residue. Miner Eng 2018;123:35–48. https://doi.org/10.1016/j.mineng.2018.04.025.

[144] Mongelli G, Boni M, Oggiano G, Mameli P, Sinisi R, Buccione R, et al. Critical metals distribution in Tethyan karst bauxite: The cretaceous Italian ores. Ore Geol Rev 2017;86:526–36. https://doi.org/10.1016/j.oregeorev.2017.03.017.

[145] Cusack PB, Courtney R, Healy MG, O' Donoghue LMT, Ujaczki É. An evaluation of the general composition and critical raw material content of bauxite residue in a storage area over a twelve-year period. J Clean Prod 2019;208:393–401. https://doi.org/10.1016/j.jclepro.2018.10.083.

[146] Deng B, Li G, Luo J, Ye Q, Liu M, Peng Z, et al. Enrichment of Sc2O3 and TiO2 from bauxite ore residues. J Hazard Mater 2017;331:71–80. https://doi.org/10.1016/j.jhazmat.2017.02.022.

[147] Pyagai IN, Pasechnik LA, Yatsenko AS, Skachkov VM, Yatsenko SP. Recovery of sludge from alumina production. Russ J Appl Chem 2012;85:1649–53. https://doi.org/10.1134/S107042721211002X.

[148] Loginova I V., Shoppert AA, Chaikin LI. Extraction of Rare-Earth Metals During the Systematic Processing of Diaspore-Boehmite Bauxites. Metallurgist 2016;60:198–203. https://doi.org/10.1007/s11015-016-0273-z.

[149] Deady ÉA, Mouchos E, Goodenough K, Williamson BJ, Wall F. A review of the potential for rare-earth element resources from European red muds: examples from Seydişehir, Turkey and Parnassus-Giona, Greece. Mineral Mag 2016;80:43–61. https://doi.org/10.1180/minmag.2016.080.052.

[150] Gu H, Wang N, Hargreaves JSJ. Sequential Extraction of Valuable Trace Elements from Bayer Process-Derived Waste Red Mud Samples. J Sustain Metall 2018;4:147–54. https://doi.org/10.1007/s40831-018-0164-6.

[151] Yang S, Wang Q, Deng J, Wang Y, Kang W, Liu X, et al. Genesis of karst bauxite-bearing sequences in Baofeng, Henan (China), and the distribution of critical metals. Ore Geol Rev 2019;115:103161. https://doi.org/10.1016/j.oregeorev.2019.103161.

[152] Deng B, Li G, Luo J, Ye Q, Liu M, Rao M, et al. Selective Extraction of Rare Earth Elements Over TiO2 From Bauxite Residues After Removal of Their Fe-, Si-, and Al-Bearing Constituents. Jom 2018;70:2869–76.

https://doi.org/10.1007/s11837-018-3130-7.

[153] Rivera RM, Xakalashe B, Ounoughene G, Binnemans K, Friedrich B, Van Gerven T. Selective rare earth element extraction using high-pressure acid leaching of slags arising from the smelting of bauxite residue. Hydrometallurgy 2019;184:162–74. https://doi.org/10.1016/j.hydromet.2019.01.005.

[154] Li W, Zhu X, Tang S. Selective separation of sodium from red mud with citric acid leaching. Sep Sci Technol 2017;52:1876–84. https://doi.org/10.1080/01496395.2017.1300591.

[155] Hodge H, Rowles MR, Hayes PC, Hawker W, Vaughan J. Bauxite residue sinter leach process – phases formation, reaction pathways and kinetics. Miner Process Extr Metall 2019;0:1–13. https://doi.org/10.1080/25726641.2019.1644778.

[156] Rivera RM, Ounoughene G, Borra CR, Binnemans K, Van Gerven T. Neutralisation of bauxite residue by carbon dioxide prior to acidic leaching for metal recovery. Miner Eng 2017;112:92–102. https://doi.org/10.1016/j.mineng.2017.07.011.

[157] Borra CR, Pontikes Y, Binnemans K, Van Gerven T. Leaching of rare earths from bauxite residue (red mud). Miner Eng 2015;76:20–7. https://doi.org/10.1016/j.mineng.2015.01.005.

[158] Zhu X, Li W, Zhang Q, Zhang C, Chen L. Separation characteristics of vanadium from leach liquor of red mud by ion exchange with different resins. Hydrometallurgy 2018;176:42–8. https://doi.org/10.1016/j.hydromet.2018.01.009.

[159] Zhou K, Teng C, Zhang X, Peng C, Chen W. Enhanced selective leaching of scandium from red mud. Hydrometallurgy 2018;182:57–63. https://doi.org/10.1016/j.hydromet.2018.10.011.

[160] Hatzilyberis K, Lymperopoulou T, Tsakanika LA, Ochsenkühn KM, Georgiou P, Defteraios N, et al. Process design aspects for scandium-selective leaching of bauxite residue with sulfuric acid. Minerals 2018;8:4–8. https://doi.org/10.3390/min8030079.

[161] Ochsenkuehn-Petropoulou M, Tsakanika LA, Lymperopoulou T, Ochsenkuehn KM, Hatzilyberis K, Georgiou P, et al. Efficiency of sulfuric acid on selective scandium leachability from bauxite residue. Metals (Basel) 2018;8. https://doi.org/10.3390/met8110915.

[162] Narayanan RP, Kazantzis NK, Emmert MH. Selective Process Steps for the Recovery of Scandium from Jamaican Bauxite Residue (Red Mud). ACS Sustain Chem Eng 2018;6:1478–88. https://doi.org/10.1021/acssuschemeng.7b03968.

[163] Onghena B, Borra CR, Van Gerven T, Binnemans K. Recovery of scandium from sulfation-roasted leachates of bauxite residue by solvent extraction with the ionic liquid betainium bis(trifluoromethylsulfonyl)imide. Sep Purif Technol 2017;176:208–19. https://doi.org/10.1016/j.seppur.2016.12.009.

[164] Anawati J, Azimi G. Recovery of scandium from Canadian bauxite residue utilizing acid baking followed by water leaching. Waste Manag 2019;95:549–59.

https://doi.org/10.1016/j.wasman.2019.06.044.

[165] Zhang X kai, Zhou K gen, Chen W, Lei Q yuan, Huang Y, Peng C hong. Recovery of iron and rare earth elements from red mud through an acid leaching-stepwise extraction approach. J Cent South Univ 2019;26:458–66. https://doi.org/10.1007/s11771-019-4018-6.

[166] Rivera RM, Ounoughene G, Malfliet A, Vind J, Panias D, Vassiliadou V, et al. A Study of the Occurrence of Selected Rare-Earth Elements in Neutralized–Leached Bauxite Residue and Comparison with Untreated Bauxite Residue. J Sustain Metall 2019;5:57–68. https://doi.org/10.1007/s40831-018-0206-0.

[167] Lymperopoulou T, Georgiou P, Tsakanika LA, Hatzilyberis K, Ochsenkuehn-Petropoulou M. Optimizing conditions for scandium extraction from bauxite residue using taguchi methodology. Minerals 2019;9. https://doi.org/10.3390/min9040236.

[168] Cánovas CR, Chapron S, Arrachart G, Pellet-Rostaing S. Leaching of rare earth elements (REEs) and impurities from phosphogypsum: A preliminary insight for further recovery of critical raw materials. J Clean Prod 2019;219:225–35. https://doi.org/10.1016/j.jclepro.2019.02.104.

[169] Abisheva ZS, Karshigina ZB, Bochevskaya YG, Akcil A, Sargelova EA, Kvyatkovskaya MN, et al. Recovery of rare earth metals as critical raw materials from phosphorus slag of long-term storage. Hydrometallurgy 2017;173:271–82. https://doi.org/10.1016/j.hydromet.2017.08.022.

[170] Zhang W, Honaker RQ. Rare earth elements recovery using staged precipitation from a leachate generated from coarse coal refuse. Int J Coal Geol 2018;195:189–99. https://doi.org/10.1016/j.coal.2018.06.008.

[171] Honaker RQ, Zhang W, Yang X, Rezaee M. Conception of an integrated flowsheet for rare earth elements recovery from coal coarse refuse. Miner Eng 2018;122:233–40. https://doi.org/10.1016/j.mineng.2018.04.005.

[172] Laudal DA, Benson SA, Addleman RS, Palo D. Leaching behavior of rare earth elements in Fort Union lignite coals of North America. Int J Coal Geol 2018;191:112–24. https://doi.org/10.1016/j.coal.2018.03.010.

[173] Yang X, Werner J, Honaker RQ. Leaching of rare Earth elements from an Illinois basin coal source. J Rare Earths 2019;37:312–21. https://doi.org/10.1016/j.jre.2018.07.003.

[174] Zhang W, Honaker R. Calcination pretreatment effects on acid leaching characteristics of rare earth elements from middlings and coarse refuse material associated with a bituminous coal source. Fuel 2019;249:130–45. https://doi.org/10.1016/j.fuel.2019.03.063.

[175] Önal MAR, Topkaya YA. Pressure acid leaching of Çaldağ lateritic nickel ore: An alternative to heap leaching. Hydrometallurgy 2014;142:98–107. https://doi.org/10.1016/j.hydromet.2013.11.011.

[176] Bonomi C, Alexandri A, Vind J, Panagiotopoulou A, Tsakiridis P, Panias D. Scandium and Titanium Recovery from Bauxite Residue by Direct Leaching with a Brønsted Acidic Ionic Liquid. Metals (Basel) 2018;8:834.

https://doi.org/10.3390/met8100834.

[177] Davris P, Marinos D, Balomenos E, Alexandri A, Gregou M, Panias D, et al. Leaching of rare earth elements from 'Rödberg' ore of Fen carbonatite complex deposit, using the ionic liquid HbetTf2N. Hydrometallurgy 2018;175:20–7. https://doi.org/10.1016/j.hydromet.2017.10.031.

[178] Davris P, Balomenos E, Panias D, Paspaliaris I. Selective leaching of rare earth elements from bauxite residue (red mud), using a functionalized hydrophobic ionic liquid. Hydrometallurgy 2016;164:125–35. https://doi.org/10.1016/j.hydromet.2016.06.012.

[179] Zhu X, Li W, Tang S, Zeng M, Bai P, Chen L. Selective recovery of vanadium and scandium by ion exchange with D201 and solvent extraction using P507 from hydrochloric acid leaching solution of red mud. Chemosphere 2017;175:365–72. https://doi.org/10.1016/j.chemosphere.2017.02.083.

[180] Zhu X, Li W, Zhang Q, Zhang C, Chen L. Separation characteristics of vanadium from leach liquor of red mud by ion exchange with different resins. Hydrometallurgy 2018;176:42–8. https://doi.org/10.1016/j.hydromet.2018.01.009.

[181] Zhang W, Koivula R, Wiikinkoski E, Xu J, Hietala S, Lehto J, et al. Efficient and Selective Recovery of Trace Scandium by Inorganic Titanium Phosphate Ion-Exchangers from Leachates of Waste Bauxite Residue. ACS Sustain Chem Eng 2017;5:3103–14. https://doi.org/10.1021/acssuschemeng.6b02870.

[182] ZHOU H, LI D, TIAN Y, CHEN Y. Extraction of scandium from red mud by modified activated carbon and kinetics study. Rare Met 2008;27:223–7. https://doi.org/10.1016/S1001-0521(08)60119-9.

[183] Roosen J, Van Roosendael S, Borra CR, Van Gerven T, Mullens S, Binnemans K. Recovery of scandium from leachates of Greek bauxite residue by adsorption on functionalized chitosan–silica hybrid materials. Green Chem 2016;18:2005–13. https://doi.org/10.1039/C5GC02225H.

[184] Al-Thyabat S, Zhang P. REE extraction from phosphoric acid, phosphoric acid sludge, and phosphogypsum. Trans Institutions Min Metall Sect C Miner Process Extr Metall 2015;124:143–50. https://doi.org/10.1179/1743285515Y.0000000002.

[185] Ramasamy DL, Puhakka V, Iftekhar S, Wojtuś A, Repo E, Ben Hammouda S, et al. N- and O- ligand doped mesoporous silica-chitosan hybrid beads for the efficient, sustainable and selective recovery of rare earth elements (REE) from acid mine drainage (AMD): Understanding the significance of physical modification and conditioning of th. J Hazard Mater 2018;348:84–91. https://doi.org/10.1016/j.jhazmat.2018.01.030.

[186] Bao S, Hawker W, Vaughan J. Scandium Loading on Chelating and Solvent Impregnated Resin from Sulfate Solution. Solvent Extr Ion Exch 2018;36:100–13. https://doi.org/10.1080/07366299.2017.1412917.

[187] Liu Z, Li H, Jing Q, Zhang M. Recovery of Scandium from Leachate of Sulfation-Roasted Bayer Red Mud by Liquid–Liquid Extraction. Jom 2017;69:2373–8. https://doi.org/10.1007/s11837-017-2518-0.

[188] Wang W, Pranolo Y, Cheng CY. Recovery of scandium from synthetic red mud leach solutions by solvent extraction with D2EHPA. Sep Purif Technol 2013;108:96–102. https://doi.org/10.1016/j.seppur.2013.02.001.

[189] Abhilash, Sinha S, Sinha MK, Pandey BD. Extraction of lanthanum and cerium from Indian red mud. Int J Miner Process 2014;127:70–3. https://doi.org/10.1016/j.minpro.2013.12.009.

[190] Liu C, Chen L, Chen J, Zou D, Deng Y, Li D. Application of P507 and isooctanol extraction system in recovery of scandium from simulated red mud leach solution. J Rare Earths 2019;37:1002–8. https://doi.org/10.1016/j.jre.2018.12.004.

[191] Ferizoglu E, Kaya Ş, Topkaya YA. Solvent extraction behaviour of scandium from lateritic nickel-cobalt ores using different organic reagents. Physicochem Probl Miner Process 2018;54:538–45. https://doi.org/10.5277/ppmp1855.

[192] Kaya Ş, Dittrich C, Stopic S, Friedrich B. Concentration and separation of scandium from Ni laterite ore processing streams. Metals (Basel) 2017;7:0–6. https://doi.org/10.3390/met7120557.

[193] Souza AGO, Aliprandini P, Espinosa DCR, Tenório JAS. Scandium Extraction from Nickel Processing Waste Using Cyanex 923 in Sulfuric Medium. Jom 2019;71:2003–9. https://doi.org/10.1007/s11837-019-03427-6.

[194] Abisheva ZS, Karshigina ZB, Bochevskaya YG, Akcil A, Sargelova EA, Kvyatkovskaya MN, et al. Recovery of rare earth metals as critical raw materials from phosphorus slag of long-term storage. Hydrometallurgy 2017;173:271–82. https://doi.org/10.1016/j.hydromet.2017.08.022.

[195] Onghena B, Borra CR, Van Gerven T, Binnemans K. Recovery of scandium from sulfation-roasted leachates of bauxite residue by solvent extraction with the ionic liquid betainium bis(trifluoromethylsulfonyl)imide. Sep Purif Technol 2017;176:208–19. https://doi.org/10.1016/j.seppur.2016.12.009.

[196] Schaeffer N, Passos H, Billard I, Papaiconomou N, Coutinho JAP. Recovery of metals from waste electrical and electronic equipment (WEEE) using unconventional solvents based on ionic liquids. Crit Rev Environ Sci Technol 2018;48:859–922. https://doi.org/10.1080/10643389.2018.1477417.

[197] Avdibegović D, Regadío M, Binnemans K. Efficient separation of rare earths recovered by a supported ionic liquid from bauxite residue leachate. RSC Adv 2018;8:11886–93. https://doi.org/10.1039/c7ra13402a.

[198] Avdibegović D, Yagmurlu B, Dittrich C, Regadío M, Friedrich B, Binnemans K. Combined multi-step precipitation and supported ionic liquid phase chromatography for the recovery of rare earths from leach solutions of bauxite residues. Hydrometallurgy 2018;180:229–35. https://doi.org/10.1016/j.hydromet.2018.07.023.

[199] Karve M, Vaidya B. Selective separation of scandium(III) and yttrium(III) from other rare earth elements using Cyanex302 as an extractant. Sep Sci Technol 2008;43:1111–23. https://doi.org/10.1080/01496390801887435.

[200] Oliveira GFR de, Botelho AB, Tenório JAS. SEPARATION OF COBALT FROM

THE NICKEL-RICH SOLUTION FROM HPAL PROCESS BY SYNERGISM USING ORGANIC EXTRACTS CYANEX 272 AND IONQUEST 290. Tecnol Em Metal Mater e Mineração 2019;16:464–9. https://doi.org/10.4322/2176-1523.20191962.

[201] Abreu RD, Morais CA. Study on separation of heavy rare earth elements by solvent extraction with organophosphorus acids and amine reagents. Miner Eng 2014;61:82–7. https://doi.org/10.1016/j.mineng.2014.03.015.

[202] Cheng CY, Barnard KR, Zhang W, Robinson DJ. Synergistic solvent extraction of nickel and cobalt: A review of recent developments. Solvent Extr Ion Exch 2011;29:719–54. https://doi.org/10.1080/07366299.2011.595636.

[203] Li D. Development course of separating rare earths with acid phosphorus extractants: A critical review. J Rare Earths 2019;37:468–86. https://doi.org/10.1016/j.jre.2018.07.016.

[204] Yudaev PA, Kolpinskaya NA, Chistyakov EM. Organophosphorous extractants for metals. Hydrometallurgy 2021;201:105558. https://doi.org/10.1016/j.hydromet.2021.105558.

[205] Rizk HE, El-Nadi YA, El-Hefny NE. Extractive Separation of Scandium from Strongly Alkaline Solution by Quaternary Ammonium Salt. Solvent Extr Ion Exch 2020;38:350–63. https://doi.org/10.1080/07366299.2020.1729327.

[206] Ye Q, Li G, Deng B, Luo J, Rao M, Peng Z, et al. Solvent extraction behavior of metal ions and selective separation Sc3+ in phosphoric acid medium using P204. Sep Purif Technol 2019;209:175–81. https://doi.org/10.1016/j.seppur.2018.07.033.

[207] Stepanov SI, P'ei K, Boyarintsev A V., Giganov VG, Aung MM, Chekmarev AM. Scandium extraction from sulfuric acid solutions by mixtures of D2EHPA and MTAA sulfate in toluene. Theor Found Chem Eng 2017;51:846–9. https://doi.org/10.1134/S0040579517050219.

[208] Le W, Kuang S, Zhang Z, Wu G, Li Y, Liao C, et al. Selective extraction and recovery of scandium from sulfate medium by Cextrant 230. Hydrometallurgy 2018;178:54–9. https://doi.org/10.1016/j.hydromet.2018.04.005.

[209] Gao LK, Rao B, Dai HX, Hong Z, Xie HY. Separation and extraction of scandium and titanium from a refractory anatase lixivium by solvent extraction with D2EHPA and primary amine N1923. J Chem Eng Japan 2019;52:822–8. https://doi.org/10.1252/jcej.18we347.

[210] Hu J, Zou D, Chen J, Li D. A novel synergistic extraction system for the recovery of scandium (III) by Cyanex272 and Cyanex923 in sulfuric acid medium. Sep Purif Technol 2020;233:115977. https://doi.org/10.1016/j.seppur.2019.115977.

[211] Kostikova G V., Mal'tseva IE, Zhilov VI. Extraction Recovery of Scandium and Concomitant Elements with Isoamyldialkylphosphine Oxide from Different Media. Russ J Inorg Chem 2019;64:277–82. https://doi.org/10.1134/S0036023619020128.

[212] Zhao Z, Kubota F, Kamiya N, Goto M. Selective Extraction of Scandium from Transition Metals by Synergistic Extraction with 2-Thenoyltrifluoroacetone and

Tri-n-octylphosphine Oxide. Solvent Extr Res Dev 2016;23:137–43.

[213] Kostikova G V., Krasnova OG, Tsivadze AY, Zhilov VI. Scandium extraction with benzo-15-crown-5 from neutral nitrate–trichloroacetate solutions. Russ J Inorg Chem 2018;63:555–60. https://doi.org/10.1134/S0036023618040125.

[214] Sharaf M, Yoshida W, Kubota F, Kolev SD, Goto M. A polymer inclusion membrane composed of the binary carrier PC-88A and Versatic 10 for the selective separation and recovery of Sc. RSC Adv 2018;8:8631–7. https://doi.org/10.1039/c7ra12697b.

[215] Zhang W, Zhang TA, Lv G, Zhou W, Cao X, Zhu H. Extraction Separation of Sc(III) and Fe(III) from a Strongly Acidic and Highly Concentrated Ferric Solution by D2EHPA/TBP. Jom 2018;70:2837–45. https://doi.org/10.1007/s11837-018-3166-8.

[216] Das S, Behera SS, Murmu BM, Mohapatra RK, Mandal D, Samantray R, et al. Extraction of scandium(III) from acidic solutions using organo-phosphoric acid reagents: A comparative study. Sep Purif Technol 2018;202:248–58. https://doi.org/10.1016/j.seppur.2018.03.023.

[217] Yuan H, Hong W, Zhou Y, Pu B, Gong A, Xu T, et al. Extraction and back-extraction behaviors of 14 rare earth elements from sulfuric acid medium by TODGA. J Rare Earths 2018;36:642–7. https://doi.org/10.1016/j.jre.2018.01.011.

[218] Fujinaga K, Yoshimori M, Nakajima Y, Oshima S, Watanabe Y, Stevens GW, et al. Separation of Sc(III) from ZrO(II) by solvent extraction using oxidized Phoslex DT-8. Hydrometallurgy 2013;133:33–6. https://doi.org/10.1016/j.hydromet.2012.11.014.

[219] Wei H, Li Y, Zhang Z, Xue T, Kuang S, Liao W. Selective Extraction and Separation of Ce (IV) and Th (IV) from RE(III) in Sulfate Medium using Di(2-ethylhexyl)-N-heptylaminomethylphosphonate. Solvent Extr Ion Exch 2017;35:117–29. https://doi.org/10.1080/07366299.2017.1292025.

[220] Fujinaga K, Nakai Y, Nakajima Y, Oshima S, Watanabe Y, Komatsu Y. The extraction separation of Sc(III) from a simulated solution of waste water by using O,O-bis(2-ethylhexyl) hydrogen thiophosphate. Solvent Extr Res Dev 2018;25:1–10. https://doi.org/10.15261/serdj.25.1.

[221] Yoshida W, Kubota F, Baba Y, Kolev SD, Goto M. Separation and Recovery of Scandium from Sulfate Media by Solvent Extraction and Polymer Inclusion Membranes with Amic Acid Extractants. ACS Omega 2019;4:21122–30. https://doi.org/10.1021/acsomega.9b02540.

[222] Sharaf M, Yoshida W, Kubota F, Goto M. A novel binary-extractant-impregnated resin for selective recovery of scandium. J Chem Eng Japan 2019;52:49–55. https://doi.org/10.1252/jcej.18we175.

[223] Zagorodni AA. Ion Exchnange Materials: Properties and Application. vol. XXXIII. First edit. Stockholm: Elsevier; 2012. https://doi.org/10.1007/s13398-014-0173-7.2.

[224] Avdibegović D, Zhang W, Xu J, Regadío M, Koivula R, Binnemans K. Selective

ion-exchange separation of scandium(III) over iron(III) by crystalline A-zirconium phosphate platelets under acidic conditions. Sep Purif Technol 2019;215:81–90. https://doi.org/10.1016/j.seppur.2018.12.079.

[225] Botelho Junior AB, Jiménez Correa MM, Espinosa DCR, Tenório JAS. Study of the reduction process of iron in leachate from nickel mining waste. Brazilian J Chem Eng 2018;35:1241–8. https://doi.org/10.1590/0104-6632.20180354s20170323.

[226] Ramasamy DL, Porada S, Sillanpää M. Marine algae: A promising resource for the selective recovery of scandium and rare earth elements from aqueous systems. Chem Eng J 2019;371:759–68. https://doi.org/10.1016/j.cej.2019.04.106.

[227] Hamza MF, Wei Y, Guibal E. Quaternization of algal/PEI beads (a new sorbent): Characterization and application to scandium sorption from aqueous solutions. Chem Eng J 2020;383:123210. https://doi.org/10.1016/j.cej.2019.123210.

[228] Ramasamy DL, Puhakka V, Repo E, Khan S, Sillanpää M. Coordination and silica surface chemistry of lanthanides (III), scandium (III) and yttrium (III) sorption on 1-(2-pyridylazo)-2-napththol (PAN) and acetylacetone (acac) immobilized gels. Chem Eng J 2017;324:104–12. https://doi.org/10.1016/j.cej.2017.05.025.

[229] Moon JY, Takajo C, Nishihama S, Yoshizuka K. Separation and Recovery of Scandium and Yttrium from Aqueous Chloride Media by Integrated Ion Exchange Method. Solvent Extr Res Dev 2020;27:91–7. https://doi.org/10.15261/serdj.27.91.

[230] Yagmurlu B, Dittrich C, Friedrich B. Effect of Aqueous Media on the Recovery of Scandium by Selective Precipitation. Metals (Basel) 2018;8:314. https://doi.org/10.3390/met8050314.

[231] da Silva RG, de Morais CA, Teixeira LV, de Oliveira ÉD. Selective removal of impurities from rare earth sulphuric liquor using different reagents. Miner Eng 2018;127:238–46. https://doi.org/10.1016/j.mineng.2018.08.007.

[232] Silva RG, Morais CA, Oliveira ÉD. Selective precipitation of rare earth from non-purified and purified sulfate liquors using sodium sulfate and disodium hydrogen phosphate. Miner Eng 2019;134:402–16. https://doi.org/10.1016/j.mineng.2019.02.028.

[233] Zhang W, Yu S, Zhang S, Zhou J, Ning S, Wang X, et al. Separation of scandium from the other rare earth elements with a novel macro-porous silica-polymer based adsorbent HDEHP/SiO 2 -P. Hydrometallurgy 2019;185:117–24. https://doi.org/10.1016/j.hydromet.2019.01.012.

[234] Ramasamy DL, Puhakka V, Repo E, Ben Hammouda S, Sillanpää M. Two-stage selective recovery process of scandium from the group of rare earth elements in aqueous systems using activated carbon and silica composites: Dual applications by tailoring the ligand grafting approach. Chem Eng J 2018;341:351–60. https://doi.org/10.1016/j.cej.2018.02.024.

[235] Ramasamy DL, Khan S, Repo E, Sillanpää M. Synthesis of mesoporous and microporous amine and non-amine functionalized silica gels for the application

of rare earth elements (REE) recovery from the waste water-understanding the role of pH, temperature, calcination and mechanism in Light REE and Hea. Chem Eng J 2017;322:56–65. https://doi.org/10.1016/j.cej.2017.03.152.

[236] Cui H, Chen J, Li H, Zou D, Liu Y, Deng Y. High-performance polymer-supported extractants with phosphonate ligands for scandium(III) separation. AIChE J 2016;62:2479–89. https://doi.org/10.1002/aic.15236.

[237] Zhao Z, Baba Y, Yoshida W, Kubota F, Goto M. Development of novel adsorbent bearing aminocarbonylmethylglycine and its application to scandium separation. J Chem Technol Biotechnol 2016;91:2779–84. https://doi.org/10.1002/jctb.4884.

[238] Giret S, Hu Y, Masoumifard N, Boulanger JF, Estelle J, Kleitz F, et al. Selective Separation and Preconcentration of Scandium with Mesoporous Silica. ACS Appl Mater Interfaces 2018;10:448–57. https://doi.org/10.1021/acsami.7b13336.

[239] Lou Z, Xiao X, Huang M, Wang Y, Xing Z, Xiong Y. Acrylic Acid-Functionalized Metal-Organic Frameworks for Sc(III) Selective Adsorption. ACS Appl Mater Interfaces 2019;11:11772–81. https://doi.org/10.1021/acsami.9b00476.

[240] Yu Q, Ning S, Zhang W, Wang X, Wei Y. Recovery of scandium from sulfuric acid solution with a macro porous TRPO/SiO2-P adsorbent. Hydrometallurgy 2018;181:74–81. https://doi.org/10.1016/j.hydromet.2018.07.025.

[241] Gedgagov EI, Zakhar'yan S V., Sinyanskaya OM, Zakhar'yan D V. Removal of Impurities from Saturated Ion-Exchange Resins by Frontal-Gradient Purification in Schemes for Recovery of Nonferrous, Rare, and Rare Earth Metals. Theor Found Chem Eng 2018;52:920–7. https://doi.org/10.1134/S0040579518050111.

[242] Van Nguyen N, Iizuka A, Shibata E, Nakamura T. Study of adsorption behavior of a new synthesized resin containing glycol amic acid group for separation of scandium from aqueous solutions. Hydrometallurgy 2016;165:51–6. https://doi.org/10.1016/j.hydromet.2015.11.016.

[243] Zhou G, Li Q, Sun P, Guan W, Zhang G, Cao Z, et al. Removal of impurities from scandium chloride solution using 732-type resin. J Rare Earths 2018;36:311–6. https://doi.org/10.1016/j.jre.2017.09.009.

[244] Ramasamy DL, Puhakka V, Repo E, Sillanpää M. Selective separation of scandium from iron, aluminium and gold rich wastewater using various amino and non-amino functionalized silica gels – A comparative study. J Clean Prod 2018;170:890–901. https://doi.org/10.1016/j.jclepro.2017.09.199.

[245] Turanov AN, Karandashev VK, Sukhinina NS, Masalov VM, Emelchenko GA. Adsorption of lanthanides and scandium ions by silica sol-gel material doped with novel bifunctional ionic liquid, trioctylmethylammonium 1-phenyl-3-methyl-4-benzoyl-5-onate. J Environ Chem Eng 2016;4:3788–96. https://doi.org/10.1016/j.jece.2016.08.024.

[246] Avdibegović D, Regadío M, Binnemans K. Recovery of scandium(III) from diluted aqueous solutions by a supported ionic liquid phase (SILP). RSC Adv 2017;7:49664–74. https://doi.org/10.1039/c7ra07957e.

[247] Chen Y, Wang H, Pei Y, Wang J. Selective separation of scandium (III) from rare earth metals by carboxyl-functionalized ionic liquids. Sep Purif Technol 2017;178:261–8. https://doi.org/10.1016/j.seppur.2017.01.058.

[248] Onghena B, Binnemans K. Recovery of Scandium(III) from aqueous solutions by solvent extraction with the functionalized ionic liquid betainium bis(trifluoromethylsulfonyl)imide. Ind Eng Chem Res 2015;54:1887–98. https://doi.org/10.1021/ie504765v.

[249] Turanov AN, Karandashev VK, Baulin VE, Kalashnikova IP, Kirillov E V., Kirillov S V., et al. Extraction of rare earths and scandium by 2-phosphorylphenoxyacetic acid amides in the presence of ionic liquids. Russ J Inorg Chem 2016;61:377–83. https://doi.org/10.1134/S0036023616030232.

[250] Sun X, Ji Y, Guo L, Chen J, Li D. A novel ammonium ionic liquid based extraction strategy for separating scandium from yttrium and lanthanides. Sep Purif Technol 2011;81:25–30. https://doi.org/10.1016/j.seppur.2011.06.034.

[251] Makanyire T, Sanchez-Segado S, Jha A. Separation and recovery of critical metal ions using ionic liquids. Adv Manuf 2016;4:33–46. https://doi.org/10.1007/s40436-015-0132-3.

[252] Parhi PK, Behera SS, Mohapatra RK, Sahoo TR, Das D, Misra PK. Separation and recovery of Sc(III) from Mg–Sc alloy scrap solution through hollow fiber supported liquid membrane (HFLM) process supported by Bi-functional ionic liquid as carrier. Sep Sci Technol 2019;54:1478–88. https://doi.org/10.1080/01496395.2018.1520730.

[253] Smith RC, Taggart RK, Hower JC, Wiesner MR, Hsu-Kim H. Selective Recovery of Rare Earth Elements from Coal Fly Ash Leachates Using Liquid Membrane Processes. Environ Sci Technol 2019;53:4490–9. https://doi.org/10.1021/acs.est.9b00539.

[254] Jyothi RK, Thenepalli T, Ahn JW, Parhi PK, Chung KW, Lee JY. Review of rare earth elements recovery from secondary resources for clean energy technologies: Grand opportunities to create wealth from waste. J Clean Prod 2020;267:122048. https://doi.org/10.1016/j.jclepro.2020.122048.

[255] Chen Z. Global rare earth resources and scenarios of future rare earth industry. J Rare Earths 2011;29:1–6. https://doi.org/10.1016/S1002-0721(10)60401-2.

[256] Favot M, Massarutto A. Rare-earth elements in the circular economy: The case of yttrium. J Environ Manage 2019;240:504–10. https://doi.org/10.1016/j.jenvman.2019.04.002.

[257] Binnemans K, Jones PT, Blanpain B, Van Gerven T, Yang Y, Walton A, et al. Recycling of rare earths: A critical review. J Clean Prod 2013;51:1–22. https://doi.org/10.1016/j.jclepro.2012.12.037.

[258] Binnemans K, McGuiness P, Jones PT. Rare-earth recycling needs market intervention. Nat Rev Mater 2021;0123456789. https://doi.org/10.1038/s41578-021-00308-w.

[259] Bray EL. Bauxite and Alumina. 2016.

[260] Bolen WP. Bauxite and Alumina Minerals Yearbook 2015. 2016.

[261] Lumley R. Fundamentals of Aluminium Metallurgy. 1st ed. Cambridge: Woodhead Publishing; 2011. https://doi.org/10.1533/9780857090256.3.655.

[262] Valeton I. Bauxites. 1972.

[263] Liu Y, Naidu R. Hidden values in bauxite residue (red mud): Recovery of metals. Waste Manag 2014;34:2662–73. https://doi.org/10.1016/j.wasman.2014.09.003.

[264] Power G, Gräfe M, Klauber C. Bauxite residue issues: I. Current management, disposal and storage practices. Hydrometallurgy 2011;108:33–45. https://doi.org/10.1016/j.hydromet.2011.02.006.

[265] Gontijo GS, Araújo ACB de, Prasad S, Vasconcelos LGS, Alves JJN, Brito RP, et al. Improving the Bayer Process productivity - An industrial case study. Miner Eng 2009;22:1130–6. https://doi.org/10.1016/j.mineng.2009.04.010.

[266] Tse P-K. China's Rare-Earth Industry. Reston: 2011.

[267] Binnemans K, Jones PT, Blanpain B, Van Gerven T, Pontikes Y. Towards zero-waste valorisation of rare-earth-containing industrial process residues: A critical review. J Clean Prod 2015;99:17–38. https://doi.org/10.1016/j.jclepro.2015.02.089.

[268] Borra CR, Blanpain B, Pontikes Y, Binnemans K, Van Gerven T. Recovery of Rare Earths and Other Valuable Metals From Bauxite Residue (Red Mud): A Review. J Sustain Metall 2016;2:365–86. https://doi.org/10.1007/s40831-016-0068-2.

[269] Liu W, Chen X, Li W, Yu Y, Yan K. Environmental assessment, management and utilization of red mud in China. J Clean Prod 2014;84:606–10. https://doi.org/10.1016/j.jclepro.2014.06.080.

[270] Perez JPH, Folens K, Leus K, Vanhaecke F, Van Der Voort P, Du Laing G. Progress in hydrometallurgical technologies to recover critical raw materials and precious metals from low-concentrated streams. Resour Conserv Recycl 2019;142:177–88. https://doi.org/10.1016/j.resconrec.2018.11.029.

[271] Jowitt SM, Mudd GM, Werner TT, Weng Z, Barkoff DW, Mccaffrey D. The Critical Metals : An Overview and Opportunities and Concerns for the Future. In: Arribas A., Broughton D., Mauk J, editors. Met. Miner. Soc. 1st ed., Lawrence: Society of Economic Geologists; 2018, p. 25–38. https://doi.org/10.5382/SP.21.02.

[272] Rollat A, Guyonnet D, Planchon M, Tuduri J. Prospective analysis of the flows of certain rare earths in Europe at the 2020 horizon. Waste Manag 2016;49:427–36. https://doi.org/10.1016/j.wasman.2016.01.011.

[273] Khairul MA, Zanganeh J, Moghtaderi B. The composition, recycling and utilisation of Bayer red mud. Resour Conserv Recycl 2019;141:483–98. https://doi.org/10.1016/j.resconrec.2018.11.006.

[274] Borra CR, Blanpain B, Pontikes Y, Binnemans K, Van Gerven T. Smelting of Bauxite Residue (Red Mud) in View of Iron and Selective Rare Earths Recovery. J Sustain Metall 2016;2:28–37. https://doi.org/10.1007/s40831-015-0026-4.

[275] Borra CR, Mermans J, Blanpain B, Pontikes Y, Binnemans K, Van Gerven T.

Selective recovery of rare earths from bauxite residue by combination of sulfation, roasting and leaching. Miner Eng 2016;92:151–9. https://doi.org/10.1016/j.mineng.2016.03.002.

[276] Fulford GD, Lever G, Sato T. Recovery of rare earth elements from Bayer Process Red Mud. 5,030,424, 1991.

[277] Kim C-J, Yoon H-S, Chung KW, Lee J-Y, Kim S-D, Shin SM, et al. Leaching kinetics of lanthanum in sulfuric acid from rare earth element (REE) slag. Hydrometallurgy 2014;146:133–7. https://doi.org/10.1016/j.hydromet.2014.04.003.

[278] Yang X, Zhang J, Fang X. Rare earth element recycling from waste nickel-metal hydride batteries. J Hazard Mater 2014;279:384–8. https://doi.org/10.1016/j.jhazmat.2014.07.027.

[279] Nadiatul N, Zainal S, Hidayah NN, Abidin SZ. The evolution of mineral processing in extraction of rare earth elements using solid-liquid extraction over liquid-liquid extraction: A review. Miner Eng 2017;112:103–13. https://doi.org/10.1016/j.mineng.2017.07.014.

[280] Davris P, Balomenos E, Panias D, Paspaliaris I. Selective leaching of rare earth elements from bauxite residue (red mud), using a functionalized hydrophobic ionic liquid. Hydrometallurgy 2016;164:125–35. https://doi.org/10.1016/j.hydromet.2016.06.012.

[281] Pepper RA, Couperthwaite SJ, Millar GJ. Comprehensive examination of acid leaching behaviour of mineral phases from red mud: Recovery of Fe, Al, Ti, and Si. Miner Eng 2016;99:8–18. https://doi.org/10.1016/j.mineng.2016.09.012.

[282] Davris P, Stopic S, Balomenos E, Panias D, Paspaliaris I, Friedrich B. Leaching of rare earth elements from eudialyte concentrate by suppressing silica gel formation. Miner Eng 2017;108:115–22. https://doi.org/10.1016/j.mineng.2016.12.011.

[283] Zhang J, Zhao B, Schreiner B. Separation Hydrometallurgy of Rare Earth Elements. Cham: Springer International Publishing; 2016. https://doi.org/10.1007/978-3-319-28235-0.

[284] Bao S, Hawker W, Vaughan J, Shenxu B, Hawker W, Vaughan J. Scandium Loading on Chelating and Solvent Impregnated Resin from Sulfate Solution. Solvent Extr Ion Exch 2018;36:100–13. https://doi.org/10.1080/07366299.2017.1412917.

[285] Page MJ, Soldenhoff K, Ogden MD. Comparative study of the application of chelating resins for rare earth recovery. Hydrometallurgy 2017;169:275–81. https://doi.org/10.1016/j.hydromet.2017.02.006.

[286] ABNT AB de NT. NBR 10006: Procedimento para obtenção de extrato solubilizado de resíduos sólidos. Abnt 2004:7. https://doi.org/01.080.10; 13.220.99.

[287] Panda I, Jain S, Das SK, Jayabalan R. Characterization of red mud as a structural fill and embankment material using bioremediation. Int Biodeterior Biodegrad 2017;119:368–76. https://doi.org/10.1016/j.ibiod.2016.11.026.

[288] Frare LM, Gimenes ML, Pereira NC, Mendes ES. Linearização do modelo log-normal para distribuição de tamanho de partículas 2000;22:1235–9.

[289] Massarani G. Fluidodinâmica em sistemas particulados. 2001. https://doi.org/10.1016/B978-85-352-7721-0/00004-4.

[290] Singh M, Kumar S, Kumar S, Nandan G, Gupta M. Characterization of Iron-ore suspension at In-situ conditions. Mater Today Proc 2018;5:17845–51. https://doi.org/10.1016/j.matpr.2018.06.110.

[291] Tarján G. A contribution to particle size distribution functions. Powder Technol 1974;10:73–7. https://doi.org/10.1016/0032-5910(74)85034-5.

[292] Zhang J, Bai Y, Dong H, Wu Q, Ye X. Influence of ball size distribution on grinding effect in horizontal planetary ball mill. Adv Powder Technol 2014;25:983–90. https://doi.org/10.1016/j.apt.2014.01.018.

[293] Liu S, Li Q, Xie G, Li L, Xiao H. Effect of grinding time on the particle characteristics of glass powder. Powder Technol 2016;295:133–41. https://doi.org/10.1016/j.powtec.2016.03.030.

[294] Parveen F, Briens C, Berruti F, McMillan J. Effect of particle size, liquid content and location on the stability of agglomerates in a fluidized bed. Powder Technol 2013;237:376–85. https://doi.org/10.1016/j.powtec.2012.12.021.

[295] Gräfe M, Power G, Klauber C. Bauxite residue issues: III. Alkalinity and associated chemistry. Hydrometallurgy 2011;108:60–79. https://doi.org/10.1016/j.hydromet.2011.02.004.

[296] Kaußen FM, Friedrich B. Phase characterization and thermochemical simulation of (landfilled) bauxite residue (“red mud”) in different alkaline processes optimized for aluminum recovery. Hydrometallurgy 2018;176:49–61. https://doi.org/10.1016/j.hydromet.2018.01.006.

[297] Pascual J, Corpas FA, López-Beceiro J, Benítez-Guerrero M, Artiaga R. Thermal characterization of a Spanish red mud. J Therm Anal Calorim 2009;96:407–12. https://doi.org/10.1007/s10973-008-9230-9.

[298] Singh S, Aswath MU, Ranganath RV. Effect of mechanical activation of red mud on the strength of geopolymer binder. Constr Build Mater 2018;177:91–101. https://doi.org/10.1016/j.conbuildmat.2018.05.096.

[299] Snars K, Gilkes RJ. Evaluation of bauxite residues (red muds) of different origins for environmental applications. Appl Clay Sci 2009;46:13–20. https://doi.org/10.1016/j.clay.2009.06.014.

[300] Li G, Liu M, Rao M, Jiang T, Zhuang J, Zhang Y. Stepwise extraction of valuable components from red mud based on reductive roasting with sodium salts. J Hazard Mater 2014;280:774–80. https://doi.org/10.1016/j.jhazmat.2014.09.005.

[301] Liu R xin, Poon C sun. Effects of red mud on properties of self-compacting mortar. J Clean Prod 2016;135:1170–8. https://doi.org/10.1016/j.jclepro.2016.07.052.

[302] Mesgari Abbasi S, Rashidi A, Ghorbani A, Khalaj G, Mesgari S, Rashidi A, et al. Synthesis, processing, characterization, and applications of red mud/carbon

nanotube composites. Ceram Int 2016;42:16738–43. https://doi.org/10.1016/j.ceramint.2016.07.146.

[303] Zhao Z, Yang Y, Xiao Y, Fan Y. Recovery of gallium from Bayer liquor: A review. Hydrometallurgy 2012;125–126:115–24. https://doi.org/10.1016/j.hydromet.2012.06.002.

[304] Gladyshev S V., Akcil A, Abdulvaliyev RA, Tastanov EA, Beisembekova KO, Temirova SS, et al. Recovery of vanadium and gallium from solid waste by-products of Bayer process. Miner Eng 2015;74:91–8. https://doi.org/10.1016/j.mineng.2015.01.011.

[305] Vind J, Alexandri A, Vassiliadou V, Panias D. Distribution of Selected Trace Elements in the Bayer Process. Metals (Basel) 2018;8:327. https://doi.org/10.3390/met8050327.

[306] Forte G, Burma J, Dufour R, Borduas J. Process for the removal of silica from an alkaline solution containing sodium aluminate. WO 99/67172, 2000.

[307] Vaughan J, Peng H, Seneviratne D, Hodge H, Hawker W, Hayes P, et al. The Sandy Desilication Product Process Concept. Jom 2019;71:2928–35. https://doi.org/10.1007/s11837-019-03617-2.

[308] Smith P. The processing of high silica bauxites - Review of existing and potential processes. Hydrometallurgy 2009;98:162–76. https://doi.org/10.1016/j.hydromet.2009.04.015.

[309] Abhilash, Sinha S, Sinha MK, Pandey BD. Extraction of lanthanum and cerium from Indian red mud. Int J Miner Process 2014;127:70–3. https://doi.org/10.1016/j.minpro.2013.12.009.

[310] Liu W, Yang J, Xiao B. Application of Bayer red mud for iron recovery and building material production from alumosilicate residues. J Hazard Mater 2009;161:474–8. https://doi.org/10.1016/j.jhazmat.2008.03.122.

[311] Zhaobo LIU, Yanbing Z, Hongxu LI, Dongmin JIA, Zihan Z, Liu Z, et al. Selectively recovering scandium from high alkali Bayer red mud without impurities of iron, titanium and gallium. J Rare Earths 2017;35:896–905. https://doi.org/10.1016/S1002-0721(17)60992-X.

[312] Klauber C, Gräfe M, Power G. Bauxite residue issues: II. options for residue utilization. Hydrometallurgy 2011;108:11–32. https://doi.org/10.1016/j.hydromet.2011.02.007.

[313] Power G, Loh J. Organic compounds in the processing of lateritic bauxites to alumina Part 1: Origins and chemistry of organics in the Bayer process. Hydrometallurgy 2010;105:1–29. https://doi.org/10.1016/j.hydromet.2010.07.006.

[314] Zhang K, Kleit AN, Nieto A. An economics strategy for criticality – Application to rare earth element Yttrium in new lighting technology and its sustainable availability. Renew Sustain Energy Rev 2017;77:899–915. https://doi.org/10.1016/j.rser.2016.12.127.

[315] Alkan G, Schier C, Gronen L, Stopic S, Friedrich B. A Mineralogical Assessment on Residues after Acidic Leaching of Bauxite Residue (Red Mud) for Titanium

Recovery. Metals (Basel) 2017;7:458. https://doi.org/10.3390/met7110458.

[316] Reid S, Tam J, Yang M, Azimi G. Technospheric Mining of Rare Earth Elements from Bauxite Residue (Red Mud): Process Optimization, Kinetic Investigation, and Microwave Pretreatment. Sci Rep 2017;7:1–9. https://doi.org/10.1038/s41598-017-15457-8.

[317] Paramguru RK, Rath PC, Misra VN. Trends in red mud utilization - A review. Miner Process Extr Metall Rev 2005;26:1–29. https://doi.org/10.1080/08827500490477603.

[318] Havlík T. Hydrometallurgy: Principles and application. vol. 61. Cambridge: Cambridge International Science Publishing Limited; 2008. https://doi.org/10.1016/S0304-386X(01)00178-5.

[319] Jordens A, Sheridan RS, Rowson NA, Waters KE. Processing a rare earth mineral deposit using gravity and magnetic separation. Miner Eng 2014;62:9–18. https://doi.org/10.1016/j.mineng.2013.09.011.

[320] Kumari A, Yoo K, Rajesh Kumar J, Lee JY, Jha MK, Panda R, et al. Review on hydrometallurgical recovery of rare earth metals. Hydrometallurgy 2016;165:2–26. https://doi.org/10.1016/j.hydromet.2016.01.035.

[321] Deng B, Li G, Luo J, Ye Q, Liu M, Peng Z, et al. Enrichment of Sc2O3 and TiO2 from bauxite ore residues. J Hazard Mater 2017;331:71–80. https://doi.org/10.1016/j.jhazmat.2017.02.022.

[322] Botelho Junior AB, Costa RH, Espinosa DCR, Tenório JAS. Recovery of Scandium by Leaching Process from Brazilian Red Mud. In: Azimi G, Kim H, Alam S, Ouchi T, Neelameggham NR, Baba AA, editors. Rare Earth Technol. 1st ed., San Antonio: Springer; 2019, p. 73–9. https://doi.org/10.1007/978-3-030-05740-4_8.

[323] Espiari S, Rashchi F, Sadrnezhaad SK. Hydrometallurgical treatment of tailings with high zinc content. Hydrometallurgy 2006;82:54–62. https://doi.org/10.1016/j.hydromet.2006.01.005.

[324] Mbedzi N, Ibana D, Dyer L, Browner R. The effect of oxidant addition on ferrous iron removal from multi-element acidic sulphate solutions. Proc. 1st Int. Process Metall. Conf., 2017, p. 9. https://doi.org/10.1063/1.4974413.

[325] Chang Y, Zhai X, Li B, Fu Y. Removal of iron from acidic leach liquor of lateritic nickel ore by goethite precipitate. Hydrometallurgy 2010;101:84–7. https://doi.org/10.1016/j.hydromet.2009.11.014.

[326] Inamuddin ML. Ion Exchange Technology I. Dordrecht: Springer Netherlands; 2012. https://doi.org/10.1007/978-94-007-1700-8.

[327] Wang W, Cheng CY. Separation and purification of scandium by solvent extraction and related technologies: a review. J Chem Technol Biotechnol 2011;86:1237–46. https://doi.org/10.1002/jctb.2655.

[328] Li G, Ye Q, Deng B, Luo J, Rao M, Peng Z, et al. Extraction of scandium from scandium-rich material derived from bauxite ore residues. Hydrometallurgy 2018;176:62–8. https://doi.org/10.1016/j.hydromet.2018.01.007.

[329] European Commission. 2020 list of critical raw materials for the EU 2021:4. https://ec.europa.eu/growth/tools-databases/regional-innovation-monitor/base-profile/berlin (accessed August 3, 2021).

[330] Swain B, Akcil A, Lee J. Red mud valorization an industrial waste circular economy challenge; review over processes and their chemistry. Crit Rev Environ Sci Technol 2020;0:1–51. https://doi.org/10.1080/10643389.2020.1829898.

[331] Souza AGO, Aliprandini P, Espinosa DCR, Tenório JAS. Scandium Extraction from Nickel Processing Waste Using Cyanex 923 in Sulfuric Medium. JOM 2019;71:2003–9. https://doi.org/10.1007/s11837-019-03427-6.

[332] Tayebi-Khorami M, Edraki M, Corder G, Golev A. Re-Thinking Mining Waste through an Integrative Approach Led by Circular Economy Aspirations. Minerals 2019;9:286. https://doi.org/10.3390/min9050286.

[333] Almeida CA, Oliveira AF de, Pacheco AA, Lopes RP, Neves AA, Lopes Ribeiro de Queiroz ME. Characterization and evaluation of sorption potential of the iron mine waste after Samarco dam disaster in Doce River basin – Brazil. Chemosphere 2018;209:411–20. https://doi.org/10.1016/j.chemosphere.2018.06.071.

[334] Alkan G, Yagmurlu B, Gronen L, Dittrich C, Ma Y, Stopic S, et al. Selective silica gel free scandium extraction from Iron-depleted red mud slags by dry digestion. Hydrometallurgy 2019;185:266–72. https://doi.org/10.1016/j.hydromet.2019.03.008.

[335] Wei D, Jun-Hui X, Yang P, Si-Yue S, Tao C, Kai Z, et al. Extraction of Scandium and Iron from Red Mud. Miner Process Extr Metall Rev 2020;00:1–8. https://doi.org/10.1080/08827508.2020.1833195.

[336] Seyed Ghasemi SM, Azizi A. Alkaline leaching of lead and zinc by sodium hydroxide: Kinetics modeling. J Mater Res Technol 2018;7:118–25. https://doi.org/10.1016/j.jmrt.2017.03.005.

[337] Senanayake G, Senaputra A, Nicol MJ. Effect of thiosulfate, sulfide, copper(II), cobalt(II)/(III) and iron oxides on the ammoniacal carbonate leaching of nickel and ferronickel in the Caron process. Hydrometallurgy 2010;105:60–8. https://doi.org/10.1016/j.hydromet.2010.07.011.

[338] Sadri F, Nazari AM, Ghahreman A. A review on the cracking, baking and leaching processes of rare earth element concentrates. J Rare Earths 2017;35:739–52. https://doi.org/10.1016/S1002-0721(17)60971-2.

[339] LIU J lian, YIN Z lan, LI X hai, HU Q yang, LIU W. Recovery of valuable metals from lepidolite by atmosphere leaching and kinetics on dissolution of lithium. Trans Nonferrous Met Soc China (English Ed 2019;29:641–9. https://doi.org/10.1016/S1003-6326(19)64974-5.

[340] Basturkcu H. Extraction of lanthanum and yttrium from red mud following elimination of ionic impurities. Sep Sci Technol 2020;00:1–10. https://doi.org/10.1080/01496395.2020.1813177.

[341] Oruê BP, Botelho Junior AB, Tenório JAS, Espinosa DCR, Baltazar M dos PG. Kinetic Study of Manganese Precipitation of Nickel Laterite Leach Based-

solution by Ozone Oxidation. Ozone Sci Eng 2020;00:1–15. https://doi.org/10.1080/01919512.2020.1796580.

[342] Zafar ZI. Determination of semi empirical kinetic model for dissolution of bauxite ore with sulfuric acid: Parametric cumulative effect on the Arrhenius parameters. Chem Eng J 2008;141:233–41. https://doi.org/10.1016/j.cej.2007.12.025.

[343] Li J, Yang Y, Wen Y, Liu W, Chu Y, Wang R, et al. Leaching Kinetics and Mechanism of Laterite with NH4Cl-HCl Solution. Minerals 2020;10:754. https://doi.org/10.3390/min10090754.

[344] Voßenkaul D, Birich A, Müller N, Stoltz N, Friedrich B. Hydrometallurgical Processing of Eudialyte Bearing Concentrates to Recover Rare Earth Elements Via Low-Temperature Dry Digestion to Prevent the Silica Gel Formation. J Sustain Metall 2017;3:79–89. https://doi.org/10.1007/s40831-016-0084-2.

[345] Han KN. Characteristics of Precipitation of Rare Earth Elements with Various Precipitants. Minerals 2020;10:178. https://doi.org/10.3390/min10020178.

[346] Aydogan S. Dissolution kinetics of sphalerite with hydrogen peroxide in sulphuric acid medium. Chem Eng J 2006;123:65–70. https://doi.org/10.1016/j.cej.2006.07.001.

[347] Cao D, Sun L, Wang G, Lv Y, Zhang M. Kinetics of hydrogen peroxide electroreduction on Pd nanoparticles in acidic medium. J Electroanal Chem 2008;621:31–7. https://doi.org/10.1016/j.jelechem.2008.04.007.

[348] Ruiz-Sánchez A, Lázaro I, Lapidus GT. Improvement effect of organic ligands on chalcopyrite leaching in the aqueous medium of sulfuric acid-hydrogen peroxide-ethylene glycol. Hydrometallurgy 2020;193:105293. https://doi.org/10.1016/j.hydromet.2020.105293.

[349] Arnout L, Beersaerts G, Liard M, Lootens D, Pontikes Y. Valorising Slags from Non-ferrous Metallurgy into Hybrid Cementitious Binders: Mix Design and Performance. Waste and Biomass Valorization 2021. https://doi.org/10.1007/s12649-020-01322-9.

[350] Hertel T, Van den Bulck A, Onisei S, Sivakumar PP, Pontikes Y. Boosting the use of bauxite residue (red mud) in cement - Production of an Fe-rich calciumsulfoaluminate-ferrite clinker and characterisation of the hydration. Cem Concr Res 2021;145:106463. https://doi.org/10.1016/j.cemconres.2021.106463.

[351] Hota S, Kar BB, Mishra M. Removal of phosphorus from contaminated water sources using composite matrix fabricated from agro-based waste materials. Mater Today Proc 2021. https://doi.org/10.1016/j.matpr.2020.11.608.

[352] Li X, Li Y, Li Y, Wu J. The phytoremediation of water with high concentrations of nitrogen and phosphorus contamination by three selected wetland plants. J Water Process Eng 2021;40. https://doi.org/10.1016/j.jwpe.2020.101828.

[353] Yuan S, Tang H, Xiao Y, Xia Y, Melching C, Li Z. Phosphorus contamination of the surface sediment at a river confluence. J Hydrol 2019;573:568–80. https://doi.org/10.1016/j.jhydrol.2019.02.036.

[354] Garanayak L. Strength effect of alkali activated red mud slag cement in ambient

condition. Mater Today Proc 2021;44:1437–43. https://doi.org/10.1016/j.matpr.2020.11.630.

[355] Krivenko P, Kovalchuk O, Pasko A, Croymans T, Hult M, Lutter G, et al. Development of alkali activated cements and concrete mixture design with high volumes of red mud. Constr Build Mater 2017;151:819–26. https://doi.org/10.1016/j.conbuildmat.2017.06.031.

[356] Xu G, Shi X. Characteristics and applications of fly ash as a sustainable construction material: A state-of-the-art review. Resour Conserv Recycl 2018;136:95–109. https://doi.org/10.1016/j.resconrec.2018.04.010.

[357] Qi D. Extraction of Rare Earths From RE Concentrates. Hydrometall. Rare Earths. 1st ed., Elsevier; 2018, p. 1–185. https://doi.org/10.1016/B978-0-12-813920-2.00001-5.

[358] Ni'am AC, Wang YF, Chen SW, You SJ. Recovery of rare earth elements from waste permanent magnet (WPMs) via selective leaching using the Taguchi method. J Taiwan Inst Chem Eng 2019;97:137–45. https://doi.org/10.1016/j.jtice.2019.01.006.

[359] Surampally R, Batchu NK, Mannepalli LK, Bontha RR. Studies on solvent extraction of Dy(III) and separation possibilities of rare earths using PC-88A from phosphoric acid solutions. J Taiwan Inst Chem Eng 2012;43:839–44. https://doi.org/10.1016/j.jtice.2012.04.009.

[360] Levin LA, Amon DJ, Lily H. Challenges to the sustainability of deep-seabed mining. Nat Sustain 2020;3. https://doi.org/10.1038/s41893-020-0558-x.

[361] Jyothi RK, Thenepalli T, Ahn JW, Parhi PK, Chung KW, Lee JY. Review of rare earth elements recovery from secondary resources for clean energy technologies: Grand opportunities to create wealth from waste. J Clean Prod 2020;267:122048. https://doi.org/10.1016/j.jclepro.2020.122048.

[362] Sovacool BK, Ali SH, Bazilian M, Radley B, Nemery B, Okatz J, et al. Sustainable minerals and metals for a low-carbon future. Science (80-) 2020;367:30–3. https://doi.org/10.1126/science.aaz6003.

[363] Kaya Ş, Dittrich C, Stopic S, Friedrich B. Concentration and Separation of Scandium from Ni Laterite Ore Processing Streams. Metals (Basel) 2017;7:557. https://doi.org/10.3390/met7120557.

[364] Kim J, Azimi G. Recovery of scandium and neodymium from blast furnace slag using acid baking–water leaching. RSC Adv 2020;10:31936–46. https://doi.org/10.1039/D0RA05797E.

[365] Zou D, Li H, Deng Y, Chen J, Bai Y. Recovery of lanthanum and cerium from rare earth polishing powder wastes utilizing acid baking-water leaching-precipitation process. Sep Purif Technol 2021;261:118244. https://doi.org/10.1016/j.seppur.2020.118244.

[366] Luo J, Li G, Rao M, Peng Z, Zhang Y, Jiang T. Atmospheric leaching characteristics of nickel and iron in limonitic laterite with sulfuric acid in the presence of sodium sulfite. Miner Eng 2015;78:38–44. https://doi.org/10.1016/j.mineng.2015.03.030.

[367] Han KN, Rubcumintara T, Fuerstenau MC. Leaching behavior of ilmenite with sulfuric acid. Metall Trans B 1987;18:325–30. https://doi.org/10.1007/BF02656150.

[368] Azimi G, Papangelakis VG. The solubility of gypsum and anhydrite in simulated laterite pressure acid leach solutions up to 250 °C. Hydrometallurgy 2010;102:1–13. https://doi.org/10.1016/j.hydromet.2009.12.009.

[369] Čermák V, Smutek M, Cermak V, Smutek M, Čermák V, Smutek M. Mechanism of decomposition of dithionite in aqueous solutions. Collect Czechoslov Chem Commun 2012;40:3241–64. https://doi.org/10.1135/cccc19753241.

[370] Lister MW, Garvie RC. Sodium dithionite decomposition in aqueous solution and in the solid state. Can J Chem 1959;37:1567–74. https://doi.org/10.1139/v59-228.

[371] Raghavan S, Fowler S, Raghavan; S, Fowler S. Use of dithionite in the removal of nickel from ammoniacal solutions. Hydrometallurgy 1983;11:125–9. https://doi.org/http://dx.doi.org/10.1016/0304-386X(83)90050-6.

[372] Terry B. The acid decomposition of silicate minerals part I. Reactivities and modes of dissolution of silicates. Hydrometallurgy 1983;10:135–50. https://doi.org/10.1016/0304-386X(83)90002-6.

[373] Ujaczki É, Zimmermann Y, Gasser C, Molnár M, Feigl V, Lenz M. Red mud as secondary source for critical raw materials - purification of rare earth elements by liquid/liquid extraction. J Chem Technol Biotechnol 2017;92:2683–90. https://doi.org/10.1002/jctb.5289.

[374] United Nations. The Sustainable Development Goals Report. 2020.

[375] Yagmurlu B, Dittrich C, Friedrich B. Precipitation Trends of Scandium in Synthetic Red Mud Solutions with Different Precipitation Agents. J Sustain Metall 2017;3:90–8. https://doi.org/10.1007/s40831-016-0098-9.

[376] Sharaf M, Yoshida W, Kubota F, Goto M. Selective Extraction of Scandium by a Long Alkyl Chain Carboxylic Acid/Organophosphonic Ester Binary Extractant. Solvent Extr Ion Exch 2018;36:647–57. https://doi.org/10.1080/07366299.2018.1532139.

[377] Wang LY, Lee MS. Separation of Zr and Hf from sulfuric acid solutions with amine-based extractants by solvent extraction. Sep Purif Technol 2015;142:83–9. https://doi.org/10.1016/j.seppur.2015.01.001.

[378] Banda R, Min SH, Lee MS. Selective extraction of Hf(IV) over Zr(IV) from aqueous H2SO4 solutions by solvent extraction with acidic organophosphorous based extractants. J Chem Technol Biotechnol 2014;89:1712–9. https://doi.org/10.1002/jctb.4249.

[379] Wang LY, Lee MS. Separation of zirconium and hafnium from nitric acid solutions with LIX 63, PC 88A and their mixture by solvent extraction. Hydrometallurgy 2014;150:153–60. https://doi.org/10.1016/j.hydromet.2014.10.009.

[380] Saratale GD, Kim HY, Saratale RG, Kim DS. Liquid–liquid extraction of yttrium from the sulfate leach liquor of waste fluorescent lamp powder: Process parameters and analysis. Miner Eng 2020;152:106341.

https://doi.org/10.1016/j.mineng.2020.106341.

[381] Zou D, Li H, Chen J, Li D. Recovery of scandium from spent sulfuric acid solution in titanium dioxide production using synergistic solvent extraction with D2EHPA and primary amine N1923. Hydrometallurgy 2020;197:105463. https://doi.org/10.1016/j.hydromet.2020.105463.

[382] Batchu NK, Vander Hoogerstraete T, Banerjee D, Binnemans K. Non-aqueous solvent extraction of rare-earth nitrates from ethylene glycol to n-dodecane by Cyanex 923. Sep Purif Technol 2017;174:544–53. https://doi.org/10.1016/j.seppur.2016.10.039.

[383] Cytec Industries Inc. CYANEX ® 923 Extractant 2008:16.

[384] Wang W, Cheng CY. Separation and purification of scandium by solvent extraction and related technologies: A review. J Chem Technol Biotechnol 2011;86:1237–46. https://doi.org/10.1002/jctb.2655.

[385] Wang LY, Lee MS. A review on the aqueous chemistry of Zr(IV) and Hf(IV) and their separation by solvent extraction. J Ind Eng Chem 2016;39:1–9. https://doi.org/10.1016/j.jiec.2016.06.004.

[386] Xie F, Zhang TA, Dreisinger D, Doyle F. A critical review on solvent extraction of rare earths from aqueous solutions. Miner Eng 2014;56:10–28. https://doi.org/10.1016/j.mineng.2013.10.021.

[387] Judge WD, Azimi G. Recent progress in impurity removal during rare earth element processing: A review. Hydrometallurgy 2020;196:105435. https://doi.org/10.1016/j.hydromet.2020.105435.

[388] Correa MMJ, Aliprandini P, Tenório JAS, Espinosa DCR. Precipitation of Metals from Liquor Obtained in Nickel Mining. In: Kirchain RE, Blanpain B, Meskers C, Olivetti E, Apelian D, Howarter J, et al., editors. REWAS 2016, vol. 1, Cham: Springer International Publishing; 2016, p. 333–8. https://doi.org/10.1007/978-3-319-48768-7_52.

[389] Kislik VS. Solvent Extraction: Classical and Novel Approaches. 2014. https://doi.org/10.1007/s13398-014-0173-7.2.

[390] Banda R, Lee HY, Lee MS. Separation of Zr from Hf in hydrochloric acid solution using amine-based extractants. Ind Eng Chem Res 2012;51:9652–60. https://doi.org/10.1021/ie3008264.

[391] Banda R, Lee HY, Lee MS. Separation of Zr and Hf from strong hydrochloric acid solution by solvent extraction with TEHA. J Radioanal Nucl Chem 2013;295:1537–43. https://doi.org/10.1007/s10967-012-1941-5.

[392] Jun L, Zhenggui W, Deqian L, Gengxiang M, Zucheng J. Recovery of Ce(IV) and Th(IV) from rare earths(III) with Cyanex 923. Hydrometallurgy 1998;50:77–87. https://doi.org/10.1016/S0304-386X(98)00051-6.

[393] Zhang N, Li H-X, Liu X-M. Recovery of scandium from bauxite residue—red mud: a review. Rare Met 2016;35:887–900. https://doi.org/10.1007/s12598-016-0805-5.

[394] Fungaro DA, Grosche LC, Izidoro J de C. Synthesis of Calcium Silicate Hydrate

Compounds From Wet Flue Gas Desulfurization (FGD) Waste. J Appl Mater Technol 2020;1:88–95. https://doi.org/10.31258/Jamt.1.2.88-95.

[395] Fungaro DA, Silva KC, Mahmoud AED. Aluminium Tertiary Industry Waste and Ashes Samples for Development Of Zeolitic Material Synthesis. J Appl Mater Technol 2021;2:66–73. https://doi.org/10.31258/Jamt.2.2.66-73.